Impacts of Land Use and Land Cover Changes on Hydrological Characteristics and Soil Erosion in Stung Sangkae Catchment, Cambodia

2023

NUT NARETH

Doctoral Dissertation

Impacts of Land Use and Land Cover Changes on Hydrological Characteristics and Soil Erosion in Stung Sangkae Catchment, Cambodia

Nareth NUT

Supervisor	:	Professor Dr. Machito MIHARA
Advisers	:	Professor Dr. Fumio WATANABE
	:	Professor Dr. Takahiko NAKAMURA
	:	Associate Prof. Dr. Toru NAKAJIMA
	:	Associate Prof. Dr. Narong TOUCH

2023

Summary

Chapter 1 Background and Objectives

The most common and widespread land use and land cover (LULC) changes across the globe are deforestation, agricultural expansion, and urbanization. The LULC changes caused by anthropogenic activities significantly affect the hydrological characteristics of the landscape. Moreover, it also was recognized as capable of greatly accelerating soil erosion. In Cambodia, the LULC changes happened dramatically in the last 2 decades which was mainly due to population growth, agricultural expansion, and economic and urban development.

Therefore, the research interests have been focused on the impacts of LULC changes on hydrological characteristics and soil erosion in Stung Sangkae Catchment, as the impacts threaten sustainable development in agriculture and local livelihoods if the targeted catchment is not properly restored through deep consideration. Accordingly, this study attempted to examine 1) What the changes of LULC and its hydrological characteristics were in the Stung Sangkae Catchment from 2002 to 2015 by the SWAT model; 2) What the soil erosion severeness was in the catchment from 2002 to 2015 by RUSLE model; 3) Based on the impacts of LULC changes on stream flow and soil erosion, how seasonal flow or soil erosion is mitigated in the catchment thought implementing countermeasures of reforestation or agroforestry practices; and 4) How the public perception on the importance of conservation strategies against flood/drought and soil loss in the catchment is deepened.

Chapter 2 Research Site Description

The Stung Sangkae Catchment (605,170 ha), which is the third-largest tributary of the Tonle Sap Basin River system, is located at the upper north-western part of Cambodia between 12◦130-13◦240 N and 102◦350-103◦420 E. The topography is level within the floodplain region and rough with slopes at the upland portion of the catchment having elevations extending from 4 m at the most reduced point to 1,413 m a.s.l at the most noteworthy point. The catchment is characterized by distinctive topographical conditions, from flat plains to rugged areas. The main river that flows through the catchment, Sangkae River, lies between the tributaries of the Tonle Sap Great Lake in the upper western part of the catchments. The length of the river is approximately 250 km. Based on meteorological data collected from six weather stations in 2007-2018, the average annual precipitation in the study area is 1,388 mm and varied from 1,308 mm at Moung Ruessei Station to 1,577 mm at Samlout Station with little change during the year. The major soil types in the catchment are (1) Luvisols (34.0%) which are a type of soil in which highly active clay migrates from the top part of the profile, usually gray, and is deposited in the B layer, usually brown; (2) Nitisols (27.4%)

which are mainly deep, well-drained soils with a stable structure and high nutrient content; (3) Gleysols (27.3%) which are wetland soils, which in the natural state are continuously water-saturated within 50 cm of the surface, for extended periods; and (4) Acrisols (11.3%) which are clay-wealthy soils which can be fairly vulnerable to erosion covering the area. In the catchment, floods, drought, and soil erosion have been happening severely.

The Stung Sangkae Catchment, located in Battambang Province, is recognized by the Royal Government of Cambodia (RGC) as an important area for agricultural investment and development. Agriculture is the main local economic activity and the main source of livelihood in the catchment. Agricultural production, in particular paddy rice production, has had significant expansion and intensification. Consequently, the catchment has experienced intensive LULC changes, particularly in the last 20 years, especially the transformation of forest land to agricultural land. Additionally, the focus has been paid to drought and flooding as well as soil erosion happening severely more in the catchment.

Accordingly, for solving facing problems in the catchment, a study on the impacts of LULC changes on hydrological characteristics and soil erosion was conducted, as the impacts threaten sustainable development in agriculture and local livelihoods if the targeted catchment is not properly restored. The impacts of LULC changes from 2002 to 2015 on the changes of hydrological characteristics, especially stream flow and soil erosion in the Stung Sangkae Catchment was analyzed, while three scenarios of reforestation or agroforestry to mitigate the excess fluctuation of stream flow and soil erosion loss in the catchment were implemented. The land use developed by the Japan International Cooperation Agency (JICA) in 2002 and land cover (Land Cover Maps of LMB) developed by Mekong River Commission (MRC) in 2015 were used in the study integrating with SWAT model and RUSLE model.

Chapter 3 Impacts of Land Use and Land Cover Changes on Hydrological Responses and Soil Erosion in Stung Sangkae Catchment in 2002-2015 by SWAT model

Based on LULC dynamics for the study periods from 2002-2015 in Stung Sangkae Catchment, the results showed that the catchment experienced a rapid conversion of forests to agricultural upland, paddy rice fields, and others. The cultivated lands (upland fields and paddy rice fields) occupied almost 50% of the total land area in the catchment in 2015, which increased from 20% in 2002, while forest cover (evergreen, deciduous, and mixed forest) occupied 43% in 2002 and declined to 30% in 2015. Among the LULCs, the areas under upland fields increased from 4.2% to 25.2%, which is the highest compared to other land use, followed by paddy rice fields that increased from 15.3% to 23.9% between the years 2002 and 2015.

The SWAT results showed that in the Stung Sangkae Catchment, the LULC changes have slightly impacted on hydrological characteristics, particularly streamflow due to the conversion from the forest area, shrubland, and grassland to agricultural upland, paddy rice, and urban area. Moreover, it was indicated that the increase of bare land and upland fields resulted in a slight increase in annual and seasonal stream flow remarkably in the catchment.

The mean annual stream flow increased in the range of approximately 0.1 m^3/s to 104 m^3/s and the highest mean annual flow changes increased by approximately 0.8 m^3/s along the mainstream of Stung Sangkae River, especially at the downstream catchment, while the soil loss was increased from 13.4 t/ha/y to 22.1 t/ha/y. The soil erosion maps also showed that 74.5 % of the surface area of the Stung Sangkae Catchment is exposed to a low to moderate risk of erosion (<10 t/ha/y) and 17.4% basin is at severe risk. The most affected areas are in the west of the catchment where the upland fields were expanded.

The simulation performances for the monthly flow were reasonably good (R^2 = 0.58, NSE = 0.55 and PBIAS = 5 including dam construction) and (R^2 = 0.64, NSE = 0.62 and PBIAS = 15 excluding dam construction). Therefore, these calibrated parameters can be used for further future hydrological and environmental studies in the Stung Sangkae Catchment without the need to perform a sensitivity analysis. Moreover, the applicability of the SWAT model in simulating the stream flow and sediment dynamics of the Stung Sangkae Catchment has been validated based on the satisfactory values of the statistical measures of the model efficiency.

Hence, the results of the model simulation provide confidence for the further application of the model to assess the hydrological response analysis due to spatial and temporal variability of the catchment characteristics having minimal bias within the Stung Sangkae Catchment. Moreover, the approach used in this research simply evaluates the contributions of individual LULC classes to the total hydrological responses, providing quantitative information for decision-makers to make better options for land and water resource planning and management.

Chapter 4 Impact of Land Use and Land Cover Changes on Soil Erosion in Stung Sangkae Catchment in 2002-2015 by RUSLE Model

The Revised Universal Soil Loss Equation (RUSLE) model integrated within a Geographic Information System (GIS) was further used to verify the result of soil loss in the catchment from the SWAT model in chapter 3. This research aimed to estimate the total amounts of soil loss in Stung Sangkae Catchment using the RUSLE model based on national LULC maps of JICA 2002 and MRC 2015.

Based on the assessment of LULC dynamics, the forest lands decreased significantly during the investigated period, notably a massive shift in deciduous and mixed forest converted to upland fields, paddy rice fields, and other types of land use. In terms of the soil loss in the catchment, the results indicated that the average soil loss was 4.6 t/ha/y and 14.4 t/ha/y for 2002 and 2015, respectively. The calculated total soil loss in the 2002 and 2015 periods was 2.8 million t/y and 8.7 million t/y, respectively. The spatial distribution of soil loss by land use types showed that the highest erosion happened to agricultural land (36.2 t/ha/y in 2002 and 48.5 t/ha/y in 2015) was recorded in upper parts of the catchment, particularly sub-catchments 11, 12, 14, 16, 18 and 19 which was agreed with the corn experimental field.

It is recommended that priority should be given to erosion hot spot areas, and appropriate soil and water conservation practices should be adopted to restore degraded lands. Therefore, it is necessary to integrate protection measures at the farm level and targeted areas of high risk of erosion, mainly the degraded lands along steep slopes, to limit the conversion of forest areas for agriculture and minimize the rate of erosion where the land is bare or with low vegetation cover.

Chapter 5 Effects of Reforestation or Agroforestry on Hydrological Responses in Stung Sangkae Catchment

From the results of Chapters 3 and 4, LULC changes slightly impacted stream flow and significantly affected soil erosion in the catchment. Hence, some scenarios of reforestation or agroforestry practices were applied to investigate its effects on streamflow and soil erosion, such as scenario 1) all areas of forest land (mixed and deciduous forest) are revived, while the other types of land use remain the same (15% in the area applied reforestation or agroforestry for achieving 30% in forest area), scenario 2) the area of agricultural upland was reforested for converting to agroforestry, while the other types of land use are the same (25% in the area applied reforestation or agroforestry for achieving 40% in forest area), and scenario 3) all the mixed forest, deciduous forest, and agricultural upland were revived (40% in the area applied reforestation or agroforestry for achieving 55% in forest area), while the other types of land use remain the same. The scenarios were based on the Royal Government of Cambodia (RGC) to maintain at least 50% of its land under forest cover to contribute to the country's Sustainable Development Goals by 2030.

The results of simulated stream flow by the SWAT model for the whole catchment of baseline land use in 2015 and three proposed scenarios showed the slight effects of reforestation or agroforestry on stream flow, especially seasonal stream flow. The results indicated that the discharge of seasonal stream flow of three scenarios decreased in the wet season (May-Oct.) and increased in the dry season (Nov.-April) compared with the baseline land uses. For the percentage of seasonal stream flow changes in scenarios 1, 2 and 3, they decreased in the wet season at about 1.4%, 3.4%, and 3.3%, and increased in the dry season at about 2.9%, 0.8%, and 0.4%, respectively. The increased stream flows are remarkably important for water resource management in the dry season and for flood reduction and soil conservation in the wet season.

However, the results of the reforestation scenarios significantly showed that 25% of reforestation in the catchment can prevent soil erosion. Reforestation beyond 25% in the catchment is not recommended from a view of soil erosion prevention, as there was no remarkable difference in preventing soil erosion under 25% reforested and under 40%.

Chapter 6 Deeping Public Perception on the Importance of Conservation Strategies against Flood/Drought and Soil Loss

Additional assessment of soil fertility changes and flood/drought was assessed through farmers' perceptions through household survey (HS) of 200 respondents (100 HS at the upstream and 100 HS at the downstream of Stung Sangkae catchment) in 2021. To overcome the problem of data scarcity and evaluate soil erosion in a relatively short period, a unique approach for assessing land degradation from the standpoint of farmers was used. It was based on farmer assessments and observations of changes in their fields. These changes were expressed as soil and productivity loss through visible and comprehensible indicators by the farmers. For the field survey, four districts were selected from each ecological zone (2 districts at the upstream and 2 districts at the downstream catchment). The villages were selected based on their agricultural practices and accessibility. Of the total participants in focus group discussion (FGDs), 35% of respondents were female. The FGDs consisted of a mixture of closed- and open-ended questions.

The results of the HS showed that during the last 18 years from 2002 to 2020, soil fertility declined significantly. In general, the soil fertility in the catchment declined from a low decline to a very strong decline at the upstream and the downstream of the catchment, **respectively**. In the catchment, mostly the soil fertility occurred from a fair decline to a strong decline, while the rate of soil fertility tended to slightly increase from a fair decline to a strong decline of 33% to 36% and 40% to 43 % at the upstream and downstream catchment, respectively. In contrast, the rate of a very strong decline in soil fertility mainly happened at the upstream catchment rather than at the downstream catchment, which was 18% and 11%, respectively. However, based on the FGD, the farmers responded that their agricultural yield only slightly declined during the study period. This was because the amounts of chemical fertilizer consumption were used more than before to sustain the yield of their products.

The catchment mostly experienced low drought at the upstream and downstream catchment in 2002 and 2015; however, in 2020 the catchment experienced extreme drought rather than low drought in the catchment, particularly in the lowland catchment. At the upstream and downstream catchment, the flooding occurred at a moderate level. In 2002, the flooding occurrence at the upstream catchment (42%) was higher than at the downstream catchment (33%); however, in 2015-2020 the flooding experienced at the downstream catchment, while the rate of flooding also increased from moderate to the extreme level, particularly in 2020. Farmers confirmed that they experienced not only drought but also flooding while there was water released from the Sek Sok multi-purpose dam at the upstream catchment.

Chapter 7 Conclusions and Recommendations

In this research, the national LULC maps of JICA 2022 and MRC 2015 were used to evaluate their impacts on the hydrological characteristics and soil erosion in Stung Sangkae Catchment. It was shown that the forest lands decreased significantly during the investigated period, especially a massive shift in deciduous and mixed forest converted to upland fields, paddy rice fields, and other types of land use. The upland fields increased 21% from 4.4% in 2002 to 25.2% in 2015, while the forest land occupied 43% in 2002 and declined to 30% in 2015 for a whole catchment area (605,170 ha). The statistical agreement of R2=0.64, NSE=0.62, and PBIAS=15 (without dam construction period) and R2=0.58, NSE=0.55, and PBIAS=5 (with dam construction period) for the SWAT model is found to be satisfactory for the Stung Sangkae Catchment. As of the 2002-2015 period, even though the LULC was significantly changed, the streamflow was slightly increased; however, soil erosion significantly impacted which was 13.4 t/ha/y in 2002 and 22.1 t/ha/y in 2015. The highest mean annual flow changes increased by approximately 0.8 m3/s along the mainstream of Stung Sangkae River, especially downstream, while medium mean annual flow increased by 0.3 m3/s across a whole catchment.

For the soil erosion analysis with the RUSLE model, the average soil loss from the catchment was 4.6 t/ha/y in 2002 and 14.4 t/ha/y in 2015, while the highest erosion area was found in parts of the upland of the Stung Sangkae Catchment, mainly due to agricultural land expansion, steep slopes, and degradation of the vegetation. Both models could capture reasonable soil loss agreement compared with the experimental corn field, while countermeasures of reforestation or agroforestry of 25% can slightly reduce streamflow, but significantly prevent erosion in the catchment.

It could be concluded that the approach used in this research simply evaluates the contributions of individual LULC classes to the hydrological characteristic, providing quantitative information for decision-makers to make better options for land and water resource planning and management. It can be widely applied to a variety of catchments, where time-sequenced digital land cover data are available, and to predict hydrological consequences of LULC changes. 25% of reforestation or agroforestry can decrease the stream flows in the wet season and increase them in the dry season which is more important for water resource management in the dry season and for flood reduction in the wet season and could significantly prevent soil erosion, while the reforestation more than 25% is not recommended in the catchment.

The outcomes of farmers' perceptions on soil fertility changes and flood/drought indicated that the rate of a very strong decline in soil fertility observed in the upstream catchment at 18% and in the downstream catchment at 11%.

As mentioned above, this study has been conducted to evaluate the impacts of land use and land cover changes on hydrological characteristics and soil erosion in Stung Sangkae catchment, Cambodia. Although the Royal Government of Cambodia (RGC) has a direction to maintain at least

50% of its land under forest cover to contribute to the country’s Sustainable Development Goals by 2030, the outcomes of this study indicated the area of agricultural upland is reforested for converting agroforestry (25% in area applied reforestation or agroforestry for achieving 40% in forest area) was very meaningful to decrease the stream flows in the wet season and increase them in the dry season, as well as to eliminate soil erosion remarkably.

和文要旨

1 章　研究の背景と目的

地球上の多くの地域で生じている土地利用と被覆の変化は、森林伐採とともに農地化や都市化の影響を受けて進んでいる。これら人為的にもたらされた土地利用と被覆の変化は、地域における水文特性に深刻な影響を及ぼしている。加えて、この人為的な土地利用と被覆の変化は、加速的に土壌侵食を引き起こしていることが認識されている。カンボジアでは最近の 20 年間に人口の増加、農業の発展、経済的および都市化の拡大によって、顕著に土地利用と被覆の変化が進行している。

カンボジア国スツゥン サンカェ流域においても、流域における土地利用と被覆の変化が水文特性および土壌侵食に与える影響について関心が注がれてきた。これは、対象の流域における土地利用と被覆の変化とその影響について調査が進められ、その結果に基づいて適切に保全対策が実施されなければ、持続可能な農業生産と生存環境に深刻な脅威になることが懸念されるためである。

従って、次の項目について研究が取り組まれた。1）どのようにカンボジア国スツゥン サンカェ流域が 2002 年から 2015 年の間に土地利用と被覆が変化し、水文学的反応に影響したのかを SWAT モデルを適用して評価する、2）RUSLE モデルに基づき 2002 年から 2015 年における土壌侵食の程度について評価する、3）この土地利用と被覆の変化による河川流量と土壌侵食への影響に基づき、流域で実施される植林やアグロフォレストリーによって、どのように河川流量の季節変動や土壌侵食を抑えられるのかについて評価する、そして 4）流域において保全対策を進めるために、侵食に伴う土壌肥沃度の低下や洪水・干ばつに対する認識度について議論を進めることである。

2 章　研究対象地域

研究対象地域は、カンボジア国北西の北緯 12◦130-13◦240 で西経 102°350-103°420 に位置するトンレサップ流域の 3 番目に大きな支流であるスツゥン サンカェ流域（流域面積 605,170 ha）である。この地域は標高 4 m から 1,413 m 範囲に広がっており、低平地から傾斜の厳しい険しい高地を擁する特徴的な地形条件を呈している。流域を流れる主河川はサンカェ川（流路延長 250 km）で、トンレサップ流域の支流間を流れている。流域内の 6 か所の観測所で 2007 年から 2018 年に記録された気象データに基づくと、Moung Ruessei 観測所では 1,308 mm で Samlout 観測所では 1,577 mm を記録するなど地域差はあるものの、平均年間降水量は 1,388 mm であった。また流域は Luvisols（34.0%）、Nitisols（27.4%）、Gleysols（27.3%）、Acrisols（11.3%）等の土壌で覆われている。この Luvisols、Nitisols、Gleysols で覆われている地域は、深刻な洪水や旱魃、土壌侵食が発生しており、関心が注がれている。

研究対象のスツゥン サンカェ流域はバッタンバン州に位置しており、カンボジア政府から農業投資と発展が期待されている地域である。農業は地域住民にとって最も重要な経済活動であり、主な収入源となっている。また、農業の中でも稲作が注目されており、拡大と強化されている。これらの農業的発展を背景に森

林域の開発が進み、結果として過去 20 年間に顕著な土地利用と被覆の変化が生じた。加えて流域で年々厳しさを増す洪水や旱魃や土壌侵食に、関心が集まっている。

そこで対象の流域で生じているこれらの問題に対処するために、カンボジア国スツゥン サンカェ流域における土地利用と被覆の変化が、流域における水文特性および土壌侵食に与える影響について研究を実施した。対象の流域において適切に保全対策が実施されなければ、この土地利用と被覆の変化が持続可能な農業生産と生存環境に深刻な脅威になるためである。具体的には 2002 年から 2015 年までの土地利用と被覆の変化が、どのように水文特性に影響したのかを SWAT モデルを適用して評価するとともに、流域で対策として実施される植林やアグロフォレストリーにあたっての 3 つのシナリオが河川流量の変動や土壌侵食を抑えられるのかについて評価に取り組んだ。2002 年の土地利用と被覆の解析にあたっては JICA から、2015 年についてはメコン委員会から発行された高解像度の土地利用・被覆図に基づき、SWAT と RUSLE のモデルを適用して研究を進めた。

3 章　SWAT モデルに基づいたスツゥン サンカェ流域における 2002 年から 2015 年の土地利用と被覆の変化が水文学的反応と土壌侵食に与える影響について

カンボジア国スツゥン サンカェ流域における 2002 年から 2015 年の土地利用と被覆の変化を解析した結果、急速に森林域が畑地、水田、その他に転用されていることが明らかとなった。2002 年に 20％であった耕作地（畑地や水田）の占める百分率は、2015 年には約 50％に達していた。一方、常緑林、落葉林、混合林等の森林域については、2002 年には 43％を占めていたが 2015 年には 30％までに低下していた。2002 年から 2015 年の土地利用と被覆の変化を詳細に見ると、畑地の占める百分率は 4.2%から 25.2%と最も拡大しており、次いで 15.3%から 23.9%に拡大した水田であった。

スツゥン サンカェ流域における SWAT モデルを適用した解析結果から、流域における土地利用と被覆の変化は、僅かではあるが明らかに水文特性に影響を及ぼしていた。特に河川流量に与える森林域、低木域や草地から畑地、水田や都市的利用への転用の影響が顕著であった。さらに、裸地や畑地の増加が河川流量の年変動と季節変動に明らかに影響していることが明らかとなった。対象の流域における 2002 年から 2015 年の土地利用と被覆の変化にともなって、平均年間河川流量の変動幅は 0.1 m^3/s から 104 m^3/s と拡大しており、さらに 2015 年の平均最大流量は 2002 年と比べて 0.8 m^3/s 増大していた。この平均最大流量の増加傾向は下流域で顕著であった。

一方、土壌侵食量も 2002 年の 13.4 t/ha/y から 2015 年には 22.1 t/ha/y に増大していた。作成した土壌侵食の危険度分類図からは、スツゥン サンカェ流域の 74.5％は低・中程度（<10 t/ha/y）に分類されたが、17.4％の地域では厳しい土壌侵食が生じる高程度に分類された。これら高程度の土壌侵食に分類された 17.4％は、主に畑地利用されていた。

2002 年と 2015 年における土地利用と被覆から、月間流量に基づいて不確実性解析および較正や検証を行った。2016 年に建設されたダムの影響下での解析結果における決定係数（R^2）は 0.58、Nash-Sutcliffe モデル効率係数（NSE）は 0.55、バイアス率（PBIAS）は 5 で、ダムの影響を除いた解析結果では、決定係数（R^2）は 0.64、Nash-Sutcliffe モデル効率係数（NSE）は 0.62、バイアス率（PBIAS）は 15 であった。この結

果から決定係数（R^2）、Nash-Sutcliffe モデル効率係数（NSE）、バイアス率（PBIAS）ともに基準値を超えており、一定の評価を与えられる結果となった。併せて、河川流量と土砂輸送の予測における SWAT モデルのモデル効率性について統計的解析が行われた結果、十分に基準値を超えて納得できる結果であることを明らかとなった。

以上の結果より、この研究で示した較正値を適用することによって、感度評価を実施しなくても今後の流出解析や環境評価に適用できることを示すことができた。よってここでのモデルシミュレーションは今後の空間的および時間的変動を見る流出解析の適用においても十分な信頼性を与えつつ実施できることを示し、流域管理に必要な事項の基礎情報を与えるものと評価できた。

4 章 RUSLE モデルに基づいたスツゥン サンカェ流域における 2002 年から 2015 年の土地利用と被覆の変化が土壌侵食に与える影響について

スツゥン サンカェ流域における GIS 解析結果に RUSLE モデルを適用して流亡土量を求め、3 章で述べた SWAT モデルによる流亡土量と比較して検証を進めた。具体的には、2002 年に JICA から、2015 年にメコン委員会から発行された各々の高解像度の土地利用・被覆図に基づいて、その間における土地利用と被覆の変化が土壌侵食による流亡土量に与える影響について評価を試みた。

土地利用と被覆の変化については、前述の通り 2002 年から 2015 年の間に森林面積は顕著に低減した。注目するべきは落葉林および混合林が畑地や水田、その他の土地利用に転用されていた点である。RUSLE モデルで算出された 2015 年の年流亡土量は 14.4 t/ha/y で 2002 年の 4.6 t/ha/y を大きく上回る結果となった。特に高い土壌侵食（36.2 t/ha/y (2002), 48.5 t/ha/y (2015)）が発生していたのが、中央部と南西部の高原地帯と畑地帯（特に、小流域 11, 12, 14, 16, 18, 19）であることが明らかとなった。併せて、これらの計算結果は、2019 年に公表された現地での実験結果とほぼ一致していた。

これらの土壌侵食におけるホットスポットでは優先的に適切な土壌および水保全対策が実施されることが望まれる。土壌侵食のリスクの高い農地では適切な土壌保全対策が実施されるとともに、急傾斜地の荒廃地では森林域からの農地転用を抑えることが重要である。

5 章 スツゥン サンカェ流域における植林やアグロフォレストリーの適用が水文学的反応に与える影響について

前述の 3 章と 4 章の結果から、土地利用と被覆の変化は僅かに河川流量に影響しているとともに、土壌侵食には顕著な影響を与えていることが明らかとなった。そこで以下のシナリオによる植林やアグロフォレストリーの適用が河川流量や土壌侵食に与える影響について評価を試みた。シナリオ 1）2002 年度に戻すように全ての混合林および落葉林が再生されるが他の土地利用は 2015 年度の状態を維持（植林面積率 15%、現有森林面積と合わせて森林率 30％）、シナリオ 2）畑地はアグロフォレスト化されるが他の土地利用は 2015 年の状態を維持（植林面積率 25%、現有森林面積と合わせて森林率 40％）、シナリオ 3）全ての混合林、落葉林、畑地は 2002 年の状態に再生するが他の土地利用は 2015 年の状態を維持（植林面積率

40%、現有森林面積と合わせて森林率 55%）、の 3 つのシナリオである。これらのシナリオは、カンボジア政府が 2030 年までの SDGs を達成するために、50%の森林率を回復する旨の方針に基づいている。

2015 年の状況下と植林やアグロフォレストリーが適用された 3 つのシナリオ下で、スツゥン サンカェ川における河川流量を比較した結果、僅かに季節流量に差異が生じることが明らかになった。つまり、3 つのシナリオ下でのスツゥン サンカェ川における河川流量は、雨期（5 月から 10 月）に減少して、乾期（11 月から 4 月）に増大する傾向が見られた。具体的には、1）から 3）のそれぞれのシナリオで、雨期における河川流量は 2015 年を基準に 1.4%、3.4% 、3.3%減少し、乾期には 2.9%、0.8%、0.4%増大する結果となった。これらの植林やアグロフォレストリーが適用された 3 つのシナリオ下で得られた河川流量の変化は僅かではあるものの、乾期には水資源の確保に繋がり、雨期には洪水や土壌保全に寄与することを意味している。

一方、これらの植林やアグロフォレストリーが適用された 3 つのシナリオ下における土壌侵食量の変化を調べた結果、植林面積率を 25%まで進めることで、顕著に土壌侵食の抑制効果が発現することが明らかとなった。しかし 25%を超えての植林は抑制効果の向上が見込まれないため、推奨できないことが分かった。

6 章 スツゥン サンカェ流域における洪水・干ばつや土壌侵食に対する保全対策に関する社会的認識の深化について

スツゥン サンカェ流域における 200 戸（上流域 100 戸、下流域 100 戸）の現地農家を対象として、洪水・干ばつや土壌肥沃度低下に対する認識調査を 2021 年に実施した。具体的な調査内容は現地農家自身が所有する農地を対象として、土壌の状態や生産量の変化等、現地農家が理解できる内容で評価した。生態学的な区分に従って上流域で 2 地区、下流域から 2 地区が選ばれ、対象の農村は農業体系に基づいて選定された。対象農家を代表して出てきた回答者の内、女性は 35%であった。また質問は選択回答形式と自由回答形式の両方で構成することとした。

先ず 2002 年から 2020 年に至る 18 年間における土壌肥沃度の変化について質問した結果、全体的には僅かにまたは著しく土壌肥沃度が低下していると回答する農家が、上流域、下流域に関わらず目立った。土壌肥沃度が僅かに改善していると農家の割合は、僅かにまたは著しく土壌肥沃度が低下していると回答した農家に対して、上流域では 33%と 36%で、下流域では 40%と 43 %に過ぎなかった。更に著しく土壌肥沃度が低下していると回答した農家率については、上流域では 18%であり下流域では 11%であった。しかし生産量については僅かに低下しているのみであり、これは投入する化学肥料によって生産量が維持されたためと考察された。

干ばつに関しては 2002 年から 2015 年にかけては僅かに影響を受けたと回答する農家が多かったが、2020 年については著しい干ばつの被害が認識されている。また、洪水に関しては 2002 年には上流域で 42%認識されており下流域の 33%を上回る結果となったが、2015 年から 2020 年に至る間は主に下流域で認識されていた。

7 章　まとめと提言

本研究では、カンボジア国スツゥン サンカェ流域を研究対象として、2002 年に JICA で、2015 年にメコン委員会で作成された高解像度の土地利用・被覆図に基づいて、2002 年から 2015 年における土地利用と被覆の変化が水文特性と土壌侵食に与える影響について、SWAT モデルと RUSLE モデルを適用して評価を試みた。その結果、2002 年に 4％の面積を占めていた畑地は 2015 年には 25％に増大し、2002 年の森林面積は 43％から 2015 年には 30％に低下していた。

SWAT モデルの適用に当たり、2002 年と 2015 年における土地利用と被覆から月間流量に基づいて不確実性解析および較正や検証を行った結果、ダムの影響を除いた解析結果では決定係数（R^2）は 0.64、Nash-Sutcliffe モデル効率係数（NSE）は 0.62、バイアス率（PBIAS）は 15 で、ダムの影響下での解析結果における決定係数（R^2）は 0.58、Nash-Sutcliffe モデル効率係数（NSE）は 0.55、バイアス率（PBIAS）は 5 であり、これらの結果から決定係数（R^2）、Nash-Sutcliffe モデル効率係数（NSE）、バイアス率（PBIAS）ともに基準値を超えており、一定の評価を与えられる結果となった。2002 年から 2015 年における土地利用と被覆は有意に変化しており、本川における 2015 年の平均最大流量は 2002 年と比べて 0.8 m^3/s の僅かな増大が見られた。

また、SWAT モデルに基づいた 2015 年の土壌侵食量は 22.1 t/ha/y で、2002 年の 13.4 t/ha/y を有意に上回っていた。同様に、RUSLE モデルで算出された 2015 年の年流亡土量は 14.4 t/ha/y で 2002 年の 4.6 t/ha/y を大きく上回る結果となった。2 つのモデルに基づいた対象の小流域における計算結果は、2019 年に公表された現地での実験結果とほぼ一致することを確認できた。

2015 年の状況下で植林やアグロフォレストリーが適用された 3 つのシナリオ下で比較した結果、雨期における河川流量は 2015 年を基準に 1.4%、3.4% 、3.3%減少し、乾期には 2.9%、0.8%、0.4%増大する結果となり、僅かではあるものの乾期には水資源の確保に繋がり、雨期には洪水や土壌保全に寄与していた。一方、土壌侵食については植林面積率を 25％まで進めることで、顕著に土壌侵食の抑制効果が発現することが明らかとなるものの、25％を超えての植林は抑制効果の向上が見込まれないため、推奨できないことが分かった。

更に、スツゥン サンカェ流域における 200 戸の現地農家を対象として、土壌肥沃度の変化や洪水・干ばつに対する認識調査を 2021 年に実施した結果、全体的には僅かにまたは著しく土壌肥沃度が低下したと回答した農家が、上流域、下流域に関わらず目立ち、著しく土壌肥沃度が低下していると回答した上流域の農家率は 18％で、下流域では 11％に昇った。

上記のようにこの研究は、カンボジア国スツゥン サンカェ流域における土地利用と被覆の変化が水文特性および土壌侵食に与える影響について扱ったものであるが、研究成果より面積率 25%を対象に植林やアグロフォレストリー化（主に畑地のアグロフォレストリー化）を進め、現有森林面積と合わせて森林率 40％を達成することにより、雨期における河川流量は 2015 年を基準に 3.4%減少し、乾期には 0.8%増大する結果となり、僅かではあるものの乾期には水資源の確保に繋がり、雨期には洪水や土壌保全に寄与することを示した。特に、土壌侵食については植林面積率を 25％まで進めて現有森林面積と合わせて森林率 40％

を達成することで、顕著に土壌侵食の抑制効果が発現することを示した。現在、カンボジア政府は 2030 年までの SDGs を達成するために、50%の森林率を回復する旨の方針を出しているものの、本研究の成果からは 50%に到達出来なくても、植林やアグロフォレストリー化で森林率 40%に至ることで十分に効果を発現できる可能性を示すことができた。

Acknowledgement

In the beginning, I would like to acknowledge my supervisor, Prof. Dr. Machito MIHARA, for guiding me throughout this research work. His immense knowledge, patience, and continuous support have motivated me to excel in this whole process.

Apart from my supervisor, I would like to express gratitude to my advisors, Professor Dr. Fumio WATANABE, Prof. Dr. Takahiko NAKAMURA, Associate Prof. Dr. Toru NAKAJIMA, and Associate Prof. Dr. Narong TOUCH, for giving me the encouragement and sharing insightful suggestions.

This research is made possible by the generous support of the American People provided to the Center of Excellence on Sustainable Agricultural Intensification and Nutrition (CE SAIN) of the Royal University of Agriculture through the Feed the Future Innovation Lab for Collaborative Research on Sustainable Intensification at Kansas State University funded by the United States Agency for International Development (USAID) under Cooperative Agreement No. AID-OAA-L-14-00006. The contents are the sole responsibility of the authors and do not necessarily reflect the views of USAID or the United States Government. I am grateful to Tokyo University of Agriculture, and this work would not have been possible without the financial support of ERECON Scholarship.

I am grateful to my parents, siblings, and my whole family. They have always provided me with endless support, encouragement, and motivation to accomplish my personal goals.

I also would like to thank to Prof. Dr. Bunthan NGO, Rector of Royal University of Agriculture, Cambodia, and Mr. Lytour LOR, Dean of Faculty of Agricultural Engineering, RUA for the encouragement and support my study in RUA, TUA and all my faculty members and students, especially Mr. Sakdanuphol CHAN who supported data analyses for my PhD Dissertation as well as ERECON staffs in Japan and Thailand, especially staffs in Cambodia Branch for the support. Also, I would like to thank Mr. Taingaun SOURN for his support and encouragement.

Last but not least, I would like to thank very much for my beloved family, my wife (Mrs. Montha LY) and daughters (Nareth Pichsoma BENG and Nareth Kossamak BENG) for supporting me so much in various ways during my academic years. I dedicate this result to all the people who have supported me and worked with me in the last three years. I do hope my dissertation can be useful to people who are engaged and make efforts for sustainable development in all areas.

TABLE OF CONTENTS

TABLE OF CONTENTS ---------- xv

LIST OF TABLES ---------- xix

LIST OF FIGURES ---------- xxi

LIST OF ABBREVIATION ---------- xxiii

CHAPTER 1 ---------- 1

Background and Objectives ---------- 1

1.1. Background ---------- 1

1.2. Land Use Change and Forest Degradation in Cambodia ---------- 3

1.3. Factors of Land Use Change in Cambodia ---------- 7

1.4. Impacts of LULC Change on Water Resources and Hydrology ---------- 10

1.4.1. LULC change impacts on water resources ---------- 10

1.4.2. LULC changes impact on streamflow ---------- 12

1.4.3. Contribution of LULC change to precipitation ---------- 13

1.4.4. Contribution of LULC change to groundwater ---------- 14

1.5. Research Conceptual Framework ---------- 15

1.6. Research Benefits ---------- 16

1.7. Scope and Limitations of the Research ---------- 17

1.8. Research objectives ---------- 18

Reference of this chapter ---------- 19

CHAPTER 2 ---------- 34

Research Site Description ---------- 34

2.1. Stung Sangkae River Catment in Battambang Province ---------- 34

2.2. Resource stresses exacerbated by climate change ---------- 37

2.3. Resource stresses and trends ---------- 39

2.4. Natural disasters ---------- 40

2.4.1. Flooding impacts ---------- 41

2.4.2. Drought impacts ---------- 41

Reference of this chapter ---------- 43

CHAPTER 3 ---------- 45

Impacts of Land Use and Land Cover Changes on Hydrological Responses in Stung Sangkae River Catchment from 2002 to 2015 ---------- 45

3.1. Introduction ---------- 45

3.2. Methodologies ---------- 46

3.2.1. Description of Study Area ---------- 46

3.2.2. Description of SWAT Model ---------- 47

3.2.2.1. Hydrological Component and Water Balance of SWAT ---------- 48

3.2.2.2. Surface Runoff Equation of SWAT ---------- 50

3.2.2.3. Flow Rate Equation of SWAT ---------- 52

3.2.2.4. Soil Loss Equation of SWAT ---------- 53

3.2.2.5. Meteorological and Hydrological Data ---------- 53

3.2.2.6. Geographical or Spatial Datasets ---------- 54

3.2.2.7. Slope Classes in Subwatershed ---------- 55

3.2.3. SWAT Model Simulation, Sensitivity Analysis, Calibration and Validation 56

3.2.3.1. Model Parameterization and Sensitivity Analysis ---------- 56

3.2.3.2. Model Performance Evaluation, Calibration and Validation ---------- 57

3.3. Results and Discussion ---------- 58

3.3.1. Analysis of Land Use and Land Cover Changes ---------- 58

3.3.2. Sensitivity Analysis, Calibration and Validation under Land Use Change Dynamics ---------- 63

3.3.2.1. Stream Flow Sensitivity Analysis ---------- 63

3.3.2.2. Stream Flow Calibration and Validation ---------- 64

3.3.3. Impact of LULC Changes on Stream Flow ---------- 71

3.3.4. Contribution of Individual LULC Changes to Catchment Water Yield ---------- 73

3.3.5. Impacts of LULC Changes on Hydrology at the Basin Scale ---------- 77

3.3.6. Impacts of LULC Changes on Hydrology at the Subbasin Scale ---------- 80

3.3.7. Impacts of LULC Changes on Soil Erosion in the Catchment ---------- 81

3.4. Conclusions of This Chapter ---------- 83

Reference of this chapter ---------- 85

CHAPTER 4 ---------- 88
Impact of Land Use and Land Cover Changes on Soil Erosion in Stung Sangkae Catchment using RUSLE Model ---------- 88
4.1. Introduction ---------- 88
4.2. Materials and Method ---------- 91
4.2.1. Description of Study Area ---------- 91
4.2.2. Description of RUSLE Model ---------- 95
4.2.2.1. Rainfall Erosivity Factor (R) ---------- 96
4.2.2.2. Soil Erodibility Factor (K) ---------- 100
4.2.2.3. Slope Length (L) and Steepness (S) Factor ---------- 103
4.2.2.4. Cover and Management Factor (C) ---------- 106
4.2.2.5. Support Practice Factor (P) ---------- 110
4.2.2.6. Limitations of (R) USLE ---------- 111
4.2.2.7. Consistency in Units ---------- 115
4.2.3. Determination of RUSLE Factor Values ---------- 115
4.2.3.1. Rainfall Erosivity (R) Factor ---------- 118
4.2.3.2. Soil Erodibility (K) Factor ---------- 119
4.2.3.3. Topographic (LS) Factor ---------- 120
4.2.3.4. Crop Management (C) Factor and Conservation Practice (P) Factor ---------- 121
4.3. Results and Discussion ---------- 122
4.3.1. RUSLE Factors ---------- 122
4.3.2. Impact of LULC Changes on Soil Erosion ---------- 125
4.3.3. Effect of Elevation and Slope on Soil Erosion ---------- 129
4.3.4. Contribution of Land Use and Land Cover Changes to Soil Erosion and Its Conversions ---------- 130
4.4. Discussions ---------- 134
4.5. Conclusions of This Chapter ---------- 137
Reference of this chapter ---------- 139

CHAPTER 5 -- 149

Effects of Reforestation or Agroforestry on Hydrological Responses in Stung Sangkae River Catchment -- 149

5.1. Introduction-- 149

5.2. Materials and Methodology -- 151

5.2.1. Reforestation scenarios --- 152

5.3. Results and Discussion -- 155

5.3.1. Stream flow response to reforestation -- 155

5.3.2. Soil loss response to reforestation--- 158

5.4. Conclusion of This Chapter -- 161

Reference of this chapter--- 162

CHAPTER 6 -- 166

Deeping Public Perception on Importance of Conservation Strategies against Flood/Drought and Soil Loss --- 166

6.1. Introduction-- 166

6.2. Research Methodology -- 167

6.3. Results and Discussion -- 169

6.3.1. Assessment of Farmers' Perceptions of Soil Erosion ------------------------ 169

6.3.2. Assessment of Farmers' Perceptions of Dought and Flooding ------------- 171

6.4. Discussion --- 172

Reference of this chapter -- 174

CHAPTER 7 -- 178

Conclusion and Recommendations-- 178

7.1. General Conclusion -- 178

7.2. Recommendations -- 180

APPEXDIX I-- 182

APPEXDIX II--- 184

APPEXDIX III-- 184

LIST OF TABLES

N⁰ NUMBER ORDER TITLE PAGE

Table 2.1. Protected areas in Battambang 38

Table 2.2. Land classification by each district, 2009 39

Table 2.3. Flood record of Stung Sangkae River 39

Table 2.4. Summary of major drought events and their impacts on agriculture in Cambodia 42

Table 3.1. Runoff curve numbers for cultivated agricultural lands........ 52

Table 3.2. Model performance evaluation classification. 58

Table 3.3. Summary analysis of land use and land cover of the Stung Sangkae catchment in 2002 and 2015. 59

Table 3.4. Transition of LULC by ignoring the area less than 500 ha 61

Table 3.5. Matrix of land use and land cover (LULC) change contribution to net change experienced by LULC types in hectare (ha) and percentage (%) for 2002–2015. 62

Table 3.6. Flow parameter sensitivity analysis result in Stung Sangkae catchment. 63

Table 3.7. Calibration performance for monthly flow at Stung Sangkae catchment 64

Table 3.8. Validation performance for monthly flow at Stung Sangkae catchment 67

Table 3.9. Annual basin values of hydrologic features for the Stung Sangkae River catchment on the different land use from 2000 to 2018 (mm). 78

Table 3.10. LULC changes and average annual hydrologic features from 2000 to 2018. 80

Table 3.11. Mean annual soil loss from 2000-2018 of Stung Sangkae catchment 81

Table 4.1. FAO slope classification in the study catchment and related susceptibility to soil erosion 93

Table 4.2. Land use and land cover of the Stung Sangkae catchment in 2002 and 2015 94

Table 4.3. Summary of some different studies that developed rainfall erosivity equations, original locations, and other studies that used their equations...... 99

Table 4.4. Summary of different studies with soil erodibility equations, original locations, and other studies that used their equations 101

Table 4.5. K-factor values from Dymond (2010) for soil texture in New Zealand....... 102

Table 4.6. K-factor values from David (1998) for soil texture in Philippines. 102

Table 4.7. Summary of methods of calculating LS factor, original locations, and other studies that used these methods........ 105

Table 4.8. C-factor equations that use NDVI 108

Table 4.9. C-factors for general types of land cover compiled from various sources... 108

Table 4.10. C-factors for specific types of land cover compiled from various sources.. 109

Table 4.11. Examples of where C-factor accounts for crop management from Morgan (2005) and David (1988) ... 109
Table 4.12. P-factors for different types of agricultural management practices ... 111
Table 4.13. Data used and data source for soil erosion modelling in the catchment. ... 117
Table 4.14. Adopted values of C and P factor for the catchment land use and land cover (LULC) classes ... 122
Table 4.15. The mean annual precipitation (mm) in the study area and the corresponding R-factor ... 123
Table 4.16. The soil types and the corresponding K-factor in the study catchment ... 124
Table 4.17. Distribution of soil erosion loss under different severity classes in Sangkae catchment from 2002 to 2015 ... 127
Table 4.18. Soil erosion severity classes and gross soil loss in Stung Sangkae catchment from 2002 to 2015 ... 127
Table 4.19. Estimation of soil erosion rates and net changes in different elevation areas ... 129
Table 4.20. Soil erosion in slope zones and net changes between the years 2002 and 2015 based on FAO slope classification ... 130
Table 4.21. Distribution of soil erosion loss under various types of land use and land cover in Stung Sangkae catchment ... 131
Table 4.22. Distribution of soil erosion loss under different LULC conversion categories in the in Stung Sangkae catchment ... 134
Table 5.1. Land use conditions in the three scenarios ... 153
Table 5.2. Annual stream flow (MCM) for baseline and reforest scenarios ... 157
Table 5.3. Annual soil loss based on baseline and 3 reforestation scenarios (ton/ha) ... 159
Table 5.4. Soil loss from subbasin of baseline land use, and with 3 reforestation land use scenarios (ton/ha) ... 160

LIST OF FIGURES

N⁰ NUMBER ORDER TITLE PAGE

Figure 1.1. Rate of forest cover change statistics from 1965-2016 7
Figure 1.2. Map of Economic Land Concession (ELC) in Cambodia 8
Figure 1.3. Flowchart of the applied methodology in the research 16
Figure 2.1. Location of the study area 36
Figure 2.2. Land use of the study area 36
Figure 3.1. Location map of the research catchment and meteorological stations within the research area. 47
Figure 3.2. Hydrological cycle in the conceptual SWAT model 49
Figure 3.3. Relationship of runoff to rainfall in SCS curve number method 51
Figure 3.4. Digital elevation model (a), soil map (b) and historical land use and land cover map of 2002 LULC (c) and 2015 LULC (d) of Stung Sangkae catchment 55
Figure 3.5. Gains and losses between 2002 and 2015 60
Figure 3.6. Net change between 2002 and 2015 60
Figure 3.7. Monthly stream flow calibration based on JICA and MRC LULC data. 65
Figure 3.8. Scatter plot of monthly stream flow calibration based on JICA and MRC LULC data 66
Figure 3.9. Monthly stream flow validation based on JICA and MRC LULC data. 68
Figure 3.10. Scatter plot of monthly stream flow validation based on JICA and MRC LULC data. 69
Figure 3.11. Correlation of observed vs. simulated flow (a) and correlation of different LULC on stream flow (b) 70
Figure 3.12. Spatial distribution of the mean annual stream flow changes in m3/s for Stung Sangkae catchment 73
Figure 3.13. Spatial distribution of the mean annual stream flow change in the percentage for Stung Sangkae catchment 73
Figure 3.14. Percentage of each LULC change and its contribution to the total average annual water yields (WY) for the Stung Sangkae River from 2002 to 2015. 75
Figure 3.15. Spatial distribution of the mean annual water yield change in millimeter for Stung Sangkae catchment 76
Figure 3.16. Spatial distribution of the mean annual water yield change in percentage for Stung Sangkae catchment 76
Figure 3.17. Spatial distribution of the mean annual ET change in millimeter for Stung Sangkae catchment 79

Figure 3.18. Spatial distribution of the mean annual ET change in percentage for Stung Sangkae catchment 79
Figure 3.19. Spatial distribution of estimated soil erosion rates (t/ha/yr) at Stung Sangkae catchment 82
Figure 4.1. Location map of the research catchment and meteorological stations within the research area 92
Figure 4.2. The distribution of annual rainfall recorded by weather stations inside and around the study catchment during 2007–2018 92
Figure 4.3. Land use and land cover (LULC) developed by JICA 2002 and MRC 2015 of the Stung Sangkae catchment 94
Figure 4.4. Flowchart of applied methodology for modelling soil erosion in the catchment. 117
Figure 4.5. Maps of R-factor (a), K-factor (b), slope (c) and LS-factor (d) of the Sangkae catchment 118
Figure 4.6. Spatial distribution of: (a,b) cover management (C-factor) and (c,d) supporting practices (P-factor) 125
Figure 4.7. Spatial distribution of soil loss in the sub-catchment within the study area 128
Figure 4.8. Total soil erosion contributed by various land use and land cover types 132
Figure 4.9. Spatial distribution of the conversions of the land use and cover (LULC) between 2002 and 2015 133
Figure 5.1. Location of the study area 152
Figure 5.2. Land use types in the study area 153
Figure 5.3. Reforestation scenario conditions in the Stung Sangkae River catchment .. 154
Figure 5.4. Annual stream flow (cms) for baseline and reforest scenarios 155
Figure 5.5. Average monthly stream flow for baseline and reforestation scenarios 156
Figure 5.6. Seasonal stream flows for baseline and reforestation scenarios 158
Figure 5.7. Monthly soil loss based on baseline and 3 reforestation scenarios 159
Figure 5.8. Soil loss based on season 160
Figure 6.1. Soil fertility 170
Figure 6.2. Perception of soil fertility decline in the catchment from 2002 to 2015...... 170
Figure 6.3. Perception of drought in the catchment from 2002 to 2020........ 171
Figure 6.4. Perception of flooding in the catchment from 2002 to 2020........ 171

LIST OF ABBREVIATION

ABBREVIATION		EXPLANATION
ADB	:	Asian Development Bank
CARDEC	:	Cambodian Conservation Agriculture Research for Development Center
CNMC	:	Cambodia National Mekong Committee
ELC	:	Economic Land Concession
FAO	:	Food and Agriculture Organization
IPCC	:	Intergovernmental Panel on Climate Change
JICA	:	Japan International Cooperation Agency
LMB	:	Lower Mekong Basin
LULC	:	Land Use and Land Cover
LULCC	:	Land Use and Land Cover Changes
MAFF	:	Ministry of Agriculture, Forestry and Fisheries, Cambodia
MOE	:	Ministry of Environment, Cambodia
MOWRAM	:	Ministry of Water Resources and Meteorology, Cambodia
MRB	:	Mekong River Basin
MRC	:	Mekong River Commission
NCDD	:	National Committee for Democratic Development and Decentralization
NSE	:	Nash Sutcliffe Efficiency
PBIAS	:	Percent bias
R^2	:	Coefficient of Determination
RGC	:	Royal Government of Cambodia
RUSLE	:	Revised Universal Soil Loss Equation
SDG	:	Sustainable Development Goal
SWAT	:	Soil and Water Assessment Tool
TSL	:	Tonle Sap Lake
USAID	:	United States Agency for International Development

CHAPTER 1

Background and Objectives

1.1. Background

Land-use change has historically always occurred around the world, is ongoing, and is likely to continue in the future (Lambin et al., 2006). These changes have positive and negative impacts on human well-being and safety. The most common and widespread land use and land cover changes (LULCC) worldwide are deforestation, agricultural expansion, and urbanization (Song and Zhang, 2012). For instance, deforestation and agricultural intensification are pervasive that they accumulate globally and significantly affect key aspects of the Earth's systems (Zhao et al., 2006). In recent centuries, the impact of human activities on the land has grown enormously, altering landscapes and ultimately impacting the earth's biodiversity, nutrient and hydrological cycles, and climate (Malhi et al., 2008; Searchinger et al., 2008; IPCC, 2007). The trend in LULC changes has been toward cash crop plantations due to various government policies, growing physical infrastructure, and social and economic development in multiple parts of mountainous areas in Southeast Asia. Forests have become the main focus for conversion to agricultural plantations (Carmona and Nahuelhual, 2012).

Understanding the hydrological process associated with the LULC changes is vital for decision-makers in improving human well-being. The LULC changes significantly affect the landscape's hydrology caused by anthropogenic activities (Engida et al., 2021). The impacts of LULC changes on hydrology can be studied by hydrological modeling, statistical analysis, and experimental catchments' comparative analysis (Elfert and Bormann, 2010). The LULC changes were a likely driver, among other factors, such as surface and groundwater abstractions for irrigated agriculture and the flow regulations due to dam construction. Another way of studying the LULC impacts is through a comparative assessment of the hydrological behavior of experimental catchments (Gebresamuel et al., 2010). This method has been rarely used due to the lack of such experimental catchments. Hydrological modeling applications for assessing the impacts of LULC changes on hydrology are the most widely used method, and several applications could be found in the literature (Birhanu et al., 2019).

In addition, it is widely recognized that land-use changes can greatly accelerate soil erosion (Hooke, 2000). It has long been known that erosion beyond soil production would ultimately reduce agricultural potential (Pimentel and Burgess, 2013). Although soil fertility generally declines with accelerated erosion, soil fertility is a function of farming methods and site conditions such as soil type, nutrient, and organic matter content (Montgomery, 2007). Soil erosion caused by human activities is reported to be 10–15 times higher than any natural process (Wilkinson and McElroy, 2007). Around 80% of the cultivated areas worldwide are exposed to high to severe erosion. The amount of generated sediments can increase waterways' turbidity and raise impurities' concentration (Tang et al., 2014).

Furthermore, soil erosion and sediment yield can severely affect people and the environment if the quantity of sediment exceeds the value of typical measurements of aquatic organisms. LULC changes led to increased soil erosion on agricultural and bare lands. This highlights the need to plan and manage changes to LULC to reduce erosion to and below sustainable levels (Eskandari Damaneh et al., 2022). The quality and quantity of water resources are strongly related to land use and land cover patterns within a local catchment. Cambodia's water resource management challenges are unsustainable natural resource development, agricultural expansion, and forest loss associated with commercial timber exploitation (Kim Phat et al. 2001). A major concern is the conversion of forests to cropland (Sourn et al., 2021; Nut et al., 2021), which can lead to habitat disturbance, soil erosion (Nut et al., 2021), sedimentation, and other issues related to water availability and quality.

The LULC changes and population growth are the most common problems in developing countries like Cambodia since their economic development mainly depends on agriculture. In recent decades, the increase in human activities led to the expansion of agricultural land, logging and urbanization, leading to deforestation in some parts of Cambodia (Kong et al., 2019), while these land cover changes affected the hydrological cycle and flooding of the local watershed, making various sub-watersheds more vulnerable (Garg et al., 2019). The modifications or transformations of natural vegetation and soil physical conditions usually cause changes in local catchment rainfall-runoff properties, which consequently alter river regimes (Shao et al., 2018; Zhang et al., 2017). Several studies show that the changes in vegetation cover, i.e., deforestation, lead to increased water yield and sedimentation (Sun et al., 2020; Vaighan et al., 2017).

A wide range of empirical, conceptual, and physically-based models have been developed to analyze hydrological processes and estimate soil loss risks. These models differ in complexity, data requirements, consideration processes, and calibration (Marondedze and Schütt, 2020; Raza et al., 2021). Among the other models, SWAT (Arnold et al., 1998), USLE/RUSLE, APEX (Williams et al., 1998), or WEPP (Laflen et al., 1991) models are the most popular, particularly the SWAT model. The SWAT model includes the statistical model of USLE (Wischmeier and Smith, 1978) and is derived from RUSLE (Renard et al., 1997). However, the SWAT and the APEX can only mechanistically simulate a limited number of different best management practices (BMPs) scenarios individually (Saleh and Gallego, 2007).

In Cambodia, land use has begun to change recently as both Cambodian and foreign investors invest in industrial crops such as palm oil, rubber, cassava, and kapok (Fox, 2002). These changes have been accompanied by expanding urban populations and the growth of huge megacities around the region, often at the expense of prime farmland. Without understanding the human dynamics behind land use change, we cannot understand changes in land cover nor predict the outcomes of policy intervention. It is vital to generate baseline data on the effects of commodification on local resource management systems to understand the impact of these changes on land cover, sustainable resource use, and landscape transformation (Nunes and Auge, 1999). For instance, as of mid-2012, 204,750 hectares ELCs have been granted to 118 companies (Chan, 2015).

Consequently, the forest cover in Cambodia decreased remarkably from 59.64% in 2006 to 45.26% in 2016 (MAFF, 2018). These changes have been accompanied by expanding urban populations and the growth of huge megacities around the region, often at the expense of prime farmland (Sourn et al., 2021). Furthermore, according to Diepart and Sem (2018), agricultural expansion and economic growth are the factors behind deforestation in Cambodia. It has been reported that the country's agricultural land expanded from 26% to 31% in 1997 and 2007 (FAO, 2010). Despite that growth, the forest cover in the northwestern uplands of Cambodia (some parts of Battambang and Pailin provinces) experienced a considerable decrease of 65% between 1976 and 2016. It was primarily converted from forest land to agricultural land for growing crops (Kong et al., 2019).

1.2. Land Use Change and Forest Degradation in Cambodia

Land use in Cambodia has undergone rapid changes, especially in the last decade, which can be attributed to development activities. In 2006, forest cover was estimated at 59.9% of the country's total land area. However, this forest cover was reduced to 57.7% of the country's total land area in 2020 (MRC, 2016). While the forest cover decreases yearly, the agricultural area has increased. The rice acreage was reported to rise from 2.72 million hectares in 2009 to 3.05 million hectares in 2013. The same trend applies to the rice acreage, the acreage of the other four main crops, namely corn, cassava, mung bean and soybean, increased from 206,058 to 239,748 ha, 160,326 to 421,375 ha, 49,599 to 54,312 ha and 96,388 to 80,680 ha from 2009 to 2013. Among the four main crops, cassava appears to be a promising case income opportunity for the local community as the total land area has increased rapidly over the past three years. According to the Ministry of Environment (MoE) the forest cover of Cambodia declined from 73.04% in 1965 to 48.14% in 2016, compared to the overall country area, primarily caused by civil war, population increase, need of land for agricultural production, and other key factors. Based on the forest cover assessment, the country's forest cover in 2016 was about 8,742,401 ha (48.14%), and the average annual loss rate from 2014 to 2016 was about 121,328 ha (0.67 %), compared to the entire country's area (MoE, 2018).

Land use in Cambodia began to change due to investment by insiders (Cambodian investors) and outsiders (foreign investors), mainly industrial crops such as palm oil (*Elaeis guineensis*), rubber (*Hevea brasiliensis*), cassava (*Manihot esculenta*), and kapok (*Ceiba pentandra*) (Fox, 2002). According to the FAO (2010), the agricultural area grew from 4,580 to 5,455,000 ha from 1997 to 2007 (26 to 31% of the total land area). The rice (*Oryza sativa*) production area increased from 2.72 million ha in 2009 to 3.05 million ha in 2013. Similar to the upward trend of the rice production area, the production areas of the other four main crops, namely: maize (*Zea mays*), cassava, mung bean (*Vigna radiata*), and soybean (*Glycine max*), increased from 206,058 to 239,748 ha, 160,326 to 421,375 ha, 49,599 to 54,312 ha, and 96,388 to 80,680 ha from 2009 to 2013, respectively (MRC, 2015), as cited in (Kityuttachai et al., 2016). According to the Ministry of Environment (MoE), Cambodia's forest area has decreased from 73.04% in 1965 to 48.14% in 2016 compared to the total country area (Figure 1.1). This was mainly caused by civil war, population growth, the need for land for agricultural production, and other key factors. Based on the forest cover assessment, the country's forest cover was about 8,742,401 ha (48.14%) in 2016, and the average annual loss rate from 2014 to 2016 was about 121,328 ha (0.67%) compared to the total Area of the country (MoE, 2018).

A recent study by Lohani et al. (2020) reported that the primary forest loss in Cambodia from 1993 to 2017 was 17,150 km^2, while in Tonle Sap, the total area of forest loss was low at 1,944 km^2; however, when analyzed as a percentage of the total forest area of all study regions, this was the highest. A portion of forest land cover in the Tonle Sap was lower as a whole (26 versus 53%) than for the Cambodia and 3S river (Srepok, Sesan, and Sekong) region. The rate of forest loss across the Tonle Sap region was relatively high and constant at 1.2% (Lohani et al., 2020). Forest loss in the Tonle Sap region seemed to occur over 25 years and mostly happened in small patches. After 2010, deforested areas have mingled into greater patches. In the western part of Cambodia, many large patches of forest loss are centered in highland regions, such as the Cardamom Mountains. In contrast, a concentrated forest loss occurred in the northwestern part of Cambodia along the border with Thailand in the early 2000s. It decreased only after nearly all remaining primary forests were lost (Lohani et al., 2020).

Based on the finding of Nalin et al. (2010), in Tonle Sap Basin, from 1990 to 2009, forest cover decreased by 43% from 20,170 km^2 to 11,436 km^2, while agricultural land increased by 34% from 14,076 km^2 to 18,858 km^2. A recent finding by Kong et al. (2019) mentioned that the total forest coverage (dense and degraded forests) remained almost unchanged, accounting for about 90% of the area between 1976 and 1997. However, about 13% of the dense forest area was transformed into degraded forestland. Forest cover was reduced dramatically during the following 20 years, from 1997 to 2016, and only 25% remained in 2016, especially along the main roads. Sixty-five (65%) percent of the forest cover loss primarily occurred between 2006 and 2016 (Kong et al., 2019). Based on the Land Degradation Neutrality Targets (LDNT) statement in Cambodia, the drivers of land degradation in Cambodia have mainly been attributed to deforestation, expanding agricultural lands, climate change, pests and diseases, unsustainable land management, and infrastructure development. In recent decades, deforestation has resulted in a significant loss of forest cover from 10.83 million ha (59.64%) in 2006 to 8.52 million ha (46.90%) in 2014 to 10.45 million ha (57.55%) in 2010, to 8.52 million ha (46.90%) in 2014 and to 8.22 million ha (45.26 %) by 2016. Over that period, croplands (paddy rice fields, field crops, horticulture, rubber and oil palm) increased by about 2.69 million ha. Agricultural land is expanding from lowland to upland, adding more pressure on forestland. Land Productivity Dynamics (LPD) indicate that in 2010, Cambodia had about 53,000 ha of land, showing an early sign of decline in productivity, as land use changed from forest to cropland. The soil organic carbon density indicates that for a period of 10 years (2000-2010), Cambodia lost about 1.98 million tons of carbon in the top 0-30 cm depth due to land use changes from forest to non-forest (MAFF, 2018). Cambodia aims to achieve an economic growth rate of 7% per annum with its aspiration to reach an upper-middle income country by 2030 and is committed to attaining zero-hunger by 2025. Agriculture continues to be a driver of economic growth and poverty reduction for Cambodia. Achieving sustainable agricultural development at 5% per annum is instrumental in addressing the objectives of the Royal Government of Cambodia (RGC) for food security, poverty reduction, and increased climate resilience (MAFF, 2018). Food production relies mainly on land and water. Land degradation and water scarcity are real challenges for food security. As one of the UNCCD (United Nations Convention to Combat Desertification) signatory States, the RGC has approved the National Action Plan (NAP) for 2018 to 2027, a fundamental document for national strategies for combating land degradation in the country. The RGC is committed to achieving 17 Sustainable Development Goals (SDGs), including SDG15, which aims to protect, restore and pro-mote sustainable use of terrestrial ecosystems, sustainably manage forests, combat desertification, and halt and reverse land degradation and halt biodiversity loss. Target 15.3 clearly aims to combat desertification, restore degraded land and soil, including land affected by desertification, drought and floods, and strive to achieve a land degradation-neutral world by 2030 (MAFF, 2018).

Because of the boom of economic land concession, some forest areas have been converted to industrial crops and forest plantations such as acacia, eucalyptus, and teak plantations, as well as rubber plantations. The area for rubber plantations has increased from 129,920 ha in 2009 to 328,771 ha in 2013. According to MAFF, till 2012, the RGC has granted Economic Land Concession to 118 companies with a total land area of 1,204,750 ha. Among these companies, 39 companies were recorded to plant forest tree species. The total cultivated area of Cambodia is about 4.37 million ha (24% of the land), while forests cover about 56%. Rice is the dominant crop, which covers approximately 3.57 million ha (80% of agricultural land), including the receding area, floating rice, and paddy rice interspersed with villages (MRC, 2016).

Cambodia has experienced rapid and extensive land use and land cover change over the last 20 years from 1990 to 2010; in particular, forest cover in Cambodia fell from 73 to 57% of the total land area (12,944 to 10,094 thousand hectares). Over the same period, the forest area designated for conservation increased from 2,776 thousand to 3,985 thousand hectares (23% of the total land area and 39% of the forest area). Available figures also show that between 1997 and 2007, Cambodia's agricultural land expanded from 4,580 to 5,455 thousand hectares (26 to 31% of land area) (FAO, 2010). The deforestation rate for the coming decades depends on many factors, such as: 1. Changes in market demand; 2. Changes in forestry management – forest concession policy; reforestation, monitoring, and control of illegal logging and forest clearing; monitoring actual logging operations; improved data on the extent and composition of the forest; harmonizing regional policy and practice regarding control of illegal timber trade, and regional cooperation in capacity building, and exchange of information and best practices; and, 3. Changes in the spontaneous growth of the agricultural settlement. Moreover, the LULC of north-east Cambodia has been changed due to agricultural enlargement; for instance, the forest cover has been converted into farmlands and paddy fields (Hor et al., 2014). Land use in mountain areas has rapidly transformed from native forests to cash crops, including rubber, acacia, cassava, sugarcane, jatropha, and other crops through economic land concessions (ELC) (ELC, 2015).

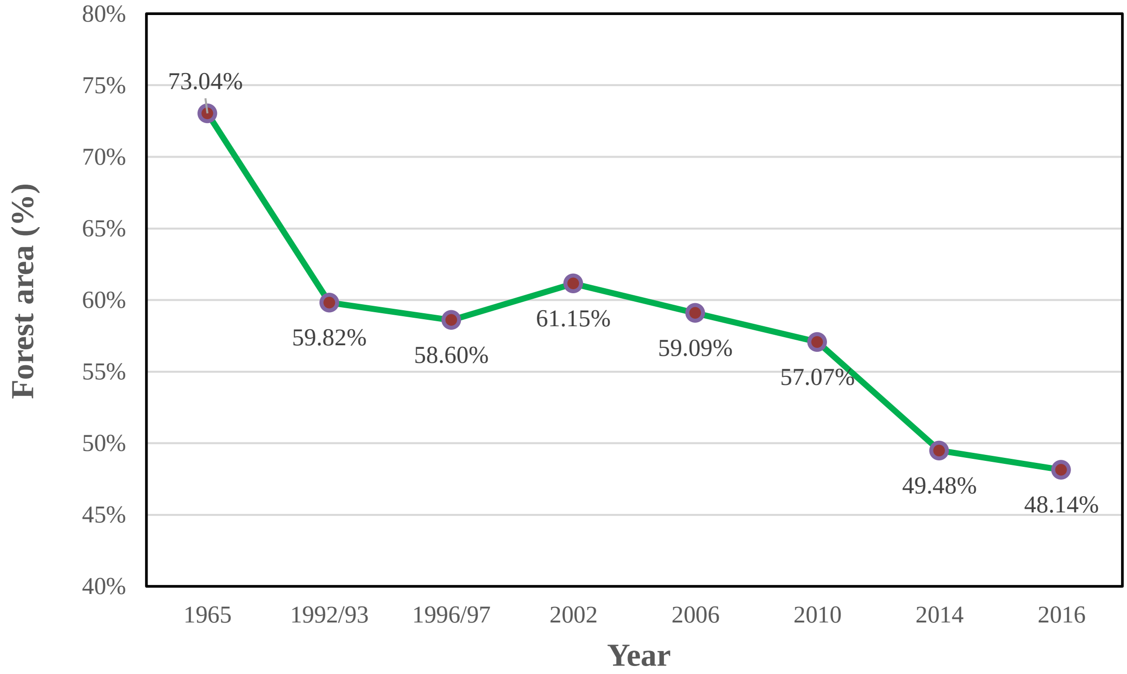

Sources: *Ministry of Environment (2018)*

Figure 1.1. Rate of forest cover change statistics from 1965-2016

1.3. Factors of Land Use Change in Cambodia

Several factors lead to forest degradation in Cambodia, as follows:

For Economic Land Concession (ELC): Cambodia's mountainous, forested areas have been transformed into agricultural land through economic land concessions (ELC). The ELC is the long-term (usually 70 to 90 years) granting the state-owned land to private sector operations for economic development through agricultural and industrial–agricultural operations, including large-scale plantations, stock rearing, and factory construction (Neef et al., 2013). A total land area of 1,204,750 hectares of ELC was granted to 118 companies, according to the report of the Ministry of Agriculture, Forestry, and Fishery (MAFF) of Cambodia (Kozak Dehlin, 2015). The ELCs granted in Cambodia which it was initially started to give to recipients in 1995 before specific laws and regulations had been in place because Land Law was just adopted in 2001, and a Sub-Degree on ELC was just also in place in 2005—a total of 6 ELCs before 2001 and 11 ELCs before 2005. Thus, offering ELCs without legal binding support and explicit instruction was unusual practices and strange. After adoption, it gradually increased to 14 ELCs only in 2006, while this trend continually increased to 43 ELCs in 2011 (Figure 1.2).

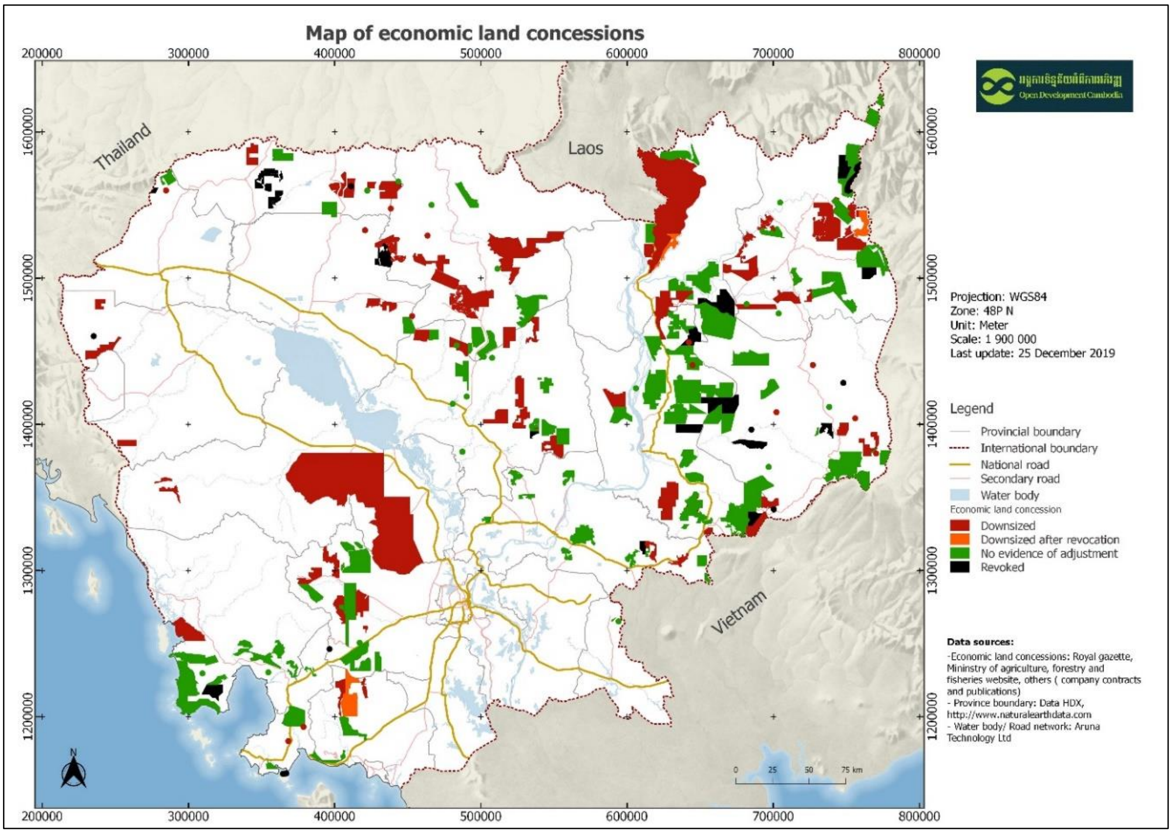

Sources: *Open Development Cambodia (2019)*

Figure 1.2. Map of Economic Land Concession (ELC) in Cambodia

For Directive 01 (D-01): Directive 01 (D-01) aims to reinforce and increase the efficiency of land management, with an emphasis on reducing land conflicts and providing titles to incumbent landholders. This was launched on July 1, 2012, by the Prime Minister. The policy aimed to systematically issue private land titles for 1.2 million hectares of land covering 350,000 families living within ELCs' forest concessions or state-owned land. To implement this initiative, thousands of student volunteers were recruited and provided basic training before being sent to the provinces to assist land titling offices and departments (Yeang, 2013).

For Market Demand Fluctuation for Crop: Commonly, Cambodia's agriculture sector has been undergone significant structural transformation decades ago and technological equipment have been integrated and used widely. Furthermore, the sector was still considered to play a major role; but it has become relatively less important in overall GDP year-by-year; for instance, in the period 2004-12, annual growth in gross production was 8.7 percent; while agricultural GDP grew by an annual average of 5.3 percent during the same period (Eliste and Zorya, 2015). It also emphasized that in many cases, farmers who expanded their land areas received higher incomes, but farmers with unchanged land areas were unable to substantially increase their incomes. The period of relatively high food prices was largely used to expand land areas rather than to build a strong foundation through productivity increases. Even poverty reduced significantly in period of last 10 years, but the number of vulnerable people also increased significantly since, most people who escaped poverty did so only by a small margin. The high rate of vulnerability was a sign of still modest agricultural productivity increases.

For Climate Change Causes Cropping Behavior and Land Use Change: Generally, local people have been considerably done farming in traditional ways; including a study by Hak, et al. (2015) at two IDs communes found that even increasing market activities and diminished natural resources, where most IPs were still huge relied on forest resources and they have still less produced the need products and not transforming them into traders nor provided it as sustained income yet. The study by Hak, et al. (2015) for specific in two communes—Dak Dam and Srae Preah; experienced a transition in agricultural production from the cultivation of upland staple crops, mainly for subsistence, to the production of cash crops for the market. As income shares from the cultivation of crops increased, those from forest products, hunting, and trapping decreased. Economic growth gave rise to land concentration and high-income inequality among households. Furthermore, Cambodia has frequently suffered catastrophic damage from natural disasters, notably drought, flood, storm, and after-effects, particularly in the many rice-producing provinces. Most rural poor rely on the regularity of the wet and dry seasons, especially for crop farming, which affects all aspects of their lives, from income generation, consumption, nutritional status, education, and health. Natural disasters especially hard hit the agricultural sector; not only crops, but infrastructure, buildings and equipment are destroyed. Given that the agricultural sector is a key contributor to the national economy, the impact of natural disasters reverberates beyond its confines (Ros, Nang and Chhim, 2011).

For Immigrant: Cambodian migration is mostly internal according to the National Institute of Statistics of Cambodia, and it was up to 35 percent of the Cambodian population migrated. Likewise, young people (aged 15-25) form a large section of migrants—30 percent. The challenge of rural is that new families cannot acquire or access land in their village. Therefore they out-migrate in search of livelihoods (Maltoni, 2005) and the current ELC and globalization. While, in Cambodia, about half of rural out-migration was to only Phnom Penh through the finding in 2012 (ADB, 2014); the garment factory sector along was accountable for up to 650,000 workers; since the majority of factories are located in urban cities and surrounding outskirts.

1.4. Impacts of LULC Change on Water Resources and Hydrology

1.4.1. LULC Change Impacts on Water Resources

The LULC change is considered one of the main factors directly affecting the hydrological cycle of the watershed (Engida et al., 2021; Gashaw et al., 2018) and directly affecting ecosystems and related services, especially water yield (Li et al., 2018). The main drivers of LULC changes are directly related to human activities such as population growth, socioeconomic development, population growth, land pressure for agriculture, foreign investment in agriculture, favorable biophysical factors, politics, and globalization (Lambin et al., 2003; Marchant et al., 2018; Kleemann et al., 2017; Msofe et al., 2019). Natural processes such as landslides, floods, droughts, and climate change affect the LULC change (Brink and Eva, 2009), although they are induced to some extent by anthropogenic activities. These conversions to cropland have negative impacts on multiple ecosystem services such as water quantity and quality (Mustard et al., 2004), and catchment water resources are a trade-off for increased agricultural yields such as food and timber production (Mustard et al., 2004; Brink et al. Eva, 2009). Hence, scientific guidance is needed to enable the sustainable development of the catchment (Leemhuis et al. 2017; Meijer et al. 2018). Land use change is also affecting climate change through vegetation clearance and changes in carbon storage and sequestration (Lambin et al., 2003), and its impact might be more severe than those of climate change in some regions with already extremely dry climate. Consequently, studies on the impacts of land use change on catchment water resources address a significant research concern in this century (Wagner et al., 2017).

Therefore, food production depends on water resources, and any likely impacts of LULC changes on water resources will negatively impact food production. Several water-related goals of the Sustainable Development Goals (SDGs) are at risk from land conversion to cropland, particularly regarding SDG 6 (Clean Water and Sanitation) and SDG 15 (Life on Land) (Meijer et al., 2018; Nhemachena et al., 2018). Several studies have examined the impacts of LULC changes and climate change on water resources separately (Faramarzi et al., 2013; Yira et al., 2016) or simultaneously (Notter et al., 2013; Op et al., 2019). The results of the studies differ for several reasons, e.g., the type of LULC changes, the regional focus, or the chosen period and model for simulating climate change.

Although there are numerous studies on the effects of LULC changes on watershed hydrology, the evidence from the different studies is still conflicting. Malmer et al. (2009) argue that the general notion that the fundamentals of forest and water relationships are well-known does not apply to watersheds with fragmented and dynamic land-use patterns, such as those observed in the tropical developing world. This means that the variation in catchment characteristics associated with LULC changes increases the uncertainty of finding commonality in observed hydrological signatures attributed to LULC changes. It is commonly argued that forests act both as pumps through increased evapotranspiration (ET) rates and as sponges through increased rates of infiltration and soil moisture retention (Bruijnzeel, 2004; Arancibia, 2013). Forested watersheds have lower runoff rates than those dominated by other managed land uses. Loss of forest cover leads to changes in albedo, a reduction in aerodynamic roughness, a decrease in leaf area, and a reduction in root depth, which consequently leads to a decrease in ET, which subsequently affects current flow (Costa et al., 2003; Farley et al., 2005). The net effect of forest loss is increased water yield (Bosch and Hewlett, 1982). In addition, a reduction in dry season flow because of deforestation is often cited (Ogden et al., 2013; Arancibia, 2013; Liu et al., 2015). Despite these general conclusions, based on experimentation at different spatial scales (e.g., property, watershed, and regional scales), empirical and physical-based (pooled and spatially distributed) modeling, and time-series analysis, they isolate the impacts of LULC changes on water resources in a landscape are problematic because uncertain interactions of factors drive these effects. Eshleman (2004) found that these increases in water yield associated with forest loss depend on several factors, including the method of forest loss (Beschta, 1998), the extent of forest clearing (Bosch and Hewlett, 1982), and the rate of plant regeneration affecting ET (Federer and Lash, 1978), climatic conditions (Bosch and Hewlett, 1982;

Whitehead and Robinson, 1993), and hydrogeology and physical properties of the catchment (Likens et al., 1978).

Previous studies have demonstrated that patterns of land use change, as well as the representation of these patterns in models, significantly affect predictions of catchment water quantity and quality (e.g. Wagner et al., 2017). Wagner et al. (2017) suggested that the static approach, with constant land use over time, can result in good streamflow predictions when land use development is linear, while land use change is approximated more realistically by means of a dynamic representation for non-linear land use changes (Chiang et al., 2010). The question arises of how the difference in land use change representations may affect water quality prediction in catchments. Furthermore, the study of Garg et al. (2019) showed that the water supply and hydrological process decreased because of LULC change, exacerbated by significantly increasing population pressure and development in the Pennar Basin of India. This can be done by increasing the water yield or reducing the flow, thereby increasing the sediment load and groundwater (Babar and Ramesh, 2015; FAO, 2014).

Therefore, maintaining the balance of native forest covers around the world is crucial because native vegetation distribution is the main factor that affects the variation of annual runoff on both national and global scales (Peel et al., 2001). It is well understood by many studies that decreasing forest cover would lead to increasing water yield (Brown et al., 2005). Still, it would be essential to look at the impact of forest cover on other aspects of hydrology, such as evapotranspiration, groundwater recharge, soil water content, and flooding.

1.4.2. LULC Changes Impact on Streamflow

Agricultural and urban expansion is a common and widespread LULC change worldwide (Hosonuma et al., 2012). LULC changes are among the most critical input data for a hydrological model. LULC changes can have significant impacts on watershed hydrology (Sadhwani et al., 2022), surface water availability, base flows (Das et al., 2018), ET (Das et al., 2018), runoff (Das et al., 2018; Farley et al., 2005), sediment yield (Sadhwani et al., 2022), and groundwater (Siddik et al., 2022) in the catchment. Many studies across the globe have shown that LULC changes significantly impact hydrological processes (Khoi and Suetsugi, 2014). Studies and reviews on the impact of land use change –particularly forest cover change-upon hydrologic processes have been done at the regional and global scales (Bradshaw et al., 2007; Brown et al., 2005; Farley et al., 2005). Brown et al. (2005) reviewed paired catchment studies on the impact of forest cover changes on water yield at different temporal scales; they reported that expansion of forest cover could reduce water yield. Likewise, Bruijnzeel (2004) reviewed various research studies on the hydrological functions of tropical forests in southeast Asia and reported that the water yield increased with decreasing forest cover. Farley et al. (2005) also found that runoff reduced as afforest based on the 26 catchments dataset globally. While removing vegetation can lead to more acute flood impacts within the denuded catchments, increasing forest cover often results in decreasing runoff rates (Calder, 2007). For example, Vertessy et al. (1998) found that a rise or fall in water yield positively correlates with the percentage of forested areas in the basin based on their research on 17 catchments in Australia. Wang et al. (2008) also concluded that mean annual runoff declined by 2.3% followed by increasing of 25% in the proportion of forestland in a mountainous catchment in China. Similarly, Khoi and Suetsugi (2014) discovered a rise of streamflow, from 0.2% to 0.4% with a decline of 16.3% in forestland in the Be River catchment, Vietnam. Consequently, LULC changes are responsible for the increased runoff of rivers across the globe (Piao et al., 2007). Besides, different forest cover types could result in various water yield. For instance, Bosh and Hewlett (1982) discovered that a 10% change in forest cover types, particularly Pine and Eucalypt, deciduous hardwood and scrub alter the water yield on average 40 mm, ~25 mm and 10 mm respectively. Therefore, maintaining the balance of native forest covers around the world is crucial because native vegetation distribution is the main factor that affects the variation of annual runoff in both national and global scales (Peel et al., 2001). It well understood by many studies that decreasing forest cover would lead to increasing water yield (Brown et al., 2005), but it would be important to look at the impact of forest cover on other aspects of hydrology such as evapotranspiration, groundwater recharge, soil water content and flooding.

1.4.3. Contribution of LULC Change to Precipitation

Forest cover can positively affect water cycles and improve water availability (Ellison et al., 2017). Conversely, deforestation led to reductions in the amount of precipitation. According to Van der Ent et al. (2010), evapotranspiration (ET) has contributed significantly to at least 40% of rainfall on Earth, and the Amazon Forest contributes more than 70% of precipitation for the Rio de Plata River basin. Transpiration contributes a significant share of the amount of ET in the atmosphere (Schlesinger and Jasechko, 2014). Kummu (2003) studied the natural environment and historical water management in the Siem Reap basin. He discovered a high rainfall distribution at the Kulen Mountain range with an average of

1,854 mm/year, which is higher than the annual average of the other two stations (Siem Reap and Banteay Srie stations), at 1,317 mm. This result indicated that the high density of forest cover along the Mount Kulen range has potentially contributed to increasing amounts of precipitation. Agricultural expansion through deforestation affects local temperature, reduces ET, and alters the rainfall and water availability in the catchment (Ellison et al., 2017). Lawrence and Vandecar (2015) and Oliveira et al. (2013) studied the effects of tropical deforestation on climate and agriculture. They found that expanding agriculture in the Amazon leads to declining precipitation and low agricultural productivity.

Moreover, forest cover is a carbon storage place, thus cooling surface temperature (Ellison et al., 2017) in the catchment. Rising mean annual temperatures affect the balance between ET and runoff and the water yield (Balist et al., 2022; Hu et al., 2005; Schmid et al., 2000). Hence, forest cover helps maintain the local precipitation and cope with future climate change in this catchment.

Likewise, Lu et al. (2015) found that forested land contributed more to water yield than any other LULC class. Still, built-up land had the most significant impact due to low initial losses and infiltration. At the basin scale, there were slight increases in average annual potential ET, actual ET, and water yield (WY), but soil water decreased between the two intervals. Moreover, Dibaba et al. (2020) also highlighted that the changes in LULC increase surface runoff and water yield and a decline in groundwater. The projected climate change shows decreased surface runoff, groundwater, and groundwater water yield. The combined study of LULC and climate change shows that the effect of the combined scenario is similar to that of the climate change-only scenario.

Furthermore, Saddique et al. (2020) reported that afforestation had reduced the WY and surface runoff at the catchment scale while enhancing the ET. Moreover, this change was more pronounced at the sub-basin scale. Some sub-basins, particularly in the northern part of the study area, showed an increase in the WY due to the rise in the snow cover area. Likewise, extreme land use scenarios also showed a significant impact on components of the water balance. The basin WY has decreased by 38 mm/year, and ET has increased by about 36 mm/year.

1.4.4. Contribution of LULC Changes to Groundwater

The forest cover is also contributed to increasing groundwater recharge and improving groundwater resources. Ilstedt et al. (2016) investigated groundwater recharge in the seasonally dry tropics, and they found that tree cover can increase groundwater recharge. Likewise, Neary et al. (2009) studied linkages between forest soils and water quality and quantity. They found that forest cover also improved the quality of groundwater and surface water in its catchment. Root systems of the forests are extensive and relatively deep compared to agricultural lands and grasslands, and it commonly plays a crucial role in improving soil conditions and groundwater through infiltration rate and percolation below their rooting zone.

Moreover, forest cover plays a crucial role in maintaining the available water storage capacity in the soil (Brown et al., 2005). While it is essential to understand the streamflow, evapotranspiration, and groundwater responses under forest cover, these might not reveal the whole story since the water stored in soil interactions also plays a vital role in water balance under the influence of forest cover (Brown et al., 2005). Besides the above-mentioned advantages, the forest cover prevents and reduces flooding (Allen and Chapman, 2001; Bradshaw et al., 2007); while removing vegetation can result in more acute flood impacts within the denuded catchment areas, increasing forest cover often reduces runoff rates (Calder and Aylward, 2006). Bradshaw et al. (2007) studied the flood risk responses under forest cover change using observation data for a decade (1990-2000) of data from 56 countries around the world. They found that the forest cover can increase interception and evapotranspiration and lead to reducing flood-related catastrophes. Floods are tropical countries' most common natural disaster (Tan-Soo et al., 2016). For instance, a flood in the Johor River basin, Malaysia, at the end of 2006 and early 2007, caused 18 deaths and the evacuation of more than 100,000 residents, costing USD 0.5 billion (Kia et al., 2012; Tan et al., 2015). Therefore, integrating forest cover for flood management and mitigation is a potential and cost-effective solution (Ellison et al., 2017; Jongman et al., 2015) for river management and development.

1.5. Research Conceptual Framework

The research implementation involves many processes, which consist of several steps to achieve the research objectives. Firstly, the research focuses on analyzing the impacts of LULC changes on streamflow and water balance in one catchment of Tonle Sap Basin, namely Stung Sangkae River catchment, which covers some parts of the Battambang province. This could be done by integrating the national LULC maps developed by Japan International Cooperation Agency (JICA) in 2002 and the Mekong River Commission

(MRC) in 2015 into the SWAT model to evaluate the hydrology changes and soil erosion from 2002 to 2015. Secondly, the research would further investigate the soil erosion in the catchment in 2002 and 2015 by integrating GIS with the RUSLE model (Figure 1.3). The result of soil erosion from the integration of GIS and RUSLE would also be used to compare and discuss with the outcome of SWAT model as well as comparing with the observed field. After that, the effective countermeasures to prevent increased streamflow and soil erosion through reforestation will be made by SWAT model. Furthermore, the field survey will also conduct to understand the perception of farmers towards hydrology changes and soil erosion as well reflect the results of the model with the farmer perception. Thus, to accomplish the research, SWAT, RUSLE, and GIS were applied with the support of field surveys, desk reviews, and discussions with relevant stakeholders. It was ensured that the collected data would meet the objectives through the careful set of data analysis and interpretation.

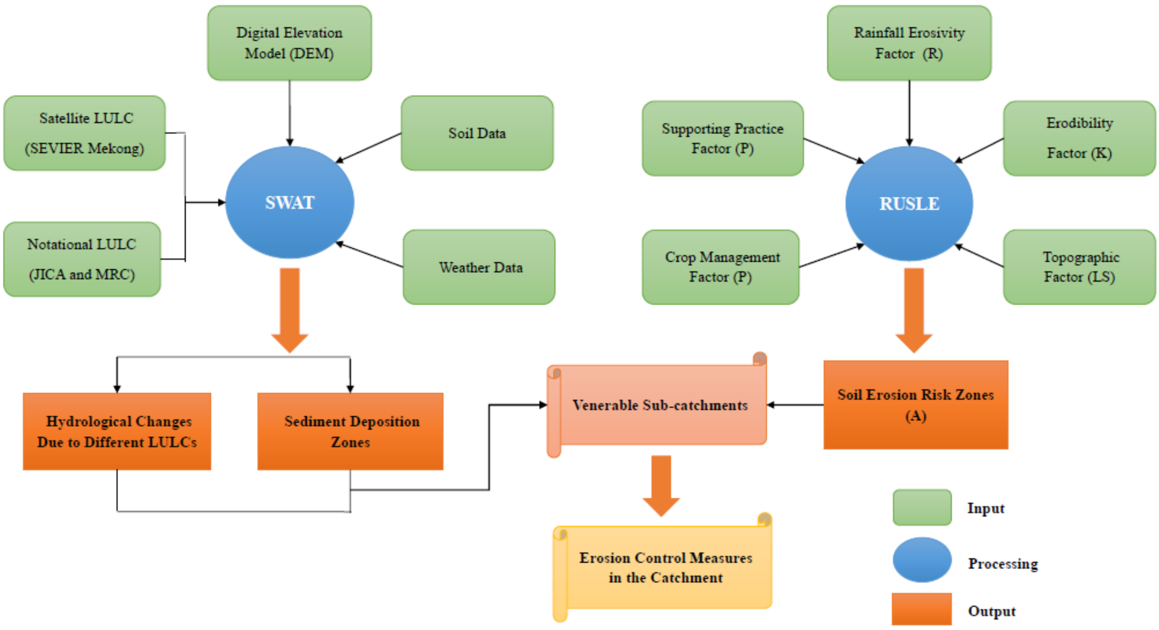

Figure 1.3. Flowchart of the applied methodology in the research

1.6. Research Benefits

The research would contribute to the development of LULC changes in Cambodia due to the trend of economic development and its impacts. It will play a vital role in establishing a land use database, which will benefit to various stakeholders while contributing to the improvement of national and sub-national understanding of researchers and relevant stakeholders on land use change database as well as contributing to government policymakers, a technical team of the Ministry of Agriculture, Forestry and Fisheries, Ministry of Land Management, Urban Planning and Construction and Ministry of Environment having a baseline study to develop agricultural zoning map or spatial planning in the catchment scale. Besides these, it will facilitate the establishment of a sustainable water resources development policy for the region, and it is essential for (i) the assessment of water yield potential, (ii) the planning of soil and water conservation measures, and (iii) reducing the sedimentation and flooding hazard at downstream. In addition, the results of this study are expected to provide helpful information that can promote soil erosion management practices in the Stung Sangkae Catchment, Battambang Province, as well as Tonle Sap Great Lake, which represents one of the world's most productive ecosystems and biodiversity. The Tonle Sap River-Great Lake system underpins the world's biggest freshwater fishery and directly or indirectly affords a livelihood for most of Cambodia's population.

1.7. Scope and Limitations of the Research

The study on hydrological characteristics and soil erosion affected by the LULC changes were carried out in one of the tributaries of Tonle Sap Lake, namely Stung Sangkae River catchment. A questionnaire survey was conducted with 200 households (HHs) in 2021 in 4 districts along Stung Sangkae River (100 HHs for upstream and 100 HHs for downstream of the catchment). All relevant information from the locations, particularly people's perspectives on hydrological changes and soil erosion occurrence, was collected. Moreover, the study analyzed the impacts of LULC on the hydrological process and soil erosion loss based on national LULC maps of JICA 2002 and MRC 2015, which would be done only in the Stung Sangkae catchment by using the SWAT and RUSLE model. However, the SWAT simulation would be done for a whole catchment which includes an ungauging part to understand the hydrological responses downstream. In contrast, model calibration and validation would be done only from the gauging station to the upstream part. There are 5 rainfall stations (2007-2018) and stream flow (2000-2018) available for the model calibration and validation. As there is no sediment record available in the catchment, the output of soil loss from RUSLE would be used to discuss and compare with the SWAT model's results to identify how the hydrology would be changed due to LULC changes in the catchment.

1.8. Research Objectives

The overall objective is to investigate the hydrological characteristic and soil erosion in Stung Sangkae catchment based on the LULC changes. To achieve overall objective, the following objectives are set below:

1). To identify the change of LULC and its hydrological responses in the catchment based on national LULC maps of JICA 2002 and MRC 2015 by SWAT model

2). To estimate soil erosion risk in the catchment based on national LULC maps of JICA 2002 and MRC 2015 by the RUSLE model

3). To investigate the effect of reforestation or agroforestry on hydrological responses in Stung Sangkae Catchment by SWAT Model

4). To deepen the public perception of the importance of conservation strategies against flood/drought and soil loss.

Reference of this chapter

Allen, A., and Chapman, D. 2001. Impacts of afforestation on groundwater resources and quality. Hydrogeol J 9:390–400. https://doi.org/10.1007/s100400100148

Asia Development Bank (ADB). 2014. Cambodia country poverty analysis, Mandaluyong City, Philippines. Available at: http://www.adb.org/sites/default/files/institutional-document/151706/ cambodiacountry-poverty-analysis-2014.

Arancibia, J.L.P. 2013. Impacts of land use change on dry season flows across the tropics forests as ‘sponges’ and ‘pumps’ University of London. PhD thesis, 262p.

Arnold, J.G., Srinivasan, R., Muttiah, R. S., and Williams, J.R. 1998. Large area hydrologic modelling and assessment Part I: Model Development. J Am Water Resources Assoc 34, 73–89. https://doi.org/10.1111/j.1752-1688.1998.tb05961.x

Babar, S., and Ramesh, H. 2015. Streamflow response to land use–land cover change over the Nethravathi River Basin, India. J. Hydrol. Eng. 20, 05015002. https://doi.org/10.10 61/(ASCE)HE.1943-5584.0001177

Balist, J., Malekmohammadi, B., Jafari, H.R., Nohegar, A., and Geneletti, D. 2022. Detecting land use and climate impacts on water yield ecosystem service in arid and semi-arid areas. A study in Sirvan River Basin-Iran. Applied Water Science, 12(1), 4. https://doi.org/10.1007/s13201-021-01545-8

Birhanu, A., Masih, I., van der Zaag, P., Nyssen, J., and Cai, X. 2019. Impacts of land use and land cover changes on hydrology of the Gumara catchment, Ethiopia. Physics and Chemistry of the Earth, Parts A/B/C, 112, 165–174. https://doi.org/10.1016/j.pce. 2019.01.006

Bosch, J.M., and Hewlett, J.D. 1982. A review of catchment experiments to determine the effect of vegetation changes on water yield and evapotranspiration J. Hydrol., 55 (1982), pp. 3-23, 10.1016/0022-1694(82)90117-2

Bradshaw, C.J.A., Sodhi, N.S., Peh, K.S.-H., and Brook, B.W. 2007. Global evidence that deforestation amplifies flood risk and severity in the developing world. Global Change Biology, 13(11), 2379–2395. https://doi.org/10.1111/j.1365-2486.2007.014 46.x

Brink, A.B., and Eva, H.D. 2009. Monitoring 25 years of land cover change dynamics in Africa: A sample based remote sensing approach. Appl. Geogr., 29, 501–512.

Brown A.E., Zhang L., McMahon, T.A., Western A.W., Vertessy, R.A. 2005. A review of paired catchment studies for determining changes in water yield resulting from alterations in vegetation. J Hydrol 310:28–61. https://doi.org/10.1016/j.jhydrol.2004.12.010

Bruijnzeel, L.A. 2004. Hydrological functions of tropical forests: not seeing the soil for the trees Agric. Ecosyst. Environ., 104, 185-228, 10.1016/j.agee.2004.01.015

Bruijnzeel, L.A. 1990. Hydrology of Moist Tropical Forests and Effects of Conversion: A State of Knowledge Review; Free University: Amsterdam, The Netherlands.

Calder, I.R., and Aylward, B. 2006. Forest and Floods: Moving to an Evidence-based Approach to Watershed and Integrated Flood Management. Water International, 31(1), 87–99. https://doi.org/10.1080/02508060608691918

Carmona, A., and Nahuelhual, L. 2012. Combining land transitions and trajectories in assessing forest cover change. Appl. Geogr., 32, 904–915.

Chan, S. 2015. Management of economic land concessions. Retrieved from http://ticambodia.org/library/wpcontent/files_mf/1451897377PB1501DRFMgtofELC.pdf

Chiang, L., Chaubey, I., Gitau, M., and Arnold, J.G. 2010. Differentiating impacts of land use changes from pasture management in a CEAP watershed using SWAT model. Trans. ASABE 53(5): 1569-1584.

Costa, M.H., Botta, A., and Cardille, J.A. 2003. Effects of large-scale changes in land cover on the discharge of the Tocantins River, Southeastern Amazonia. J. Hydrol. (Amst), 283 (2003), 206-217, 10.1016/S0022-1694(03)00267-1

Das, P., Behera, M.D., Patidar, N., Sahoo, B., Tripathi, P., Behera, P.R., Srivastava, S.K., Roy, P.S., Thakur, P., Agrawal, S.P., and Krishnamurthy, Y.V.N. 2018. Impact of LULC change on the runoff, base flow and evapotranspiration dynamics in eastern Indian river basins during 1985–2005 using variable infiltration capacity approach. Journal of Earth System Science, 127(2), 19. https://doi.org/10.1007/s12040-018-0921-8

Dibaba, W.T., Demissie, T.A., and Miegel, K. 2020. Watershed Hydrological Response to Combined Land Use/Land Cover and Climate Change in Highland Ethiopia: Finchaa Catchment. Water, 12(6), 1801. https://doi.org/10.3390/w12061801

Diepart J.-C. and Sem T. 2018. Cambodian peasantry and formalisation of land right: Historical perspectives and current issues. Research series. Paris, French Technical Committee on Land Tenure and Development (AFD-MEAE). Retrieved from http://www.foncier-developpement.fr/wp-content/uploads/2018_Cambodian-peasantry-and-formalisation-of-land-rights_FINAL2.pdf

Economic Land Concessions (ELC). 2015. Available online: https://opendevelopment cambodia.net/profiles/economic-land-concessions/(accessed on 1 December 2020).

Elfert, S., and Bormann, H. 2010. Simulated impact of past and possible future land use changes on the hydrological response of the Northern German lowland 'Hunte'catchment. J. Hydrol. 383 (3), 245–255.

Eliste, P., and Zorya, S. 2015. Cambodian Agriculture in Transition: Opportunities and Risks. Washington, D.C.: World Bank Group. Availble at: http://documents. worldbank.org/curated/en/805091467993504209/Cambodianagriculture-in-transition-opportunities-and-risks.

Ellison, D., Morris, C.E., Locatelli, B., Sheil, D., Cohen, J., Murdiyarso, D., Gutierrez, V., Van Noordwijk, M., Creed, I.F., Pokorny, J. 2017. Trees, forests and water: cool insights for a hot world. Global Environ. Change 43, 51–61. https://doi.org/10.1016/ j.gloenvcha.2017.01.002.

Engida, T.G., Nigussie, T.A., Aneseyee, A.B., and Barnabas, J. 2021. Land Use/Land Cover Change Impact on Hydrological Process in the Upper Baro Basin, Ethiopia. Applied and Environmental Soil Science 2021, 1–15. https://doi.org/10.1155/2021/6617541

Eshleman, K.N. 2004. Eshleman Hydrological consequences of land use change: a review of the state-of-science R.S. Defries, G.P. Asner, R.A. Houghton (Eds.), Ecosystems and Land Use Change, American Geophysical Union, Washington, D.C (2004), 10.1029/153GM03

Eskandari Damaneh, H., Khosravi, H., Habashi, K., Eskandari Damaneh, H., and Tiefenbacher, J.P. 2022. The impact of land use and land cover changes on soil erosion in western Iran. Natural Hazards, 110(3), 2185–2205. https://doi.org/10.1007/s11069-021-05032-w

Faramarzi, M., Abbaspour, K.C., Ashraf Vaghefi, S., Farzaneh, M.R., Zehnder, A.J.B., Srinivasan, R., and Yang, H. 2013. Modeling impacts of climate change on freshwater availability in Africa.J. Hydrol, 480, 85–101.

Farley, K.A., Jobbagy, E.G., and Jackson, R.B. 2005. Effects of afforestation on water yield: a global synthesis with implications for policy Glob. Change Biol., 11 (10) (2005), pp. 1565-1576, 10.1111/j.1365-2486.2005.01011.x

Federer, C.A., and Lash, D. 1978. Simulated streamflow response to possible differences in transpiration among species of hardwood trees Water Resour. Res., 14 (1978), pp. 1089-1097, 10.1029/WR014i006p01089

Food and Agriculture Organiztion (FAO). 2010. Assessment of land use, forest policy and governance in Cambodia.

Food and Agriculture Organization (FAO). 2014. World reference base for soil resources, international soil classification system for naming soils and creating legends for

soil maps," Tech. Rep., Food and Agriculture Organization, Rome, Italy, 2014, World Soil Resources Report 106.

Fox, J. 2002. Understanding a Dynamic Landscape: Land Use, Land Cover, and Resource Tenure in Northeastern Cambodia. Linking People, Place, and Policy 113–130. https://doi.org/10.1007/978-1-4615-0985-1_6

Garg, V., Nikam, B.R., Thakur, P.K., Aggarwal, S.P., Gupta, P.K., and Srivastav, S.K. 2019. Human-induced land use land cover change and its impact on hydrology. HydroResearch 1, 48–56. https://doi.org/10.1016/j.hydres.2019.06.001

Gashaw, T., Tulu, T., Argaw, M., and Worqlul, A.W. 2018. Modeling the hydrological impacts of land use/land cover changes in the Andassa watershed, Blue Nile Basin, Ethiopia. Science of The Total Environment 619–620, 1394–1408. https://doi.org/10.1016/ j.scitotenv.2017.11.191

Gebresamuel, G., Singh, B.R., and Dick, Ø. 2010. Land-use changes and their impacts on soil degradation and surface runoff of two catchments of Northern Ethiopia. Acta Agric. Scand. Sect. B Soil Plant Sci 60 (3), 211–226. https://doi.org/10.1080/ 09064710902821741

Hak, C., So, D., Oeur, L., and McAndrew, J. 2015. Prosperity and Poverty: Livelihood transitions emerging from land use change in Two Mondulkiri Commune, Chapter 5; from Diepart, J.-C., ed. "Learning for resilience: Insights from Cambodia's Rural Communities". Phnom Penh: The Learning Institute.

Hooke, R.L.B. 2000. On the history of humans as geomorphic agents. Geology 28, 843–846. https://doi.org/10.1130/0091-7613(2000)282.0.CO;2

Hosonuma, N., Herold, M., De Sy, V., De Fries, R.S., Brockhaus, M., Verchot, L., Angelsen, A., and Romijn, E. 2012. An assessment of deforestation and forest degradation drivers in developing countries. Environ. Res. Lett, 7, 044009. https://doi.org/10.1088/ 1748-9326/7/4/044009

Hor, S., Saizen, I., Tsutsumida, N., Watanabe, T., and Kobayashi, S. 2014. The impact of agricultural expansion on forest cover in Ratanakiri Province, Cambodia, Kyoto University. Available at: https://doi.org/10.5539/jas.v6n9p46

Hu, Q., Willson, G.D., Chen, X., and Akyuz, A. 2005. Effects of climate and landcover change on stream discharge in the Ozark Highlands, USA, vol. 10. Environmental Modeling & Assessment, pp. 9–19. https://doi.org/10.1007/s10666-004-4266-0.

Ilstedt, U., Tobella, A.B., Bazié, H.R., Bayala, J., Verbeeten, E., Nyberg, G., Sanou, J., Benegas, L., Murdiyarso, D., and Laudon, H. 2016. Intermediate tree cover can maximize groundwater recharge in the seasonally dry tropics. Sci Rep 6:21930. https://doi.org/10.1038/srep2 1930

Intergovernmental Panel on Climate Change (IPCC). 2007. Climate Change. The Physical Science Basis. Summary for Policymakers, Contribution of Working Group I to the Fourth Assessemt Report of the Intergovernmental Panel on Climate Change (IPCC), Paris.

Jongman, B., Winsemius, H.C., Aerts, J.C.J.H., Coughlan de Perez, E., van Aalst, M.K., Kron, W., and Ward, P.J. 2015. Declining vulnerability to river floods and the global benefits of adaptation. Proceedings of the National Academy of Sciences, 112(18). https://doi.org/10.1073/pnas.1414439112

Khoi, D.N., and Suetsugi, T. 2014. The responses of hydrological processes and sediment yield to land-use and climate change in the Be River Catchment, Vietnam: Impact of land-use and climate changes on hydrology and sediment yield. Hydrol. Process. 28, 640–652. https://doi.org/10.1002/hyp.9620

Kozak Dehlin, S. 2015. Economic Land Concessions in Cambodia-At the Expense of Adequate Housing? A Minor Field Study. Available online: http://lup.lub.lu.se/student papers/ record/5434299 (Accessed on 15 October 2019)

Kummu, M. 2003. The Natural Environment and Historical Water Management of Angkor, Cambodia. Leith, C., 2019. Challenges Facing the Siem Reap Tuk-Tuk Workforce in a Changing Tourism Environment, p. 166.

Kia, M. B., Pirasteh, S., Pradhan, B., Mahmud, A. R., Sulaiman, W. N. A., and Moradi, A. 2012. An artificial neural network model for flood simulation using GIS: Johor River Basin, Malaysia. Environmental Earth Sciences, 67(1), 251–264. https://doi.org/10.1007/s12665-011-1504-z

Kityuttachai, K., Heng, S., and Sou, V. 2016. Land Cover Information Catalogue of the Lower Mekong Basin. MRC Technical Paper No. 58, Information and Knowledge Management Programme, Mekong River Commission, Phnom Penh, Cambodia 83 pp.

Kleemann, J., Baysal, G., Bulley, H.N.N., and Fürst, C. 2017. Assessing driving forces of land use and land cover changeby a mixed-method approach in north-eastern Ghana, West Africa.J. Environ. Manag.196, 411–442.

Kong, R., Diepart, J.-C., Castella, J.-C., Lestrelin, G., Tivet, F., Belmain, E., and Bégué, A. 2019. Understanding the drivers of deforestation and agricultural transformations in the Northwestern uplands of Cambodia. Applied Geography 102, 84–98. https://doi.org/10.1016/j.apgeog.2018.12.006

Laflen, J. M., Lane, L. J., and Foster, G.R. 1991. WEPP: A new generation of erosion prediction technology. Journal of Soil and Water Conservation 34–38.

Lambin, E. F., Geist, H. J., and Lepers, E. 2003. Dynamics of land-use and land-cover change in tropical regions. Annual review of environment and resources, 28, 205–241.

Lambin, E.F., and Geist, H. 2006. Land-use and land-cover change: local processes and global impacts. The IGBP series 1619-2435. Berlin: Springer.

Leemhuis, C., Thonfeld, F., Näschen, K., Steinbach, S., Muro, J., Strauch, A., López, A., Daconto, G., Games, I., and Diekkrüger, B. 2017. Sustainability in the food-water ecosystem nexus: The role of land use and land cover change for water resources and ecosystems in the Kilombero Wetland, Tanzania. Sustainability, 9, 1513.

Legates, D.R., and McCabe, G.J. 1999. Evaluating the use of “goodness-of-fit” measures in hydrologic and hydroclimatic model validation. Water Resour. Res. 35(1): 233-241. Lewis, S.L. 2006. Tropical forests and the changing earth system. Philosophical Transactions of the Royal Society B: Biological Sciences 361(1465), 195-210.

Lawrence D, and Vandecar K. 2015. Effects of tropical deforestation on climate and agriculture. Nat Clim Chang 5:27. https://doi. org/10.1038/nclimate2430

Li, S., Yang, H., Lacayo, M., Liu, J., and Lei, G. 2018. Impacts of land-use and land-cover changes on water yield: A case study in Jing-Jin-Ji, China. Sustainability 10, 960. https://doi.org/10.3390/su10040960

Likens, G.E., Bormann, F.H., Pierce, R.S., and Reiners, W.A. 1978. Recovery of a deforested ecosystem Science, 199, pp. 492-496, 10.1126/science.199.4328.492

Lohani, S., Dilts, T., Weisberg, P., Null, S., and Hogan, Z. 2020. Rapidly accelerating deforestation in Cambodia's Mekong River Basin: a comparative analysis of spatial patterns and drivers. Water 12, 2191. https://doi.org/10.3390/w12082191

Lu, Z., Zou, S., Qin, Z., Yang, Y., Xiao, H., Wei, Y., Zhang, K., and Xie, J. 2015. Hydrologic Responses to Land Use Change in the Loess Plateau: Case Study in the Upper Fenhe River Watershed. Advances in Meteorology, 2015, 1–10. https://doi.org/10.1155/2015/676030

Malmer, A., Murdiyarso, D., Bruijnzeel, L. A., and Ilstedt, U. 2009. Carbon sequestration in tropical forests and water: a critical look at the basis for commonly used generalizations Glob. Change Biol., 16, pp. 1-6, 10.1111/j.1365-2486.2009.01984.x

Maltoni, B. 2005. Impact of Remittances on local Communities in Cambodia: The Case of Prey Veng Province.

Marchant, R., Richer, S., Boles, O., Capitani, C., Courtney-Mustaphi, C.J., Lane, P., Prendergast, M.E., Stump, D., De Cort, G., Kaplan, J.O., et al. 2018. Drivers and trajectories of land cover change in East Africa: Human and environmental interactions from 6000 years ago to present. Earth-Sci. Rev,178, 322–378.

Marondedze, A. K., and Schütt, B. 2020. Assessment of soil erosion using the RUSLE model for the Epworth district of the Harare Metropolitan province, Zimbabwe. Sustainability 12, 8531. https://doi.org/10.3390/su12208531

Malhi, Y., Roberts, J.T., Betts, R.A., Killeen, T.J., Li, W., and Nobre, C.A. 2008. Climate Change, Deforestation, and the Fate of the Amazon. Science 319(5860), 169-172.

Meijer, J., Shames, S., Scherr, S. J., and Giesen, P. 2018. Spatial Scenario Modelling to Support Integrated Landscape Management in the Kilombero Valley Landscape in Tanzania; PBL Netherlands Environmental Assessment Agency: The Hague, The Netherlands.

Mekong River Commission (MRC). 2016. Land Cover Map of the Lower Mekong Basin (MRC Technical Paper No. 59), Information and Knowledge Management Programme. Mekong River Commission, Phnom Penh, Cambodia.

Mekong River Comission (MRC). 2005. Overviews of Hydrology of the Mekong Basin. Mekong River Comission, Vientiane.

Ministry of Agriculture, Forestry and Fisheries (MAFF). 2018. Land Degradation Neutrality Targets. Ministry of Agriculture, Forestry and Fisheries, Phnom Penh, Cambodia.

Ministry of Environment (MoE). 2018. Cambodia Forest Cover 2016. Ministry of Environment, Phnom Penh, Cambodia.

Montgomery, D.R. 2007. Soil erosion and agricultural sustainability. Proceedings of the National Academy of Sciences 104, 13268–13272. https://doi.org/10.1073/pnas.0611508104

Msofe, N. K., Sheng, L., and Lyimo, J. 2019. Land use change trends and their driving forces in the Kilombero ValleyFloodplain, Southeastern Tanzania.Sustainability,11, 505.

Mustard, J., DeFries, R., Fisher, T., and Moran, E.F. 2004. Land use and land cover change pathways and impacts M.A. Cochrane (Ed.), Land Change Science: Observing, Monitoring, and Understanding Trajectories of Change on the Earth's Surface, SpringerVerlag, Dordrecht, the Netherlands.

Nalin, S., Mony, K., Hazarika, M.K., and Samarakoon, L. 2010. Land cover/land use change detection in Tonle Sap Watershed, Cambodia, in: Asian Conference on Remote Sensing. Presented at the Asian Conference on Remote Sensing, Hanoi, Vietnam.

Neary, D.G., Ice, G.G., and Jackson, C.R. 2009. Linkages between forest soils and water quality and quantity. Forest Ecology and Management, 258(10), 2269–2281. https://doi.org/10.1016/j.foreco.2009.05.027

Neef, A., Touch, S., and Chiengthong, J. 2013. The politics and ethics of land concessions in rural Cambodia. J. Agric. Environ. Ethics, 26, 1085–1103.

Nhemachena, C., Matchaya, G., Nhemachena, C., Karuaihe, S., Muchara, B., and Nhlengethwa, S. 2018. Measuring Baseline Agriculture-Related Sustainable Development Goals Index for Southern Africa. Sustainability,10, 849.

Notter, B., Hurni, H., Wiesmann, U., and Ngana, J.O. 2013. Evaluating watershed service availability under futuremanagement and climate change scenarios in the Pangani Basin.Phys. Chem. Earth,61–62, 1–11.

Nunes, C., and Auge, J.I. 1999. Land-use and land-cover change (LUCC): Implementation strategy. IGBP Report No. 48, IHDP Report No. 10, Stockholm, Bonn.

Nut, N., Mihara, M., Jeong, J., Ngo, B., Sigua, G., Prasad, P.V.V., and Reyes, M.R. 2021. Land use and land cover changes and its impact on soil erosion in Stung Sangkae catchment of Cambodia. Sustainability, 13(16), 9276. https://doi.org/10.3390/su13169276

Ogden, F.L., Crouch, T.D., Stallard, R.F., and Hall, J.S. 2013. Effect of land cover and use on dry season river runoff, runoff efficiency, and peak storm runoff in the seasonal tropics of Central Panama Water Resour. Res., 49 (2013), pp. 8443-8462, 154 10.1002/2013WR013956

Op de Hipt, F., Diekkrüger, B., Steup, G., Yira, Y., Hoffmann, T., Rode, M., Näschen, K. 2019. Modeling the impactof climate change on water resources and soil erosion in a tropical catchment in Burkina Faso, West Africa.Sci. Total Environ. 653, 431–445.

Oliveira, L.J., Costa, M.H., Soares-Filho, B.S., Coe, M.T. 2013. Lrge-scale expansion of agriculture in Amazonia may be a no-win scenario. Environ Res Lett 8:024021. https://doi.org/10.1088/17489326/8/2/024021

Peel, M.C., McMahon, T.A., Finlayson, B.L., and Watson, F.G.R. 2001. Identification and explanation of continental differences in the variability of annual runoff. Journal of Hydrology, 250: 224-240.

Pimentel, D., and Burgess, M. 2013. Soil erosion threatens food production. Agriculture 3, 443–463. https://doi.org/10.3390/agriculture3030443

Piao, S., Friedlingstein, P., Cias, P., de Noblet-Ducoudré, N., Labat, D., and Zaehle, S. 2007. Changes in climate and land use have a larger direct impact than rising CO2 on global river runoff trends. Proc. Natl. Acad. Sci. USA, 104, 15 242–15 247.

Raza, A., Ahrends, H., Habib-Ur-Rahman, M., and Gaiser, T. 2021. Modeling approaches to assess soil erosion by water at the field scale with special emphasis on heterogeneity of soils and crops. Land 10, 422. https://doi.org/10.3390/land10040422

Renard, K.G., Foster, G.R., Weesies, G.A., McCool, D.K., and Yoder, D.C. 1997. Predicting soil erosion by water: a guide to conservation planning with the Revised Universal Soil Loss Equation (RUSLE), Handbook No. 703. United States Department of Agriculture.

Ros, B., Nang, P., and Chhim, C. 2011. Agricultural development and climate Change: The case of cambodia. CDRI working pater series No. 65. Cambodia’s leading independent development policy research institute, Phnom Penh, Cambodia.

Sadhwani, K., Eldho, T.I., Jha, M.K., and Karmakar, S. 2022. Effects of Dynamic Land Use/Land Cover Change on Flow and Sediment Yield in a Monsoon-Dominated Tropical Watershed. Water, 14(22), 3666. https://doi.org/10.3390/w14223666

Saddique, N., Mahmood, T., and Bernhofer, C. 2020. Quantifying the impacts of land use/land cover change on the water balance in the afforested River Basin, Pakistan. Environmental Earth Sciences, 79(19), 448. https://doi.org/10.1007/s12665-020-09206-w

Saleh, A., and Gallego, O. 2007. Application of SWAT and APEX using the SWAPP (SWATAPEX) program for the Upper North Bosque River Watershed in Texas. Transactions of the ASABE 50, 1177–1187. https://doi.org/10.13031/2013.23632

Schmid, H.P., Grimmond, C.S.B., Cropley, F., Offerle, B., and Su, H. 2000. Measurements of CO2 and energy fluxes over a mixed hardwood forest in the mid-western United States. Agric. For. Meteorol. 103, 357–374. https://doi.org/10.1016/S0168-1923(00)00140-4.

Searchinger, T., Heimlich, R., Houghton, R.A., Dong, F., Elobeid, A., Fabiosa, J., Tokgoz, S., Hayes, D. and Yu, T.-H. 2008. Use of U.S. Croplands for Biofuels Increases Greenhouse Gases Through Emissions from Land-Use Change. Science 319(5867), 1238-1240.

Schlesinger, W.H., and Jasechko, S. 2014. Transpiration in the global water cycle. Agricultural and Forest Meteorology, 189–190, 115–117. https://doi.org/10.1016/j.agrformet.2014.01.011

Shao, G., Guan, Y., Zhang, D., Yu, B., and Zhu, J. 2018. The Impacts of Climate Variability and Land Use Change on Streamflow in the Hailiutu River Basin. Water 10, 814. https://doi.org/10.3390/w10060814

Siddik, M.S., Tulip, S.S., Rahman, A., Islam, Md. N., Haghighi, A.T., and Mustafa, S.M.T. 2022. The impact of land use and land cover change on groundwater recharge in northwestern Bangladesh. Journal of Environmental Management, 315, 115130. https://doi.org/10.1016/j.jenvman.2022.115130

Song, L., and Zhang, J. 2012. Hydrological response to climate change in Beijiang River Basin based on the SWAT model. Procedia Engineering 28, 241–245. https://doi.org/10.1016/j.proeng.2012.01.713

Sourn, T., Pok, S., Chou, P., Nut, N., Theng, D., Rath, P., Reyes, M.R., and Prasad, P.V.V. 2021. Evaluation of land use and land cover change and its drivers in Battambang Province, Cambodia from 1998 to 2018. Sustainability, 13(20), 11170. https://doi.org/10.3390/su132011170

Sun, P., Wu, Y., Wei, X., Sivakumar, B., Qiu, L., Mu, X., Chen, J., and Gao, J. 2020. Quantifying the contributions of climate variation, land use change, and engineering measures for dramatic reduction in streamflow and sediment in a typical loess watershed, China. Ecological Engineering 142, 105611. https://doi.org/10.1016/j.ecoleng.2019.105611

Tang, W., Shan, B., Zhang, H., Zhang, W., Zhao, Y., Ding, Y., Rong, N., and Zhu, X. 2014. Heavy metal contamination in the surface sediments of representative limnetic ecosystems in Eastern China. Sci Rep 4, 7152. https://doi.org/10.1038/srep07152

Tan, J., Jakob, C., Rossow, W. B., and Tselioudis, G. 2015. Increases in tropical rainfall driven by changes in frequency of organized deep convection. Nature, 519(7544), 451–454. https://doi.org/10.1038/nature14339

Tan-Soo, J.-S., Adnan, N., Ahmad, I., Pattanayak, S. K., and Vincent, J. R. 2016. Econometric Evidence on Forest Ecosystem Services: Deforestation and Flooding in Malaysia. Environmental and Resource Economics, 63(1), 25–44. https://doi.org/10.1007/s10640-014-9834-4

Van der Ent, R.J., Savenije, H.H.G., Schaefli, B., and Steele-Dunne, S.C. 2010. Origin and fate of atmospheric moisture over continents: Origin and fate of atmopheric moisture. Water Resources Research, 46(9). https://doi.org/10.1029/2010WR009127

Vaighan, A.A., Talebbeydokhti, N., and Bavani, A.M. 2017. Assessing the impacts of climate and land use change on streamflow, water quality and suspended sediment in the Kor River Basin, Southwest of Iran. Environ Earth Sci 76, 543. https://doi.org/10.1007/s12665-017- 6880-6

Vertessy, R.A., Watson, F., O'Sullivan, S., Davis, S., Campbell, R., Benyon, R., and Haydon, S. 1998. Predicting water yield from mountain ash forest catchments. Ind. Rep, 98, 38.

Wang, G.Q., Zhang, J.Y., He, R.M., Jiang, N.Q., and Jing, X.A. 2008. Runoff reduction due to environmental changes in the Sanchuanhe River basin. Int J Sedim Res 23:174–180

Wagner, P.D., Bhallamudi, S.M., Narasimhan, B., Kumar, S., Fohrer, N., and Fiener, P. 2017. Comparing the effects of dynamic versus static representations of land use change in hydrologic impact assessments. Environ. Model. Softw. https://doi.org/10.1016/j.envsoft.2017.06.023.

Whitehead, P.G., and Robinson, M. 1993. Experimental basin studies-an international and Historical perspective of forest impacts J. Hydrol., 145, pp. 217-230, 10.1016/0022-1694(93)90055-E

Wilkinson, B.H., and McElroy, B.J. 2007. The impact of humans on continental erosion and sedimentation. Geological Society of America Bulletin 119, 140–156. https://doi.org/10.1130/B25899.1

Williams, J.R., Arnold, J.G., Srinivasan, R., and Ramanarayanan, T.S. 1998. APEX: A New Tool for Predicting the Effects of Climate and CO2 Changes on Erosion and Water Quality, in: Boardman, J., Favis-Mortlock, D. (Eds.), Modelling Soil Erosion by Water. Springer Berlin Heidelberg, Berlin, Heidelberg, pp. 441–449. https://doi.org/10.1007/978-3-642- 58913-3_33

Wischmeier, W.H., and Smith, D.D. 1978. Predicting rainfall erosion Losses: A guide to conservation planning. Department of Agriculture, Science and Education Administration, Washington, DC, USA.

Yeang D. 2013. Improving Tenure Security in Urban Informal Settlements: Improving Tenure Security in Urban Informal Settlements: The Case of Battambang Province in Cambodia.

Yira, Y., Diekkrüger, B., Steup, G., and Bossa, A.Y. 2016. Modeling land use change impacts on water resources in atropical West African catchment (Dano, Burkina Faso).J. Hydrol.,537, 187–199.

Zhang, L., Karthikeyan, R., Bai, Z., and Srinivasan, R. 2017. Analysis of streamflow responses to climate variability and land use change in the Loess Plateau region of China. CATENA 154, 1–11. https://doi.org/10.1016/j.catena.2017.02.012

Zhao, B.Z., Jia, W.W., and Li, F.R. 2006. Effect evaluation of natural forest protection project for forestry enterprises in Daxing'anling of Inner Mongolia. Journal of Northeast Forestry University, 34(2), 84.

CHAPTER 2
Research Site Description

2.1. Stung Sangkae River Catment in Battambang Province

Battambang is part of the greater natural landscape of the Cardamom region (Figure 2.1 and 2.2). The natural habitats of this region form a complex network of interconnected landscapes and watersheds that provide important ecosystem services to the region (Killeen 2012). Sangkae River is one of the key water sources for the foundation of city development in Battambang. It originates from the range of the Elephant and Cardamom Mountains at an elevation of about 1,391-meter sea level (msl), flows from the southwest to North across Battambang Town and joins the Stung Mongkol Borey River at Bac Prea village about 40 kilometers downstream from Battambang Town, and the Stung Sreng River at another further 10 kilometers downstream. It then flows into the Tonle Sap Great Lake. The upper Stung Sangkae River combines two rivers: the Stung Sangkae and the Stung Chamlang Kuoy (CNMC, 2012). At O Dambang, located about five kilometers upstream from Battambang Town, the river splits into the Sangkae and the Stung Chas Rivers, then flows directly into the Tonle Sap Great Lake.

Battambang Province is approximately 11,803 km², and comprises 13 districts, one municipality, 96 communes and 741 villages. In 2005, the total population was 952,306 (185,868 families). By 2008, it had increased to 1,025,174 with 205,351 families, while in 2019 the total population had dramatically declined to 987,400 with 218,584 households (NIS, 2019) due to the migration to work abroad. According to the Report of Annual General Meeting 2018, Ministry of Labour and Vocational Training, the total of migrants working abroad amounted to 1,235,993, in which Thailand: 1,146,685, Republic of Korea: 49,099, Japan: 9,195, Malaysia: 30,113, Singapore: 831, Hong Kong: 54 and Saudi Arabia: 16.

The Sangkae River (or Stung Sangkae in the Khmer language) is one of the main rivers in Battambang province. It is approximately 250 kilometers long and flows through 27 communes of 6 districts in Battambang before draining into the Tonle Sap Great Lake. The river's average depth is 2.35 meters and 6.79 meters in dry and wet seasons, respectively (PDOWRAM, 2013). It provides primary water sources to feed into the minor irrigation system, mainly to irrigate dry-season rice. The Sangkae River delivers a pathway for fish to migrate from the Tonle Sap Lake (TSL) to flooded forests, open fields, and other river channel networks in the wet season. Thus, the Sangkae River is a great fishing ground for local people in Battambang province (Try et al., 2015).

Moreover, it is recognized by the Royal Government of Cambodia (RGC) as an important area for agricultural investment and development. A number of stakeholders have invested in developing land and water resources at Stung Sangkae, including local farmers, donors, national and local government agencies, and business communities. Agricultural production, especially paddy rice production, was expanded and intensified considerably. As a result, the catchment has experienced intense land use and land cover change (LULC), particularly in the last 20 years. With the increase in forest use and other unsustainable land use practices, an examination of the changing patterns of LULC is needed. The geographical context of the Sangkae River catchment is considered to be the province in which flooding has the second highest impact on agriculture, while Prey veng province is considered as the most vulnerable province in Cambodia (RGC, 2006). The site at Prek Toal, which is a floodplain of Sangkae River connected to TSL, consists of forest and floodplain areas that are seasonally submerged, and which are managed for fishing located on either side of the Stung Sangkae, which empties into the Tonle Sap Lake. These are highly productive areas of flooded forest and floodplain that contain areas highly important to migratory birds and that have importance for fish conservation such as the Prek Toal Core Area (e.g. Davidson, 2006; Goes, 2005).

The Stung Sangker River catchment has a total area of 6,052 km², and more than one third of this catchment area is within an elevation from four to 13 meters and is 1,391 meters at the highest point. The catchment at Battambang town gauging station is 3,230 km² (CNMC, 2012). The province is situated in the northwest part of Cambodia about 300 kilometers from Phnom Penh via National Road No. 5. The province borders Beanteay Meanchey, Siem Reap, and Pursat Province. The enclave of Pailin Province and the national border with Thailand frames the western boundary. At its eastern tip, the province is connected to Tonle Sap Lake.

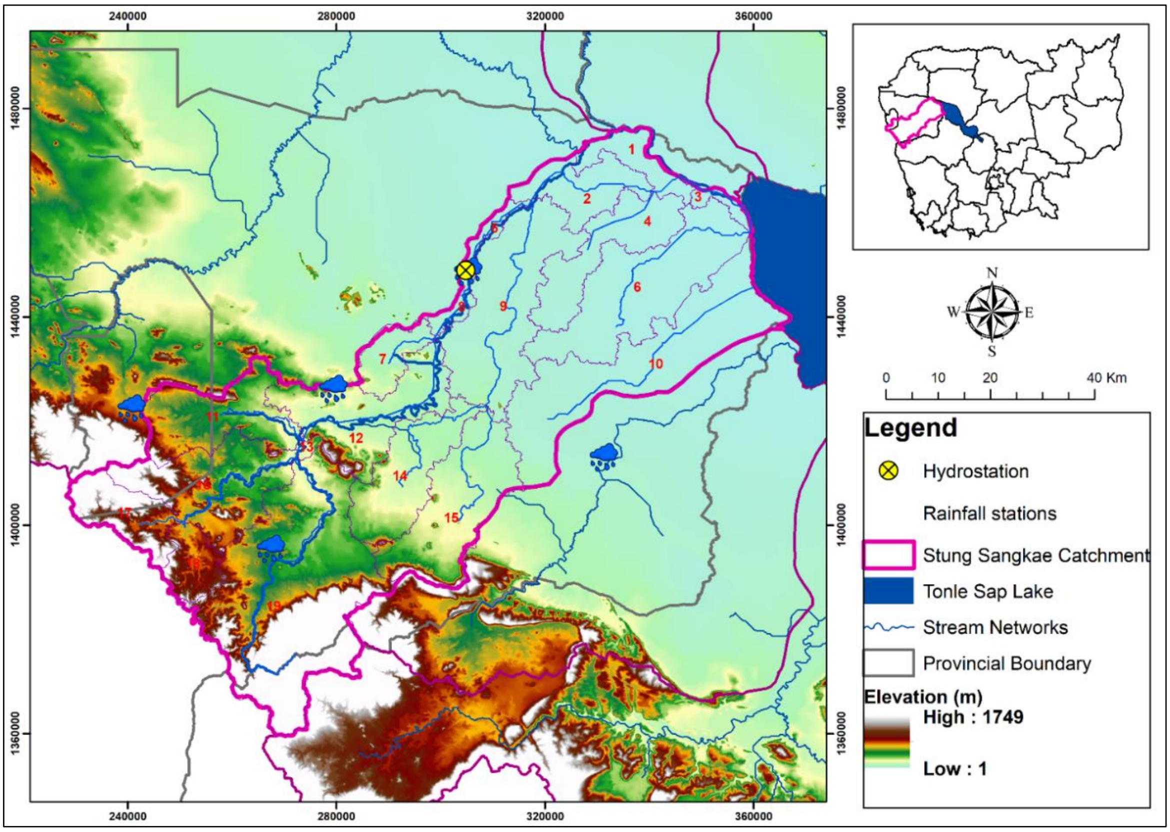

Figure 2.1. Location of the study area

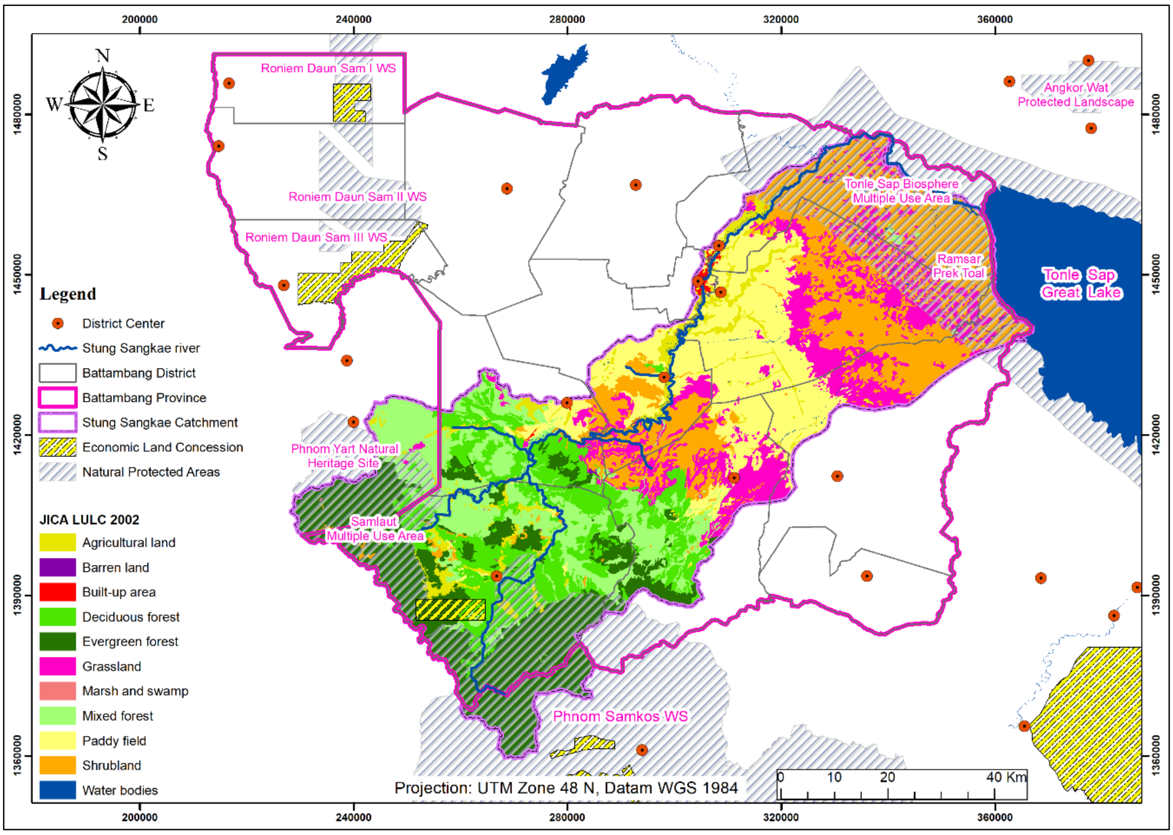

Figure 2.2. Land use of the study area

LULC changes could affect not only on the environment but also on local people consequently. Bürgi et al. (2004) and Wu and Hobbs (2002) indicate that changes in land use are the primary cause of various environmental issues such as soil erosion and water quality. Moreover, the research shows the water quality decline is caused by nitrogen loading increases, resulting in fertilizer use in the expansion of agricultural lands (Mattikalli and Richards, 1996). In developing countries, LULC changes may influence on socioeconomics or local environment (microclimate).

In Cambodia, forest cover has declined dramatically in the last few decades, while agricultural production, especially the cultivation of paddy rice, was expanded and intensified considerably. For instance, the Stung Sangkae catchment has experienced intensive land use and land cover change (LULC), particularly in the last 20 years. With the increase in forest use and other unsustainable land use practices, an examination of the changing patterns of LULC is required. Moreover, the research on hydrological responses and soil erosion loss caused by LULC changes is limited, particularly in the Stung Sangkae catchment, where there is little research on soil erosion reported to date. Most soil erosion, sediment and hydrological studies with SWAT model or other applications were conducted at a large river basin scale such as Tonle Sap River Basin, Lower Mekong Basin (LMB) and Mekong River Basin (MRB). Moreover, there are no specific soil erosion rates that have been investigated in sub-catchments of Tonle Sap Lake (TSL), particular in Stung Sangkae catchment in term of spatial distribution of soil erosion losses in each individual TSL's sub-catchment. Furthermore, the geographic context of the Stung Sangkae River catchment is the province where flooding has the second greatest impact on agriculture in Cambodia after Prey Veng province which is considered to be the most vulnerable province (RGC, 2006). Aside from these, while climate change is causing climate variability in some parts of the world, particularly rainfall patterns, this will intensify and exacerbate soil erosion and lead to drought problems in some regions, particularly areas where land use change is occurring.

This is a new research in Cambodia in terms of using the RUSLE model to estimate soil erosion loss in the catchment scale based on the changes of LULC.

2.2. Resource stresses exacerbated by climate change

There are three protected areas associated with the Sangker River system (Sometimes known as the Battambang River Basin). These partly encompass: Phnom

Samkos Wildlife Sanctuary, Sam Lout Multiple Use Area, and Tonle Sap Multiple Use Area, totalling 710,000 ha. These areas are characterized below (Table 2.1):

Table 2.1. Protected areas in Battambang

Protected area	Provinces	Total area (ha)	Area in basin (ha, %)	Some uniques characteristics
Phnom Samkos Wildlife Sanctuary	Crosses Battambang and Pursat Province	333,750	62,700 (10.8%)	High altitude areas with a wide diversity of forest types. Supports a range of threatened birds in the area.
Samlaut Multiple Use Areas	Crosses Battambang and Pursat Province	60,000	44,900 (74.8%)	An evergreen forest area within the watershed of the Sangke River. It has been degraded by mining, causing severe erosion and increased sedimentation of the river, which flows into the Tonle Sap Lake.
Tonle Sap Biosphere Multiple Use Areas	Battambang (Aek Pnhom and Sangkae district)	316,250	81,900 (25.9%)	Long-standing fish reserve; Great biological, hydrological, and cultural/economic importance.

Source: *Japan International Cooperation Agency, Ministry of Water Resource and Meteorology, Ministry of Agriculture, Forestry and Fisheries (2007)*

Both Phnom Samkos and Samlaut are located upstream of most irrigation systems; therefore, there would be no adverse environmental impact through irrigation promotion in this basin. On the other hand, Tonle Sap Biosphere Multiple Use Area is situated downstream of Sangkae River and it will be affected by water infrastructure development such as irrigation schemes and the increased usage in fertilizer and pesticides. Attention needs to be paid so as to refrain from negatively impacting downstream areas through irrigation (JICA, MOWRAM, and MAFF 2007). The Tonle Sap Biosphere Multiple Use Area is biologically diverse, with over 110 species of fish present. It is home to 11 globally threatened bird species and four near-threatened species such as the Spot-billed Pelican, Greater Adjutant, Bengal Florican, and Oriental Darter, and also supports important populations of reptiles such as Siamese Crocodiles. The planned rehabilitation of existing irrigation schemes located upstream of Tonle Sap Lake does not appear to cause any additional negative impact on the environment. However, if there is an expansion beyond existing schemes, then the environmental monitoring plan must be considered as one of the project components in order to minimize future negative impacts on Tonle Sap Areas (JICA, MOWRAM, and MAFF 2007). The land classification is shown in Table 2.2.

Table 2.2. Land classification by each district, 2009

District	Total area (ha)	Forest land area (ha)		Cultivation area (ha)	Construction area (ha)	Other area (ha)
		Total	Flooded forest area			
Banan	79,600	33,443	-	32,171	12,843	1,143
Thmar Koul	81,700	15,400	15,400	60,100	3,540	1,660
Battambang	11,544	-	-	8,558	8,558	117
Bavel	92,300	17,471	601	49,293	4,541	20,995
Ek Phnom	63,500	46,940	46,940	13,700	2,860	-
Moung Russei	124,995	28,319	28,319	73,965	6,696	16,015
Rotanak Mondul	79,200	25,520	-	46,400	3,780	3,500
Sangkae	83,00	35,200	35,200	40,017	7,763	20
Samlaut	180,300	80,181	-	5,520	6,410	38,509
Sampov Luon	51,900	9,100	-	36,396	450	5,954
Phnom Proek	70,400	8,276	-	32,397	2,602	27,125
Kam Rieng	56,600	5,821	-	47,009	2,100	1,670
Koas Kralor	105,000	30,000	-	60,000	15,000	-
Rukh Kiri	57,688	10,805	-	41,291	5,592	-
Total	1,137,727	246,476	126,460	596,497	78,047	116,708

Source: *National Committee for Democratic Development and Decentralization (NCDD), Battambang Provincial Data Book 2009*

2.3. Resource stresses and trends

More natural forest areas, in particular from protected areas, are being granted to or taken by local communities or businessmen for large-scale agricultural development. Since 2005, people have cleared forested areas to cultivate maize and/or cassava to market to private factories. Most of such products are exported to Thailand. Newly cleared land requires limited amounts of fertilizer, but later on more and more fertilizer will be used as the land productivity, watershed, and water resources degrade if no countermeasures are taken.

Currently, an estimated 191,492 ha of forest cover is left, of which 150,992 ha is under the forestry administration's management and 40,000 ha is under the provincial department of the environment. However, protected areas are increasingly under threat from land encroachment for large-scale agricultural land development (Provincial Development of Planning, 2015).

Key informants from the provincial department of agriculture reveal that the area under agricultural land will increase to 500,000 ha from 2015 to 2018, of which 100,000 ha will be dry season rice cultivation as well as upland rice crop. This trend for commercial cash crop production is likely to encroach significantly on both protected areas and recession flooded forest areas (Interview with deputy director, provincial department of environment, dated 22 December 2014).

Interviews with officials from the provincial department of environment also confirm the significant loss of protected areas, including:

• Samkos Wildlife Sanctuary: 14,000 ha of land has been taken from these protected areas, of which 8,000 ha was provided to local community members with legal title while the land title to an additional 6,000 ha was in a process of being issued to farmers.

• Roneam Dounsar Wildlife Sanctuary: Covers an area of more than 170,000 ha in two provinces: Banteay Meanchey and Battambang (70,000 to 80,000 ha). Now there are only around 3,000 to 4,000 ha left in Battambang due to land concession and encroachment.

• Samlout Multiple Use Area: More than 60,000 ha in Battambang and Pailin, of which 40,000 ha is located in Battambang. Currently, there are around 10,000 ha left due to land clearance for cash crops and commercial farming.

2.4. Natural disasters

2.4.1. Flooding impacts

According to the provincial water resource department in Battambang, a river with water levels above 12.5 meters high would flood the city. Flooding has been recorded in every Sangkat (commune) of Battambang municipality during the rainy season from June to December. In 2013, serious floods affected the whole province (flooding occurred mostly in October to December). The highest level of flooding occurred in Sangkats Svay Por and Preak Preak Sdach with water depths ranging from oneto two meters. Table 2.3 below summarizes the annual flooding capacity happened in Stung Sagnkae River.

Official records from various documents show that in 2011 (with water levels up to 13.95 m) floods affected 31,458 people (7,111 households in 31 communes in nine districts), inundated 52,503 ha, and destroyed 36,266 ha of rice fields. Flooding in 2013 was even more serious as water levels reached a historical height of 14.2 meters high along Sangke

River (normally 12.5 meters, water started to overflow from the river to the town and areas in lowlands or wetlands).

Floods in late 2013 are considered as the worst in 70 years (MoWRAM, 2013). Various sources of water from upstream, including torrential rain, concentrated throughout the Sangker River including other watershed areas down the river and across the province.

Table 2.3. Flood record of Stung Sangkae River

Year	Max. Annual water level (m)	Annual Flood (m^3/s)	Year	Max. Annual water level (m)	Annual Flood (m^3/s)
1999	12.37	634	2010	11.12	337
2000	13.44	1009	2011	13.95	1235
2001	12.14	569	2012		
2002	11.59	433	2013		
2003	13.02	846	2014		
2004	12.08	552	2015		
2005	13.39	988	2016		
2006	13.71	1125	2017		
2007	13.50	1034	2018		
2008	12.14	569	2019		
2009	12.08	552	2020		

Source: Cities Development Initiative for Asia and Asian Development Bank (2010) and Provincial Department of Water Resource and Meteorology (2013)

2.4.2. Drought impacts

Climate change is impacting Cambodia through more frequent, abnormal climate events with increasing temperatures, decreasing rainfall, and the delay of the monsoon onset – all contributing to the occurrence of droughts. Tonle Sap provides Cambodians with between 60 and 70 percent of their annual protein intake. In 2019, the amount of water flooding into the Tonle Sap was low, and fishing communities had lower fish catches than the previous years. Some districts, cities and provinces had a shortage of domestic water such as Khemarak Phumin city of Koh Kong, Stung Staung of Kampong Thom province, stung Maung Russey and Stung Sangker of Battambang, Ta Pon reservoir of Koh Kong, stung Mongkulborey, Trapaing Thmar reservoir of Bateay Meanchey. The drought expanded into the rainy season because of the delay of the onset of rains. This had an impact on the agricultural sector in 16 provinces, which affected 324,641 ha of rice and damaged 67,663 ha, of which 25,539 ha of rice could be recovered; 44,734 ha of other crops were affected and 7,746 ha damaged (Table 2.4).

Table 2.4. Summary of major drought events and their impacts on agriculture in Cambodia

Affected region	Affected rice (ha)	Affected crop (ha)	Recovered (ha)
Tboung Khmum	5,150		467
Kampong Cham	6,003		
Prey Veng	16,211		
Kandal	503		
Kampong Thom	15,957		648
Preah Vihear	4,610		
Mondulkiri	223		
Udormeanchey	872		
Siem Reap	36,410		
Banteay Meanchey	67,681		
Battambang	104,718	44,734	23522
Pailin	1,610		
Svay Rieng	1,736		580
Pursat	62,381		312
Takeo	185		
Kampong Chhnang	266		
Phnom Penh	125		

Source: *Mekong Annual Hydrology Report (2019)*

Reference of this chapter

Bürgi, M., Hersperger, A.M. and Schneeberger, N. 2004. Driving forces of landscape change -current and new directions. In: Landscape Ecology 19 (8): 857-868. doi:10.1007/s10 980- 005-0245-3.

Cities Development Initiative for Asia and Asian Development Bank. 2010. Battambang Urban Improvements to Mitigate Climate Change, Cambodia. Cities Development Initiative in Asia and Asian Development Bank: Manila.

Cambodia National Mekong Committee (CNMC). 2012. Basin development plan programme: Profile of Tonle Sap sub-area (SA-9C). Cambodia National Mekong Committee: Phnom Penh.

Davidson, P.J.A. 2006. The biodiversity of the Tonle Sap Biosphere Reserve. 2005 status review. Prep. by Wildlife Conservation Society for the Tonle Sap Conservation Project.

Goes, F. 2005. Four years of waterbird conservation activities in Prek Toal Core Area, Tonle Sap Biosphere Reserve (2001-2004). Wildlife Conservation Society (WCS) Cambodia Program, Phnom Penh.

Japan International Cooperation Agency (JICA), Ministry of Water Resource and Meteorology (MWRAM), and Ministry of Agriculture, Forestry and Fisheries (MAFF). 2007. Basin-Wide Basic Irrigation and Drainage Master Plan Study in the Kingdom of Cambodia: Interim Report. Japan International Cooperation, Ministry of Water Resource and Meteorology, and Ministry of Agriculture, Forestry and Fisheries: Phnom Penh.

Killeen, T.J. 2012. The Cardamom Conundrum: Reconciling Development and Conservation in the Kingdom of Cambodia. National University of Singapore Press: Singapore.

Mattikalli, N.M., and Richards, K.S. 1996. Estimation of surface water quality changes in response to land use change: Application of the export coefficient model using remote sensing and geographical information system. Journal of Environmental Management, 48(3), pp. 263-282, DOI: 10.1006/jema.1996.0077

Ministry of Water Resource and Meteorology and Asian Development Bank. 2013. Cambodia Water Resource Profile. TA 7610-CAM: Supporting Policy and

Institutional Reforms and Capacity Development in Water Sector. Ministry of Water Resource and Meteorology and Asian Development Bank: Phnom Penh.

National Committee for Democratic Development and Decentralization (NCDD). 2010. Battambang Provincial Profile. National Committee for Democratic Development and Decentralization: Phnom Penh.

National Institute of Statistics (NIS). 2019. General population census of the Kingdom of Cambodia 2019. Ministry of Planning, Phnom Penh, Cambodia.

Provincial Department of Water Resource and Meteorology (PDOWRAM). 2013. Presentation of Flood Damage in Battambang (Khmer version). Provincial Department of Water Resource and Meteorology: Battambang.

Royal Government of Cambodia (RGC). 2006. National Adaptation Programme of Action to Climate Change (NAPA). Phnom Penh, Cambodia.

Try, T., Dyna, E., Ferrer, A.J., Yen, B.T., Kura, Y., and Sebastian, L.S. 2015. Situation Analysis and Needs Assessment Report for Rohal Soung Village and Battambang Province, Cambodia. CGIAR Research Program on Climate Change, Agriculture and Food Security (CCAFS), Copenhagen, Denmark.

CHAPTER 3

Impacts of Land Use and Land Cover Changes on Hydrological Responses in Stung Sangkae River Catchment from 2002 to 2015

3.1. Introduction

Generally, regional impacts of land use change on hydrology vary from place to place and need to be considered for specific circumstances and environments (Wang et al. 2014). Rapid population growth, urbanization, and economic development increase water, energy, and food demands, accelerating pressures on land and water resources across the globe (Aghsaei et al., 2020). Recently, many regions worldwide have undergone considerable land-use and land cover (LUC) changes, especially in developing countries. These LUC changes significantly influence various hydrological components such as evapotranspiration, soil infiltration, groundwater recharge, surface runoff generation, and sediment generation (Öztürk et al., 2013). As such, LUC is considered an important input in many applications related to water resources assessment as well as soil erosion and degradation assessment (DeFries and Eshleman, 2004). In the context of LUC change, understanding and evaluating the responses of hydrology and sediment yield are indispensable for the sustainable management of land and water resources of a river basin. Effective management and conservation of water and soils under changing LUC scenarios can be attainable through reliable runoff and sediment generation estimations in a river basin.

Previous studies have analyzed the impact of land use and land cover changes in some watersheds (Kalantari et al., 2014; Noda et al., 2017; Muto et al., 2022), as they are considered the two key drivers exerting influence on water and sediment dynamics. Moreover, in Mekong Basin, some research has also been done on the impacts of land use change on hydrology (Markert et al., 2018; Shrestha et al., 2018), but research on the contribution of individual LULC to the total runoff and the impacts of LULC changes on watershed hydrology is lacking. In particular, there is a lack of information for evaluating the benefits of soil and water conservation in the Stung Sangkae River catchment, where it is difficult to distinguish the impacts of LULC changes on hydrology. A greater understanding of the contribution of individual LULC change to runoff and the effects of LULC changes on the hydrology at different scales is needed to guide comprehensive natural resources management in this region.

Methods for assessing the hydrological impacts of land use changes in watersheds include comparisons of paired catchments, statistical analysis, and hydrological modeling (Li et al., 2009; Khoi and Suetsugi, 2014; Li et al., 2012). Hydrological modeling is the most suitable for scenario studies at different scales among these approaches. Widely used hydrological models in studies on the impacts on watershed hydrology include the Hydrologic Simulation Program, FORTRAN, the Soil and Water Assessment Tool (SWAT), and WaTEM/SEDEM (Mango et al. 2011; Nie et al. 2011; Khoi and Suetsugi, 2014; Wang et al. 2014). It is readily available and user-friendly for data input (Arnold et al. 1998).

The overall objectives of this study are to investigate the contributions of individual LULC change to runoff and to determine the impacts of LULC changes on the hydrology of the Stung Sangkae River catchment by an integrated approach that combines hydrological modeling and national LULC 2002 and LULC 2015. The specific objectives are (1) to investigate the LULC changes in the catchment from 2000 to 2018 with national LULC maps in 2002 and 2015; (2) to assess the hydrological effects of individual land uses, and (3) to simulate responses of hydrologic components to land use changes at basin and subbasin scales. The results should assist decision-makers in target water resources planning and vegetation restoration on the Stung Sangkae River catchment.

3.2. Methodologies

3.2.1. Description of Study Area

The Stung Sangkae catchment (605,170 ha), which is the third-largest tributary of the Tonle Sap Basin River system, is located in the upper north-western part of Cambodia between 12°13′–13°24′ N and 102°35′–103°42′ E (Figure 3.1). The topography is level within the floodplain region and rough with slopes at the upland portion of the catchment, having elevations extending from 4 m at the most reduced point to 1,413 m a.s.l at the most noteworthy point. The main river that flows through the catchment, Sangkae River, lies between the tributaries of the Tonle Sap Great Lake in the upper western part of the catchments. Agriculture is the main local economic activity and the main source of livelihood. Meteorological data collected from six weather stations in 2007–2018 showed that the average annual precipitation in the study area varied from 1,308 mm at Moung Ruessei station to 1,577 mm at Samlout station, with little change during the year. The major soil types in the region are categorized into 4: (1) Gleysols are wetland soils, which in the natural state are continuously water-saturated within 50 cm of the surface for extended periods; (2) Luvisols are a type of soil in which highly active clay migrates from the top part of the profile, usually gray, and is deposited in the B layer, usually brown; (3) Nitisols are mainly deep, well-drained soils with a stable structure and high nutrient content; and (4) Acrisols are clay-wealthy soils which can be fairly vulnerable to erosion.

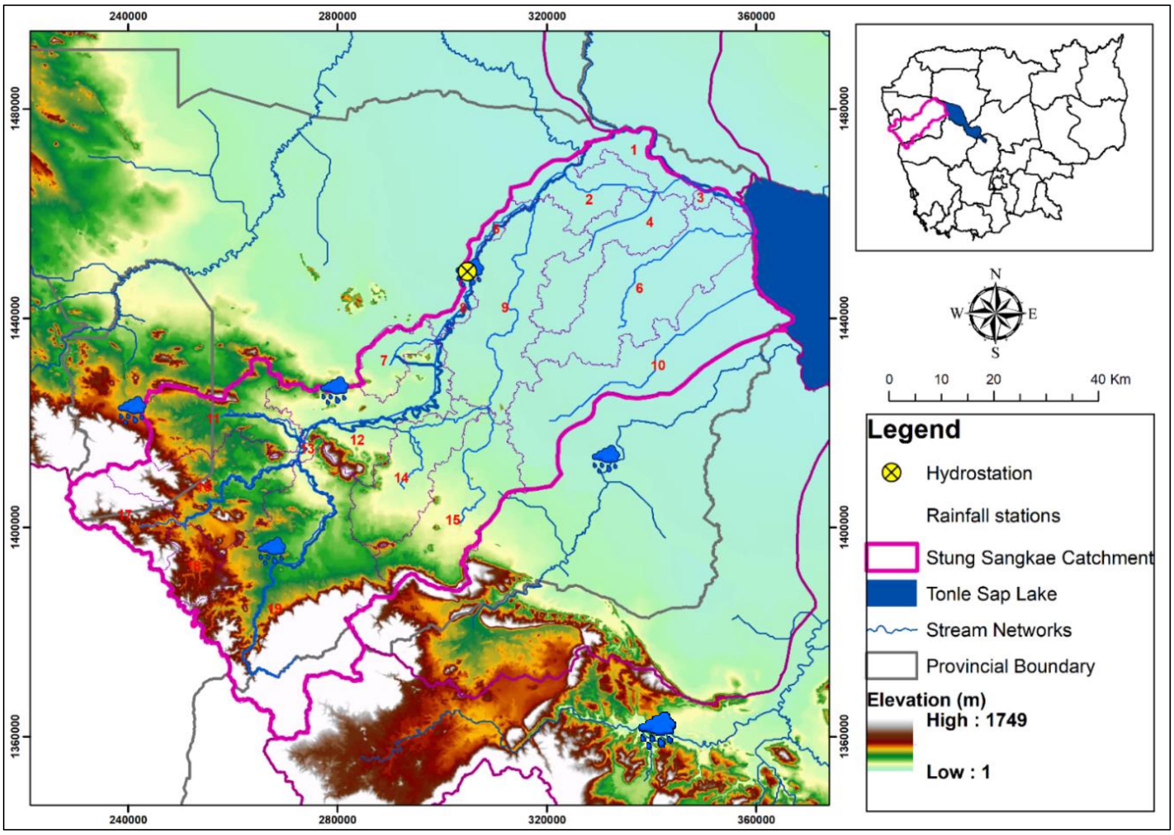

Figure 3.1. Location map of the research catchment and meteorological stations within the research area

3.2.2. Description of SWAT Model

The Soil and Water Assessment Tool (SWAT) model was developed by the US Department of Agriculture-Agriculture Research Service (Neitsch et al., 2005). It is a conceptual, physically-based, daily-time-stepped, basin-scale, semi-distributed model operating on a continuous time-step. Model components include weather, hydrology, erosion/sedimentation, plant growth, nutrients, pesticides, agricultural management, channel management, and pond/reservoir management. This model has several advantages as it has integrated multiple environmental processes, uses readily available inputs, is user-friendly, is physically based, and is computationally efficient to work in large basins in a reasonable time (Pai et al., 2012). SWAT was used with ArcSWAT 2012 release in an ArcGIS 10.x extension. This interface streamlines data entry, creation of required input files, and manipulation of parameters while allowing easy observation of spatial parameters in the ArcGIS environment. In ArcSWAT, the watershed has been delineated into a series of sub-basins, which have been further subdivided into Hydrological Response Units (HRUs) consisting of homogeneous land use, management, and soil properties. The model calculations were performed on an HRU basis and flow and water quality variables were routed from HRU to sub-basins and then to the watershed. SWAT estimates soil erosion using the Modified Universal Soil Loss Equation (MUSLE) (Zhang and Nearing, 2005). The strong emphasis on vegetation and hydrological interactions within SWAT makes it a preferred model for this land-use-based hydrological analysis.

3.2.2.1. Hydrological Component and Water Balance of SWAT

The catchment area hydrology simulation was conducted in two separate phases. The first phase was the land phase of the water cycle, which controls the amount of water, sediment, nutrients, and pesticides entering the main channel in each sub-basin. The second division was the conducting phase of the water cycle, defined as the movement of water, sediment, nutrients, and organic chemicals through the watershed's network of channels to the outlet (Figure 3.2). In the land phase of the water cycle, SWAT simulates the water cycle based on the water balance equation.

$$\mathrm{SWt} = \mathrm{SWo} + \sum_{i=0}^{t} (R_{day} - Q_{surf} - E_{a} - W_{sweep} - Q_{qw}) \tag{1}$$

Where: SWt is the final soil water content (mm), SWo is the initial soil water content on day i (mm), t is the time (days), R_{day} is the amount of precipitation on day i (mm), Q_{surf} is the amount of surface runoff on day i (mm), E_a is the amount of evapotranspiration on day i (mm), W_{sweep} is the amount of water entering the vadose zone from the soil profile on day i (mm), and Qgw is the amount of return flow on day i (mm) (Arnold, 1998; Neitsch, 2005).

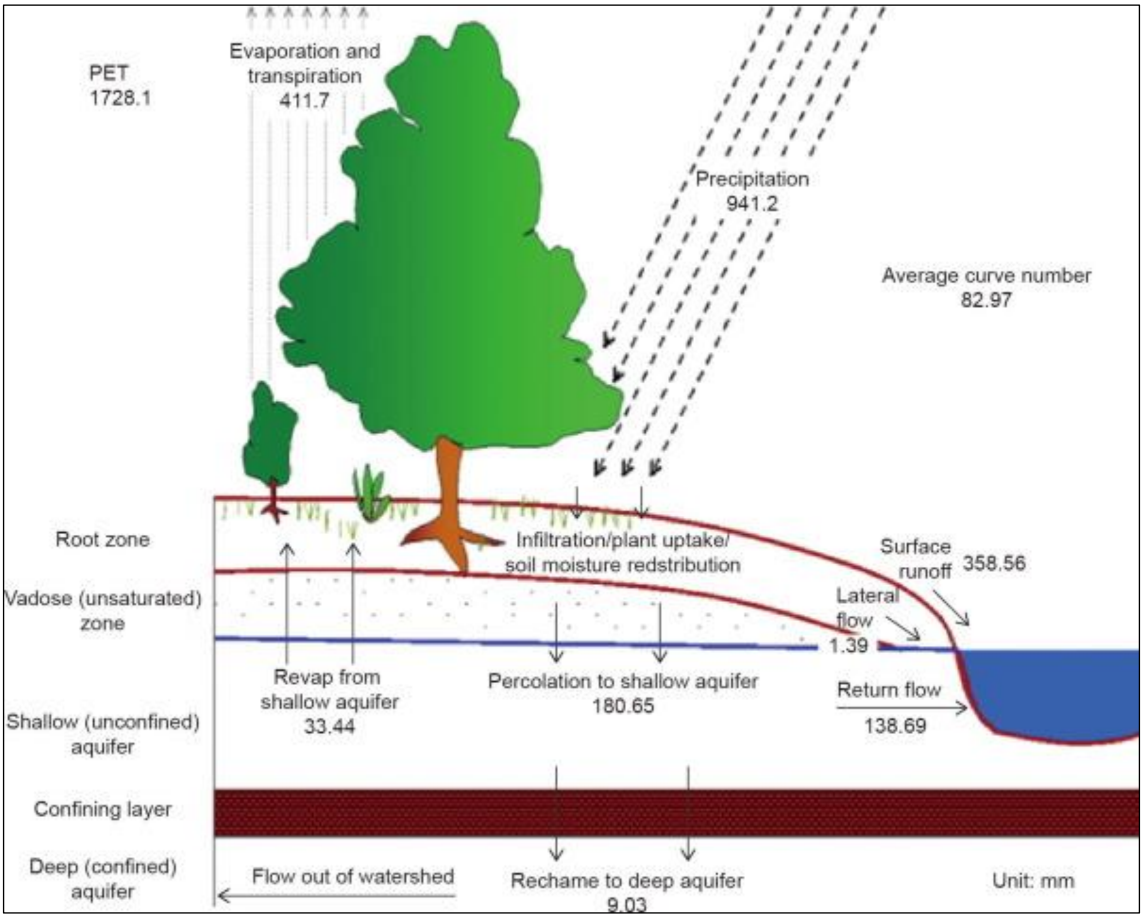

Figure 3.2. Hydrological cycle in the conceptual SWAT model

One critical parameter evaluated for sustainable water resource management of the study area is the water yield. Water yield is the aggregate sum of water leaving the HRU and entering the principle channel during the time step (Arnold et al., 2011). Water yield within a watershed is evaluated by the model based on Eq. (2):

$$W_{yld} = Q_{surf} + Q_{qw} + Q_{lat} - T_{loss} \tag{2}$$

where W_{yld} is the measure of water yield (mm), Q_{surf} is the surface runoff (mm), Q_{lat} is the lateral flow contribution to stream (mm), Q_{qw} is the groundwater contribution to streamflow (mm), and $T_{loss}$is the transmission losses (mm) from tributary in the Hydraulic Response Units (HRU) by means of transmission through the bed. The estimation of surface runoff can be performed by the model using the SCS curve number system by the USDA Soil Conservation Service (Eq. (3)).

3.2.2.2. Surface Runoff Equation of SWAT

Surface runoff occurs whenever the rate of precipitation exceeds the rate of infiltration. The runoff from each HRU is predicted separately and routed for the determination of the aggregate yield for the catchment separately in the SWAT model, thereby increasing the precision and giving an improved physical description of water balance. The concept of infiltration excess runoff is used in SWAT 2012, where it is assumed that runoff occurs whenever the infiltration rate exceeds the rainfall intensity. SWAT offers two methods for estimating surface runoff: the Soil Conservation Service (SCS) curve number procedure (Neitsch, 2005) and the Green and Ampt infiltration method (Green, 1911). Using daily or sub-daily rainfall, SWAT simulates surface runoff volumes and peak runoff rates for each HRU. The SCS curve number equation is:

$$Q_{\mathrm{surf}} = \frac{\left(\mathrm{R}_{\mathrm{day}} - 0.2\mathrm{S}\right)^2}{\left(\mathrm{R}_{\mathrm{day}} + 0.8\mathrm{S}\right)} \tag{3}$$

where, Q_{surf} is the surface runoff or rainfall excess (mm), $\mathrm{R}_{\mathrm{day}}$ is the rainfall depth for the day (mm) and S is the retention parameter.

The retention parameter varies spatially due to changes in soil, land use, management and slope and temporally due to changes in soil water content. The retention parameter is defined as:

$$\mathrm{S} = 254\left(\frac{100}{\mathrm{CN}} - 1\right) \tag{4}$$

where, S is the retention parameter, CN is the curve number for the day.

The SCS curve number is a function of the soil's permeability, land use and antecedent soil water conditions. The curve number value is range from 0 to 100 (Figure 3.3).

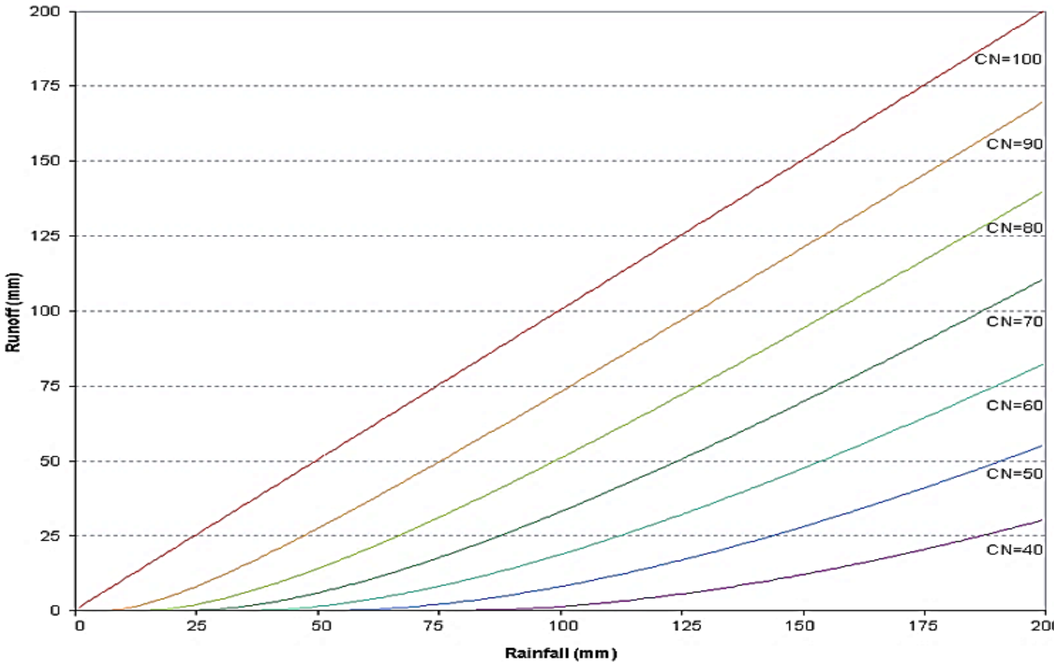

Figure 3.3. Relationship of runoff to rainfall in SCS curve number method

In the SWAT model, the antecedent moisture condition is defined on the basis of Curve- Number Antecedent moisture condition (CN-AMC) (USDA – NRCS, 2004). This is done on the basis of soil moisture content calculated by the model (Neitsch et al., 2011) to determine CN.

Antecedent moisture condition (AMC) is defined as the initial moisture content which exists in the soil at the start of the rainfall-runoff event under consideration. AMC governs the infiltration and initial abstraction. SCS recognizes three levels of AMC for the purpose of practical application, which is mentioned below:

- **AMC-I**: Soils are dry but not to the wilting point
- **AMC-II**: Average condition
- **AMC-III**: Sufficient rainfall has occurred within the immediate last 5 days. Saturated soil condition prevails.

The variation of CN according to AMC-I, AMC-II, AMC-III is known as CN_I, CN_{II} and CN_{III} respectively. CN_{II} can be converted to the other two moisture conditions through the use of equations (5) and (6):

$$\mathrm{CN_I} = \mathrm{CN_{II}} - \left(\frac{20 \cdot (100 - \mathrm{CN_{II}})}{(100 - \mathrm{CN_{II}} + \exp[2.533 - 0.0636 \cdot (100 - \mathrm{CN_{II}})])}\right) \quad (5)$$

$$CN_{III} = CN_{II} \cdot \exp[0.00673 \cdot (100 - CN_{II})] \quad (6)$$

The soil and land use properties are merged into a single parameter in the SCS-CN method (White and Chaubey, 2005). On the basis of infiltration properties of soil, the Natural Resources Conservation Service (NRCS) soil classification is used in SWAT (Neitsch et al., 2011), where soils are categorized to four classes (A, B, C, D) with high, moderate, low and very low infiltration rate respectively (Table 3.1). Permeability, average clay content, infiltration characteristics, and effective depth of soil are some of the significant soil characteristics which affect the hydrological classification of soils. In this classification, under similar cover and storm conditions, a soil group has a similar hydrologic classification.

Table 3.1. Runoff curve numbers for cultivated agricultural lands

Land use	**Hydrologic condition**	**Hydrologic Soil Group**			
		A	B	C	D
Pasture, grassland, or range - continuous forage for grazing	Poor	68	79	86	89
	Fair	49	69	79	84
	Good	39	61	74	80
Meadow - continuous grass, protected from grazing and generally mowed for hay	————	30	58	71	78
Brush - brush - weed - grass mixture with brush the major element	Poor	48	67	77	83
	Fair	35	56	70	77
	Good	30	48	65	73
Woods - grass combination (orchard or tree farm)	Poor	57	73	82	86
	Fair	43	65	76	82
	Good	32	58	72	79
Woods	Poor	45	66	77	83
	Fair	36	60	73	79
	Good	33	55	70	77
Farmsteads - buildings, lanes, driveways, and surrounding lots	————	59	74	82	86

3.2.2.3. Flow Rate Equation of SWAT

Manning's equation for uniform flow in a channel is used to calculate the rate and velocity of flow in a reach segment for a given time step:

$$q_{ch} = \frac{A_{ch} \cdot R_{ch}^{2/3} \cdot slp_{ch}^{1/2}}{n} \quad (7)$$

$$v_c = \frac{R_{ch}^{2/3} \cdot slp_{ch}^{1/2}}{n} \quad (8)$$

where, q_{ch} is the rate of flow in the channel (m^3/s), A_{ch} is the cross-sectional area of flow in the channel (m^2), R_{ch} is the hydraulic radius for a given depth of flow (m), slp_{ch} is the slope along the channel length (m/m), n is Manning's n coefficient for the channel, and v_c is the flow velocity (m/s).

3.2.2.4. Soil Loss Equation of SWAT

The SWAT model comprises two phases: a land phase solved at HRU level, and a stream phase solved at reach (subbasin) level (Neitsch et al., 2011). The land phase comprises the computation of HRU daily water balance and sediment yields. The HRU daily water balance considers precipitation, irrigation, evapotranspiration, surface runoff, lateral flow, and percolation to shallow and/or deep aquifers (Neitsch et al., 2011).

HRU sediment yields for non-urban land use types are estimated with the MUSLE (Williams, 1975):

$$SY_{MUSLE} = 11.8\left(Q \times q_p \times A\right)^{0.56} K.LS.C.P.F_{CRFG} \tag{9}$$

SY = HRU sediment yield (t/day); *Q* = daily runoff volume (mm); *qp* = runoff peak discharge (m3/s); A = HRU area (ha); *C*, *P*, *K*, and *LS* are dimensionless factors accounting for HRU crop cover, soil protection, soil erodibility, and topography as defined in the original Universal Soil Loss Equation (USLE) (Wishmeier and Smith, 1978); and *FCRFG* is a dimensionless factor to account for coarse fragment cover (stoniness). Contrary to the USLE, the MUSLE uses the energy of surface runoff rather than of rainfall to estimate sediment yields, which makes it suitable for application at daily time scale. Since it estimates sediment yields and not gross erosion, the MUSLE already accounts for sediment deposition within the HRU. Conversely, sediment yields from urban HRUs are estimated based on precipitation or with a 'build up/wash off' approach; the latter method was selected in this study, keeping the default settings (Neitsch et al., 2011).

Daily outputs of all HRUs of a subbasin are routed through the stream network (stream phase). The stream phase comprises the routing of water, sediments and other pollutants in the cascading sequence of reaches composing the stream network. All streamflow components (surface runoff, lateral flow, and baseflow) are routed to the reach and along the stream network (Neitsch et al., 2011).

3.2.2.5. Meteorological and Hydrological Data

The long-term records of meteorological data (1995-2018) were collected from five stations (Battambang, Moung Ruessei, Rotanak Mondol, Samlout, and Pailin) which lie inside and outside the border of the study catchment. The observations of meteorological variables of each station were obtained from the Ministry of Water Resources and Meteorology (MOWRAM) of Cambodia. Since temperature, relative humidity, wind speed, and solar radiation data records were limited for all the stations except for the Battambang and Pailin stations, weather generator capabilities of the SWAT model were used to generate those data by using Lalibela station records. Daily stream flow records (2000–2018) at Stung Sangkae gauging station located in Battambang city, in the middle of the catchment, were also obtained from the Department of Hydrology and River Work (DHRW) of MoWRAM.

3.2.2.6. Geographical or Spatial Datasets

The digital elevation model (DEM) of Stung Sangkae River catchment with 30 by 30 m DEM resolution (Figure 3.4.a) was obtained from the United States Geological Survey (USGS) Earth Explorer at https://earthexplorer.usgs.gov. This DEM was used to delineate the catchment and the drainage patterns of the surface area analysis. Subbasin parameters such as slope length of the terrain, slope gradient, and stream network characteristics such as channel length, slope, and width were derived from this DEM. It was also used to determine the hydrological parameters of the catchment, such as flow accumulation, direction, and stream network.

A digitized soil map of Stung Sangkae catchment as shown in Figure 3.4b was acquired from the FAO/UNESCO Soil Map of the World database through the Harmonized World Soil Database (HWSD) because the observed data of the local soil properties in Cambodia is limited and difficult to access. The HWSD is a 30-arc-second raster database (approximately 1 km of spatial resolution) with over 15,000 different soil mapping units that combine existing regional and national updates of soil information around the world. The soil data needed for the physical and chemical characteristics of the soil both play a large role in determining the movement of water and air within the HRU. The properties required by SWAT for each layer of each soil type include the depth of the soil layer, soil texture, hydraulic conductivity, bulk density, and organic carbon content, and soil depth for the different layers of soil were obtained mainly from Tonle Sap River basin integrated development master plan and major soils of the world (FAO, 2006).

The digital land use and land cover data of JICA in 2002 and MRC in 2015 (Figure 3.4.c,d) of the study area was obtained from the Ministry of Agriculture, Forestry and Fisheries (MAFF) of Cambodia and Mekong River Commission (MRC).

For comparative use of the land use land cover evolution, LULC of 2002 was obtained from MAFF, and LULC of 2015 was obtained from MRC with the same scale (Figure 3.4 d). The LULC of the study area is categorized into eleventh groups for JICA 2002 and MRC 2015 respectively. Even though there have been marked changes in coverage but in both reference land uses of forest land (evergreen, deciduous and mixed forests), paddy rice, agricultural land, shrub land and grasslands were the dominant land uses in the study area.

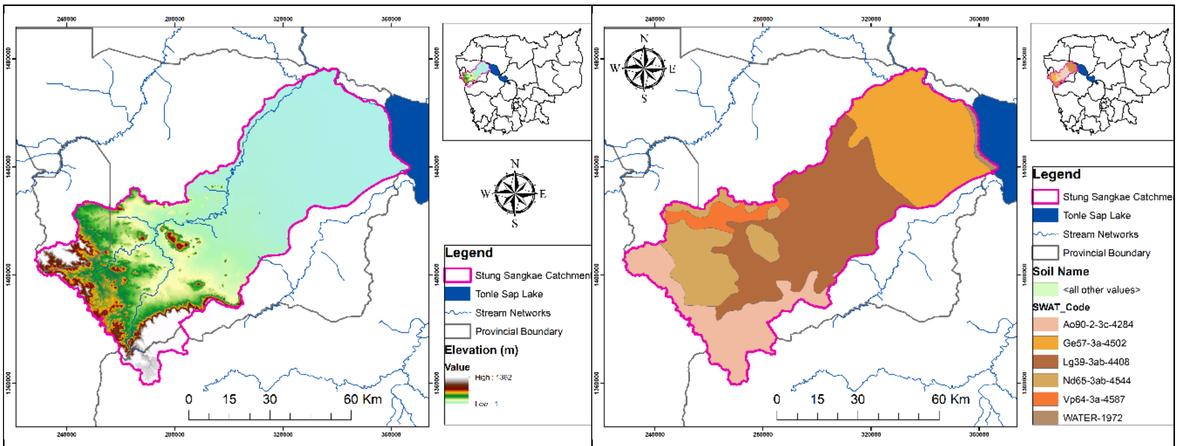

(a) Elevation in meter of the study area | (b) FAO/UNESCO soil of thee study area

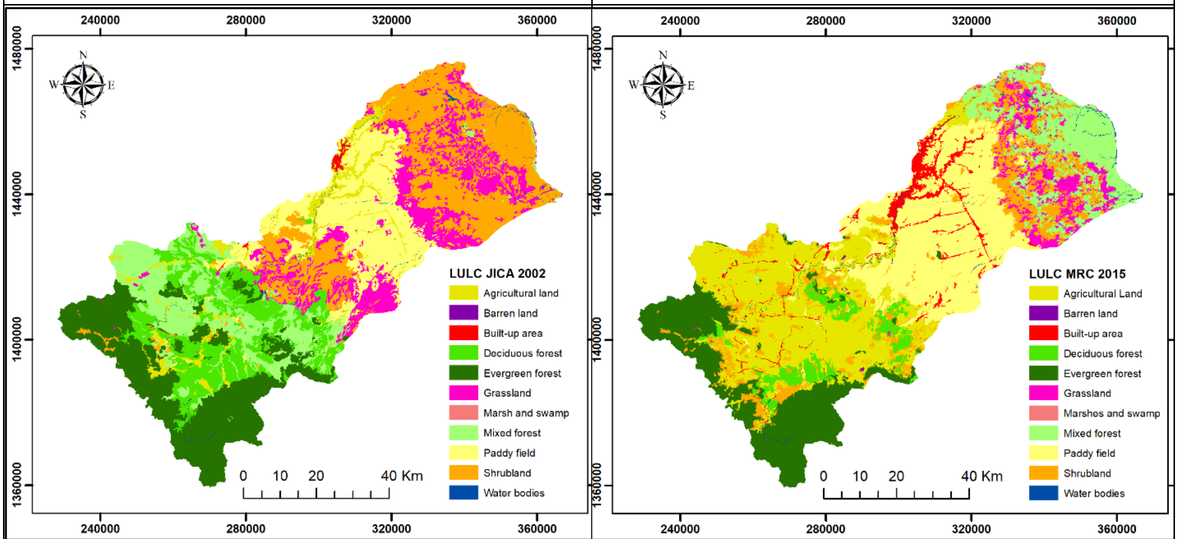

(c) 2002 LULC Map of JICA | (d) 2015 LULC Map of MRC

Figure 3.4. Digital elevation model (a), soil map (b) and historical land use and land cover map of 2002 LULC (c) and 2015 LULC (d) of Stung Sangkae catchment

3.2.2.7. Slope Classes in Subwatershed

To develop the hydrological response unit (HRU) in the SWAT model, the slope is essential. It generates from the resolution of 30 m x 30 m DEM for the study area. Slope classification may be single class or multiclass. For this study, the slope option (an option for considering different slope classes for HRU definition) was selected. Therefore, the slope class in this study was classified into four classes. According to Setegn, et al. (2008), slope classification was used to account for lower range in hydrological modelling. Depending on the slope of 0–2%, 2–5%, 5–10%, 10–25% and >25% were selected for HRU creation of the study Stung Sangkae River catchment. Finally, HRU definition analysis in SWAT helps to load LULC and soil type projects.

3.2.3. SWAT Model Simulation, Sensitivity Analysis, Calibration and Validation

The simulation result cannot be directly used for further analysis. Instead, the ability of the model to sufficiently predict the constituent streamflow should be evaluated through sensitivity analysis, model calibration, and model validation (White and Chaubey, 2005). The first step in the calibration and validation process in SWAT is the determination of the most sensitive parameters for a given watershed or subwatershed (Arnold et. al. 2012).

3.2.3.1. Model Parameterization and Sensitivity Analysis

Parameter sensitivity analysis provides insights as to which parameters contribute most to the output variance due to input variability (Holvoet, et al., 2005). The sensitivity analysis method implemented in SWAT model is called the Latin hypercube One-At-a–Time (LH-OAT) design as proposed by Mories (1991). Sensitivity analysis was then performed to identify those parameters that model outputs were sensitive to. In general, a parameter should be included in calibration if sensitivity analysis identifies that there is a 95% probability that the sensitivity of a variable to a particular parameter is significant. Stream flow sensitivity analysis followed by sediment yield sensitivity analysis was performed for each time reference land uses (2002 LULC and 2015 LULC). For each reference land uses stream flow sensitivity analysis was done with 12 number of interval within latin hypercube for a total of 12 flow parameters (324 iterations) for each LULC maps. The sensitivity of parameters were categorized in to classes of small $0 < RS < 0.05$, Medium $0.05 < RS < 0.2$, High $0.2 < RS < 1$, very high $RS > 1.0$ according to Lenhart, Eckhardt, Fohrer, and Frede (2002). Flow parameters were selected for calibration those their value ranges between very high to medium classes of sensitivity class above.

3.2.3.2. Model Performance Evaluation, Calibration and Validation

Before calibration proceeds, the performance of the model was evaluated for the initial simulation with the model default parameter values. But the default SWAT simulation result was with the discrepancy between measured and simulated outputs. Hence both automatic and manual calibrations was done respectively. SWAT model calibration for stream flow was performed for 2002 LULC and 2015 LULC separately at the catchment outlet located in the middle of Stung Sangkae River. Only sensitive parameters were included in the calibration of the model at a weekly and monthly time-step against observations of discharge loads recorded data at the outlet located in the middle of the Stung Sangkae catchment.

After running of the model for analysis of results, simulated stream flow was evaluated by visual inspection and quantitative statistics i.e. to evaluate how the model simulates well. For quantitative statistics the model performance was evaluated using three statistical criteria, the coefficient of determination (R^2), Nash-Sutcliffe efficiency (NSE) and percent bias (PBIAS) as recommended by Moriasi et al. (2007). NSE is a normalized statistic that describes the relative magnitude of the residual variance as compared to the observed and demonstrates how well the plot of observed versus simulated value fits the 1:1 line. The Nash-Sutcliffe Efficiency (NSE) coefficient proposed by Nash and Sutcliffe (1970) is defined by Eq. (1). R^2 ranges from 0 to 1 and explains the proportion of variance in the observed data with higher value indicating less error variance. R^2 is defined by Eq. (2). PBIAS measures the average tendency of the simulated data to be larger or smaller than their observed counterparts and is defined by Eq. (3). A positive value PBIAS indicates model under estimation bias and negative value indicates model over estimation bias. In general model simulation can be judged as satisfactory if NSE >0.4 and R^2>0.5 and PBIAS ±25% (Table 3.2) for stream flow and PBIAS ±55% for sediment yield (Ajai, Mohd, Isaacc, & Denisc, 2014). For the visual inspection, the scatter plots were used.

All simulated results from calibration and validation were evaluated by three quantitative statistics: Coefficient of determination (R^2), the Nash-Sutcliffe efficiency (NSE), and percent bias (PBIAS) (Moriasi et al. 2007).

$$\mathrm{NSE} = 1 - \frac{\sum_{i=1}^{n}(O_i - S_i)^2}{\sum_{i=1}^{n}(O_i - \bar{O})^2} \quad (1)$$

$$R^2 = \left(\frac{\sum_{i=1}^{n}(O_i - \bar{O})(S_i - \bar{S})}{\sqrt{\sum_{i=1}^{n}(O_i - \bar{O})^2} \sqrt{\sum_{i=1}^{n}(S_i - \bar{S})^2}} \right)^2 \quad (2)$$

$$\text{PBIAS} = \frac{\sum_{i=1}^{n}(O_i - S_i)}{\sum_{i=1}^{n} O_i} \text{ x } 100\% \quad (3)$$

where O_i is the observed value at time i, $\bar{O}$ is the average observed value, S_i is the simulated value at time i, $\bar{S}$ is the average simulated value, and n is the number of registered observed data.

Table 3.2. Model performance evaluation classification

Statistic	Evaluation rating			
	Unsatisfactory	Satisfactory	Good	Very good
R^2	< 0.50	0.50 – 0.60	0.60 – 0.70	0.70 – 1
NSE	< 0.50	0.50 – 0.65	0.65 – 0.75	0.75 – 1
PBIAS	> ±25	±15 < PBIAS < ±25	±10 < PBIAS < ±15	< ±10

Model validation was done to ensure that the calibrated set of parameters performs reasonably well under an independent data set. To utilize any predictive watershed model for estimating the effectiveness of feature potential management practices, the model was validated against an independent dataset without adjusting calibrated parameters. The period of 2000–2010 and 2011–2018 daily stream flow data was used for model calibration and validation for 2002 and 2015 LULC, respectively in a monthly time scale.

3.3. Results and Discussion

3.3.1. Analysis of Land Use and Land Cover Changes

The dominant land use types of the Stung Sangkae catchment in both reference land uses are forest land (evergreen, deciduous and mixed forests), paddy rice, agricultural land, shrub land and grasslands, which in the total account over 92% of the total area. However, their individual percentage coverage of these dominant land uses in each reference land use is different (Table 3.3).

Table 3.3. Summary analysis of land use and land cover of the Stung Sangkae catchment in 2002 and 2015

SWAT Code	LULC Types	JICA 2002		MRC 2015		Net Change	
		Area (ha)	Area (%)	Area (ha)	Area (%)	Area (ha)	Area (%)
AGRL	Agricultural land	25,627.2	4.24	152,742.3	25.24	127,115.0	21.00
BARR	Barren land	149.2	0.02	274.0	0.04	124.8	0.02
URML	Built-up area	1,702.8	0.28	20,870.1	3.45	19,167.3	3.17
FRSD	Deciduous forest	74,524.7	12.31	24,144.9	3.99	−50,379.8	−8.32
FRSE	Evergreen forest	110,474.4	18.26	90,338.0	14.93	−20,136.4	−3.33
FRST	Mixed forest	75,361.5	12.45	64,710.9	10.69	−10,650.6	−1.76
RICE	Paddy field	92,784.8	15.33	144,931.5	23.95	52,146.7	8.62
RNGE	Grassland	79,496.0	13.14	29,394.2	4.86	−50,101.8	−8.28
RNGB	Shrubland	141,689.0	23.41	74,019.0	12.23	−67,670.0	−11.18
WETN	Marsh and swamp	280.3	0.05	35.8	0.01	−244.6	−0.04
WATR	Water bodies	3,080.1	0.51	3,709.4	0.61	629.3	0.10
	Total	605,170.0	100.00	605,170.0	100.0		

The results of the transition matrix of LULC changes between 2002 and 2015 are shown in (Figure 3.5., Figure 3.6, Table 3.4 and Table 3.5). The transformations among shrubland, forest land (Evergreen, mixed and deciduous forest), and grassland were the main forms of land use changes in the Stung Sangkae catchment; the area of agricultural land and paddy field increased and the area of forest land decreased. Agricultural land showed the largest change (Figure 3.5 and 3.6). Meanwhile, due to social development, the area of built-up land increased markedly at the expense of farmland. Finally, a tiny proportion of it was changed into water or wetland and unused land. In the southeast, a part of the watershed grassland was turned into farmland. Among other classes of transition of LULC, the mixed forest transformed to agricultural land the most (57,794 hectares); however, there was also a transformation of shrubland to mixed forest (57,623 hectares) which was almost the same area as its conversion to agricultural land (Table 3.3).

Table 3.4 shows the LULC change detection matrices for different time periods from 2002 to 2015 of the conversion from each class to other individual classes. For instance, considering the entire study period of 2002-2015, 11,300 hectares of agricultural land remained unchanged, 141,440 hectares of new agricultural land were created from conversions of mixed forest (57,780 hectares), deciduous forest (38,330 hectares), evergreen forest (19,860 hectares), shrubland (14,330 hectares), grassland (6,650 hectares), paddy field (4,180 hectares) and the other categories (330 hectares). Moreover, 14,330 hectares of agricultural land were lost from conversions to the built-up area (11,820 hectares), paddy fields (1,470 hectares), shrubland (660 hectares), water bodies (250 hectares), deciduous forest (120 hectares) and other types (7 hectares). Agricultural land was the LULC type that expanded the most (141,440 hectares), followed by mixed forest (63,250 hectares), paddy field (62,290 hectares), shrubland (46,400 hectares), built-up areas (19,220 hectares), and grassland (17,000 hectares). At the same time, the LULC types with the highest loss were shrubland, mixed forest, grassland, and deciduous forest, with loss areas of 114,000 hectares, 73,900 hectares, 67,100 and 53,820 hectares, respectively (Table 3.4).

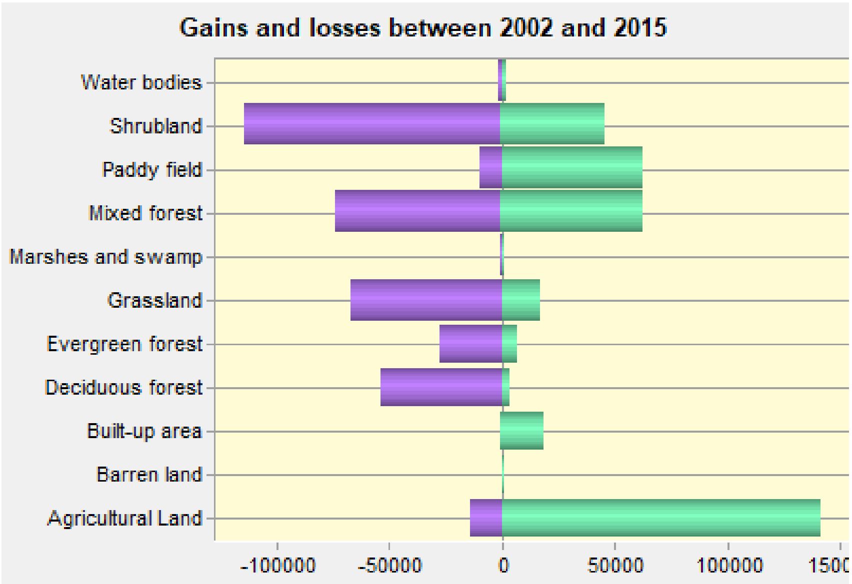

Figure 3.5. Gains and losses between 2002 and 2015

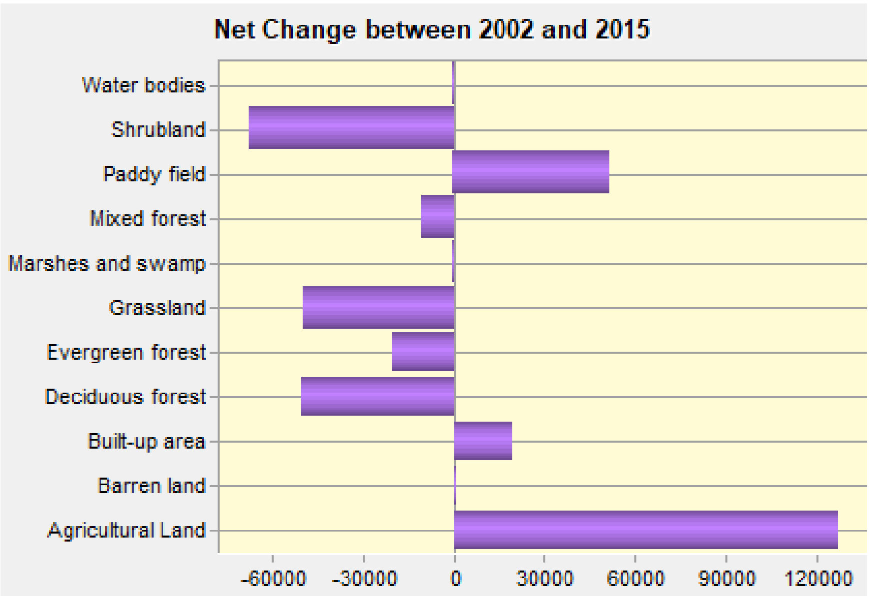

Figure 3.6. Net change between 2002 and 2015

Table 3.4. Transition of LULC by ignoring the area less than 500 ha

Category	Hectares	Legend
1	38,315	Deciduous forest to Agricultural land
2	19,848	Evergreen forest to Agricultural land
3	6,648	Grassland to Agricultural land
4	57,794	Mixed forest to Agricultural land
5	4,168	Paddy field to Agricultural land
6	14,332	Shrubland to Agricultural land
7	11,825	Agricultural Land to Built-up area
8	738	Deciduous forest to Built-up area
9	595	Grassland to Built-up area
10	580	Mixed forest to Built-up area
11	4,969	Paddy field to Built-up area
12	653	Evergreen forest to Deciduous forest
13	2,576	Mixed forest to Deciduous forest
14	3,714	Deciduous forest to Evergreen forest
15	2,568	Mixed forest to Evergreen forest
16	753	Shrubland to Evergreen forest
17	16,774	Shrubland to Grassland
18	5,080	Grassland to Mixed forest
19	57,623	Shrubland to Mixed forest
20	1,462	Agricultural Land to Paddy field
21	1,394	Deciduous forest to Paddy field
22	35,490	Grassland to Paddy field
23	23,447	Shrubland to Paddy field
24	658	Agricultural Land to Shrubland
25	9,400	Deciduous forest to Shrubland
26	6,719	Evergreen forest to Shrubland
27	18,714	Grassland to Shrubland
28	9,578	Mixed forest to Shrubland
29	853	Paddy field to Shrubland
30	661	Shrubland to Water bodies

Table 3.5. Matrix of land use and land cover (LULC) change contribution to net change experienced by LULC types in hectare (ha) and percentage (%) for 2002–2015

	LULC Class	LULC 2015																							
		AL		BL		BA		DF		EF		GL		MS		MF		PF		SL		WB		Grand Total	Loss
		ha	%	ha	%	ha	%	ha	%	ha	%	ha	%	ha	%	ha	%	ha	%	ha	%	ha	%		
LULC 2002	Agricultural land	11300	7	0	0	11821	57	116	0	4	0	1	0	0	0	2	0	1470	1	662	0.9	252	7	25627	14328
	Barren land	110	0	6	2	24	0	7	0	0	0	0	0	0	0	0	0	1	0	2	0.0	0	0	150	144
	Built-up area	19	0	0	0	1646	8	0	0	0	0	0	0	0	0	0	0	13	0	0	0.0	24	1	1703	57
	Deciduous forest	38328	25	23	9	746	4	20706	86	3709	4	0	0	0	0	157	0	1399	1	9390	12.7	66	2	74525	53818
	Evergreen forest	19856	13	70	26	19	0	651	3	83183	92	3	0	0	0	0	0	0	0	6725	9.1	34	1	110542	27359
	Grassland	6646	4	59	22	592	3	18	0	28	0	12394	42	19	54	5090	8	35494	24	18704	25.3	452	12	79496	67102
	Marsh and swamp	0	0	0	0	0	0	0	0	4	0	0	0	0	0	42	0	0	0	233	0.3	0	0	280	280
	Mixed forest	57777	38	45	16	584	3	2579	11	2612	3	178	1	12	32	1460	2	326	0	9580	12.9	208	6	75361	73901
	Paddy field	4175	3	0	0	4966	24	9	0	39	0	3	0	4	11	10	0	82640	57	850	1.1	88	2	92785	10144
	Shrubland	14330	9	71	26	329	2	56	0	787	1	16753	57	1	2	57630	89	23457	16	27636	37.3	662	18	141710	114075
	Water bodies	201	0	0	0	144	1	3	0	39	0	63	0	0	0	318	0	130	0	258	0.3	1923	52	3080	1157
	Grand Total	152742		274		20870		24145		90405		29394		36		64711		144931		74040		3710		605259	362366
	Expansion	141443		269		19224		3439		7222		17000		36		63251		62291		46405		1787		362366	

Note: AL: agricultural land, BL: barren land, BA: built-up area, DF: deciduous forest, EF: evergreen forest, MF: mixed forest, PF: paddy field, GL: grassland, SL: shrubland, MS: marsh and swamp, and WB: water bodies; ha = hectare.

3.3.2. Sensitivity Analysis, Calibration and Validation under Land Use Change Dynamics

3.3.2.1. Stream Flow Sensitivity Analysis

Sensitivity analysis results of SWAT model stream flow parameters were identified as significant for a period of 10 years (2000−2010) and show a range of most sensitive parameters for JICA 2002 LULC (Table 3.6). Almost similar results were obtained by Ying, Chen, Wang, and Peng (2011). These parameters are related to groundwater, runoff, and soil process and thus influence the stream flow in the catchment. The analysis result was found that the ALPHA_BF, which is a direct index of groundwater flow response to a change in rechanges, is the most significant factor influencing stream flow. The remaining 11 parameters are identified as slightly important influencing stream flow parameters in this analysis such as the curve number (CN2), the soil available water capacity (SOL_AWC), the threshold depth of water in the shallow aquifer required for return flow (GWQMN), the groundwater delay (GW_DELAY), the threshold depth of water in the shallow aquifer for "revap" to occur (REVAPMN), the effective hydraulic conductivity in tributary channel alluvium (CH_K1), the lateral flow travel time (LAT_TTIME), the rate of decline in radiation use efficiency per unit increase in vapor pressure deficit (WAVP), the fraction of growing season when leaf area starts declining (DLAI), the max leaf area index (BLAI) and the total heat units for cover/plant to reach maturity (HEAT_UNITS). These may be additional support to the result of the sensitivity analysis.

Table 3.6. Flow parameter sensitivity analysis result in Stung Sangkae catchment

ID	Parameter	Default range	Fitted value
1	v__ALPHA_BF.gw	0−1	0.5
2	v__GW_DELAY.gw	0−500	15
3	v__GWQMN.gw	0−5000	750
4	v__REVAPMN.gw	0−1000	745
5	v__CH_K1.sub	0.01−500	176
6	v__LAT_TTIME.hru	0−180	30
7	v__WAVP{6-8}.plant.dat____FRST,FRSD,FRSE	0−50	42
8	v__DLAI{6-8}.plant.dat____FRST,FRSD,FRSE	0.15−1	0.23
9	v__BLAI{6-8}.plant.dat____FRST,FRSD,FRSE	0.5−10	9
10	r__HEAT_UNITS{[],1}.mgt	0−3500	-0.5
11	r__CN2.mgt	35−98	-0.02
12	r__SOL_AWC().sol	0−1	0.05

Note: v__ means that the existing parameter value is to be replaced by the given value; r__ means that the existing parameter value is multiplied by 1 plus a factor in the given value.

3.3.2.2. Stream Flow Calibration and Validation

The simulation of the SWAT model with the default value of parameters in the Stung Sangkae catchment showed relatively good matching on a monthly basis between the simulated and observed streamflow hydrographs. Hence, calibration was done for sensitive flow parameters of SWAT with observed monthly stream flow data. Based on the available information in the literature, the sensitivity flow parameters were adjusted by the manual calibration procedure. In this procedure, the values of the parameters were varied iteratively within the allowable ranges until the simulated flow as close as possible to the observed stream flow. The SWAT model was calibrated for stream flow in the 2000–2010. Calibration performance for the monthly flow was reasonably good in both JICA 2002 (R^2 = 0.62, NSE = 0.61 and PBIAS = 14) and MRC 2015 (R^2 = 0.62, NSE = 0.60 and PBIAS = 13) for Stung Sangkae catchment. The calibration performance was reasonably good with limited rainfall data as Table 3.7. This is found to be satisfactory for the Stung Sangkae catchment according to the performance evaluation criteria.

Table 3.7. Calibration performance for monthly flow at Stung Sangkae catchment

LULC	Calibration period	Statistic	Value	Evaluation
JICA 2002	(2000-2010)	R^2	0.62	Good
		NSE	0.61	Satisfactory
		PBIAS	14	Good
MRC 2015	(2000-2010)	R^2	0.62	Good
		NSE	0.60	Satisfactory
		PBIAS	13	Good

Figure 3.7 presented that the calibrated results of stream flow were not significantly different. Both observed and simulated hydrographs had a similar seasonal pattern for Stung Sangkae catchment; however, the SWAT model has been shown to underestimate peak flows and base flows in some years. Graphically, the monthly simulated peak flow based on both JICA and MRC land uses in 2000-2001 and 2003-2006 periods have been underestimated by comparing with the monthly observed peak flow. Moreover, the monthly simulated peak flow based on both JICA and MRC land uses in 2002 and 2015 periods have been overestimated by comparing with the monthly observed peak flow. As represented by the calibration period by Figure 3.7 the monthly simulated flow based on MRC land use in 2015 has slightly increased in both peak and base flow by comparing with the monthly

simulated flow based on JICA land use in 2002.

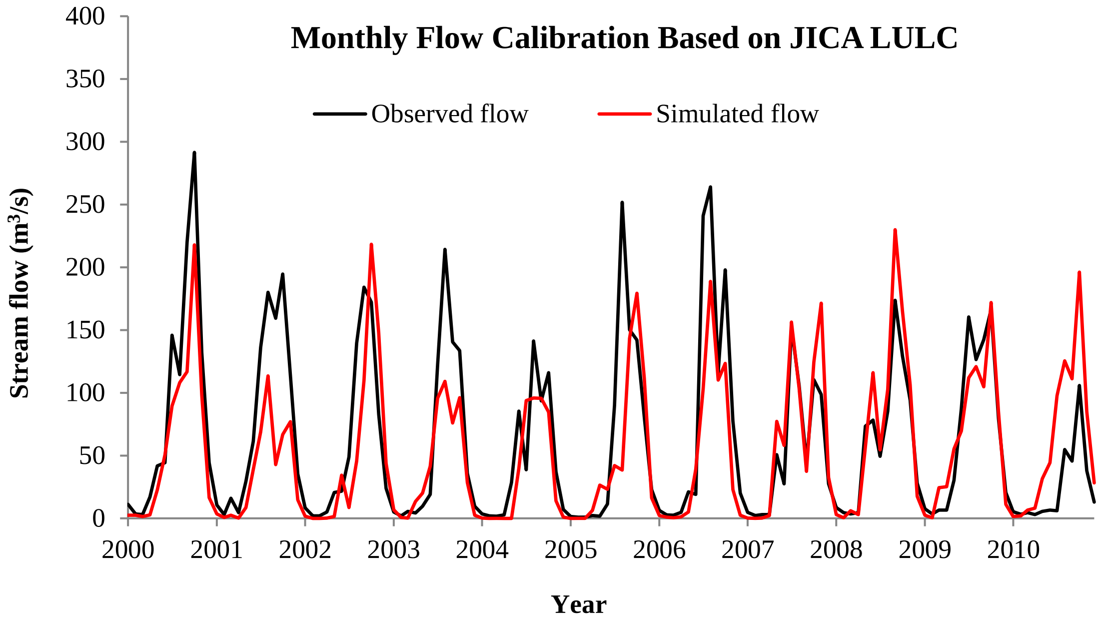

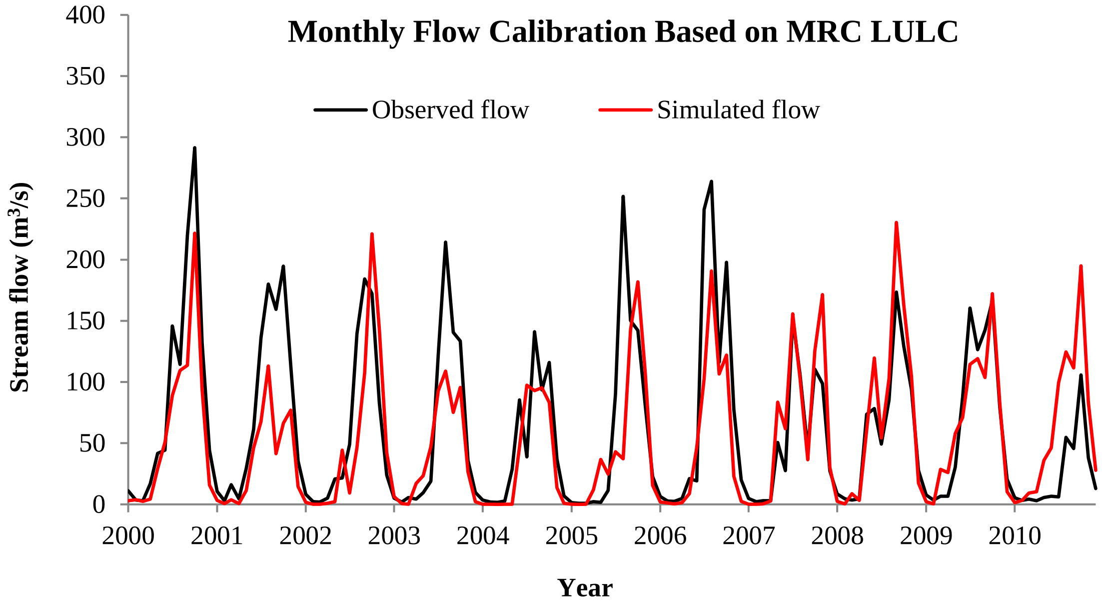

Figure 3.7. Monthly streamflow calibration based on JICA and MRC LULC data

Scatter plots between the monthly simulated and observed flow for the calibration period of Stung Sangkae catchment had been also shown in Figure 3.8. The calibrated results were performed well for Stung Sangkae catchment according to the performance evaluation criteria. According to these scatter plots, the correlations between observed and simulated flow are positive correlations for calibration in monthly simulation. This positive correlation illustrates that observed and simulated has the same thing due to one variable will be followed by changes in the other variables regularly in the same direction. However, the highest correlation is in the calibration period based on JICA land use in monthly simulation.

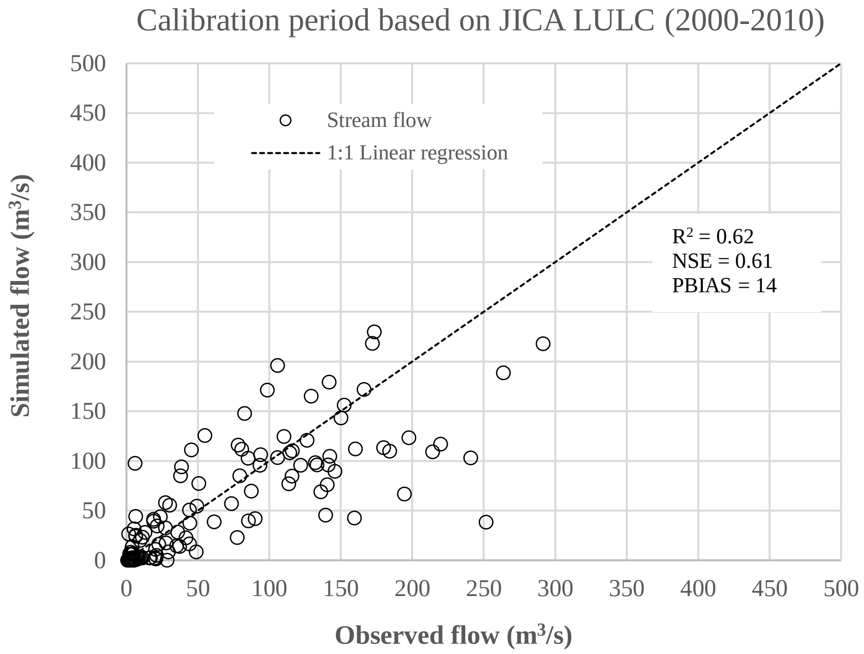

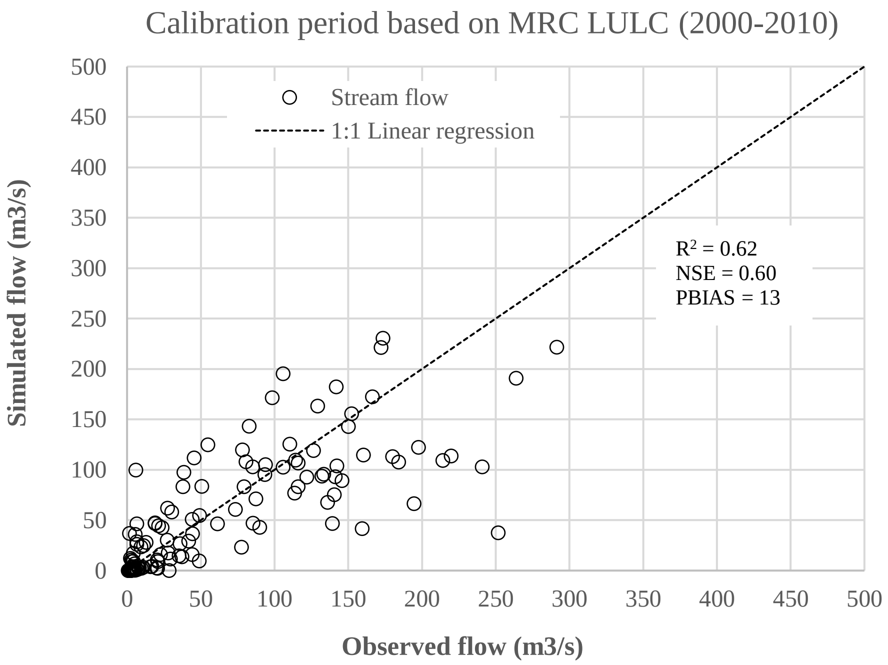

Figure 3.8. Scatter plot of monthly stream flow calibration based on JICA and MRC LULC data

The SWAT model validation was carried out from 2011 to 2018 without further adjusting the calibrated parameters. However, validation performance for the monthly flow was acceptable in both JICA 2002 (R^2 = 0.56, NSE = 0.48 and PBIAS = −8) and MRC 2015 (R^2 = 0.56, NSE = 0.48 and PBIAS = −9) for Stung Sangkae catchment, except for the NSE value; however, the R^2 and PBIAS value were found to be good in this river (Table 3.8). Due to the data scarcity, the inaccuracy in rainfall, the budget constraints, and the low investment in water infrastructure in Stung Sangkae catchment, the hydrological simulation did not perform well for one quantitative statistic (NSE value < 0.5) in the validation period (2011-2018).

Table 3.8. Validation performance for monthly flow at Stung Sangkae catchment

LULC	Validation period	Statistic	Value	Evaluation
JICA 2002	(2011-2018)	R^2	0.56	Satisfactory
		NSE	0.48	Unsatisfactory
		PBIAS	−8	Very good
MRC 2015	(2011-2018)	R^2	0.56	Satisfactory
		NSE	0.48	Unsatisfactory
		PBIAS	−9	Very good

Figure 3.9 presented that the validated results of stream flow were not significantly different. The both observed and simulated hydrograph had the similar seasonal pattern as the model validation for Stung Sangkae catchment; however, the SWAT model has been shown to overestimate peak flows and base flows in some years. Graphically, the monthly simulated peak flow based on both JICA and MRC land uses in 2012 and 2015-2018 periods have been overestimated by comparing with the monthly observed peak flow. Moreover, the monthly simulated peak flow based on both JICA and MRC land uses in 2011 and 2013-2014 periods have been underestimated by comparing with the monthly observed peak flow. As represented the validation period by Figure 3.9, the monthly simulated flow based on MRC land use in 2015 has been slightly increased in both peak flow and base flow by comparing with the monthly simulated flow based on JICA land use in 2002.

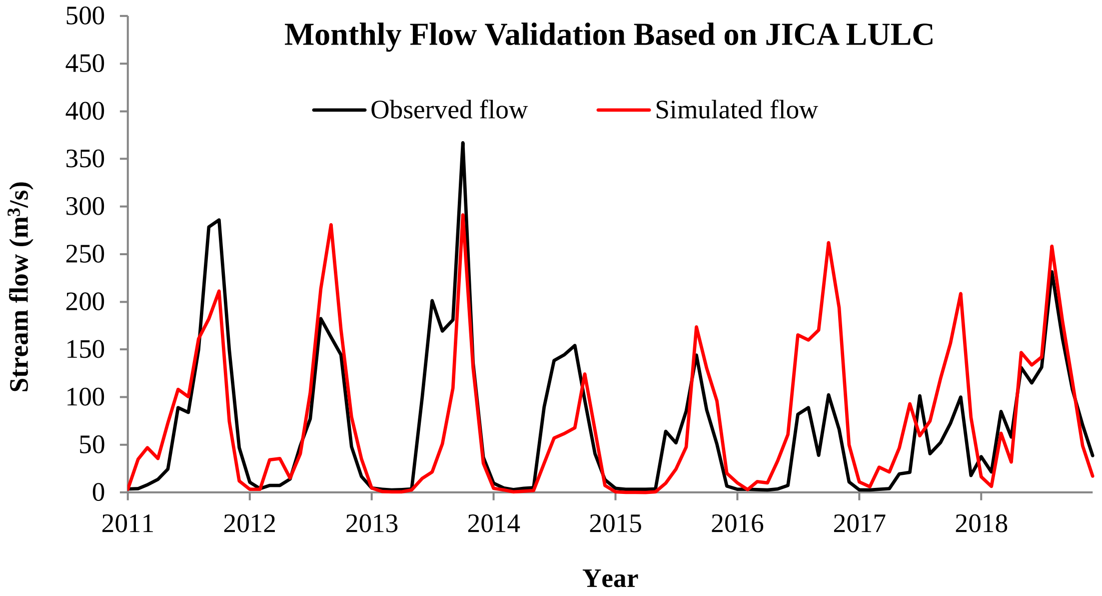

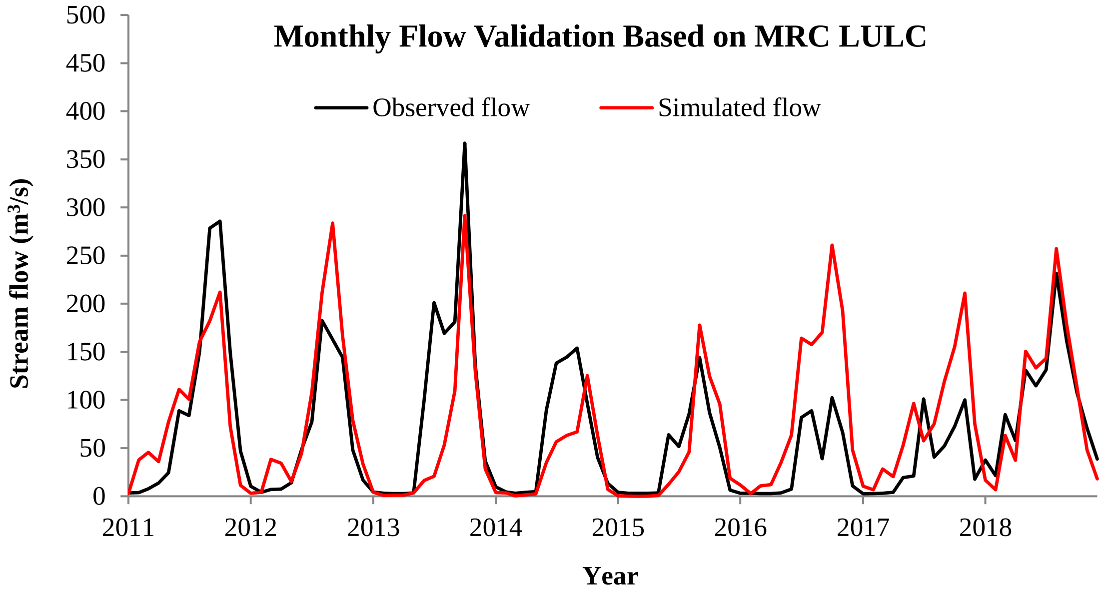

Figure 3.9. Monthly streamflow validation based on JICA and MRC LULC data

Scatter plots between the simulated and observed flow for the validation period of Stung Sangkae catchment had been also shown in Figure 3.10. The validated results were performed adequately satisfactory for Stung Sangkae catchment according to the performance evaluation criteria, except for the NSE value. According to these scatter plots, the correlations between observed and simulated flow are also positive correlations for validation in monthly simulation. Positive correlation in the validation period also shows that observed and simulated has the same thing due to one variable will be followed by changes in the other variables regularly in the same direction. However, the highest correlation is in the validation period based on JICA land use in monthly simulation according to R^2 and PBIAS value, which R^2 is in the satisfactory evaluation and PBIAS is in the very good evaluation.

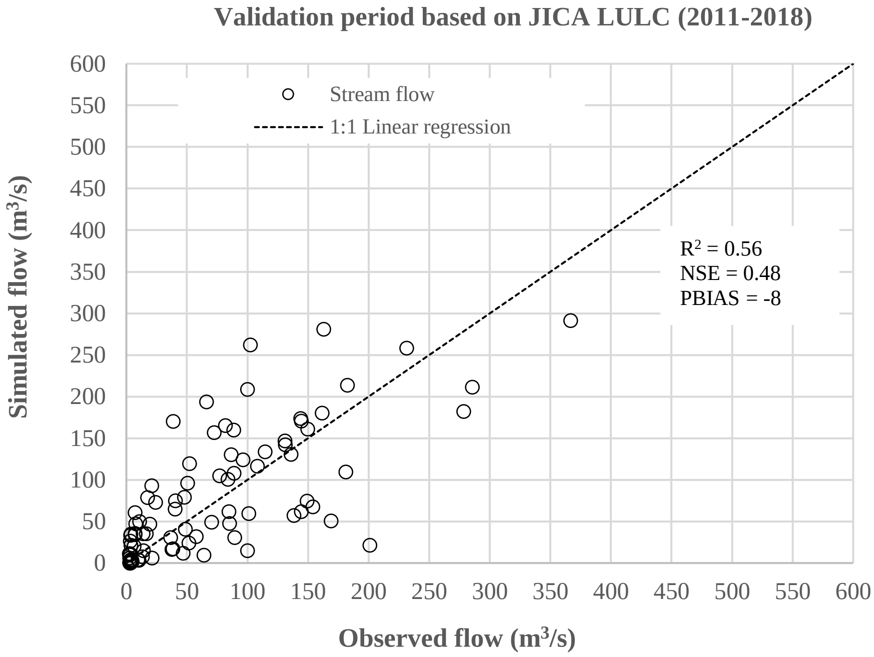

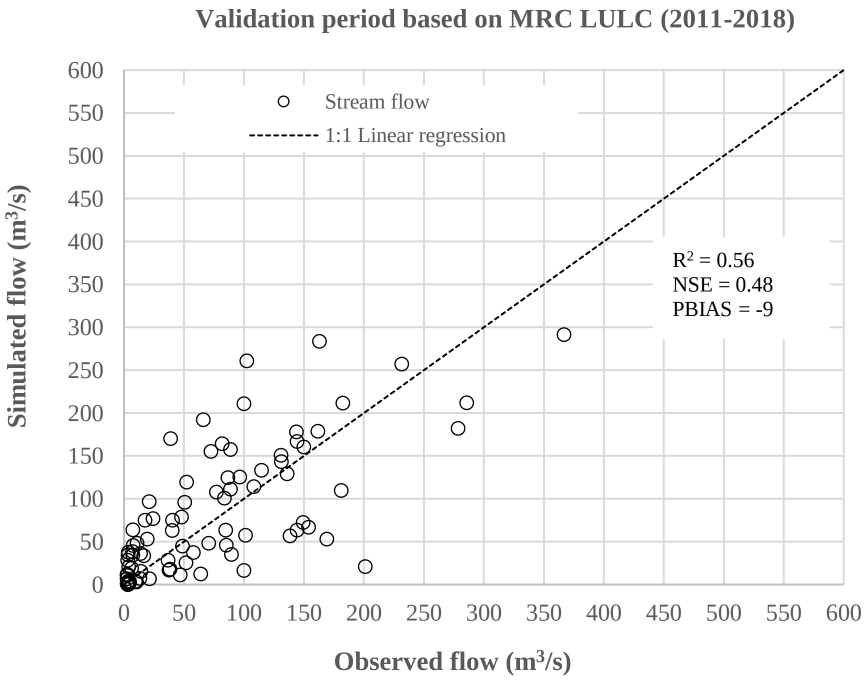

Figure 3.10. Scatter plot of monthly stream flow validation based on JICA and MRC LULC data

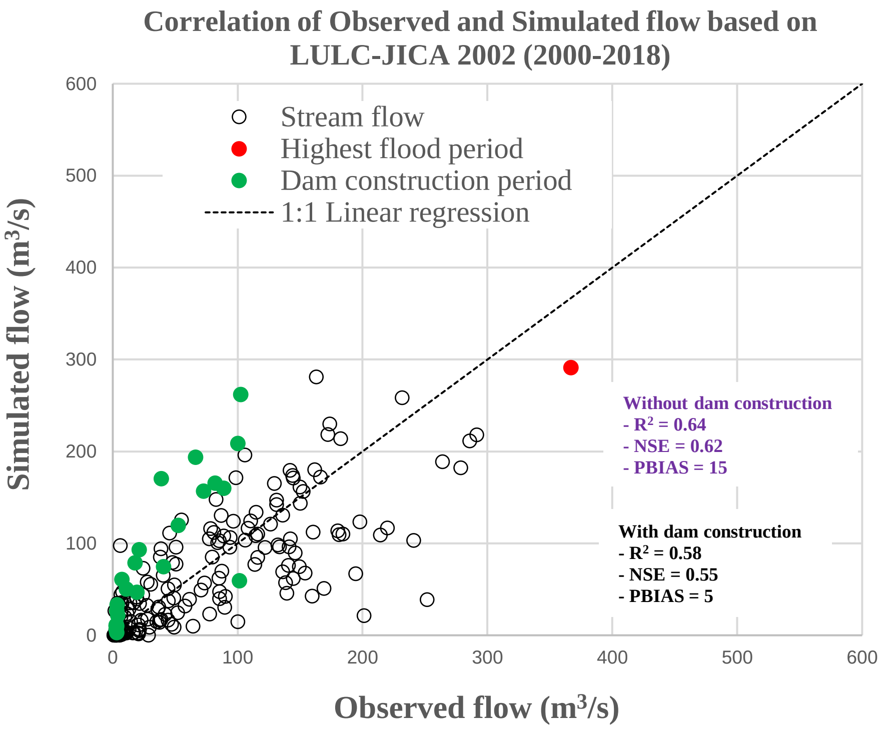

a). Correlation of observed and simulated flow based on LULC in 2022 in 2000-2018

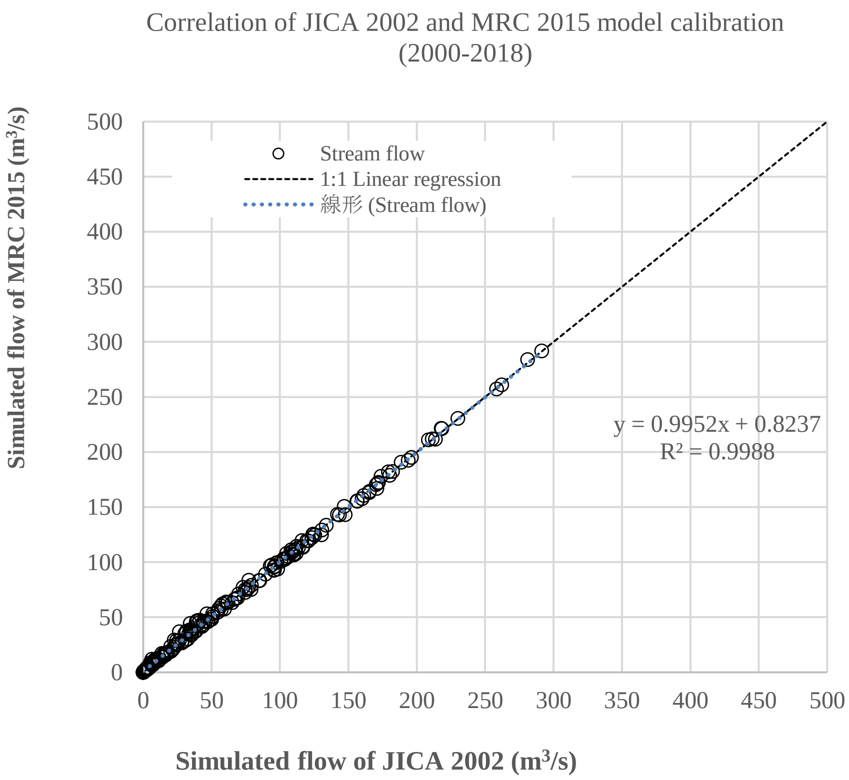

b). Correlation of simulated flow of JICA 2002 and MRC 2015 in 2000-2018

Figure 3.11. Correlation of observed vs. simulated flow (a) and correlation of different LULC on stream flow (b)

In the comparison between the correlation of the observed and simulated flow based on JICA LULC in 2000-2018 (Figure 3.11a), the values of the statistical indicators were high (R^2=0.64, NSE=0.62, and PBIAS=15) if the periods of construction Sek SoK multi-purpose dam from 2016 to 2017 was not included. The dam was operated in 2018. This may be related to the location of the stream gauge as it was installed in the middle of the catchment due to the expansion of the areas of Tonle Sap Lake during the rainy season, so only half of the catchment was evaluated. Moreover, the collected stream flow data for model calibration and validation was not measured data as it was done by rating curve (H-Q curve) estimated from the water level of the Stung Sangkae. The equation of the rating curve developed to estimate stream flows for the monitored water levels at the outlets of the 11 Tonle Sap sub-catchments (Kummu, et al., 2014) is shown in appendix 2 (Table A.1). Moreover, comparing the correlation of the LULC of JICA 2002 and MRC 2015 found that there was a non-significant change in streamflow during the investigation period, even though the LULC from 2002 to 2015 significantly occurred. This was because at the upstream catchment, the forest cover was changed to agricultural land; however, for the agricultural land (upland), many fruit trees were grown; as a result, their robust root system can absorb the runoff during the rain. At the downstream, shrubland was changed into forest land; however, it was mainly the riparian forest of the Tonle Sap Lake (TSL) floodplain.

3.3.3. Impact of LULC Changes on Stream Flow

One of the most important things of the study was to evaluate the impact of land use and land cover (LULC) changes on the hydrological response of Stung Sangkae catchment. The effects of change in LULC on the hydrology (stream flow) in Stung Sangkae catchment was analysed on an annual time scale. The yearly output from SWAT model has been employed to assess the hydrologic impacts of LULC changes, in which two separate simulations of the SWAT model were performed using LULC map of JICA 2002 and MRC 2015 with the same climatic record (2000-2018), by comparing the annual stream flow data from the baseline of LULC in 2002. The mean annual flow was estimated on the basis of continuous simulations for 18 years (2000-2018). The simulated average annual stream flow maps of two LULC situations were then compared to explore the spatial pattern of changes and to assess the hydrologic impacts of LULC changes between 2002 and 2015. A good model performance of simulations with change in land use established the contribution of land use change to changes in stream flow. Spatial changes in both cubic meter per second and percentage for the mean annual stream flow caused by LULC changes in this study area were investigated in many of the sub-catchments as represented in Figure 3.12 and 3.13.

As shown in Figure 3.12, the study demonstrated that the most significant increases of mean annual flow mainly occurred along the main stream of Stung Sangkae river, largely matching the spatial distribution pattern of the expansion of agricultural land (21%), paddy rice (8.62%), and urban area (3.17%) and the total loss of forest area (13.41%). The result of mean annual stream flow in cubic meters per second has increased with the range approximately from 0.1 m^3/s to 104 m^3/s. Figure 3.13 illustrates the mean annual flow in each sub-catchment of along the main stream showing the highest mean annual flows with the range from 31 m^3/s to 101 m^3/s. In comparison, the medium mean annual flows occurred in the midstream and downstream of the river region with the range from approximately 11 m^3/s to 30 m^3/s and the lowest mean annual flows occurred mainly in the downstream region with the range from 0.1 m^3/s to 10 m^3/s. Additionally, due to impacts of LULC change in the 2002-2015 period, the highest mean annual flow changes have increased approximately 0.8 m^3/s along the main stream of Stung Sangkae river, especially the downstream, while the medium mean annual flow changes have increased around 0.3 m^3/s for most sub-catchments surrounding the main stream of the catchment; however the lowest mean annual flow changes have decreased approximately 0.2 m^3/s in the sub-catchment 4 and 6 of the downstream in Stung Sangkae river. Moreover, the SWAT model produced the percentage change in some areas of sub-catchment as shown in Figure 3.13. The percentage change for mean annual flow has increased in the maximum approximately 7% for most of upstream areas in Stung Sangkae River while the mean annual flow has increased in the average approximately 0.8%, except some areas have decreased approximately 5% such as sub-catchments of 4, 6, and 15 in Stung Sangkae catchment.

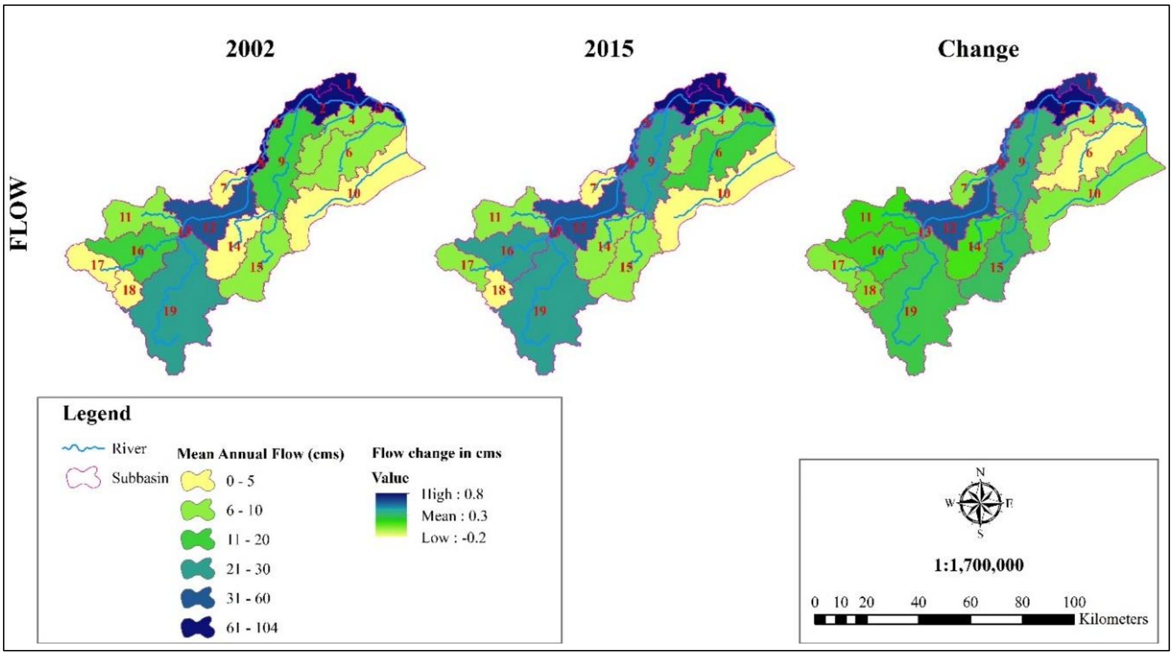

Figure 3.12. Spatial distribution of the mean annual stream flow changes in m^3/s for Stung Sangkae catchment

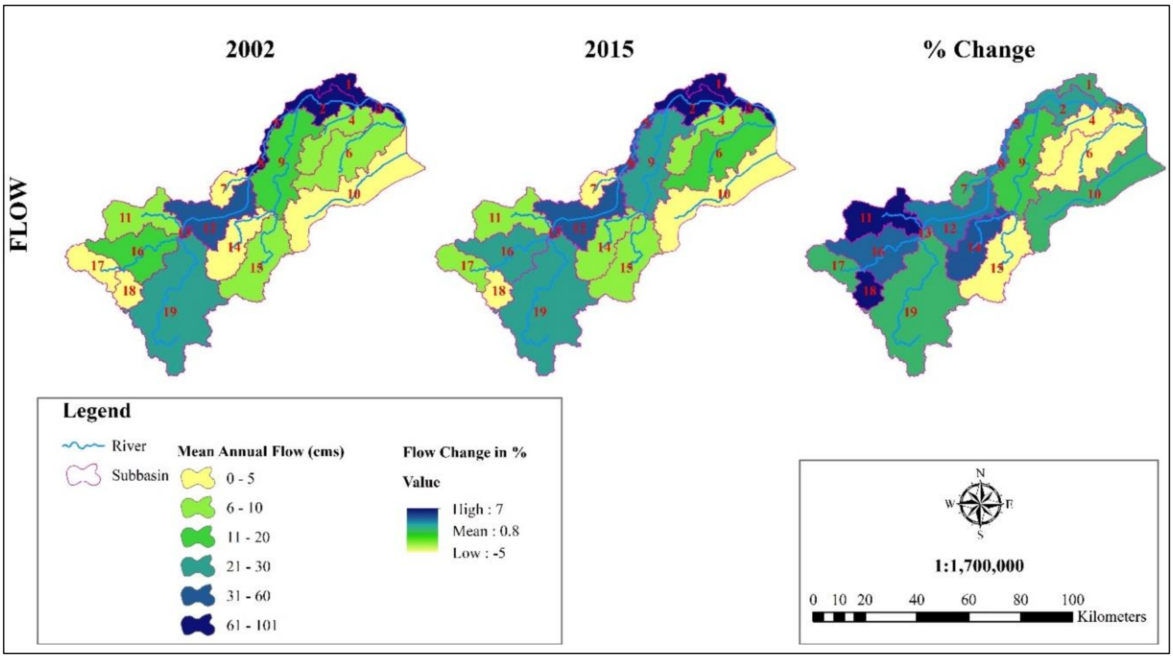

Figure 3.13. Spatial distribution of the mean annual stream flow change in the percentage for Stung Sangkae catchment

3.3.4. Contribution of Individual LULC Changes to Catchment Water Yield

The proportional contributions of six LULC changes (i.e., agricultural land, rice, forest land, urban area, grassland and shrubland) and simulated water yield (WY) are shown in Figure 3.14. Forest land, rice, agricultural land, grassland and shrubland were the main

LULC changes in the Stung Sangkae catchment from 2002 to 2015 and the sum of their areas accounted for 99.7% in 2002 and 96.6% in 2015 of the total area. Their contributions to water yield were up to about 89% but there was no obvious positive correlation between the area of individual LULC changes and their proportional contributions to watershed WY. The forest land class includes mainly deciduous, evergreen, and mixed forest, so its water-yielding capacity was large up to approximately 39.5%.

Due to modernization and urbanization, expansions of agricultural land, rice, and urban area have decreased the forest land, grassland, and shrubland. Although the area of forested land, grassland, and shrubland were decreased much less than that of the agricultural land, rice, and urban area, their contributions to catchment WY were slightly changed such as an increase of 0.1% forest land, 0.4% grassland, and a decrease of 1.1% shrubland. The area of agricultural land was increased about 21.2%, while its water-yielding capacity was increased about 0.3%. In contrast, the area of rice was increased approximately 8.6%, but its water-yielding capacity was decreased approximately 0.4% In addition, the paddy rice in the Stung Sangkae catchment used to grow close and straight row-seeded rice which considerably reduce the water yield. Although the area of urban area was extremely modest, it was discovered that a growth in urban area was the main reason of increases in runoff by comparing the percentage of area of each land use type and their contribution to water yield. This is because it had the highest water-yielding capacity due to low intial loss and infiltration, as well as rapid rainfall-runoff process.

Spatial changes in both millimeter and percentage for the mean annual water yield caused by LULC changes in this study area were investigated in many of the sub-catchments as represented in Figure 3.15 and 3.16. As shown in Figure 3.14, the study demonstrated that the most significant increases of mean annual WY mainly occurred in the upstream of Stung Sangkae River. The result of mean annual WY in millimeter has increased with the range approximately from 425 mm to 837 mm. Figure 3.13 illustrated the mean annual WY in each sub-catchment of the upstream and midstream showing the highest mean annual WY with the range from 601 mm to 837 mm, while the medium mean annual WY occurred in the downstream of the Sangkae river region with the range from approximately 501 mm to 600 mm and the lowest mean annual WY occurred also mostly in the downstream region with the range from 425 mm to 500 mm. Additionally, due to impacts of LULC change in the 2002-2015 period, the highest mean annual WY changes have increased approximately 17 mm in the upstream and midstream of Stung Sangkae river, while the medium mean annual

WY changes have increased around 1 mm for most sub-catchments in the downstream; however the lowest mean annual WY changes have decreased about 16 mm in the sub-catchment 1, and 6 of the downstream in Stung Sangkae river. Moreover, the SWAT model produced the percentage change in some areas of sub-catchment as shown in Figure 3.16. The percentage change for mean annual WY has increased in the maximum approximately 4% for most of upstream and midstream areas in Stung Sangkae River while the mean annual WY has increased in the average approximately 0.8%, except some areas have decreased approximately 2.5% such as sub-catchments of 1, and 6 in Stung Sangkae catchment.

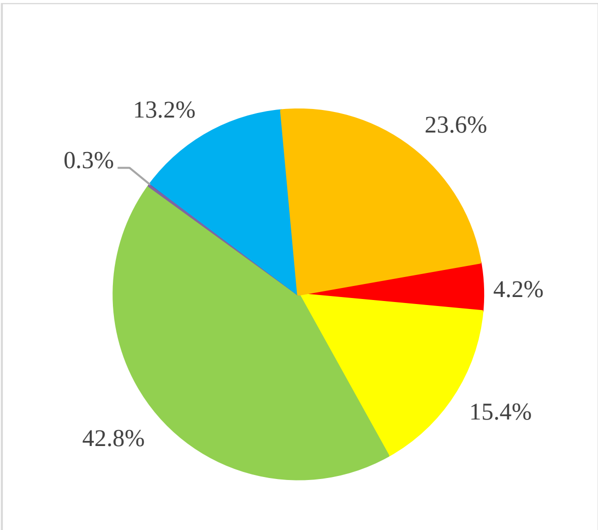

(a) Land use 2002

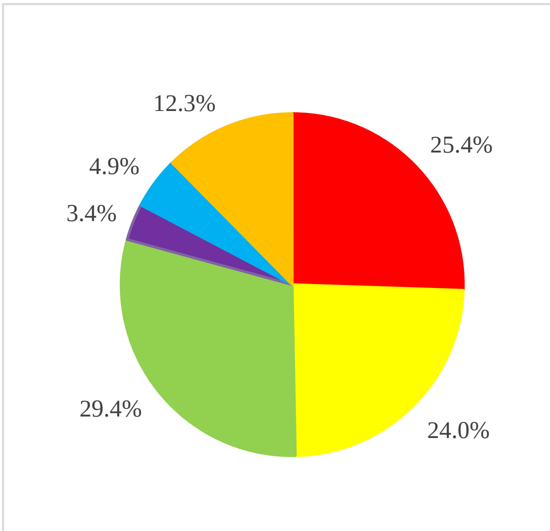

(b) Land use 2015

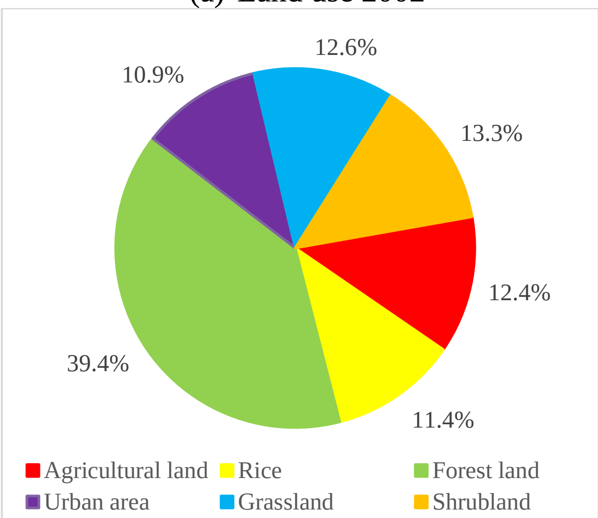

(c) WY with land use 2002

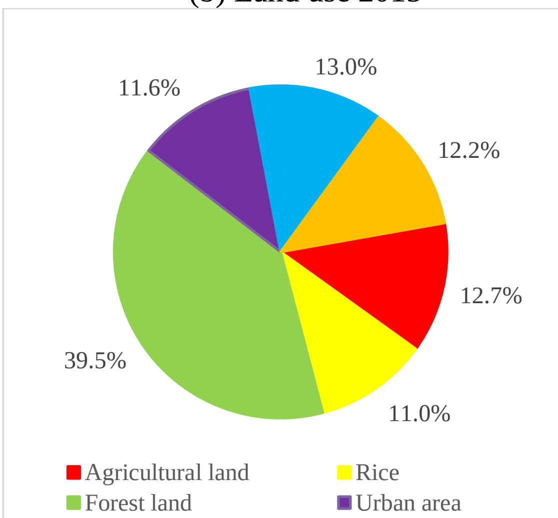

(d) WY with land use 2015

Figure 3.14. Percentage of each LULC change and its contribution to the total average annual water yields (WY) for the Stung Sangkae River from 2002 to 2015.

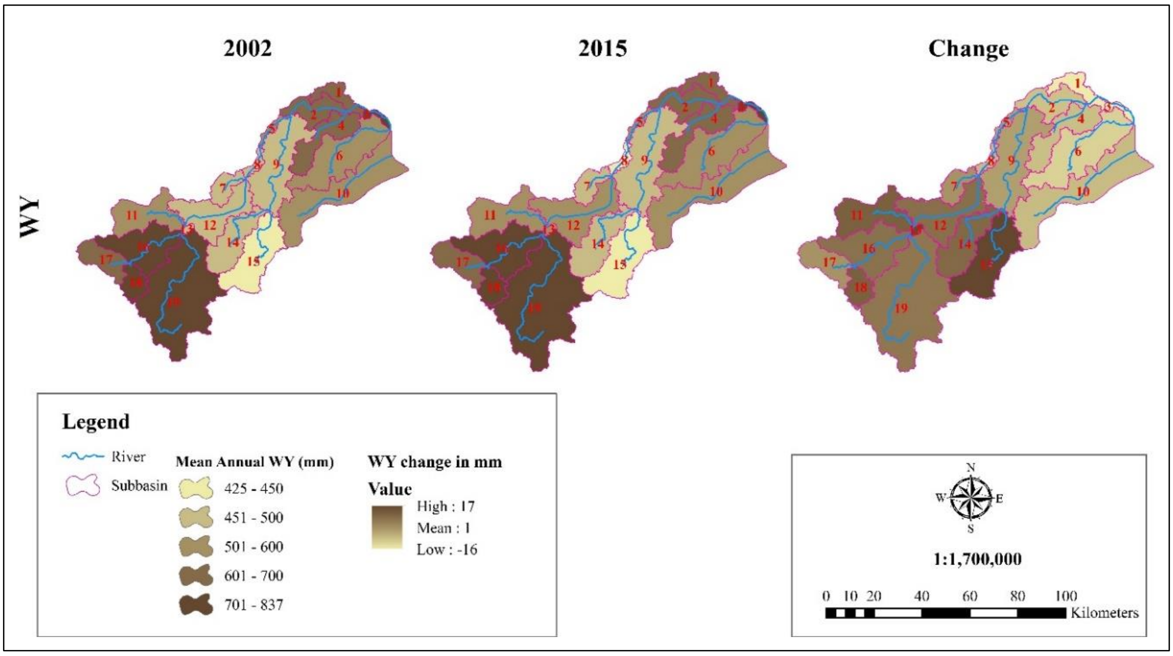

Figure 3.15. Spatial distribution of the mean annual water yield change in millimeter for Stung Sangkae catchment

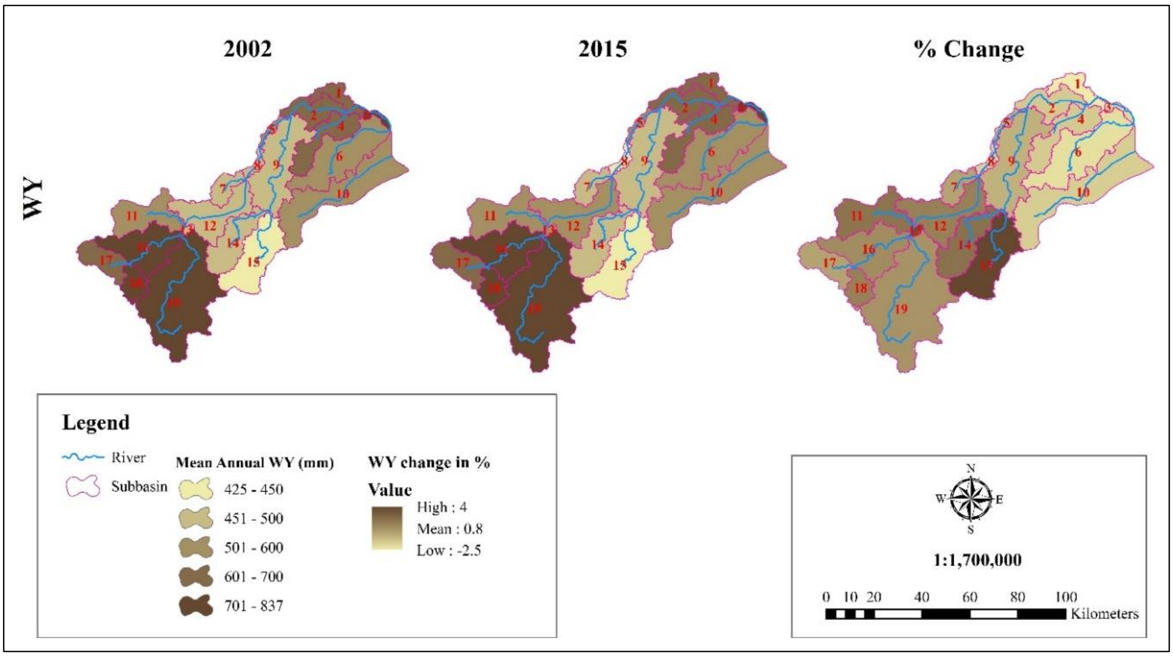

Figure 3.16. Spatial distribution of the mean annual water yield change in percentage for Stung Sangkae catchment

As LULCs changed from 2002 to 2015, the contribution of individual LULC change to catchment WY changed too, but the change process was complex, because the WY is an integrated result of LULCs, soil, topography, and climate.

3.3.5. Impacts of LULC Changes on Hydrology at the Basin Scale

The average basin values of PCP, PET, ET, SW, and WY simulated from each LULC map in 2002 and 2015 are represented in Table 3.9. Compared to the LULC change baseline year of 2002, the average annual WY over the catchment was 0.2 mm higher in 2010. Similar to WY, average annual PET with LULC in 2002 was 1619.9 mm; it increased to 1621.2 mm by 2015. The ET increased from 646.5 mm for LULC in 2002 to 648.1 mm for LULC in 2015. On the contrary, the average annual SW for LULC in 2015 was 0.1 mm lower than that in 2002.

Furthermore, compared to the LULC baseline year 2002, the annual PET, ET, and SW for each year from 2000 to 2018 for LULC change in 2015 changed in a similar manner as the average annual PET, ET, and SW. But in contrast to the size of the average annual WY for LULC in 2002 and 2015, the annual WY for each year in this period did not increase consistently. For example, in years of abundant precipitation, such as 2008 and 2017, the annual WY for the LULC change in 2002 was higher than that in 2015. This indicated that the precipitation could affect the impacts of the LULC changes on the hydrology in this region.

The comparison of variations of PET and ET and changes in LULCs suggested that the increase of annual PET could be mainly attributed to returning agricultural land and rice to forest, grassland, and shrubland and to urban expansion from 2002 to 2015. Further comparison between WY changes and LULCs changes showed that the increase in WY was mainly due to increased urbanization, which can increase the impervious surface area, increase runoff, and reduce infiltration. An association between the decreases of SW and agricultural land, rice, and urban area expansion from 2002 to 2015 could be indicated from the comparison between variations of average annual SW and changes in LULC from 2002 to 2015. Loss of forest land, grassland, and shrubland by replacing them with agricultural land could promote water infiltration and drainage because of well-developed root systems and prevention of infiltration due to increases in the areas of impervious surfaces.

Spatial changes in both millimeters and percentage for the mean annual actual evapotranspiration caused by LULC changes in this study area were investigated in many of the sub-catchments as represented in Figures 3.17 and 3.18. As shown in Figure 3.17, the study demonstrated that the most significant increases of mean annual ET mainly occurred in the downstream of Stung Sangkae River. The result of mean annual ET in millimeter has increased with the range approximately from 462 mm to 786 mm. Figure 3.18 illustrated the mean annual ET in each sub-catchment of the downstream showing the highest mean annual ET with the range from 651 mm to 786 mm, while the medium mean annual ET occurred in the midstream of the Sangkae river region with the range from about 551 mm to 650 mm and the lowest mean annual ET occurred also mostly in the upstream region with the range from 462 mm to 550 mm. Additionally, due to impacts of LULC change in the 2002-2015 period, the highest mean annual ET changes have increased about 34 mm in the downstream of Stung Sangkae river, while the medium mean annual ET changes have increased around 9 mm for most sub-catchments in the midstream; however the lowest mean annual ET changes have decreased about 17 mm in the sub-catchment 11, 15, and 18 of the upstream in Stung Sangkae river. Moreover, the SWAT model produced the percentage change in some areas of sub-catchment as shown in Figure 3.17. The percentage change for mean annual ET has increased in the maximum about 7.4% for most of downstream areas in Stung Sangkae River while the mean annual ET has increased in the average about 2.5%, except some areas have decreased approximately 2.3% such as sub-catchments of 11, 15, and 18.

Table 3.9. Annual basin values of hydrologic features for the Stung Sangkae River catchment on the different land use from 2000 to 2018 (mm)

Year	PCP	Scenario with land use in 2002				Scenario with land use in 2015			
		PET	ET	SW	WY	PET	ET	SW	WY
2000	1330.3	1531.4	664.4	92.9	675.1	1532.8	664.2	92.9	677.0
2001	1083.3	1630.3	682.5	95.7	417.3	1631.6	682.5	95.7	418.9
2002	1199.5	1704.2	630.7	96.4	559.8	1705.4	631.5	96.3	561.2
2003	1056.9	1660.3	606.2	82.2	466.1	1661.5	608.4	82.2	465.4
2004	985.8	1630.5	586.9	79.5	388.1	1631.7	588.1	79.3	388.7
2005	1241.7	1703.7	642.0	98.8	555.7	1704.8	639.4	98.4	560.4
2006	1207.1	1665.3	681.5	82.5	530.8	1666.5	682.3	82.3	531.5
2007	1370.4	1635.0	641.2	91.0	697.9	1636.2	641.2	91.1	699.8
2008	1558.7	1637.7	685.1	94.5	853.4	1639.0	689.0	94.5	851.0
2009	1291.8	1660.3	665.6	88.9	620.7	1661.5	669.2	88.9	618.7
2010	1285.0	1643.2	642.6	93.1	620.7	1644.4	643.7	92.9	621.7
2011	1624.9	1521.3	688.1	89.0	926.3	1522.6	688.9	89.1	926.7
2012	1441.4	1560.4	686.4	93.7	735.4	1561.8	688.3	93.8	735.4
2013	1222.8	1537.1	576.7	101.4	627.8	1538.5	580.0	101.3	626.5
2014	942.2	1599.0	599.3	88.2	347.0	1600.2	598.4	88.0	349.7
2015	1049.5	1642.2	568.5	94.8	456.3	1643.3	573.8	94.5	453.1
2016	1192.1	1577.8	610.7	94.4	563.6	1578.8	614.3	94.3	561.7
2017	1391.9	1618.3	727.3	98.3	642.1	1619.5	729.2	98.3	641.8
2018	1326.7	1620.5	698.6	97.0	621.5	1621.8	701.9	96.6	620.1
Mean	1252.7	1619.9	646.5	92.2	595.0	1621.2	648.1	92.1	595.2

Note: PCP: precipitation; PET: potential evapotranspiration; ET: actual evapotranspiration; SW: soil water; WY: water yield.

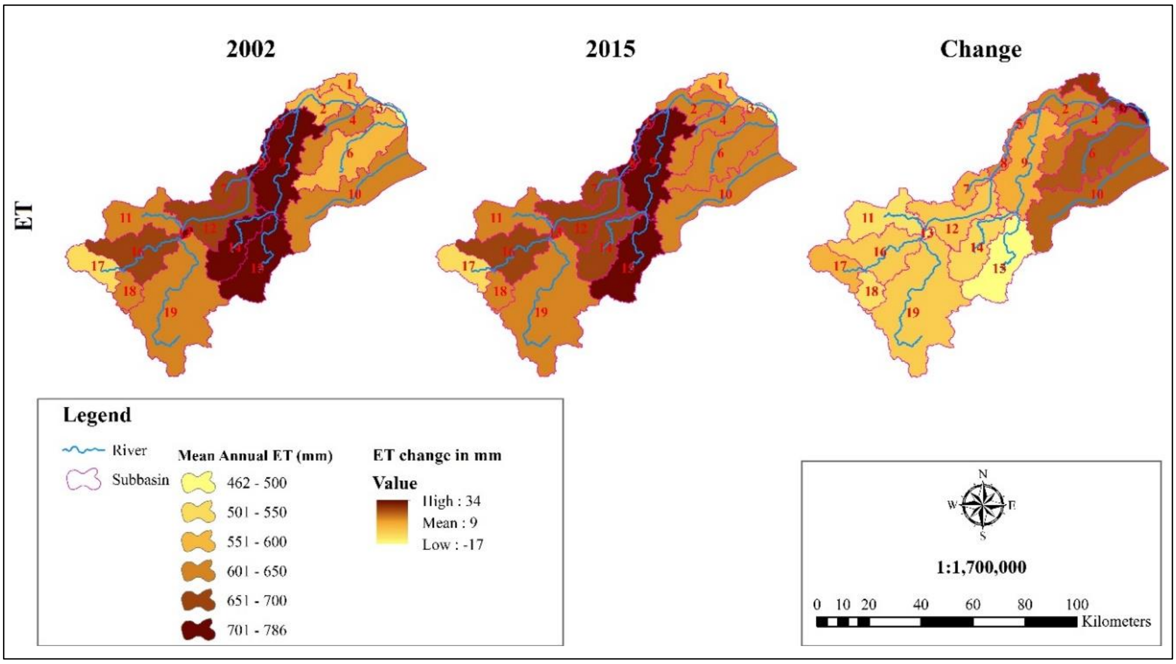

Figure 3.17. Spatial distribution of the mean annual ET change in millimeter for Stung Sangkae catchment

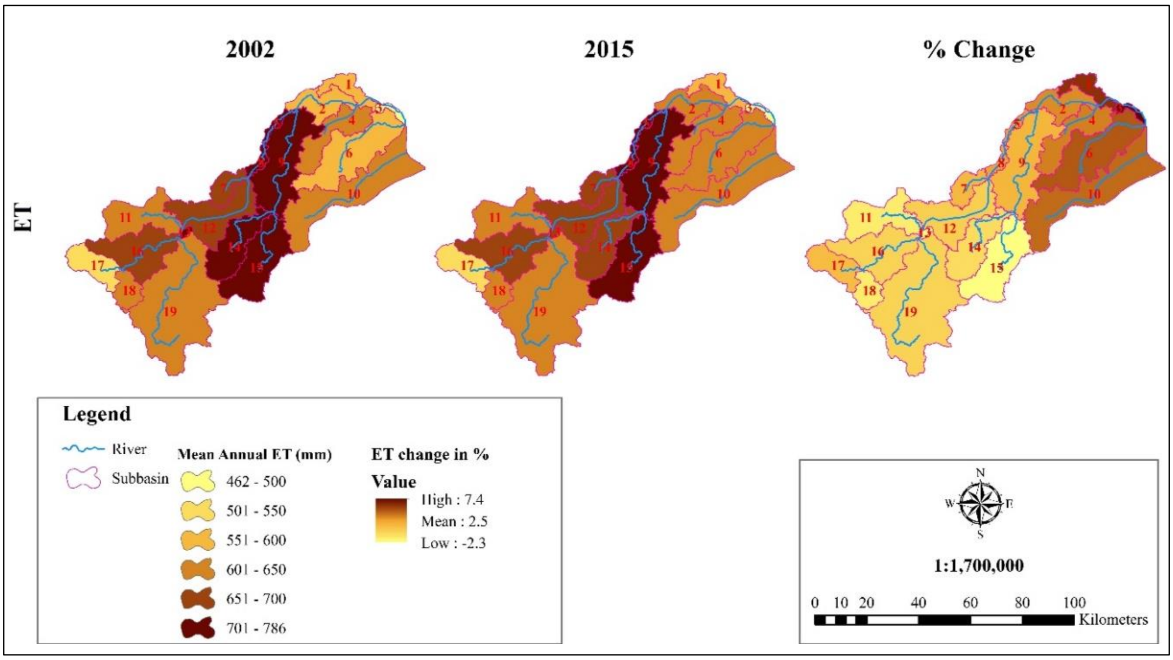

Figure 3.18. Spatial distribution of the mean annual ET change in percentage for Stung Sangkae catchment

3.3.6. Impacts of LULC Changes on Hydrology at the Subbasin Scale

Three subbasins (numbers 2, 8, and 15 in Figure 3.1) with noticeable LULC changes were selected to analyze the impacts of LULC changes on hydrology at the subbasin scale. The results in Table 3.10 shows that the precipitation (PCP) decreased along the stream from downstream (No.2), middle stream (No.8) and upstream catchment (No.15). In subbasin number 2, the area of agricultural land, rice, forest land, grassland, and urban area increased sharply, and the areas of shrubland, and water decreased from 2002 to 2015, which led to the decrease of the potential evapotranspiration (PET) and water yield (WY), and in contrast, the actual evapotranspiration (ET) increased and soil water (SW) stable. In subbasin number 8, only the urban area increased, and agricultural land, rice, shrubland, barren, and water decreased considerably. Hence, the impacts on hydrology were that ET increased and WY and SW decreased. In subbasin, number 15, areas of agricultural land, rice, urban area, wetland, and barren increased and forest land, grassland, and shrubland decreased, and WY increased, and ET and SW decreased. By comparing the LULC changes and their hydrological responses in these three sub-basins, the obvious LULC changes may not show a clear hydrological impact, meaning that different combinations of the LULC can produce similar hydrological effects. In addition, the impacts of the same LULC changes on hydrology may vary under conditions of different precipitation intensity and distribution.

Table 3.10. LULC changes and average annual hydrologic features from 2000 to 2018

Subbasin	Number 2		Number 8		Number 15	
LULC scenario	2002	2015	2002	2015	2002	2015
Total area (ha)	3634.8	3634.8	4397.1	4397.1	45216.5	45216.5
Agricultural land (%)	3.30	7.23	50.06	0.00	0.51	32.98
Rice (%)	0.16	5.37	37.61	28.80	11.44	34.94
Forest land (%)	0.00	40.97	0.00	0.00	56.16	19.38
Urban area (%)	0.00	0.03	9.47	68.51	0.00	1.77
Grassland (%)	8.16	19.12	0.00	0.00	18.60	0.17
Shrubland (%)	87.13	26.16	0.03	0.00	12.32	9.53
Wetland (%)	0.00	0.00	0.00	0.00	0.00	0.04
Barren (%)	0.00	0.00	0.03	0.00	0.00	0.21
PCP (mm)	1245.0	1245.0	1242.4	1242.4	1174.7	1174.7
PET (mm)	1725.5	1724.5	1731.7	1731.0	1791.9	1791.9
ET (mm)	594.8	602.1	786.4	792.7	721.3	704.6
SW (mm)	43.7	43.7	145.2	144.7	119.8	119.4
WY (mm)	636.5	627.7	453.4	445.9	425.1	442.0

3.3.7. Impacts of LULC Changes on Soil Erosion in the Catchment

Stung Sangkae catchment was divided into 19 sub-basins (Figure 3.19). After the calibration and validation processes, the SWAT model was executed for 19 years (2000-2018) to estimate the soil erosion in each sub-basin for both scenarios with land use in 2002 and 2015. As shown in Table 3.11, the average annual values recorded of soil loss at the Stung Sangkae catchment were approximately 12.0 t/ha/yr and 21.8 t/ha/yr for the 2002 and 2015 periods, respectively. Based on the results presented in Figure 3.19, most sub-basins show a low (2-5 ton/ha) to moderate (5-10 ton/ha) sediment yield for both scenarios. The sub-basin 16, 18, and 19 increased the sediment yield from a low to a high erosion rate, especially sub-basin 16. This was because the agricultural land was expanded from 2002 to 2015.

Table 3.11. Mean annual soil loss from 2000-2018 of Stung Sangkae catchment

Year	Flow (m^3/s)	Scenario with land use in 2002	Scenario with land use in 2015
		Soil loss (t/ha/yr)	Soil loss (t/ha/yr)
2000	61.4	11.9	21.9
2001	37.1	3.3	5.4
2002	51.6	13.4	23.5
2003	41.3	12.4	21.9
2004	35.8	8.1	14.0
2005	50.1	11.5	20.9
2006	50.6	13.0	21.4
2007	64.2	17.9	37.5
2008	72.3	18.3	26.0
2009	65.8	8.6	16.5
2010	62.3	19.2	23.5
2011	87.5	13.4	22.6
2012	85.2	13.8	27.2
2013	54.9	22.1	33.4
2014	35.8	6.5	14.9
2015	41.9	9.2	22.1
2016	94.1	7.8	18.0
2017	75.8	10.1	22.5
2018	97.3	7.1	21.9

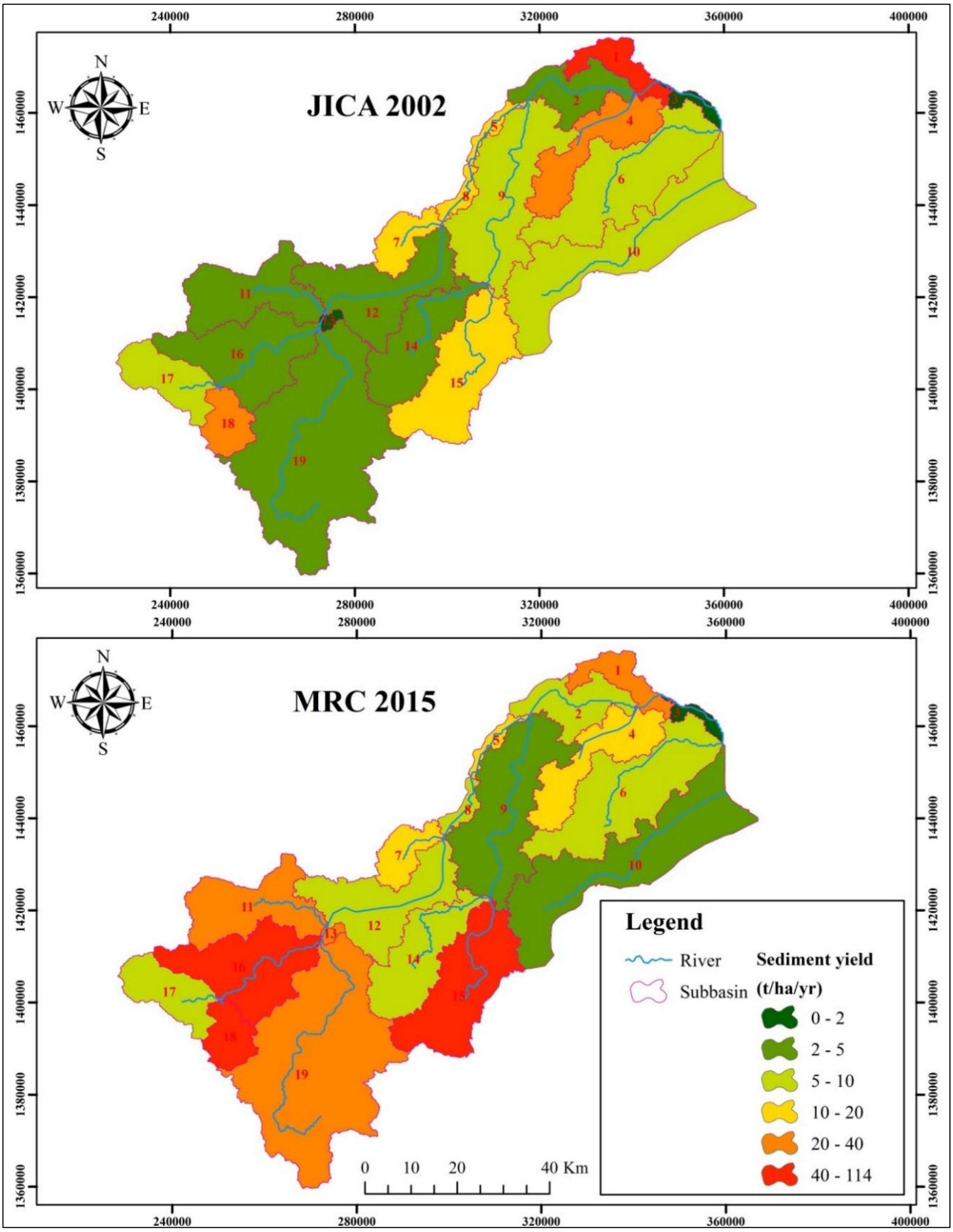

Figure 3.19. Spatial distribution of estimated soil erosion rates (t/ha/yr) at Stung Sangkae catchment

Figure 3.19 shows that the soil erosion was significantly affected by the LULC changes, particularly at the upstream catchment of sub-catchment 11-19, even though the streamflow was not significantly changed from 2022 to 2015. The finding was reasonable with the corn field experiment of 10.45 to 41.89 tons/ha in 2019 (CARDEC, 2019).

3.4. Conclusions of This Chapter

In this chapter, we investigated the impacts of LULC changes on hydrological responses in Cambodia's Stung Sangkae River catchment. The catchment experienced significant changes in the LULC over the 18-year interval from 2002 to 2015. The main land use changes were the transformations of forested area, shrubland, and grassland to agricultural land, rice, and urban area increased at the expense of cropland. These changes were due to implementation of catchment management measures and social and economic development. For the contribution of each LULC to the total WY of the catchment, the forested area, shrubland, and grassland were the main contributors, with up to about 40%, 12%, and 13%, respectively. The land use that generated the most significant water yield was agricultural activities and urban area, higher than any other land use type, followed by forested area, shrubland, and grassland.

For both reference land uses (2002 LULC and 2015 LULC), the sensitive parameters of stream flow were the same, although the sensitivity rank of the same parameters varies. Therefore, these calibrated parameters can be used for further future hydrological and environmental studies in the Stung Sangkae River catchment without needing to do sensitivity analysis. Moreover, the applicability of the SWAT model in simulating stream flow dynamics of Stung Sangkae River catchment has been validated based on the satisfactory values of the statistical measures of the model efficiency (R^2 = 0.58, NSE = 0.55, and PBIAS = 5 if included dam construction and R^2 = 0.64, NSE = 0.62 and PBIAS = 15 if exclude dam construction). Therefore, the model simulation results provide confidence for the further application of the model to assess the hydrologic response analysis due to spatial and temporal variability of the catchment characteristics will have minimal bias within the Stung Sangkae River catchment.

The soil erosion map obtained by the hydro-agricultural model (SWAT) also shows that 74.5 % of the surface area of the Stung Sangkae catchment is exposed to a low to moderate risk of erosion (<10 t/h/y) and 17.4% basin is at severe risk. The most affected areas are located in the west of the catchment, where the upland agriculture was expanded. The results of soil loss SWAT model is higher.

However, based on the evaluation, accompanying the LULC changes in the Stung Sangkae catchmnet, increases in PET, ET, and WY indicated that soil and water conservation practices increased stream flow, while the expansion of the agricultural land, rice, and urban area increased the ET and WY.

Moreover, the approach used in this research simply evaluates contributions of individual LULC classes to the total hydrological responses, providing quantitative information for decision-makers to make better options for land and water resource planning and management. This approach also provides a solid example of the potential of hydrologic modeling using remotely sensed digital LULCs in understanding the impacts of landscape change on water provisioning, a vital ecosystem service in the Stung Sangkae of Cambodia. It can be widely applied to a variety of catchments, where time-sequenced digital land cover data are available, and to predict hydrological consequences to LULC changes.

Reference of this chapter

Aghsaei, H., Dinan, N. M., Moridi, A., Asadolahi, Z., Delavar, M., Fohrer, N., and Wagner, P. D. 2020. Effects of dynamic land use/land cover change on water resources and sediment yield in the Anzali wetland catchment, Gilan, Iran, Sci. Total Environ., 712, 136449, https://doi.org/10.1016/j.scitotenv.2019.136449.

Ajai, S., Mohd, I., Isaacc, R.K., and Denisc, D.M. 2014. Assessing the performance and uncertainty analysis of the SWAT and RBNN models for simulation of sediment yield in the Nagwa watershed, India. Hydrological science journal, 2(2), 65–74.

Arnold, J.G., Srinivasan, R., Muttiah, R. S., and Williams, J. R. 1998. Large Area Hydrologic Modelling and Assessment Part I: Model Development. J Am Water Resources Assoc 34, 73–89. https://doi.org/10.1111/j.1752-1688.1998.tb05961.x

Cambodian Conservation Agriculture Research for Development Center (CARDEC). 2019. Conservation agriculture-related research activities in Cambodia. General of the General Directorate of Agriculture, Ministry of Agriculture, Forestry and Fisheries, Phnom Penh, Cambodia.

DeFries, R., and Eshleman, K.N. 2004. Land-use change and hydrologic processes: a major focus for the future. Hydrological Processes 18: 2183–2186.

Food and Agriculture Organization of the United Nations (FAO). 2006. Guidelines for Soil Description, 4th ed.; Food and Agriculture Organization of the United Nations: Rome, Italy; ISBN 978-92-5-105521-2.

Green, W.H., and Ampt, G.A. 1911. Studies on soil physics, 1. The flow of air and water through soils, J. Agr. Sci., 4, 11–24.

Holvoet, K., Van Griensven, A., Seuntjens, P., and Vanrolleghem, P.A. 2005. Sensitivity analysis for hydrology and pesticide supply towards the river in SWAT. Physics and Chemistry of the Earth, Parts A/B/C, 30(8–10), 518–526. https://doi.org/10.1016/j.pce. 2005.07.006

Kalantari, Z., Lyon, S.W., Folkeson, L., French, H.K., Stolte, J., Jansson, P.-E., and Sassner, M. 2014. Quantifying the hydrological impact of simulated changes in land use on peak discharge in a small catchment. Science of The Total Environment 466–467, 741–754. https://doi.org/10.1016/j.scitotenv.2013.07.047

Khoi, D.N., and Suetsugi, T., 2014. The responses of hydrological processes and sediment yield to land-use and climate change in the Be River Catchment, Vietnam: Impact of land use and climate changes on hydrology and sediment yield. Hydrol. Process. 28, 640–652. https://doi.org/10.1002/hyp.9620

Kummu, M., Tes, S., Yin, S., Adamson, P., Józsa, J., Koponen, J., Sarkkula, J. 2014. Water balance analysis for the Tonle Sap Lake-floodplain system. Hydrological Processes, 28(4), 1722–1733. https://doi.org/10.1002/hyp.9718

Li, H., Zhang, Y., Vaze, J., and Wang, B. 2012. Separating effects of vegetation change and climate variability using hydrological modelling and sensitivity-based approaches. Journal of Hydrology 420–421, 403–418. https://doi.org/10.1016/j.jhydrol.2011.12.033

Li, Z., Liu, W., Zhang, X., Zheng, F. 2009. Impacts of land use change and climate variability on hydrology in an agricultural catchment on the Loess Plateau of China. Journal of Hydrology 377, 35–42. https://doi.org/10.1016/j.jhydrol.2009.08.007

Mango, L.M., Melesse, A.M., McClain, M.E., Gann, D., and Setegn, S.G. 2011. Land use and climate change impacts on the hydrology of the upper Mara River Basin, Kenya: results of a modeling study to support better resource management, Hydrology and Earth System Sciences, vol. 15, no. 7, pp. 2245–2258.

Markert, K.N., Griffin, R.E., Limaye, A.S., and McNider, R.T. 2018. Spatial modeling of land cover/land use change and its effects on hydrology within the Lower Mekong Basin, in: Vadrevu, K.P., Ohara, T., Justice, C. (Eds.), Land-Atmospheric Research Applications in South and Southeast Asia, Springer Remote Sensing/Photogrammetry. Springer International Publishing, Cham, pp. 667–698. https://doi.org/10.1007/978-3-319-67474- 2_29

Moriasi, D.N., Arnold, J.G., Van Liew, M.W., Binger, R.L., Harmel, R.D. and Veith, T. 2007. Model evaluation guidelines for systematic quantification of accuracy in watershed simulations. Trans. ASABE 50(3): 885-900.

Muto, Y., Noda, K., Maruya, Y., Chibana, T., and Watanabe, S. 2022. Impact of climate and land- 153 use changes on the water and sediment dynamics of the Tokoro River Basin, Japan. Environmental Advances 7, 100153. https://doi.org/10.1016/j.envadv.2021.100153

Neitsch, S.L., Arnold, J.G., Kiniry, J.R., Srinivasan, R., and Williams, J.R. 2005. Soil and water assessment tool user's manual. GSWRL Report.

Neitsch, S.L., Arnold, J.G., Kiniry, J.R., and Williams, J.R. 2011. Soil and Water Assessment Tool Theoretical Documentation Version 2009; Texas Water Resources Institute: College Station, TX, USA.

Nie, W., Yuan, Y., Kepner, W., Nash, M. S., Jackson, M., and Erickson, C. 2011. Assessing impacts of landuse and landcover changes on hydrology for the upper San Pedro watershed. Journal of Hydrology, vol. 407, no. 1–4, pp. 105–114. https://doi.org/10.1016/j.jhydrol.2011.07.012

Noda, K., Yoshida, K., Shirakawa, H., Surahman, U., and Oki, K. 2017. Effect of land use change driven by economic growth on sedimentation in River Reach in Southeast Asia: A case study in Upper Citarum River Basin. J. Agric. Meteorol. 73, 22–30. https://doi. org/10.2480/agrmet.D-15-00021

Öztürk, M., Copty, N.K., and Saysel, A.K., 2013. Modeling the impact of land use change on the hydrology of a rural watershed. Journal of Hydrology 497, 97–109. https://doi.org/ 10.1016/j.jhydrol.2013.05.022

Pai, N., Saraswat, D., Srinivasan, R. 2012. Field-SWAT: A tool for mapping SWAT output to field boundaries. Computers and Geosciences 40, 175–184. https://doi.org/10.1016/ j.cageo.2011.07.006

Shrestha, B., Cochrane, T.A., Caruso, B.S., and Arias, M.E. 2018. Land use change uncertainty impacts on streamflow and sediment projections in areas undergoing rapid development: A case study in the Mekong Basin. Land Degrad. Develop. 29, 835–848. https://doi.org/10.1002/ldr.2831

Wang, G., Yang, H., Wang, L., Xu, Z., and Xue, B. 2014. Using the SWAT model to assess impacts of land use changes on runoff generation in headwaters, Hydrological Processes, 28 (3), 1032–1042.

White, K.L., and Chaubey, I. 2005. Sensitivity analysis, calibration, and validations for a multisite and multivariable SWAT model 1, JAWRA Journal of the American Water Resources Association, vol. 41, pp. 1077–1089.

Zhang, X.C. and Nearing, M.A. 2005. Impact of climate change on soil erosion, runoff, and wheat productivity in central Oklahoma, Catena, 61, 185–195.

CHAPTER 4

Impact of Land Use and Land Cover Changes on Soil Erosion in Stung Sangkae Catchment Using RUSLE Model

4.1. Introduction

Soil erosion is a major environmental and economic concern in most parts of the world (Ozsahin et al., 2018; Pimentel and Burgess, 2013; Chuenchum et al., 2019; Benavidez et al., 2018) and poses a threat to land, freshwater, and oceans (Borrelli et al., 2020). This threat may result in low agricultural productivity (Mihara et al., 2005), ecological degradation, and high sedimentation (Chuenchum et al., 2019; Pham et al., 2018; Bonilla et al., 2010). According to Marondedze and Schütt (2020), the estimated average soil erosion rate globally ranges between 12 and 15 t/ha/y and almost 84% of global soil loss results from soil erosion processes.

It is estimated that the average soil erosion by water exceeds 2000 t/km^2/y, which mainly occurs on croplands in tropical areas (Chuenchum et al., 2019; Van Oost et al., 2007). It is reported that soil erosion caused by human activities is 10–15 times higher than any natural process (Wilkinson and McElroy, 2007). For instance, approximately 80% of cultivated areas worldwide face high to severe erosion. The number of generated sediments can increase waterways' turbidity and impurities' concentration (Tang et al., 2014). Furthermore, soil erosion and sediment yield can severely affect people and the environment if the quantity of sediment exceeds the value of the typical measurement of aquatic organisms. Soil erosion is the central part of the early development of sediment conveyance to streams. In this early development process, evacuated soil particles are converted into sediments due to the effect of the erosion agent (Chuenchum et al., 2019). Rainfall, topography, soil characteristics, vegetation or land cover changes, cropping systems, and land management practices are the main fundamental factors causing the rate and severity of soil erosion (Panagopoulos et al., 2019; Kogo et al., 2020).

In the past, soil erosion studies were done through physical field assessments (Mihara et al., 2005). It was more challenging, costly, and unfeasible to do mapping of soil erosion risks in huge spatial areas with complex environments in most cases (Kogo et al., 2020; Chen et al., 2011). However, even though it is challenging, field-based assessments are needed to provide accurate and reliable data, which are essential for calibrating and validating results from soil loss models (Mihara et al., 2005; Evans, 2002; Evans and Brazier, 2005). Previously, soil loss and erosion risk mapping has been assessed using altered empirical and stochastic models at local and global levels (Renschler and Harbor, 2002). A review study by Benavidez et al. (2018) summarized 35 previous studies that have applied the USLE (Universal Soil Loss Equation) and RUSLE (Revised Universal Soil Loss Equation) from 1988 to 2017. The review identified modeling techniques developed and used to study soil loss from a field, a hill slope, or a catchment/watershed and discussed the different sub-factors of USLE and RUSLE, and analyzed how various studies around the globe have adapted the equations to local environments (Benavidez et al., 2018). These models have different geomorphological parameters that vary in extent and period of application, manipulating factors, processes, features examined, algorithms used, and type of assessment. Among the models, RUSLE by Renard et al. (1997), which is used to estimate sheet and rill erosion of annual soil loss per unit land area, has arisen as the most widely and globally used model.

A wide range of empirical, conceptual, and physical-based models have been developed to estimate soil loss risks. These models vary in complexity, data requirements, consideration processes, and calibration (Marondedze and Schütt, 2020; Merritt et al., 2003; Raza et al., 2021). Empirical models such as USLE, MUSLE and RUSLE are primarily based on observed data and the relationships between different factors and soil erosion levels. The empirical models require relatively fewer input data than conceptual or physical-based models. Thus, empirical models are often used when there is a limitation in data availability. Most empirical models do not provide information about the deposition of stream sedimentation, which limits their application in modeling mass balance (Raza et al., 2021). According to Stefanidis et al. (2021), the most commonly used empirical erosion model is USLE, and the revised version is RUSLE. The main advantages of the USLE/RUSLE model are flexibility, data availability, and extensive literature research, making this method suitable for almost all types of conditions and environments (Alewell et al., 2019). Conceptual models, such as Agricultural Policy/Environmental eXtender (APEX) and Soil and Water Assessment Tool (SWAT), are primarily based on sediment and runoff continuity equations and essentially are hybrids of physical-based and empirical models (Beck, 1987). Most of the conceptual models use equations from empirical approaches. For instance, empirical models like USLE and MUSLE are carried out in APEX and SWAT to estimate soil erosion. Physical-based models such as Environmental Policy Integrated Climate (EPIC), APEX, and Water Erosion Prediction Project (WEPP), are more capable of responding to event-based or continuous storms to simulate surface runoff, soil detachment, transportation, and sediment yield (Raza et al., 2021). For example, the EPIC model considers the effect of several best management practices (BMPs) related to crop, soil, and nutrient management on soil erosion and soil productivity.

Recently, due to climate change which causes climate variation in some parts of the world, particularly rainfall patterns, this will increase and enhance soil erosion, especially in areas where land use changes occur. Rainfall erosivity is the potential ability of rain to cause erosion (Reyes et al., 2004), and it is a major driving force of soil erosion and nutrient losses worldwide, which may leave farmers vulnerable to crop failures. The rainfall erosivity, derived from 30-min or daily rainfall events, is characterized by a large variability in space and time (Bezak et al., 2020; Panagos et al., 2017). This may lead to inaccurate estimates of soil erosion. However, daily rainfall amount is the simplest erosivity factor and it may poorly explain the amount of soil loss (Wischmeier and Smith, 1978) because erosivity is also a function of the raindrop's diameter, mass, and velocity. In most countries, soil loss measurement is not available. Therefore, an erosivity index cannot be determined empirically (Reyes et al., 2004). The impact of future climate change on soil erosion susceptibility can be estimated by calculating the predicted R-Factor value. The spatial correlation between climate change, soil erosion, and land cover change using global models, such as RUSLE, can effectively assist in the spatial management process (Hateffard et al., 2021).

Soil erosion changes in the future can be done by developing modeling scenarios of the two most dynamic factors in soil erosion, i.e., rainfall erosivity and land cover change Panagos et al., 2017). Currently, it is believed that large-scale estimation of soil loss rates under climate change conditions is possible. According to Panagos et al. (2017), predicting soil erosion changes in the future mainly depends on modeling future rainfall erosivity, land use changes, and impacts of policies on soil loss. Recently, developing the Rainfall Erosivity Database at European Scale (REDES) and statistical methods for spatially interpolating rainfall erosivity data can become valuable insights for predicting future rainfall erosivity based on climate scenarios (Bezak et al., 2020). Using a comprehensive statistical modeling method (Gaussian Process Regression) will help to predict rainfall erosivity according to climate change scenarios by selecting the most appropriate covariates (monthly precipitation, temperature datasets, and bioclimatic layers (Panagos et al., 2017). Extreme rainfall will be more intense, and natural disasters will be related to more frequent rain; as a result, soil erosion rates are expected to increase in response to climate change (Borrelli et al., 2020;

Stefanidis et al., 2021). Moreover, climatologists have discovered that the earth is warming, and as the global temperature rises, the water cycle becomes more vigorous. Therefore, it is clear that climate change will affect soil erosion and its consequences (Stefanidis and Chatzichristaki, 2017).

Thus, the overall goal of this chapter was to evaluate the land use and land cover changes and their impact on soil erosion in Stung Sangkae catchment in 2002 and 2015. The study's specific objectives were to: (1) estimate the magnitude of annual soil erosion and its spatial distribution in the catchment; and (2) evaluate how land use and land cover types contributed to soil erosion in the catchment. The results of this study are expected to provide useful information that can promote soil erosion management practices in Stung Sangkae Catchment, Battambang Province, as well as Tonle Sap Great Lake, which represents one of the world's most productive ecosystems and biodiversity. The Tonle Sap River-Great Lake system underpins the world's biggest freshwater fishery and directly or indirectly affords a livelihood for most of Cambodia's population (MRC, 2005).

4.2. Materials and Method

4.2.1. Description of Study Area

The Stung Sangkae catchment (605,170 ha), which is the third-largest tributary of the Tonle Sap Basin river system, is located at the upper north-western part of Cambodia between 12°13′–13°24′ N and 102°35′–103°42′ E (Figure 3.1). The topography is level within the floodplain region and rough with slopes at the upland portion of the catchment, having elevations extending from 4 m at the most reduced point to 1,413 m a.s.l at the most noteworthy point. The main river that flows through the catchment, Sangkae River, lies between the tributaries of the Tonle Sap Great Lake in the upper western part of the catchments. Agriculture is the main local economic activity and the main source of livelihood. Meteorological data collected from six weather stations in 2007–2018 showed that the average annual precipitation in the study area varied from 1308 mm at Moung Rues-sei station to 1,577 mm at Samlout station, with little change during the year (Figure 4.2). The major soil types in the region are categorized into 4: (1) Gleysols are wetland soils, which in the natural state are continuously water-saturated within 50 cm of the surface for extended periods; (2) Luvisols are a type of soil in which highly active clay migrates from the top part of the profile, usually gray, and is deposited in the B layer, usually brown; (3)

Nitisols are mainly deep, well-drained soils with a stable structure and high nutrient content; and (4) Acrisols are clay-wealthy soils which can be fairly vulnerable to erosion.

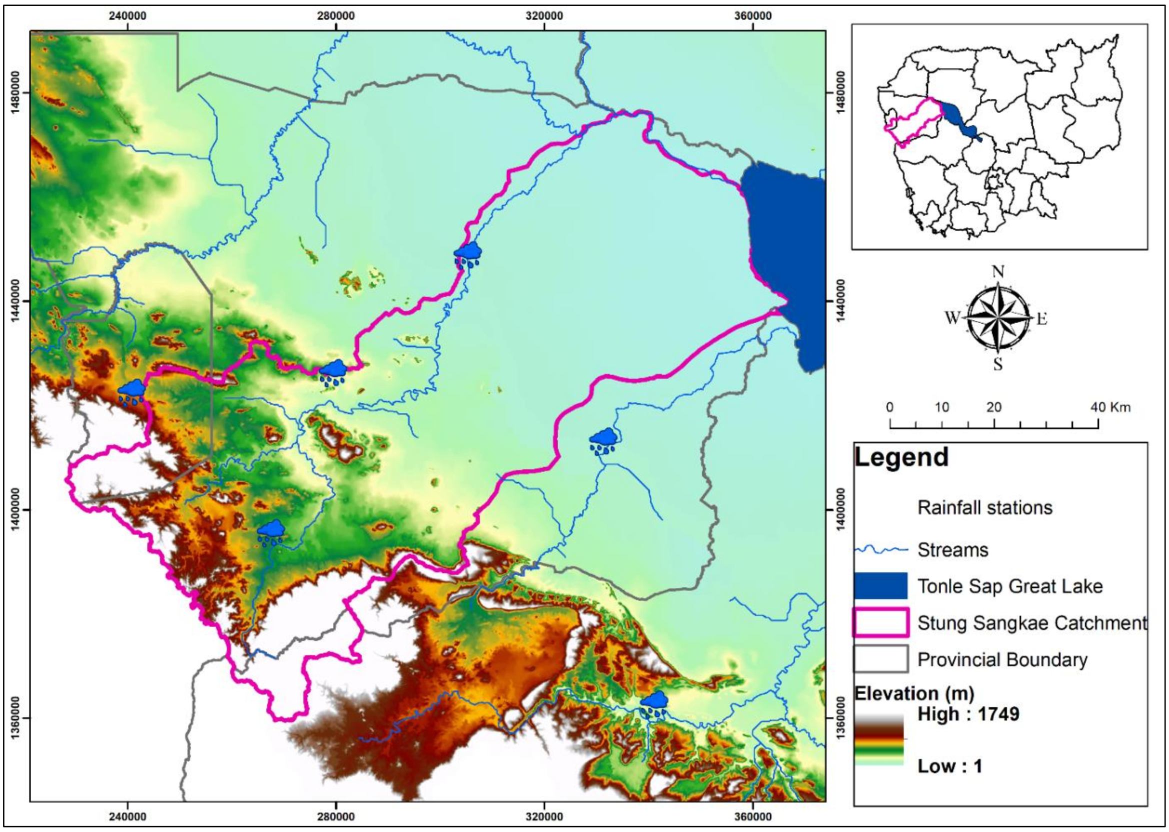

Figure 4.1. Location map of the research catchment and meteorological stations within the research area

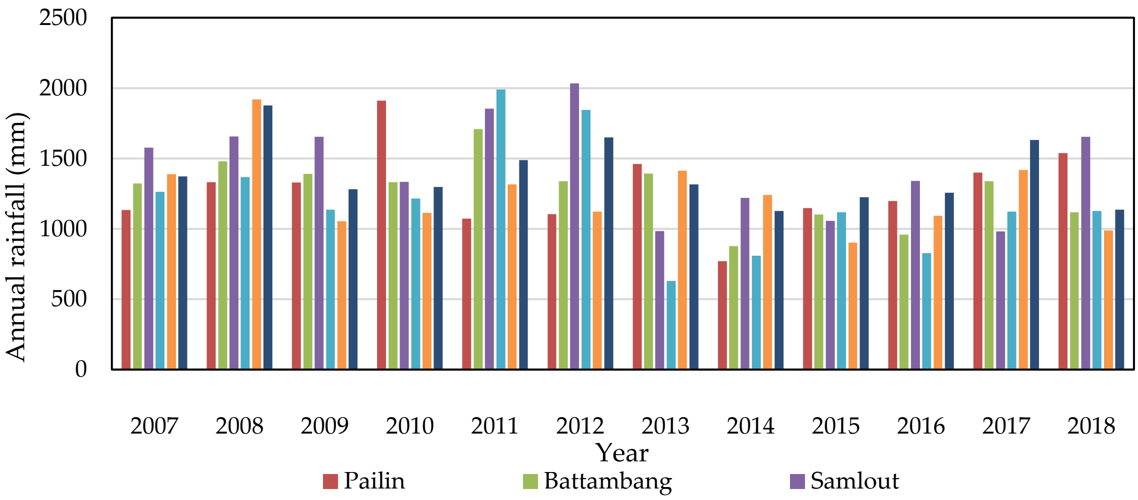

Figure 4.2. The distribution of annual rainfall recorded by weather stations inside and around the study catchment during 2007–2018

The catchment is characterized by distinctive topographical conditions, from flat plains to rugged areas. After dividing the digital elevation model (DEM) into six FAO slope grades (FAO, 2006); 16.6% of the total area has very gently sloping (0–2°), whereas 35.2% and 28.3% of the entire areas are characterized as gently sloping (2–5°) and sloping (5–10°). The remaining land slopes are divided into strongly sloping, moderately steep, and steep, which covered areas of 9.8% (10–15°), 9.1% (15–30°), and 1.0% (>30°), respectively (Table 4.1).

Table 4.1. FAO slope classification in the study catchment and related susceptibility to soil erosion

No	Slope Classes (Degree)	Characteristics	Susceptibility	Area	
				(ha)	(%)
1	0–2	Flat to very gently sloping	Very low	100,579	16.6%
2	2–5	Gently sloping	Low	212,830	35.2%
3	5–10	Sloping	Medium	171,084	28.3%
4	10–15	Strongly sloping	High	59,375	9.8%
5	15–30	Moderately steep	Very high	55,173	9.1%
6	>30	Steep	Extremely high	6129	1.0%

The land use developed by the Japan International Cooperation Agency (JICA) in 2002 (JICA, 2003) and land cover (Land Cover Maps of LMB) developed by Mekong River Commission (MRC) in 2015 (MRC, 2015) were used in the study (see Table 4.2 and Figure 4.3). The land cover maps of the Lower Mekong Basin, which covers the Lower Mekong countries such as Cambodia, Lao PDR, Thailand and Vietnam, was developed by MRC following the FAO Land Cover Classification System based on the target surveyed points and the satellite image classifications. In Cambodia, the number of target surveyed points were 2595 points (Kityuttachai et al., 2016). However, due to site conditions, not all points could be inspected; only 9357 points were collected from field data, which accounted for 89% of the target (10,575 points). The samples covered all 19 land cover types. This approach would have resulted in 12,825 samples for the entire LMB. However, the targeted sample size was reduced to 10,575 samples; as a result, only 9357 samples were collected on-site.

Table 4.2. Land use and land cover of the Stung Sangkae catchment in 2002 and 2015

LULC Classes	JICA 2002 Area (ha)	JICA 2002 Area (%)	MRC 2015 Area (ha)	MRC 2015 Area (%)	Net Change Area (ha)	Net Change Area (%)
Agricultural land	25,627.2	4.24	152,742.3	25.24	127,115.0	21.00
Barren land	149.2	0.02	274.0	0.04	124.8	0.02
Built-up area	1,702.8	0.28	20,870.1	3.45	19,167.3	3.17
Deciduous forest	74,524.7	12.31	24,144.9	3.99	−50,379.8	−8.32
Evergreen forest	110,474.4	18.26	90,338.0	14.93	−20,136.4	−3.33
Grassland	79,496.0	13.14	29,394.2	4.86	−50,101.8	−8.28
Marsh and swamp	280.3	0.05	35.8	0.01	−244.6	−0.04
Mixed forest	75,361.5	12.45	64,710.9	10.69	−10,650.6	−1.76
Paddy field	92,784.8	15.33	144,931.5	23.95	52,146.7	8.62
Shrubland	141,689.0	23.41	74,019.0	12.23	−67,670.0	−11.18
Water bodies	3,080.1	0.51	3,709.4	0.61	629.3	0.10
Total	605,170.0	100.00	605,170.0	100.0		

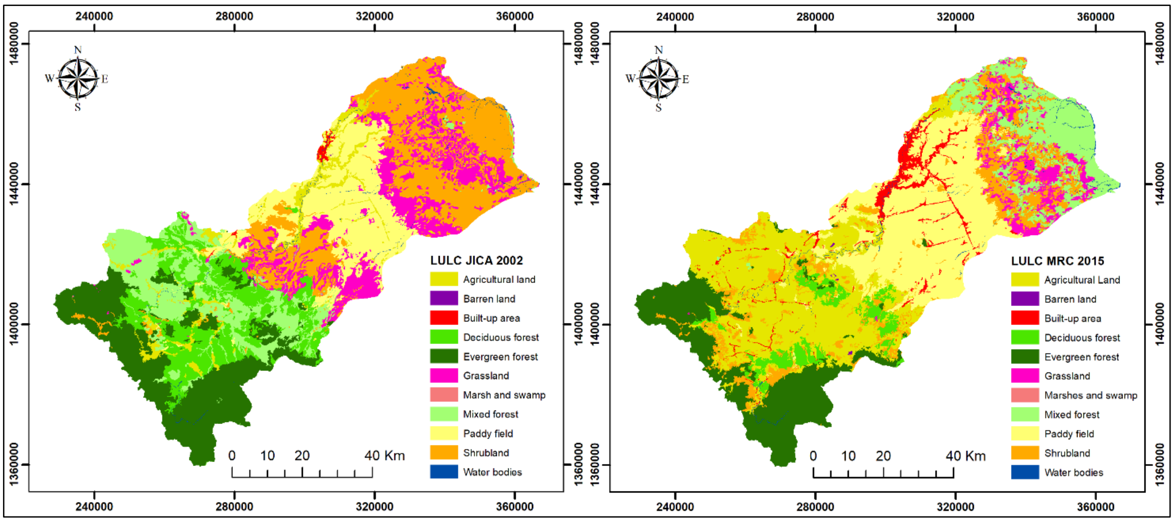

Figure 4.3. Land use and land cover (LULC) developed by JICA 2002 and MRC 2015 of the Stung Sangkae catchment

From the land use and land cover assessment in Table 4.2, cultivated lands (agricultural land and paddy rice fields) occupied almost 50% of the total land area in the region in 2015, which increased from 20% in 2002, while forest cover (evergreen, deciduous and mixed forest) occupied 43% in 2002 and declined to 30% in 2015. Among the land use and land covers, areas under agricultural land increased from 4.24% to 25.24%, which is the highest compared to others, followed by paddy rice fields that increased from 15.33% to 23.95% between the years 2002 and 2015. The built-up areas also increased from 0.28% in 2002 to 3.45% in 2015, while water bodies also increased slightly from 0.51% to 0.61% between 2002 and 2015. On the contrary, evergreen forest, deciduous forest, mixed forest, grassland, shrubland and marsh and swamp areas decreased from 18.26%, 12.31%, 12.45%, and 23.41% in 2002 to 14.93%, 3.99%, 10.69%, 4.86% and 12.23% in 2015, respectively.

4.2.2. Description of RUSLE Model

The Revised Universal Soil Loss Equation (RUSLE) is a well-known and widely accepted and implemented empirical model for estimating soil erosion. The RUSLE, an empirical model, is simple and the most commonly used computerized version of the Universal Soil Loss Equation (USLE), a statistical model developed to estimate annual soil loss per unit area based on erosion factors (Renard et al., 1997). The RUSLE model has been widely used to predict average annual soil losses caused by sheet and rill erosion and to display the spatial distribution of potential erosion risk.

The empirical models such as USLE (Wischmeier and Smith, 1978), MUSLE (Williams and Berndt, 1977) and RUSLE (Renard et al., 1997) are mostly based on observed data and the relationships between different factors and soil erosion levels. The empirical models require considerably less input data compared to conceptual or physical-based models. Thus, the empirical models are often used when there is a limitation of data availability. Most empirical models do not provide information about deposition of stream sedimentation which limits their application in modeling mass balance (Raza et al., 2021). According to Stefanidis et al., (2021) the most commonly used empirical erosion model is USLE (Wischmeier and Smith, 1978), and the revised version RUSLE (Renard et al., 1997). The main advantages of the USLE/RUSLE model are flexibility, data availability and extensive literature research, making this method suitable for almost all types of conditions and environments (Alewell et al., 2019).

The principal equation for the USLE model family (Wischmeier and Smith, 1958 and 1978) is below:

$$\boldsymbol{A} = \boldsymbol{R} \times \boldsymbol{K} \times \boldsymbol{L} \times \boldsymbol{S} \times \boldsymbol{C} \times \boldsymbol{P} \quad (1)$$

where A is mean annual soil loss (metric tons per hectare per year), R is the rainfall and runoff factor or rainfall erosivity factor (megajoule millimeters per hectare per hour per year), K is the soil erodibility factor (metric ton hours per megajoules per millimeter), L is the slope length factor (unitless), S is the slope steepness factor (unitless), C is the cover and management factor (unitless), and P is the support practice factor (unitless).

The USLE was initially developed at the farm-plot scale for agricultural land in the United States of America, but has seen use in many other countries, at many different scales, and in many other geoclimatic regions. Although the name implies that the model can be applied to all soils, the original USLE is more accurate for soils of medium texture and slopes less than 400 ft in length with a gradient ranging between 3% and 18%, and it is managed with consistent cropping practices that are well represented in plot-scale erosion studies (Wischmeier and Smith, 1978). Hence, applying the USLE family of models to soils and sites exceeding these limits requires careful parameterisation of the model and being mindful of the increased uncertainty in model predictions.

In the original development of the model, this farm plot is called the "unit plot" and is defined as a plot that is 22.1 meters long, 1.83 meters wide, and has a slope of 9% (Wischmeier and Smith, 1978). Although the model accounts for rill and interrill erosion, it does not account for soil loss from gullies or mass wasting events such as landslides (Thorne et al., 1985).

4.2.2.1. Rainfall Erosivity Factor (R)

The R factor represents the effect that precipitation has on soil erosion and was included after observing sediment deposits after an intense storm (Wischmeier and Smith, 1978). The annual R factor is a function of the mean annual EI_{30} that is calculated from detailed and long-term records of storm kinetic energy (E) and maximum 30 min intensity (I_{30}) (Morgan, 2005; Renard et al., 1997). Due to the detailed data requirements for the standard (R)USLE calculation of rainfall erosivity, studies in areas with less detailed data have used alternative equations depending on the temporal resolution and availability of the rainfall data. These compiled studies have used long-term datasets with at least daily temporal resolution to construct their R-factor equation. Extensive work by Naipal et al. (2015) attempted to apply the (R)USLE at a coarse global scale (30 arcsec) by using USA and European databases to derive rainfall erosivity equations. These equations use a combination of annual precipitation (millimeters), mean elevation (meters), and simple precipitation intensity index (millimeters per day) to calculate the R factor for different Köppen–Geiger climate classifications (Naipal et al., 2015). Loureiro and Coutinho (2001) used 27 years of daily rainfall data from Portugal and the (R)USLE method of calculating EI_{30} to construct an equation that uses the number of days that received over 10mm of rainfall and the amount of rainfall per month when the day's rainfall exceeded 10 mm. The Loureiro and Coutinho (2001) equation was modified by Shamshad et al. (2008) for use in tropical Malaysia by using long-term rainfall data to construct a regression equation relating monthly rainfall and annual rainfall with the R factor.

Similarly, Sholagberu et al. (2016) used 23 years of daily rainfall data to create a regression equation relating annual rainfall and the R factor for the highlands of Malaysia. These simplified equations may be transferable to areas of similar climate that do not have the long-term detailed rainfall data required by the original (R)USLE. The imperial units of erosivity are in hundreds of foot tonforce (tonf) inch per acre per hour per year, and multiplying by 17.02 will give the SI units of megajoule millimeter per hectare per hour per year (Renard et al., 1997).

In tropical areas such as Southeast Asia, the R factor by El-Swaify et al. (1987) as cited in Merritt et al. (2004) was used extensively in Thailand, the Philippines, and Sri Lanka. However, the units for the R factor in this equation are given as metric tons per hectare per year, which do not correspond to the original units used by (R)USLE (Merritt et al., 2004). This lack of consistency regarding units is not uncommon in the reviewed literature, which sometimes fails to explicitly report the units used for the different factors. For example, Renard and Freimund (1994) report that the units of R-factor equations by Arnoldus (1977) were presumed to be in metric units. By being clear and consistent about units in the (R)USLE literature, future researchers can be more certain about the accuracy of their borrowed R-factor equations instead of presuming the units to be the same as the original (R)USLE.

The usage of monthly precipitation data to determine the R factor is due to monthly rainfall data being more readily available compared to detailed storm records (Renard and Freimund, 1994). Although annual rainfall estimates are sufficient, using monthly rainfall data to construct sub-annual R factors and then aggregating those R factors to an annual scale is useful in sites with large temporal variability in rainfall. Renard and Freimund (1994) used data from 155 stations with known R factors based on the original USLE approach and related their R factors to observed annual and monthly precipitation. These equations developed by Renard and Freimund (1994) on the west coast of USA were used in Ecuador

(Ochoa-Cueva et al., 2015), and Honduras and El Salvador (Kim et al., 2005). Work by Arnoldus (1980) developed R-factor equations in West Africa that use monthly and annual precipitation. However, as described earlier, these equations present a problem in terms of consistent units. In Southeast Asia, Shamsad et al. (2008) developed an R-factor equation in Malaysia that was used in the Philippines by Delgado and Canters (2012). In New Zealand, the monthly precipitation can be aggregated to seasonal precipitation and used in the equation for seasonal R factor derived by Klik et al. (2015).

Monthly or better precipitation records are very useful in (R)USLE applications because of the option of estimating soil loss at a monthly or seasonal scale, which can be useful in countries with high temporal variation of rainfall throughout the year. Monthly and seasonal erosion has been estimated by varying the R factor depending on the monthly precipitation while leaving all the other factors constant (Ferreira and Panagopoulos, 2014; Kavian et al., 2011). Klik et al. (2015) emphasized the need to understand the drivers of soil erosion, including whether rainfall intensity had a stronger effect compared to mean annual rainfall. In an assessment of spatial and temporal variations in rainfall erosivity over New Zealand, December and January were associated with higher erosivities, while August was associated with lowest erosivity (Klik et al., 2015). Similar work by Diodato (2004) has cited the use of monthly erosivity data to be more useful with respect to managing crop growing cycles and tillage practices, especially during seasons where high rainfall erosivity is expected. In locations where there is a large temporal variation in rainfall throughout the year, the seasonal approach of estimating soil erosion is more important for sustainable land management (Ferreira and Panagopoulos, 2014).

In summary, there are many rainfall erosivity datasets and equations in the (R)USLE literature that can be used by new researchers applying the RUSLE to their study area (Table 4.3). The erosivity dataset produced by Panagos et al. (2017) is recommended for areas with no rainfall data or in ungauged catchments since this is a raster dataset with global coverage (~30 arcsec resolution) and is freely available. For areas in the European Union, work by Panagos et al. (2015a) has produced a rainfall erosivity map with regional coverage at (~1 km resolution. These datasets can also be used to validate the erosivity factors calculated at the national or catchment scale. For study areas in which annual precipitation and the Köppen–Geiger classification are known, Naipal et al. (2015) has published rainfall erosivity equations and values for 17 different climate zones. Several studies have published erosivity equations for tropical areas: da Silva (2004) for Brazil, Shamshad et al. (2008) for Malaysia, and Jain and Das (2010) for India. For arid areas, Arnoldus (1980) as cited in Renard and Freimund (1994) has derived erosivity equations for Morocco and other locations in West Africa. Many other equations are found in Table 4.3, and choosing several for sensitivity testing is recommended for future (R)USLE applications. It is also important to test against observed data or R factors derived by previous applications in the same study area or in study areas with similar climatic regimes.

Table 4.3. Summary of some different studies that developed rainfall erosivity equations, original locations, and other studies that used their equations

No.	Author	Original location	Resolution	Equation and requirements
1	Fernandez et al. (2003), originally developed by the USDA-ARS (2002)	USA	Annual	$\mathrm{R} = -823.8 + 5.123P$ P: annual precipitation Units: MJ mm ha^{-1} h^{-1} year^{-1}
2	Nakil (2014) as cited in Nakil and Khire (2016)	India	Annual	$\mathrm{R} = 839.15 + e^{0.0008P}$ P: annual precipitation Units: MJ mm ha^{-1} h^{-1} year^{-1}
3	Land Development Department (2000) as cited in Nontananandh and Changnoi (2012)	Thailand	Annual	$\mathrm{R} = 0.04669\mathrm{P} - 12.1415$ P: mean annual precipitation Units: MJ mm ha^{-1} h^{-1} year^{-1}
4	Renard and Freimund (1994)	West coast of USA	Monthly and annual	$R = 0.0483 \times P^{1.610}$ $R = 587.8 - 1.219P + 0.004105\,P^2$ Using MFI (Arnoldus, 1980): $R = 0.07397 \times \mathrm{MFI}^{1.847}$ $R = 95.77 - 6.081\mathrm{MFI} + 0.4770\mathrm{MFI}^2$ $\mathrm{MFI} = \sum_{i=1}^{12} \frac{P_i^2}{P}$ MFI: modified Fournier index P_i: monthly precipitation P: annual precipitation Units: MJ mm ha^{-1} h^{-1} year^{-1}
5	Zhou et al. (1995) as cited in Li et al. (2014)	Southern China	Monthly	$R = \sum_{i=1}^{12} -1.15527 + 1.792P_i$ P_i: monthly precipitation Units: MJ mm ha^{-1} h^{-1} year^{-1}
6	Roose (1975) and Morgan (1974) as cited in Morgan (2005)	Peninsular Malaysia and Africa	Annual	Africa (Roose, 1975): $R = 0.5 \times P \times 17.3$ Peninsular Malaysia: $R = (9.28 \times P - 8838)\left(\frac{75}{1000}\right)$ P: mean annual precipitation (mm) Units: MJ mm ha^{-1} h^{-1} year^{-1}

7	El-Swaify et al. (1987) as cited in Merritt et al. (2004)	Possible USA	Annual	$R = 38.5 + 0.35\,P$ P: mean annual precipitation Units: MJ mm ha^{-1} h^{-1} $year^{-1}$
8	Hurni (1985)	Ethiopia	Annual	$R = 0.562P - 8.12$ P: mean annual precipitation Units: MJ mm ha^{-1} h^{-1} $year^{-1}$

4.2.2.2. Soil Erodibility Factor (K)

The K factor represents the influence of different soil properties on the slope's susceptibility to erosion (Renard et al., 1997). It is defined as the "mean annual soil loss per unit of rainfall erosivity for a standard condition of bare soil, recently tilled up-and-down slope with no conservation practice" (Morgan, 2005). The K factor essentially represents the soil loss that would occur on the (R)USLE unit plot, which is a plot that is 22.1m long, is 1.83m wide, and has a slope of 9% (Lopez-Vicente et al., 2008).

The values of the K-factor are in the range from 0 to 1. Higher K-factor values indicate the soil's higher susceptibility to soil erosion by water (Adornado et al., 2009). In the (R)USLE, Wischmeier and Smith (1978) and Renard et al. (1997) use an equation that relates textural information, organic matter, information about the soil structure, and profile permeability with the K factor or soil erodibility factor. However, other soil classifications might not include soil structure and profile permeability information that matches the information required by (R)USLE nomograph. Hence, alternative equations have been developed that exclude the soil structure and profile permeability (Table 4.3). The question of which equation to use depends on the availability of soil data. Where only the textural class and organic matter content are known, Stewart et al. (1975) have approximated K-factor values based on these inputs. Like the R factor, the imperial units of soil erodibility are in ton acre hour per hundreds of acres per foot per tons per inch. Multiplying by 0.1317 gives the erodibility in SI units of metric tons hectare hour per hectare per megajoule per millimeter (Renard et al., 1997).

Although seemingly relatively straightforward, the K- factor equation proposed by Wischmeier and Smith (1978) has a few soil type limitations. This equation was developed using data from medium-textured surface soils in the Midwestern USA, with an upper silt fraction limit of 70% (Renard et al., 1997). An equation for volcanic soils in Hawaii was proposed by El-Swaify and Dangler (1976) as cited in Renard et al. (1997) but is only appropriate for soils similar to Hawaiian soils and not for all tropical soils. Despite these limitations, many studies outside the USA have used the original Wischmeier and Smith

(1978) K-factor equation. Being aware of the regional specificity of K-factor equations is important, and using different K-factor equations in one study area to find a range of soil erodibility could be a way of testing their applicability.

Similar to the sensitivity analysis of the R-factor equations, testing different K-factor equations to see the variation in erodibility values and then comparing these K factors with published values from similar soils would be a good way to test applicability. For the spatial coverage of the European Union, a soil erodibility raster dataset (500m resolution) is available for validation (Panagos et al., 2014). David (1988) and Dymond (2010) have published K-factor values for soils of different textural classes (e.g. clay, loam) that can be used if only soil texture is known (Table 4.4 and 4.5). However, the values published by Dymond (2010) are broad and do not account for soils with mixed texture, while the values of David (1988) are based on soils in the Philippines. Like the R factor, it is important to check the derived K-factor values for the site-specific soil against previously published K-factor values for comparable sites and soil types.

Table 4.4. Summary of different studies with soil erodibility equations, original locations, and other studies that used their equations

No.	Author	Original location	Data requirements	Equation
1	Wischmeier and Smith (1978) and Renard et al. (1997)	USA	Very fine sand (%), clay (%), silt (%), organic matter (%), soil structure, profile permeability	$M = \text{Silt} \times (100 - \text{Clay})$ $K = \{[2.1 \times M^{1.14} \times (10^{-4}) \times (12 - a)] + [3.25 \times (b - 2)] + [2.5 \times (c - 3)]\} \div 100$ M: Particle-size parameter Silt: silt (%) as well as the percentage of very fine said (0.1 to 0.05 mm) Clay: clay (%) a: organic matter (%) b: soil structure code used in soil classification: 1: Very fine granular 2: Fine granular 3: Medium or coarse granular 4: Blocky, platy, or massive c: profile permeability class: 1: Rapid 2: Moderate to rapid 3: Moderate 4: Slow to moderate 5: Slow 6: Very slow
2	Williams and Renard (1983) as	USA	Sand (%), silt (%),	$K = 0.2 + 0.3 \exp\left(0.0256 \times \text{Sa} \times \left(1 - \frac{S_i}{100}\right)\right) \times \left(\frac{S_i}{Cl+S_i}\right)^{0.3} \times \left(1.0 -\right.$

	cited in Chen et al. (2011)		clay (%), organic carbon (%)	$\frac{0.25 \times C}{C + \exp(3.72 - 2.95C)}\Big) \times \Big(1.0 - \frac{0.7 \times SN}{SN + \exp(-5.51 + 22.9SN)}\Big)$ Sa: sand (%) Si: silt (%) Cl: clay (%) SN = 1 - (Sa/100) C: organic carbon
3	David (1988), a simplified version of Wischmeier and Mannering (1969)	USA	Sand (%), clay (%), silt (%), organic matter (%), pH	$K = [(0.043 \times \mathrm{pH}) + (0.62 \div \mathrm{OM}) + (0.0082 \times S) - (0.0062 \times C)] \times S_i$ pH: pH of the soil OM: organic matter (%) S: sand content (%) C: clay ratio = % clay = (% sand + % silt) Si: silt content = % silt/100
4	El-Swaify and Dangler (1976) as cited in Renard et al. (1997)	Hawaii, USA	Textural information, base saturation	$K = -0.03970 + 0.00311x_1 + 0.00043x_2 + 0.00185x_3 + 0.00258x_4 - 0.00823x_5$ x_1: unstable aggregate size fraction (<0.250mm) (%) x_2: modified silt (0.002–0.1 mm) (%) -modified sand (0.1–2 mm) (%) x_3: % base saturation x_4: silt fraction (0.002–0.050 mm) (%) x_5: modified sand fraction (0.1–2 mm) (%)

Note: All of the equations in Table 4.4 use imperial units of soil erodibility: ton acre hour per hundreds of acres per foot per tonf per inch. Multiply by 0.1317 for conversion into SI units of metric ton hours per megajoules per millimeter.

Table 4.5. *K*-factor values from Dymond (2010) for soil texture in New Zealand

No.	Soil texture	K-factor (Dymond, 2010)
1	Clay	0.20
2	Loam	0.25
3	Sand	0.05
4	Silt	0.35

Table 4.6. *K*-factor values from David (1998) for soil texture in Philippines

No.	Soil texture	K-factor (Dymond, 2010)
1	Loamy fine sand	0.07
2	Clay	0.13-0.26
3	Clay loam	0.22-0.30
4	Loam	0.19-0.63
5	Sandy clay	0.09-0.20
6	Sandy loam	0.23-0.30
7	Silt loam	0.30-0.60
8	Silty clay	0.19-0.27
9	Silty clay loam	0.28-0.35

4.2.2.3. Slope Length (L) and Steepness (S) Factor

The LS factor represents the effect of the slope's length and steepness on sheet, rill, and inter-rill erosion by water. It is the ratio of expected soil loss from a field slope relative to the original USLE unit plot (Wischmeier and Smith, 1978). The USLE method of calculating the slope length and steepness factor was initially applied at the unit plot and field scale. The RUSLE extended this to the one-dimensional hill slope scale, with different equations depending on whether the slope had a gradient of more than 9% (Renard et al., 1997; Wischmeier and Smith, 1978). Further research extends the LS factor to topographically complex units using a method that incorporates contributing area and flow accumulation (Desmet and Govers, 1996). The USLE and RUSLE method of calculating the LS factor uses slope length, angle, and a parameter that depends on the steepness of the slope in percent (Wischmeier and Smith, 1978).

One of the criticisms of the original USLE method of calculating LS factor is its limited applicability to complex topography. With advances in GIS technology, the method of determining the LS factor as a function of upslope contributing area or flow accumulation and slope has risen in popularity (Table 4.6). Using DEMs to calculate the upslope contributing area and the resulting LS factor allows researchers to account for more topographically complex landscapes (Moore and Burch, 1986; Desmet and Govers, 1996). Desmet and Govers (1996) have also built on this method by showing its application in a GIS environment over topographically complex terrain compared to the original method proposed by Wischmeier and Smith (1978). This method of using flow accumulation for slope length and steepness explicitly accounts for flow convergence and divergence, which is important when considering soil erosion over a complex landscape (Wilson and Gallant, 2000). It is possible to use this method to calculate the LS factor over a large extent, but a high-resolution DEM is needed for an accurate representation of the topography. The resolution required depends on the study area's scale. The relatively coarse globally available DEMs (30m at best) are less suited to field and sub-catchment scale studies where capturing microtopography's effects may be important.

The original equations for the LS factor assume that slopes have uniform gradients and any irregular slopes would have to be divided into smaller segments of uniform gradients for the equations to be more accurate (Wischmeier and Smith, 1978). This manual measurement of slopes and dividing them into segments may be manageable at the plot or small field scale, but it is less valuable at larger scales. In terms of practicality, Desmet and Govers (1996) have reported studies of this method applied at a watershed scale with the disadvantages of it being time-consuming. Studies in Iran and the Philippines have implemented the (R)USLE methods within a GIS environment by calculating the LS factor for each raster cell in a DEM, essentially treating each pixel as its segment of uniform slope (Bagherzadeh, 2014; Schmitt, 2009).

As explained above, using flow accumulation, upslope contributing area, and slope in a GIS environment has gained popularity due to its ability to account for flow convergence and divergence explicitly, thus capturing more complex topography (Wilson and Gallant, 2000). The flow accumulation method was applied at the scales of watersheds and regions (as shown in Table 4.7) and has even been applied by Panagos et al. (2015a) at the scale of the European Union using a 25m DEM. The only thing limiting users is the availability of high-resolution DEMs and the trade-off between processing time and accuracy. The original (R)USLE methods require only slope angle and length, operate over a single cell in a DEM by treating it as a uniform slope, and take less processing time than the flow accumulation method. However, the user must remember that this cannot capture the convergence and divergence of flow, thus sacrificing accuracy for time.

Additionally, the issue of limited vertical accuracy in global and many national DEMs confounds the uncertainties associated with coarse cell sizes. Further work is suggested to understand the appropriate horizontal resolution and vertical accuracy of DEMs used for soil erosion predictions at the sub-catchment or field scales. Benavidez (2018) investigated the use of high-resolution DEMs (15m and finer), finding the methods that only used slope length and steepness were adequate for delineating large vulnerable areas at the watershed scale. However, flow accumulation methods performed significantly better at the sub-watershed or field scale (Benavidez, 2018). In summary, the choice of which LS-factor method to use depends on the DEM's spatial resolution, availability of computing resources, and scale of the study site. DEMs with spatial resolution coarser than 100m do not accurately capture the flow network of a catchment (Panagos et al., 2015a). The LS-factor methods that account for only slope length and steepness are recommended for sites with such coarse DEMs. At the national, regional, or watershed scale, delineating large areas vulnerable to soil loss is more useful due to the ease of managing these areas at such large scales. The methods that use only slope length and steepness are recommended. For sub-watershed or field studies and with sufficiently fine DEMs (15m or finer), using LS-factor methods that account for flow accumulation is more useful for identifying the most critical areas of vulnerability for targeted management approaches.

Table 4. 7. Summary of methods of calculating LS factor, original locations, and other studies that used these methods

No.	Author	Original location	Data requirements	Equation
1	Wischmeier and Smith (1978)	USA	Slope length and angle	$LS = \left(\frac{\lambda}{72.6}\right)^m \times [(65.41 \times \sin^2\theta) + (4.56 \times \sin\theta) + 0.065]$ λ: slope length (ft) θ: angle of slope m: dependent on the slope - 0.5 if slope is greater than 0.5% - 0.4 if slope is 3.5 - 4.5% - 0.3 if slope is 1-3% - 0.2 if slope is less than 1%
2	Renard et al. (1997)	USA	Slope length and angle	$L = \left(\frac{\lambda}{72.6}\right)^m$ $m = \frac{\beta}{1+\beta}$ $\beta = \frac{\left(\frac{\sin\theta}{0.0896}\right)}{[3.0 \times (\sin\theta)^{0.8} + 0.56]}$ If slope is less than 9%: $S = 10.8 \times \sin\theta + 0.03$ If slope is greater or equal to 9%: $S = 16.8 \times \sin\theta + 0.50$ But if the slope is shorter than 15 ft: $S = 3.0 \times \sin\theta^{0.8} + 0.56$ λ: slope lenght (ft) θ: angle of slope m: dependent on the slope - 0.5 if slope is greater than 0.5% - 0.4 if slope is 3.5 - 4.5% - 0.3 if slope is 1-3% - 0.2 if slope is less than 1%
3	David (1988), based on work by Madarcos (1985) and Smith and Whitt (1947)	Philippines, but based on work from the USA	Slope rise in percent	$LS = a + b \times S_L^{4/3}$ $a = 0.1$ $b = 0.21$ S_L: slope (%)
4	Morgan (2005) but previously published in earlier editions	Britain	Slope length and gradient in percent	$LS = \left(\frac{l}{22}\right)^{0.5}$ + 0.065 + 0.045s + 0.0065s^2) l: slope length (m) s: slope steepness (%)

5	Moore and Burch (1986) as cited in Mitasova et al. (1996) Desmet and Govers (1996); Mitasova et al. (2013)	USA	Upslope contributing area per unit width, which can be approximated through flow accumulation, cell size, slope	$LS = (m+1)\left(\frac{U}{L_0}\right)^m \left(\frac{\sin\beta}{S_0}\right)^n$ U (m^2 m^{-1}): upslope contributing area per unit width as a proxy for discharge $U =$ flow accumulation × cell size L_0: lenght of the unit plot (22.1) S_0: slope of the unit plot (0.09) β: slope m (sheet) and n (rill) depend on the prevailing type of erosion ($m = 0.4$ to 0.6) and n (1.0 to 1.3)

4.2.2.4. Cover and Management Factor (C)

The cover and management factor (C) is defined as the ratio of soil loss from a field with a particular cover and management to that of a field under "clean-tilled continuous fallow" (Wischmeier and Smith, 1978). The (R)USLE uses a combination of sub-factors such as impacts of previous management, canopy cover, surface cover and roughness, and soil moisture on potential erosion to produce a value for the soil loss ratio, which is used with the R factor to produce a value for the C-factor (Renard et al., 1997). This method requires extensive knowledge of the study area's cover characteristics, including agricultural management. It may be suitable at the field or farm scale, but monitoring all these characteristics at the watershed scale may not be feasible.

A simpler method of determining the C-factor is referencing studies with reported values for similar land cover or studies done in the same area or region. Table 4.8 and 4.9 give a broad overview of C factors for cover types and common crops. Wischmeier and Smith (1978) also include the effect of percent ground cover, reporting C-factor values for the same cover type over a cover percentage and condition range. Morgan (2005) and David (1988) have reported values for the different growth stages of the same kinds of trees. A simple method of creating a C-factor layer is using lookup tables to assign C-factor values to the land cover classes in the study area. When using C factors from the literature, it is essential to note that the definition of land cover type between two countries may vary. For example, land classified as forest in one country may be different regarding vegetation cover or type compared to the forest in another (e.g. differences in pine forests and tropical forests). Therefore, it is crucial to understand the differences between land cover classifications before applying C-factor values from the literature. Van der Knijff et al. (2000) cite the large spatial and temporal variations in cover and crop over a large region such as the European

Union as another reason why using the lookup-table-based approach is inadequate and tedious. Another method of determining the C-factor is the normalized difference vegetation index (NDVI) estimated from satellite imagery to address this. Although there are NDVI layers available, these are limited by geographical coverage, date of acquisition, and resolution. The MODIS NDVI dataset made by Caroll et al. (2004) at 250m resolution covers the USA and South America. NASA produced a global dataset of NDVI values at 1^0 resolutions for the time span of July 1983 to June 1984, making it suitable for studying historical soil erosion but not necessarily for the current state of land cover3. In areas where ready-made NDVI products are unavailable, authors have used satellite imagery to obtain NDVI such as AVHRR or Landsat ETM (Van der Knijff et al., 2000; De Asis and Omosa, 2007; Ma et al., 2010, as cited in Li et al., 2014). De Asis and Omasa (2007) related the C-factor and NDVI through fieldwork and image classification – determining the C-factor at several points within the study area using the (R)USLE approach and relating it to the NDVI through regression correlation analysis. This may not be feasible in larger study areas such as the European Union, where Van der Knijff et al. (2000) determined NDVI from satellite imagery and created an equation based on its positive correlation with green vegetation (Table 4.8). This approach enabled them to create a C-factor map over the European Union. However, C factors were unrealistically high in some areas such as woodland and grassland, so values for those areas were taken from the literature.

An advantage of using NDVI is that researchers can determine sub-annual C factors if there is satellite imagery available, which can lead to understanding the contribution of cover to seasonal soil erosion and identifying critical periods within the year where soil erosion is a risk (Ferreira and Panagopoulos, 2014). Similar methods have been applied in Brazil by Durigon et al. (2014) and Kyrgyzstan by Kulikov et al. (2016). Determining C factors at the seasonal scale is important because vegetation cover can change throughout the year due to agricultural and forestry practices. In study areas with a high temporal variation of rainfall throughout the year, seasonal vegetation can greatly exacerbate or mitigate soil erosion.

To summarize, the choice of which method to use depends on the scale of the study area, reported C factors for a similar cover, and availability of high-resolution imagery. For small-scale studies, it is more feasible to determine the C factors through fieldwork (Table 4.10). If previous (R)USLE studies have reported C factors for a cover similar to the study area, those values can be used for the table-based approach. Lastly, high-resolution imagery can be used to determine the study area's NDVI. At small scales and with a good understanding of differences in land cover classifications, pulling values from the literature may be the most efficient choice, but at larger regional scales, this may become tedious. At larger scales, high-resolution satellite imagery may be available to determine NDVI. Still, authors must be mindful of its acquisition date in relation to their study period, as well as data quality and image processing issues such as dealing with cloud cover and aggregating images from multiple satellite passes (Van der Knijff et al., 2000; Kulikov et al., 2016).

Table 4.8. C-factor equations that use NDVI

No.	Author	Original location	Equation
1	Van der Knijff et al. (2000)	Europe	$C = \exp\left[\propto\left(\frac{\text{NDVI}}{\beta - \text{NDVI}}\right)\right]$ $\propto = 2$ $\beta = 1$
2	Ma et al. (2010) as cited in Li et al. (2014)	China	$f_g = \frac{\text{NDVI} - \text{NDVI}_{\text{min}}}{\text{NDVI}_{\text{max}} - \text{NDVI}_{\text{min}}}$ $C = \begin{cases} 1 & f_g = 0 \\ 0.6508 - 0.343 \times \log?(f_g) & 0 < f_g < 78.3\% \\ 0 & f_g \geq 78.3\% \end{cases}$

Table 4.9. C-factors for general types of land cover compiled from various sources

No.	Cover	Dymond (2010), New Zealand	David (1988), Philippines	Morgan (2005), USA	Fermandez et al. (2003), USA	Dumas and Fossey (2009), Vanuatu	Land Development Department (2002), Thailand as cited in Nontananandh and Changnoi (2012)
1	Bare ground	1	1	1	NA	NA	NA
2	Urban	NA	0.2	NA	0.03	0	0
3	Crop	NA	NA	NA	0.128	0.01	0.255-0.525
4	Forest	0.005	0.001-0.006	0.001	0.001	0.001	0.003-0.048
5	Pasture	0.01	NA	0.1	NA	NA	NA
6	Scrub	0.005	0.007-0.9	0.01	0.003	0.16	0.01-0.1

Table 4.10. C-factors for specific types of land cover compiled from various sources

Cover	Panagos et al. (2015b) (Europe)	David (1988) (Philippines)	Morgan (2005) (Varous)
Bananas	NA	0.1-0.3	NA
Barley	0.21	NA	NA
Chili	NA	NA	0.33
Cocoa	NA	NA	0.1-0.3
Coffee	NA	NA	0.1-0.3
Common wheat and spelt	0.2	NA	0.1-0.4
Cotton seed	0.5	0.4-0.6	0.4-0.7
Dried pulses (legumes) and protein crop	0.32	0.3-0.5	0.04-0.7
Durum wheat	0.2	NA	NA
Fallow land	0.5	NA	NA
Grain-maize/corn	0.38	0.3-0.6	0.02-0.9
Groundnuts	NA	NA	0.3-0.8
Linseed	0.25	NA	0.1-0.2
Oilseeds	0.28	NA	NA
Palm with cover crops	NA	0.05-0.3	0.1-0.3
Pineapple	NA	0.2-.05	0.01-0.4
Potatoes	0.34	NA	0.1-0.4
Rape and turnip rape	0.3	NA	NA
Rice	0.15	0.1-0.2	0.1-0.2
Rye	0.2	NA	NA
Soya	0.28	NA	0.2-0.5
Sugar beet	0.34	NA	NA
Sugarcane	NA	NA	0.13-0.4
Sunflower seed	0.32	NA	NA
Tobacco	0.49	0.4-0.6	NA
Yams	NA	NA	0.4-0.5

Table 4.11. Examples of where C-factor accounts for crop management from Morgan (2005) and David (1988)

Crop	Management	*C* factor
Maize, sorghum, or millet	High productivity; conventional tillage	0.20-0.55
	Low productivity; conventional tillage	0.50-0.90
	High productivity; chisel plowing into residue	0.12-0.20
	Low productivity; chisel plowing into residue	0.30-0.45
	High productivity; no or minimum tillage	0.02-0.10
Coconuts	Tree intercrops	0.05-0.1
	Annual crops as intercrop	0.1-0.30

4.2.2.5. Support Practice Factor (P)

The support practice factor (P) is defined as the ratio of soil loss under a specific soil conservation practice (e.g. contouring, terracing) to that of a field with upslope and downslope tillage (Renard et al., 1997). The P factor accounts for management practices that affect soil erosion through modifying the flow pattern, such as contouring, strip cropping, or terracing (Renard et al., 1997). The more effective the conservation practice is at mitigating soil erosion, the lower the P factor (Bagherzadeh, 2014). Like the C factor, values for P factors can be taken from the literature; if no support practices are observed, the P factor is 1.0 (Adornado et al., 2009). The P factor can also be estimated using sub-factors, but the difficulty of accurately mapping support practice factors or not observing support practices leads to many studies ignoring it by giving their P factor a value of 1.0 (Adornado et al., 2009; Renard et al., 1997; Schmitt, 2009).

Another possible reason why studies may ignore the P factor is due to the nature of their chosen C factors. Some C factors already account for a support factor, such as intercropping or contouring. For example, Morgan (2005) and David (1988) give C factors for one type of crop but with different types of management (Table 4.10). Despite the P factor being commonly ignored, a number of studies have reported possible P factors for different kinds of tillage, terracing, contouring, and strip cropping (Table 4.12). The P factor has a significant impact on the estimation of soil loss. For example, a P factor of 0.25 for zoned tillage reflects the potential for this management factor to reduce soil by 75% loss compared to conventional tillage (P factor: 1.00). At suitably detailed scales and with enough knowledge of farming practices, using these P factors may lead to a more accurate estimation of soil loss. Additionally, these P factors can be used in scenario analysis to understand how changing farming practices may mitigate or exacerbate soil loss. An application of (R)USLE in the Cagayan de Oro catchment in the Philippines showed, through scenario analysis, that soil conservation practices such as agroforestry and alley cropping could potentially lead to large decreases in soil loss compared to the baseline scenario (Benavidez, 2018).

In summary, including the P factor in (R)USLE applications is important because of the significant effects of some management practices on reducing soil loss compared to conventional tillage. The P factor is useful for studies where different management practices are being considered for the same site, as it can elucidate which practices are more beneficial for soil conservation.

Table 4.12. P-factors for different types of agricultural management practices

David (1988)				
Tillage and residue management	*P* factor			
Conventional tillage	1.00			
Zoned tillage	0.25			
Mulch tillage	0.26			
Minimum tillage	0.52			
Slope (%)	Terracing		Contouring	Contour strip cropping
	Bench	Broad-based		
1–2	0.10	0.12	0.60	0.30
3–8	0.10	0.10	0.50	0.15
9–12	0.10	0.12	0.60	0.30
13–16	0.10	0.14	0.70	0.35
17–20	0.12	0.16	0.80	0.40
21–25	0.12	0.18	0.90	0.45
> 25	0.14	0.20	0.95	0.50
Panagos et al. (2015c)				
Slope (%)	Contouring *P* factor			
9–12	0.6			
13–16	0.7			
17–20	0.8			
21–25	0.9			
> 25	0.95			

4.2.2.6. Limitations of (R) USLE

This section presents a few of the key limitations of the (R)USLE: regional applicability, uncertainties associated with the model, input data and validation, and representing other types of erosion. The original USLE was formulated based on soil erosion studies on agricultural land in the USA. When applied to different climate regimes and land cover conditions, this may lead to greater uncertainties associated with estimates of average annual soil loss (Kinnell, 2010). Since the (R)USLE parameters were developed based on small-scale studies of agricultural plots, there are also uncertainties associated with upscaling the original USLE to the catchment or regional scale (Nagle et al., 1999; Naipal et al., 2015). Wischmeier and Smith (1978) have also warned that using the (R)USLE in conditions extremely different from the agricultural conditions the model was formulated under may lead to extrapolation error.

Sensitivity analysis and testing which (R)USLE subfactors suit particular study sites is one method of addressing the (R)USLE's regional applicability. To reduce uncertainty in accounting for land use, work by Post and Hartcher (2005) recommended using C-factor values for specific land cover classifications (e.g. specific crops, forest growth stages) instead of values for broad land cover categories (e.g. agriculture, forest). Although C-factor values can be taken from the literature or determined in situ, an extensive literature review compiling potential soil loss rates of different crop and forest covers compared to likely soil loss rates of bare soil can be used to determine likely C-factor values of a particular site. Improvements and modifications to the (R)USLE subfactors have made it applicable to larger spatial scales, including a coarse-resolution **r**epresentation at the global scale (Naipal et al., 2015). The pan-European application by Panagos et al. (2015a) showed setting a maximum value for slope steepness of 50% (26.6^0) would prevent significantly large LS-factor values and account for the absence of soil on such steep slopes. Assembling published estimates of (R)USLE sub-factors from different climatic regions and soil types would help in sensitivity testing (R)USLE equations, deciding the most appropriate equation to use, and verifying the derived (R)USLE sub-factor values.

The uncertainties associated with the (R)USLE, and arguably soil erosion modelling in general, stem from several factors: the inability of models to capture the complex interactions involved in soil loss, the low availability of long-term reliable data for modelling, and the lack of soil erosion observational data for model validation, especially in datascarce environments. The simplicity of the (R)USLE allows usage in locations where there are insufficient data for more complex models that require large input datasets (Hernandez et al., 2012). Of the studies reviewed, very few critically discuss the uncertainties associated with the (R)USLE, but those that do offer several ways to overcome these uncertainties. Since the (R)USLE does not account for all the complex interactions associated with soil erosion, its predicted soil erosion rates should be taken as best estimates rather than absolute values (Wischmeier and Smith, 1978). Some applications have chosen to display their soil loss results as categorical to produce maps that show low, medium, or high areas of vulnerability instead of showing annual average amounts (Adornado et al., 2009; Schmitt, 2009). The (R)USLE is a good first attempt at identifying vulnerable areas and estimating soil loss for a landscape at the baseline scenario due to the model's relative simplicity and few data requirements (Aksoy and Kavvas, 2005). The (R)USLE is also useful for doing scenario analysis to check whether changing land use or management practices would either exacerbate or mitigate soil loss, making it useful for comparison purposes (Merritt et al., 2004; Nigel and Rughooputh, 2012).

Validating the soil erosion rates produced by the (R)USLE is difficult because of the lack of easily obtainable observational soil erosion records, especially in data-scarce environments. Out of the (R)USLE applications reviewed for this paper, 30% presented explicit comparisons between their modelled soil loss from (R)USLE and observed soil loss, modelled soil loss from (R)USLE and other models (one study), and soil loss from multiple models and observed soil loss (one study).

Based on the remaining studies that reported comparisons of modelled RUSLE soil loss to observed soil loss, the modelled-to-observed ratio ranged from extreme under prediction at 0.04 to over-prediction at over 3 times the observed values. The applications where RUSLE severely under-predicted soil loss cited the model's inability to account for gully erosion and mass wasting as one of the reasons for estimation errors, thus underscoring the importance of including these types of erosion in future improvements to RUSLE (Dabney et al., 2012; Gaubi et al., 2017). Another issue is temporal and/or spatial resolution differences and sometimes differing timescales between modelled and observed estimates. Average observations based on occasional grab samples of sediment in streams may not well represent the monthly to annual sediment loads the (R)USLE is attempting to estimate. In another example, López-Vicente et al. (2008) compared observed to modelled values and had a ratio of modelled to observed soil loss of 0.62. However, the "observed" soil loss was based on 137Cs measurements that were indicative of average soil loss values for the past 40 years, while the model values were based on 1997–2006 driving data. During this period, the study area experienced lower precipitation and thus had lower modelled soil loss measurements compared to the soil loss derived from the 137Cs records (López-Vicente et al., 2008).

As stated earlier, the regional applicability of the RUSLE is a limitation that requires the sub-factors to be adjusted and modified based on the specific characteristics of the researcher's study site. Nakil and Khire (2016) and Abu Hammad et al. (2005) show this important practice in RUSLE applications in their studies. Through testing and refining their method of accounting for topography through the LS factor, the ratio of modelled to observed soil loss ranged from 0.8 to almost unity (Nakil and Khire, 2016). The initial application of RUSLE of Abu Hammad et al. (2005) over-estimated soil loss by a factor of 3, but with adjustments to the subfactors based on local data on soil moisture, land cover, and support practices, the model error was reduced to 14 %. The importance of adjusting RUSLE with the availability of more detailed data was further shown in the pan-European study of Panagos et al. (2015b), where detailed soil, topography, land cover, and management practices allowed the researchers to refine their application where most of the ratios of modelled to observed soil loss were very good (0.9 to 1.3). In the validation areas where the soil loss comparisons were not good, further local testing and refining of the RUSLE subfactors is seen as an area in which to improve the model results (Beskow et al., 2009; Panagos et al., 2015b).

A global soil erosion study using RUSLE was accomplished by Borrelli et al. (2017) using the rainfall erosivity map generated by Panagos et al. (2017) that showed comparable results to regional and local soil erosion estimates, and good agreement with global soil erosion datasets such as the Global Assessment of Human-induced Soil Degradation (GLASOD) dataset.

Future work in the soil erosion literature could include assembling a comprehensive database of global, regional, and national soil erosion rates to allow comparison between soil erosion modelling methods, not just (R)USLE results. A proxy for understanding soil erosion is water quality data such as total suspended solids (TSS) that includes sediment delivery and organic sources (Schmitt, 2009). However, TSS usually excludes the larger and heavier bed load sediments that could be resulting from mass wasting events or erosion (Nagle et al., 1999). Nevertheless, water quality data are useful for inferring likely temporal patterns of soil erosion or the sediment yield during seasons of heavy rainfall or after extreme events. Ground truthing or analysis of satellite imagery is another useful method of validating the (R)USLE results, as the areas of extreme erosion risk can be checked for physical evidence of soil loss occurrence (De Asis and Omasa, 2007; Adornado and Yoshida, 2010; Nontananandh and Changnoi, 2012). The soil loss estimates can be validated against observations from similar catchments, recorded events of mass wasting, or larger-scale soil loss studies at the national or regional scale (Panagos et al., 2015b; Nakil and Khire, 2016).

Lastly, a frequently cited limitation is that the (R)USLE estimates soil loss through sheet and rill erosion, but not from other types of erosion such as gully erosion, channel erosion, bank erosion, or mass wasting events such as landslides (Nagle et al., 1999; Wischmeier and Smith, 1978). By excluding these types of erosion, the (R)USLE may underestimate the actual soil loss (Thorne et al., 1985). The model also does not account for deposition, leading to overestimation, or sediment routing (Desmet and Govers, 1996; Wischmeier and Smith, 1978). One of the possible methods for linking the (R)USLE results to sediment delivery to streams is using the sediment delivery ratio (SDR), defined as “the ratio of the sediment delivered at a location in the stream system to the gross erosion from the drainage area above that point”. This parameter varies depending on the gradient, slope shape, and length and can also be influenced by land cover, roughness, etc. Given that it is influenced by characteristics similar to those of the (R)USLE, future work can include combining the (R)USLE with the SDR to estimate sediment delivery to streams and avoiding possible double counting. These two limitations of deposition and routing are linked to the model’s representation of more topographically complex terrain. Previous studies have attempted to address them by improving the LS factor by incorporating upstream contributing area (Desmet and Govers, 1996; Moore et al., 1991).

Despite these drawbacks, the USLE family of models is still widely used because of is relative simplicity and low data requirements compared to more complex physically based models. Worldwide studies continue to improve (R)USLE parameterization and application in different climate regimes and locations.

4.2.2.7. Consistency in Units

The USLE was originally developed using imperial units; although the handbook provides conversion factors to convert to metric, there are still issues within the scientific literature regarding units. In the process of this review, it was noted that, although most studies used the metric units for R factor and K factor, there were other studies that did not report their units or had units that were not the imperial or metric units of (R)USLE. Since the original (R)USLE was formulated with US customary units, researchers must be careful to use the correct units and conversions to metric (Renard and Freimund, 1994). Renard et al. (1997) recommends a conversion factor of 17.02 for the R factor and 0.1317 for the K factor to convert from imperial to metric units. As mentioned, uncertainties are associated with the (R)USLE, and publishing sub-factor values and soil loss estimates for future reference by other researchers is a potential way to reduce some of those uncertainties. The problem of unclear or inconsistent units causes problems for future researchers in terms of adapting the rainfall erosivity or soil erodibility equations for their own study sites, underscoring the need for clear and explicit reporting of units in the (R)USLE literature.

4.2.3. Determination of RUSLE Factor Values

The applied methodology (as shown in Figure 4.4) to estimate soil erosion rate in the study catchment was employed with the GIS-based Revised Universal Soil Loss Equation

(RUSLE) model (Renard et al., 1997). The obtained geospatial input parameters for the RUSLE model (Table 4.13) were used to produce thematic maps to estimate potential soil erosion risk. RUSLE is an extension of the Universal Soil Loss Equation (USLE) model by adjusting the input factors for the local conditions (Renard et al., 1997; McCool et al., 1995). The application of the RUSLE model is simple and applicable in limited data conditions. Because of its suitable capacity and relatively simple computational inputs, RUSLE has been widely used around the world, including in Ethiopia (Gashaw, et. al., 2019; Kebede, et. al., 2019), Kenya (Kogo, et. al., 2020), Zimbabwe (Marondedze and Schütt, 2020); China (Hui, et. al., 2019; Kolli, et. al., 2021), Japan (Mihara, et. al., 2005), India (Prasannakumar et. al., 2012), Nepal (Talchabhadel, et. al., 2020; Koirala et. al., 2019); Sri Lanka (Jayasinghe et. al., 2010), South-East Asian countries (Philippines (Adornado, et. al., 2009; De Asis and Omasa, 2007; Hernandez, et. al., 2012), Thailand (Krishna Bahadur, 2009; Merritt, et. al., 2004), and Mekong River Basin (Chuenchum, et. al., 2019; Thuy and Lee, 2017; Chuenchum, et. al., 2020). Furthermore, the RUSLE also provides international applicability and comparability for the results and methods because the model can be adjusted and applied in many parts of the world. The RUSLE model and its predecessor USLE (Wischmeier and Smith, 1978) estimate the rate of mean annual soil loss by considering multiple factors expressed in Equation (1):

$$A = R \times K \times LS \times C \times P \tag{1}$$

where: A is the mean annual soil loss (t/ha/y); R is the rainfall erosivity factor (MJ/mm/ha/hr/y); K is the soil erodibility factor (t/hr/MJ/mm); LS is the topographiC-factor (dimensionless); C is the cropping management factor (dimensionless); and P is the support practice factor (dimensionless).

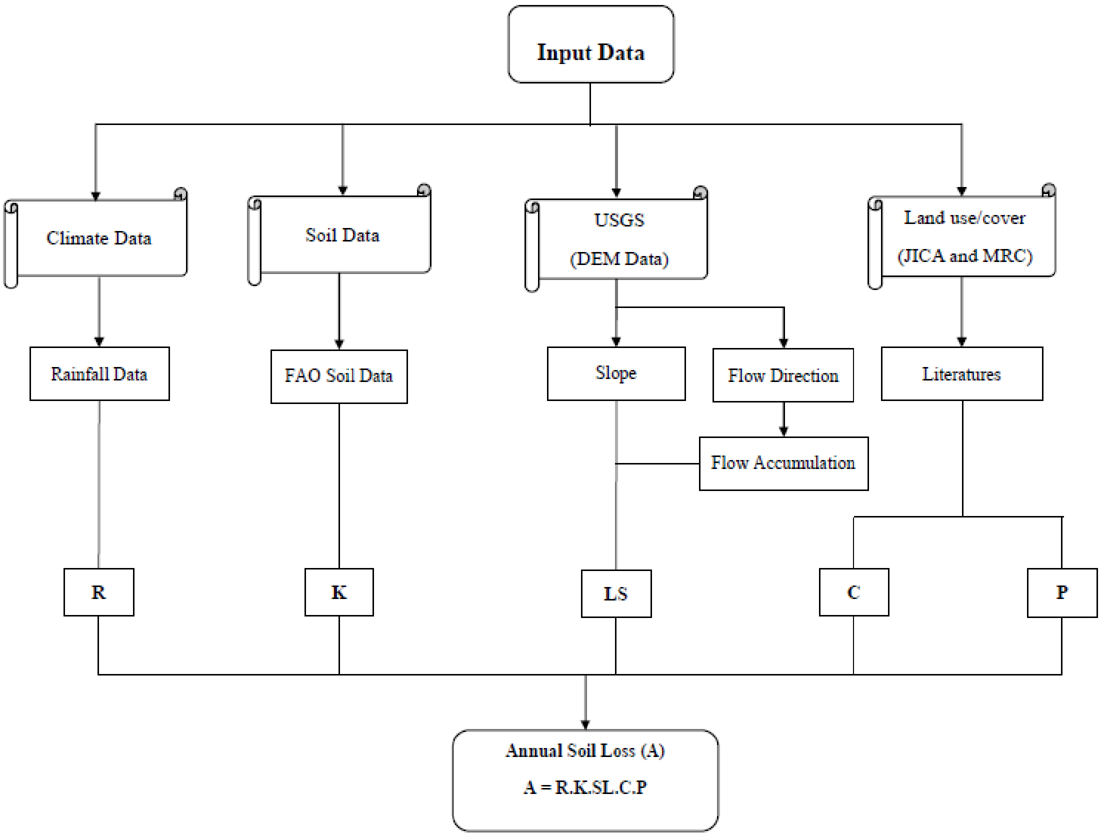

Figure 4.4. Flowchart of applied methodology for modelling soil erosion in the catchment.

Table 4.13. Data used and data source for soil erosion modelling in the catchment

No.	Factors	Resolution	Data Source	Format
1	R Factor	-	Daily rainfall data (2007–2018) from Ministry of Water Resources and Meteorology in Cambodia (MORWAM).	Raster
2	K Factor	1 km	FAO/UNESCO Soil Map of the World database through the Harmonized World Soil Database (HWSD).	Raster
3	LS Factor	30 m	Digital Elevation Model (DEM) from the United States Geological Survey (USGS) website.	Raster
4	C Factor	30 m	Obtained by assigning weighted C-factor values to the LULC based on the literatures.	Raster
5	P Factor	30 m	Obtained by assigning weighted P factor values to the LULC based on the literature as suggested by Yang et al. (2003).	Raster

4.2.3.1. Rainfall Erosivity (R) Factor

The R-factor accounts for the erosive force of a specific rainfall (Wischmeier and Smith, 1978). The erosive power of a particular precipitation is determined by the amount, intensity and distribution of precipitation; where intensity is the most important property determining the amount of erosion (Blanco-Canqui and Lal, 2008). Therefore, in the original USLE and its revised version (RUSLE), the R-factor was represented in the rainfall intensity data. The annual R-factor is a function of the average annual EI30 that is calculated from detailed and long-term records of storm kinetic energy (E) and the 30-min maximum intensity (I30) of the storm (Renard et al., 1997; Adornado et al., 2009). In general, rainfall intensity data is rarely available in Cambodia, especially in the research areas. For this reason, daily rainfall data collected from six weather stations (Figure 4.5) in 2007–2018 were obtained from the Ministry of Water Resources and Meteorology (MOWRAM) of Cambodia. Then, the average annual rainfall of the stations (2007–2018), required for the calculation of the R-factor was drawn from the daily data set. The calculated R-factor was interpolated using the inverse distance weighting (IDW) method and converted into a 30 m cell size grid (Figure 4.5a).

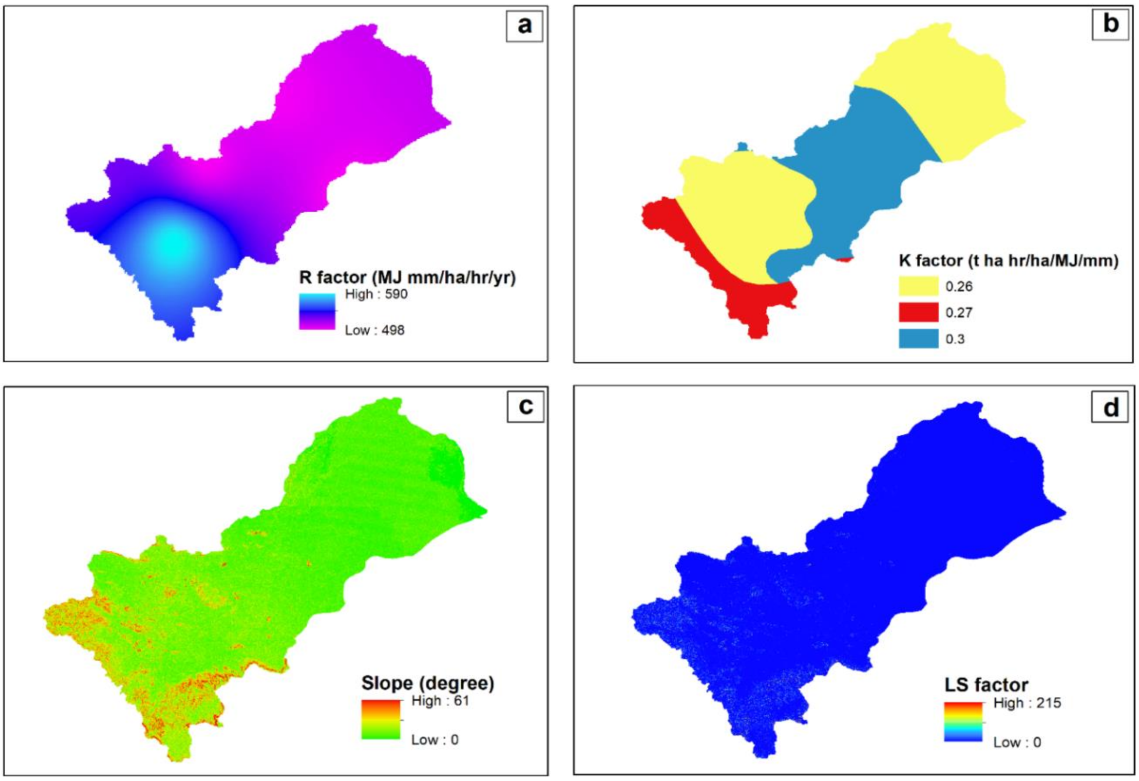

Figure 4.5. Maps of R-factor (a), K-factor (b), slope (c) and LS-factor (d) of the Sangkae catchment

In this study, the equation (Equation (2)) was chosen to calculate the R-factor from Reference (El-Swaify et al., 1987). The equation has been adopted by many users in Southeast Asian countries and has been extensively used in Thailand (Merritt et al., 2004; Eiumnoh, 2000), Philippines (Adornado et al., 2009; De Asis and Omasa, 2007; Hernandez et al., 2012) and also Sri Lanka (Jayasinghe et al., 2010), Nepal (Koirala et al., 2019) and African countries of Rwanda (Byizigiro et al., 2020), and Zimbabwe (Marondedze and Schütt, 2020).

$$\mathrm{R} = 38.5 + 0.35\ \mathrm{P} \tag{2}$$

where R = rainfall erosivity (MJ/mm/ha/hr/y) and P = mean annual rainfall amount (mm).

4.2.3.2. Soil Erodibility (K) Factor

The K-factor corresponds to the influence of the soil's physical and chemical properties on erosion during storm events in upland areas (Renard et al., 1997); Wischmeier and Smith, 1978). Some of the soil properties that affect soil erodibility include soil texture, drainage condition, soil depth, structural integrity and organic content (Prasannakumar et al., 2012). Among the different methods for computing the K-factor, the soil nomograph method, which uses the relative ratios of soil texture, permeability, soil structure and organic matter content (Wischmeier and Smith, 1978), is the most commonly used method. In this study, soil data were acquired from FAO/UNESCO Soil Map of the World database through the Harmonized World Soil Database (HWSD) because the observed data of the local soil properties in Cambodia is limited and difficult to access. The HWSD is a 30 arc-second raster database (approximately 1 km of spatial resolution) with over 15,000 different soil mapping units that combine existing regional and national updates of soil information around the world. The soil information extracted from the database for assessing soil erodibility includes sand, silt, clay, and organic carbon. The mentioned soil parameters were used to compute the K-factor based on the following Equations.

$$K_{USLE} = f_{csand} \times f_{cl-si} \times f_{orgC} \times f_{hisand} \tag{3}$$

$$f_{csand} = \left(0.2 + 0.3 \times \exp\left[-0.256 \times m_s \times \left(1 - \frac{m_{silt}}{100}\right)\right]\right) \tag{4}$$

$$f_{cl-si} = \left(\frac{m_{silt}}{m_c + m_{silt}}\right)^{0.3} \tag{5}$$

$$f_{orgC} = \left(1 - \frac{0.25 \times OrgC}{OrgC + \exp[3.72 - (2.95) \times OrgC]}\right) \tag{6}$$

$$f_{hisand} = \left(1 - \frac{0.7 \times \left(1 - \frac{m_s}{100}\right)}{\left(1 - \frac{m_s}{100}\right) + \exp\left[-5.51 + 22.9 \times \left(1 - \frac{m_s}{100}\right)\right]}\right) \quad (7)$$

where K is the soil erodibility factor, fcsand is a function of the high coarse sand content of the soil, fcl-si is a function of the clay and silt of the soil, forgC is a function of the organic carbon content of the soil, fhisand is the function of high sand content in the soil, ms is the % sand content (0.05–2.00 mm diameter particles), msilt is % silt content (0.002–0.05 mm diameter particles), mc is the % clay content (<0.002 diameter particles), and orgC is % organic carbon content of the layer (%). The values of the K-factor are between 0 to 1, where values tending towards 1 indicate an increase in susceptibility to erosion by water (Byizigiro et al., 2020). The same value of K-factor was used for both LULC of JICA 2002 and MRC 2015 as there were no separate data for the different periods.

4.2.3.3. Topographic (LS) Factor

The topographiC-factor is one of the most important parameters of the RUSLE model for determining soil erosion since the gravity force plays an important role in surface runoff (Moore and Burch, 1986; Zhang et al., 2013). This factor combines the slope length (L), which measures the distance from the source to the top of the intercalation, and the slope steepness (S). The slope length measurement is incomplete, in which the catchment is characterized as heterogeneous, and considers the topographic scale and aspects related to LULC (Moore and Burch, 1986; Van Remortel et al., 2001). The LS-factor combines both the length and steepness of the land slope, so it noticeably affects the soil loss rate. This factor was calculated from the DEM of Cambodia at a 30-m spatial resolution obtained from the United States Geological Survey (USGS) Earth Explorer at https://earthexplorer.usgs.gov. The LS factor maps were created using ArcGIS 10.3 and the ArcHydro extension tools to undertake DEM sink filling prior to creating the flow direction and flow accumulation. Then, the surface slope angle was calculated from the DEM, and the LS factor was computed using the following equation as recommended by Van Remortel et al. (2001). This equation has been adopted by several researchers (Kogo et al., 2020; Nakil and Khire, 2016; Rozos et al., 2013; Van Remortel et al., 2001; Yoshino and Ishioka, 2005).

$$LS = \left(Flow\ accumulation \times \frac{cell\ size}{22.13}\right)^m \times (0.065 + 0.045s + 0.0065s^2) \quad (8)$$

where: cell size is the resolution of the DEM pixels (30 m resolution pixel), s is the slope gradient in %; m = dimensionless exponent based on the steepness of the land. The values of m are assigned as: 0.5, 0.4, 0.3 and 0.2 for slopes of >5%, 3–5%, 1–3% and <1%, respectively (Renard et al., 1997; McCool et al., 1995). The same LS-factor was used for both study years of JICA 2002 and MRC 2015.

4.2.3.4. Crop Management (C) Factor and Conservation Practice (P) Factor

The cover and management factor (C) is expressed as the soil loss ratio from an area with a certain cover and management, in which the C-factor accounts for the role of vegetative covers against water erosion (Wischmeier and Smith, 1978; Morgan, 2009). In the areas without vegetation, soil erosion by water is high. Conversely, due to the high protection of the soil surface by the vegetation against erosion, the soil erosion from the land with vegetation cover is low. Therefore, this can reduce soil erosion by returning the LULC types into more vegetation surface covers. For this reason, the C-factor is probably the most crucial factor in reducing soil erosion. An easier way to determine the C-factor is to report similar land cover values and refer to previous studies, or to studies conducted in the same area or region (Benavidez et al., 2018). However, it is important to note that the definition of land cover type may differ among countries when using the C-factor in the literature. For Instance, land classified as a forest in one country may have a different vegetation cover or type than forests in another country (e.g., the difference between a pine forest and a tropical rainforest). Therefore, it is important to understand the differences in land cover classifications before applying the C-factor values from the literature (Benavidez et al., 2018). To develop C-factor maps of the study catchment from the corresponding LULC temporal layers, C factors were assigned for each LULC type based on the literature (Table 4.14).

Table 4.14. Adopted values of C and P factor for the catchment land use and land cover (LULC) classes

LULC Classes	C-factor	P Factor
Agricultural land	0.5	0.5
Barren land	0.35	1.0
Built-up area	0.1	1.0
Deciduous forest	0.01	1.0
Evergreen forest	0.001	1.0
Grassland	0.08	1.0
Marsh and swamp	0.05	1.0
Mixed forest	0.1	0.8
Paddy field	0.1	0.5
Shrubland	0.014	1.0
Water bodies	0.01	1.0

The P-factor represents the role of conservation practices in reducing erosion (Wischmeier and Smith, 1978). The value of P-factor is between 0 and 1. In general, 1 is assigned to areas without protection measures (Adornado et al., 2009; Gashaw et al., 2021), and a minimum value close to 0 is given for areas with suitable protection measures. Therefore, the lower the P value is, the more effective the protection against erosion is (Prasannakumar et al., 2012). A review of the RUSLE model by Benavidez et al. (2018) emphasized that the P-factor could also be estimated using sub-factors. Even so, the difficulty of accurately mapping supporting practice factors or not observing support practices has led many studies to ignore it by setting the value of its P-factor to 1, as seen in other studies (Marondedze and Schütt, 2020; Adornado et al., 2009; Gashaw et al., 2021). However, in the studied catchment, the P factor was determined based on the land cover type from the C-factor (Table 4.14) as suggested by Yang et al. (2003).

4.3. Results and Discussion

4.3.1. RUSLE Factors

The various RUSLE factors identified in this study are shown in Table 4.15 and Figure 4.6. The rainfall erosivity (R-factor) value ranged from 496 to 590 MJ mm/ha/hr/y (mean of 524). The rainfall erosivity factor map for Stung Sangkae catchment depicts moderate variations over the study periods between 2002 and 2015. In parts of the lowland areas, the value of R-factor was below 500 MJ mm/ha/hr/y, while in the upland parts of the catchment, the R-factor was higher reaching up to almost 600 MJ mm/ha/hr/y (Figure 4.6a).

The R-factor is the main driver of soil erosion. There are many equations to estimate the rainfall erosivity factor based on the preferences of the individual researchers and the regions. Benavidez et al. (2018) showed that due to the detailed data requirements for the standard (R)USLE computation of rainfall erosivity, alternative equations have been used when studying in areas with less detailed data, depending on the temporal resolution and availability of the precipitation data. In the study, the equation recommended by El-Swaify et al. (1987), adopted by many researchers around the world, mostly in Africa (e.g., Ethiopia, Kenya, Zimbabwe) and the Asia (e.g., China, India, Malaysia, Nepal, Thailand, Philippine), particularly the South-East Asian countries and MRB countries were chosen for soil erosion analysis. At the same time, the K-factor was calculated following the equation (Williams, 1995). According to Yang et al. (2013), soil loss is proportional to rainfall erosivity index when all the other factors are held constant; therefore, it is an important factor in the model. The study showed that the spatial distribution of rainfall-runoff erosivity in the catchment was consistent with the amount of precipitation received in various parts of the study catchment. The highest calculated erosivity indices were more in the southwestern regions of the study area, mainly in Phnom Samkos Wildlife Sanctuary, compared with central areas and floodplain areas (Figure 4.6). In Cambodia, the average annual rainfall is 1400 mm in the central lowland regions and can reach 4000 mm in some coastal areas or in the highlands (Thoeun, 2015). As a result, the high rainfall erosivity indices in the region are more likely to occur during the rainy season which runs from mid-May to early October.

Table 4.15. The mean annual precipitation (mm) in the study area and the corresponding R-factor

Station	Location		Elevation (m)	Mean Annual Rainfall (2007–2018)	R Factor (MJ/mm/ha/hr/y)
	Longitude	Latitude			
Pailin	102.61	12.85	95	1399.8	528.4
Battambang	103.20	13.09	94	1318.7	500.1
Samlout	102.85	12.61	153	1576.9	590.4
Rotanak Mondol	102.96	12.89	258	1313.1	498.1
Moung Ruessei	103.44	12.77	29	1308.3	496.4
Pursat	103.54	12.33	22	1410.7	532.3

Soils in the catchment upland areas were dominated by Nitosols (clay), which covers 27% of the catchment and Acrisols (clayey loams), which covered 12% of the catchment, while in the lowland and floodplain areas, the soil was dominated by Luvisols (34%) and Gleysols (12%). Thus, the soils varied from clay to clay loams in the catchment based on the soil texture classification (Table 4.16). The soil erodibility (K-factor) values ranged from 0.26 to 0.3 tons h/MJ/mm (Figure 4.6b). The slope in the catchment varied from 0–61 degrees, and the LS factor values ranged from 0 to 215 (Figure 4.6 c,d).

Table 4.16. The soil types and the corresponding K-factor in the study catchment

Soil Type	**Soil Texture**	**K Factor (t ha h/ha/MJ/mm)**	**Area**	
			(ha)	**(%)**
Eutric Gleysols (Ge)	Clay	0.26	164,959	27%
Gleyic Luvisols (Lg)	Clay Loam	0.30	204,534	34%
Dystric Nitosols (Nd)	Clay	0.26	165,639	27%
Orthic Acrisols (Ao)	Clay Loam	0.27	70,040	12%
	Total		605,170	100%

The values of land cover management factor (C-factor) and the values of conservation practice (P-factor) were based on the literatures. As shown in Figure 4.6, the spatial distribution of the value of C-factors was in the range of 0.001 to 0.5, while the value of P-factor ranged from 0.5 to 1 (Figure 4.6c,d).

The study also determined that the highest erodibility values were found in the upper regions of the catchment. This indicates that the soils in these areas have stability and low infiltration rates; therefore, they are susceptible to erosion in the event of large flows.

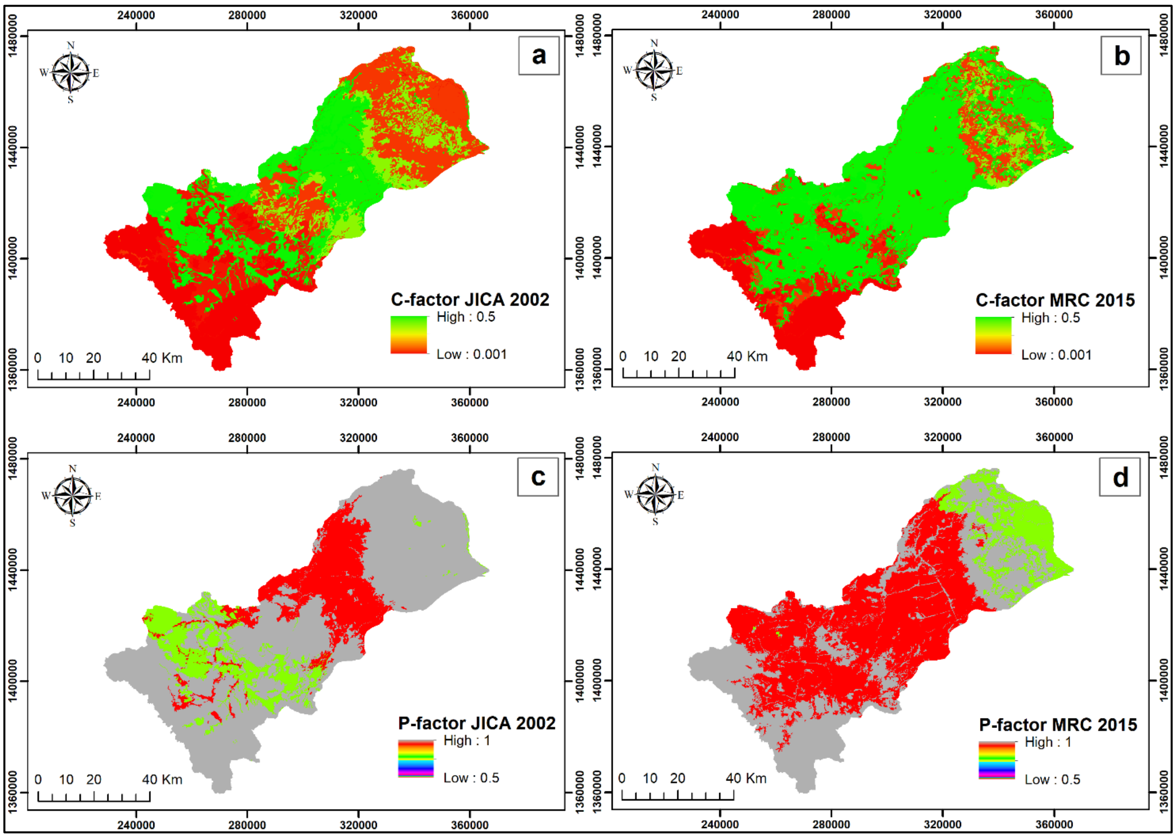

Figure 4.6. Spatial distribution of: (a,b) cover management (C-factor) and (c,d) supporting practices (P-factor)

4.3.2. Impact of LULC Changes on Soil Erosion

The RUSLE factors were multiplied in ArcGIS 10.3 spatial analyst tool (zonal statistic) to get the spatiotemporal variations in annual soil erosion rate for the period 2002–2015, and the results are provided in Tables 4.17 and 4.18 and Figure 4.7. The study revealed that the soil loss caused by sheet and rill erosion in Stung Sangkae catchment was in the range of 0–60 t/ha/y in 2002 to 0–63 t/ha/y in 2015 (Table 4.17). In 2002, the total soil loss was 1,604,234 tons distributed over the catchment, while the amount of total soil loss in 2015 was 3,343,216 tons (Table 4.18), which happened mainly in the upland of the catchment (Figure 4.7).

In terms of the severity classes of soil loss, the results illustrated that 76.6% of the study areas experienced a very low rate of severe soil erosion. Cumulatively, the annual contribution of the low severe soil erosion class is highest due to the expansive extent of their occurrence. These areas cannot be ignored in the agricultural management of soil erosion, because soil loss in these areas will systematically reduce soil quality by removing silt, clay, and organic components that play a vital role in keeping the soil water holding capacity and structural integrity (Sanchez et al., 2003).

The study also determined that the highest erodibility values (Figure 4.7) were found in the upper regions of the catchment. This indicates that the soil in these areas have stability and low infiltration rates; therefore, they are susceptible to erosion in the event of large flows. The soil erosion rates between 0.2 and 62.9 t/ha/y (Table 4.17) estimated for the catchment were within similar studies carried out in the MRB. According to Chuenchum et al. (2020), in the Lancang MRB, soil erosion loss was mainly classified as moderate erosion in 45% of the study area. Furthermore, in the area around Tenle Sap's soil erosion, it was found that its erosion level was extreme, with more than 80 t/ha/y (Chuenchum et al., 2020). Chuenchum et al. (2020) reported that the soil erosion of the lower MRB was 198.2 t/km^2/y (1.9 t/ha/y), which represents approximately 64% of the total occurrence of soil erosion in the MRB. However, the results of Chuenchum et al. (2020) were close to the average values from the previous studies (Thuy and Lee, 2017), where soil erosion average was found to be between 1,400 to 8,500 t/km^2/y. The differences in these findings may be mainly because of R-factor and LS-factor values, as Chuenchum et al. (2020) found that the values of R-factor and LS-factor were 65.6–524.3 MJ.mm/(ha.hr.y) and LS-factor were in the range of 0–336. Meanwhile, Thuy et al. (2017) found that the R-factor was 1,886–9,725 MJ.mm/(ha.hr.y), and LS-factor was from 0.001 to 31.9. Kogo et al. (2020) emphasized that due to the variability of topographic features, erodibility, erosivity, and vegetation entrances, the estimated soil erosion rate varies between regions. Based on the Marondedze et al. (2020), in the tropical condition, the average soil loss rates of 5/t/ha/y were found in the previous studies (Bamutaze, 2015; Lufafa et al., 2003) while it also mentioned that a soil loss limit could be 11t/ha/y accepted as reasonably average annual loss due to soil erosion. However, Hudson (1995) believes that for sensitive and fragile lands, the rate of average soil loss tolerance of 2 t/ha/y can be recommended. Additionally, the potential and actual case studies of soil erosion have verified the sensitivity of the C and the P-factors to soil erosion. Natural vegetation covers, such as the forests (evergreen forest, deciduous forest, and mixed forest) in catchment decreased dramatically around 50,379.8 ha (8.32%), 20,136.4 ha (3.33%), and 10,650.6 ha (1.76%) from 2002 to 2015 (Tables 4.2 and 4.11 and Figure 4.7). Therefore, if forest area is converted into agricultural lands, the rate of soil erosion will increase significantly, especially in the upper reaches (Rangsiwanichpong et al., 2018). However, it is reported that the RUSLE model lacks the ability to calculate soil losses caused by gully or river channel erosion caused by raindrops (Wischmeier and Smith, 1978; Renard et al., 1997). Hence, it should be considered that the soil erosion rates found in this study mainly comes from sheet, rill (produced by runoff) and inter-rill (affected by raindrops on the ground) erosion. However, these are the most common processes leading to extensive soil loss in farmland (Borrelli et al., 2017).

Table 4.17. Distribution of soil erosion loss under different severity classes in Sangkae catchment from 2002 to 2015

Severity Classes	Soil Loss (t/ha/y)	JICA 2002			MRC 2015			Net Change (ha)
		Area		Soil Loss	Area		Soil Loss	
		(ha)	(%)	(t/ha/y)	(ha)	(%)	(t/ha/y)	
Very low	<2	484,089	80.0	0.2	443,439	73.3	0.2	−40,650
Low	2–5	52,646	8.7	3.2	50,897	8.4	3.3	−1,749
Moderate	5–10	28,854	4.8	7.0	33,416	5.5	7.1	+4,562
Severe	10–20	18,961	3.1	13.9	25,023	4.1	14.3	+6,062
Very severe	20–40	11,463	1.9	27.5	22,940	3.8	28.5	−11,477
Extremely Severe	>40	9,157	1.5	60.0	29,455	4.9	62.9	−20,298
Total Area		605,170	100.0		605,170	100.0		

Table 4.18. Soil erosion severity classes and gross soil loss in Stung Sangkae catchment from 2002 to 2015

Severity Classes	Soil Loss (t/ha/y)	JICA 2002		MRC 2015		Total Annual Soil Loss			
		Area		Area		2002		2015	
		(ha)	(%)	(ha)	(%)	(tons)	(%)	(tons)	(%)
Very low	<2	484,089	80.0	443,439	73.3	104,958	6.5	77,615	2.3
Low	2–5	52,646	8.7	50,897	8.4	169,155	10.5	166,630	5.0
Moderate	5–10	28,854	4.8	33,416	5.5	201,419	12.6	237,254	7.1
Severe	10–20	18,961	3.1	25,023	4.1	263,691	16.4	357,164	10.7
Very severe	20–40	11,463	1.9	22,940	3.8	315,430	19.7	653,124	19.5
Extremely Severe	>40	9157	1.5	29,455	4.9	549,581	34.3	1,851,429	55.4
Total Area		605,170	100.0	605,170	100.0	1,604,234	100.0	3,343,216	100.0

The estimated rate of soil erosion was categorized into five severity classes such as very low (0–2 t/ha/y), low (2–5 t/ha/y), moderate (5–10 t/ha/y), severe (10–20 t/ha/y), very severe (20–40 t/ha/y) and extremely severe (>40 t/ha/y), as shown in Tables 4.7 and 4.8. The results show that the areas experienced very low erosion rates, which were dominant in the study area, covering 484,089 ha (80.0%) that the average soil loss was 0.2 t/ha/y and 443,439 ha (73.3%) that the average soil loss was 0.2 t/ha/y in the years 2002 and 2015, respectively, while the areas affected by the extreme erosion was 9157 ha (1.5%) and 29,455 ha (4.9%) with the average soil loss of 60 t/ha/y and 63 t/ha/y in the years 2002 and 2015, respectively. In 2002, the areas that experienced moderate erosion (7 t/ha/y), severe erosion (13.9 t/ha/y) and very severe erosion (27.5 t/ha/y) were 28,854 ha, 18,961 ha and 11,463 ha, respectively. In 2015, areas that experienced moderate erosion (7.1 t/ha/y), severe erosion (14.3 t/ha/y) and very severe erosion (28.5 t/ha/y) were 33,416 ha, 25,023 ha and 22,940 ha, respectively.

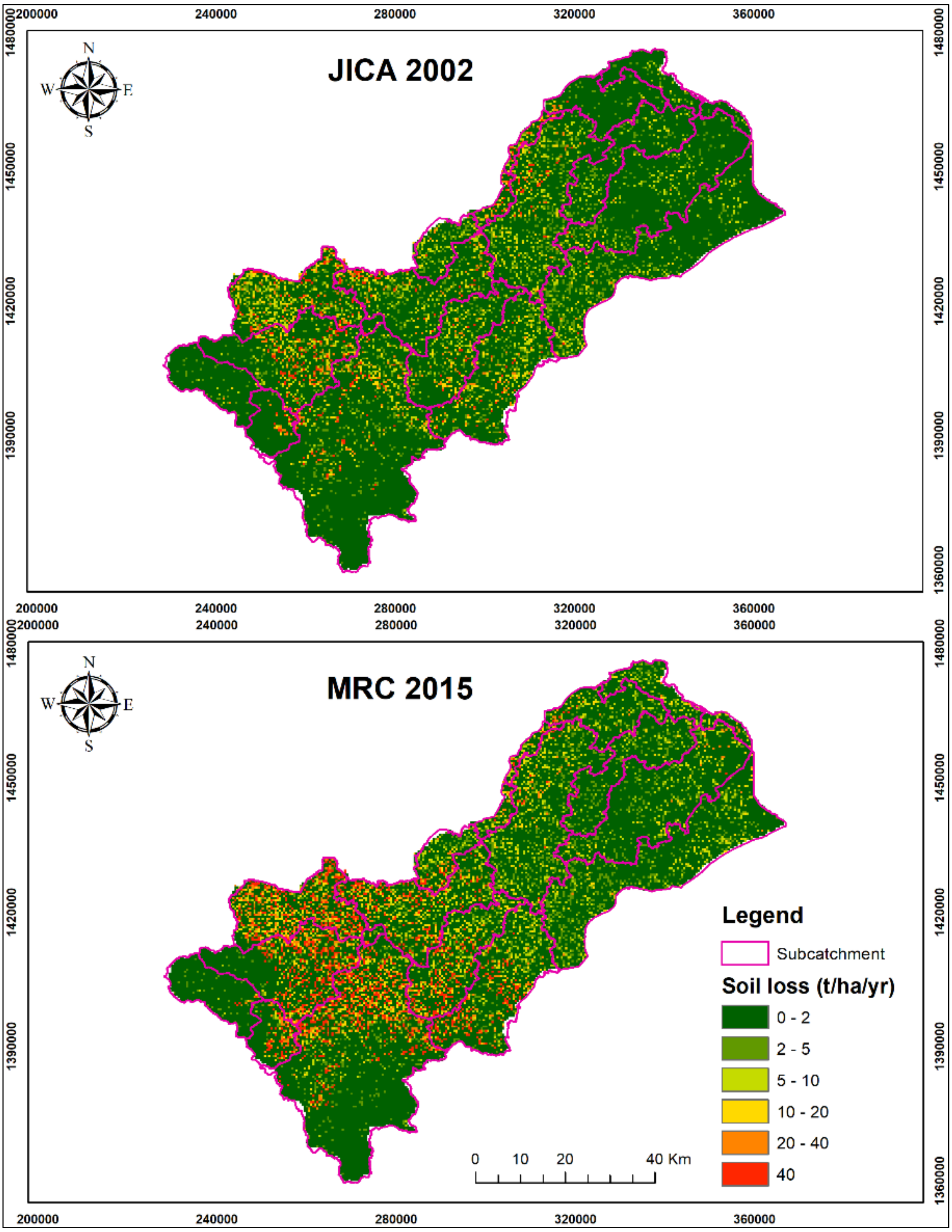

Figure 4.7. Spatial distribution of soil loss in the sub-catchment within the study area

4.3.3. Effect of Elevation and Slope on Soil Erosion

The elevation of the study catchment was divided into five different zoning areas, and the corresponding soil erosion rates were computed accordingly (Table 4.19). The soil loss rate at elevations less than 300 m (529,855 ha) was 2.7 t/ha/y in 2002, and 5.2 t/ha/y in 2015, and the change was the highest soil loss amounts to 2.5 t/ha/y. The rate of soil loss for the elevation of 300–600 m (39,347 ha) was 0.8 t/ha/y in 2002 and 0.9 t/ha/y in 2015. In contrast, the rate of soil loss for the elevation of 600–900 m (29,454 ha) and 900–1200 m (6,065 ha) was 0.4 t/ha/y and 0.9 t/ha/y in 2002 and 0.3 t/ha/y and 0.7 t/ha/y in 2015. The results indicated a decrease in soil loss of about 0.1 t/ha/y and 0.3 t/ha/y that was realized at elevations of 600–900 m (29,454 ha) and those below 1200 m (6,065 ha), respectively, while at the elevation of 1200–1500 m (449 ha), the amount of soil erosion was not changed (0.4 t/ha/y).

Table 4.19. Estimation of soil erosion rates and net changes in different elevation areas

No	Elevation (Meters)	Area (ha)	Area (%)	Erosion (t/ha/y) 2002	Erosion (t/ha/y) 2015	Net Change (t/ha/y)
1	0–300	529,855	87.6	2.7	5.2	2.5
2	300–600	39,347	6.5	0.8	0.9	0.1
3	600–900	29,454	4.8	0.4	0.3	−0.1
4	900–1200	6,065	1.0	0.9	0.7	−0.3
5	1200–1500	449	0.1	0.4	0.4	0.0

The amount of soil loss was additionally distributed according to the slope of occurrence (Table 4.20). The soil erosion rate increased with the increase of slope. The lowest was 0.8 t/ha/y in 2002 and 1.7 t/ha/y in 2015, which occurred in slopes that were less than 2° (100,579 ha). In slopes of 2–5° (212,830 ha), the soil loss rates were 1.7 t/ha/y in 2002 and 3.6 t/ha/y in 2015. In addition, the soil loss rates of slopes of 5–10° (171,084 ha) were 3.6 t/ha/y in 2002 and 9.6 t/ha/y in 2015, while the slope of 10–15° (59,375 ha) was 6.4 t/ha/y in 2002 and 17.7 t/ha/y in 2015. For the slopes of 15–30° (55,173 ha), was 7.2 t/ha/y in 2002 and 16.1 t/ha/y in 2015. Slopes of more than 30° (6,129 ha) had soil erosion rates of 16.3 t/ha/y in 2002 and 27.6 t/ha/y in 2015.

Table 4.20. Soil erosion in slope zones and net changes between the years 2002 and 2015 based on FAO slope classification

No	Slope Classes (Degree)	Area (ha)	(%)	Erosion (t/ha/y) 2002	2015	Net Change (t/ha/y)
1	0–2	100,579	16.6%	0.8	1.7	0.8
2	2–5	212,830	35.2%	1.7	3.6	1.9
3	5–10	171,084	28.3%	3.6	9.6	6.0
4	10–15	59,375	9.8%	6.4	17.7	11.3
5	15–30	55,173	9.1%	7.2	16.1	8.9
6	>30	6,129	1.0%	16.3	27.6	11.3

4.3.4. Contribution of Land Use and Land Cover Changes to Soil Erosion and Its Conversions

The relationship between LULC and estimated soil erosion was analyzed by overlaying LULC and the soil erosion maps in 2002 and 2015 (Table 4.11). This relationship is considered to be a valuable tool to monitor patterns of LULC change and the risk of soil erosion (Marondedze and Schütt, 2020; Khosrokhani and Pradhan, 2014). In comparison with the soil erosion based on the types of land use and land cover, the results revealed that human activities mainly influenced soil erosion concerning soil erosion risk, which was higher in rain-fed agricultural land and paddy field, highlighting their vulnerability to water-induced erosion, as compared to areas under forests (evergreen forest and deciduous forest), grassland, shrubland and built-up area. This can be explained by the intensive cultivation of crops in the Battambang province of Cambodia, the country's largest rice-producing province. As stated in the introduction (MRC, 2016) the area of rice production increased from 2.72 million ha in 2009 to 3.05 million ha in 2013. In the catchment, farmers practice conventional agricultural methods for crop production, leading to soil degradation. This tends to cause a higher rate of erosion and loss of soil organic matter content, which affects the stability of soil aggregate (Kogo et al., 2020; Barbera et al., 2012).

The results indicated that under LULC conditions in 2002, it is estimated that about 1,903,554 tons of soil were lost, while the estimated average soil loss in 2015 was 4,538,331 tons (Table 4.21). The results also revealed that the amount of soil loss increased almost twice during the investigated periods. For the agricultural land areas in Stung Sangkae catchment, averagely 463,962 tons (24.6%) of soil loss was estimated for 2002, while an increase of up to 3,757,018 tons (81.5%) of soil loss was estimated for the same land use type for 2015. Likewise, the estimated soil loss of land use types of "barren land" and "built-up area" increased slightly from 1240 tons (0.1%) in 2002 to 51,823 tons (1.2%) in 2015 and from 14,748 tons (1.2%) in 2002 to 147,967 tons (3.2%) in 2015. In contrast, estimates of soil loss for land use types such as deciduous forests, evergreen forests, grasslands, mixed forests, and paddy field and so on were decreased. Particularly there was a significant decline of soil loss for the land use of grassland where the estimated soil loss was 241,922 tons (12.5%) in 2002 to 49,179 tons (1.0%) in 2015; and for the mixed forest it decreased from 797,562 tons (41.9%) in 2002 to 129,349 tons (2.8%) in 2015. For the land use types of deciduous and evergreen forest, the estimated soil losses were 83,370 tons (4.4%) and 37,189 tons (1.9%) in 2002 and 28,244 tons (0.6%) and 33,443 tons (0.7%) in 2015, respectively.

Table 4.21. Distribution of soil erosion loss under various types of land use and land cover in Stung Sangkae catchment

LULC Classes	JICA 2002			MRC 2015		
	Soil Loss (tons)	Area		Soil Loss (tons)	Area	
		(ha)	(%)		(ha)	(%)
Agricultural land	463,962 (24.6%)	25,627.2	4.24	3,757,018 (81.5%)	152,742.3	25.24
Barren land	1240 (0.1%)	149.2	0.02	51,823 (1.2%)	274.0	0.04
Built-up area	14,748 (0.7%)	1702.8	0.28	147,967 (3.2%)	20,870.1	3.45
Deciduous forest	83,370 (4.4%)	74,524.7	12.31	28,244 (0.6%)	24,144.9	3.99
Evergreen forest	37,189 (1.9%)	11,0474.4	18.26	33,443 (0.7%)	90,338.0	14.93
Grassland	241,922 (12.5%)	79,496.0	13.14	49,179 (1.0%)	29,394.2	4.86
Marsh and swamp	305 (0.1)	280.3	0.05	73 (0.1)	35.8	0.01
Mixed forest	797,562 (41.9%)	75,361.5	12.45	129,349 (2.8%)	64,710.9	10.69
Paddy field	185,115 (9.7%)	92,784.8	15.33	234,464 (6.3%)	144,931.5	23.95
Shrubland	78,143 (4.1%)	141,689.0	23.41	106,771 (2.6%)	74,019.0	12.23
Water bodies	0	3080.1	0.51	0	3709.4	0.61
Total Area	1,903,554	605,170.0	100.0	4,538,331	605,170.0	100.0

The soil loss distribution of different types of LULC showed that the amount of soil loss from agricultural land increased the most, from 463,962 tons (24.6%) to 3,757,018 tons (81.5%). In comparison, soil erosion in the built-up areas also increased dramatically from 14,748 tons (0.7%) in 2002 to 147,967 tons (3.2%) in 2015 (Table 4.21). In contrast, other LULC types that had significantly lower soil loss were forest lands, paddy field and grass/shrubland, accounting for 48.2%, 4.1%, and 9.7% of soil loss in 2002 and 6.3%, 16.6%, and 3.7% in 2015, respectively (Figure 4.8).

Forests, grassland and shrubland areas are also prone to soil erosion. However, due to better soil cover, the rate of erosion in these areas is lower than that of agricultural land and paddy fields. Table 4.21 shows that the forest lands under mixed forest experienced the highest soil erosion among the other types of land uses caused by the forest clearance by farmers to expand agricultural productivities. This observation aligns with a recent finding by Kong et al. (2019), which demonstrated that from 2002 to 2010, forest conversion was relatively more intensive and homogenous in Pailin Province where the Stung Sangkae catchment covers almost one-third part of it. If the trend of transforming forestlands to agricultural lands continues to increase, the possibility of soil erosion will be further expanded, which will affect the sustainability of agricultural lands in the catchment for crop production. Therefore, agricultural deforestation must be minimized, especially on steep slopes. Additionally, it is necessary to implement agricultural management practices, such as on-farm conservation agriculture practices (CAP), water conservation and management, agroforestry practices, vegetation cover restoration and the creation of slopes terraces (Kogo et al., 2020) to achieve sustainable control of soil erosion to improve the productivity of growing crops.

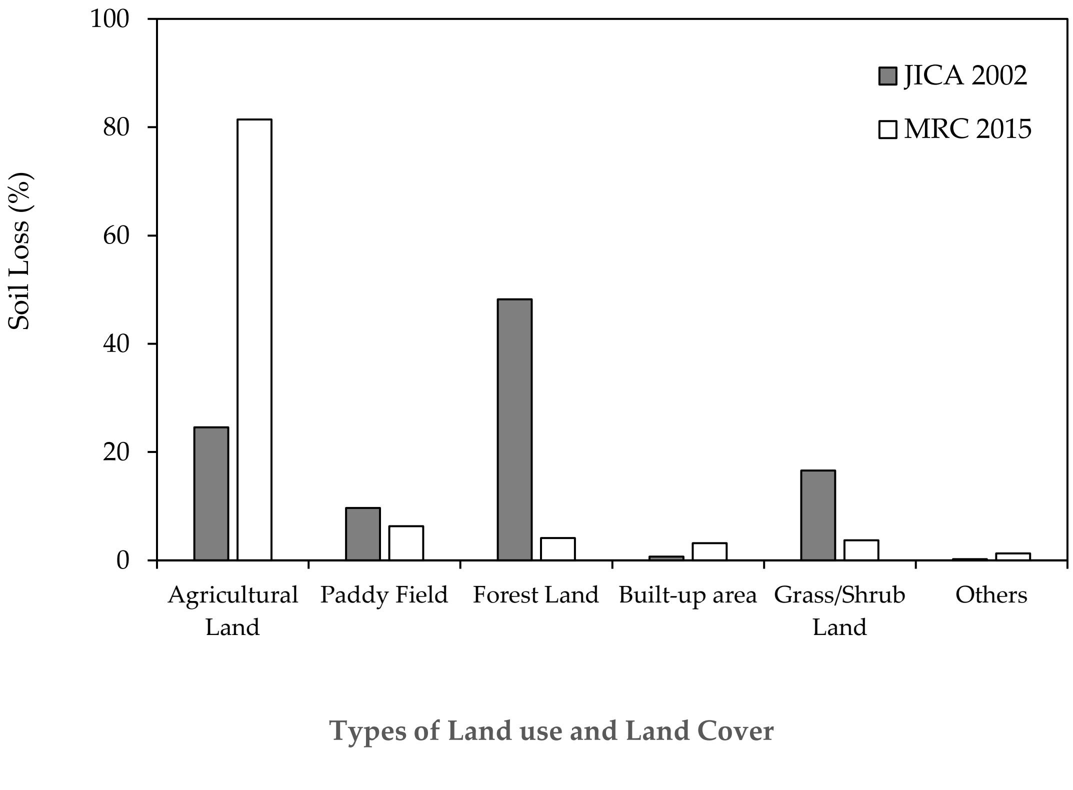

Figure 4.8. Total soil erosion contributed by various land use and land cover types

The spatial distribution of LULC conversion and its contribution to soil erosion are shown in Figure 4.9 and Table 4.22. It should be noted that each LULC category were converted to different land use types during the studied period between 2002 and 2015. However, Table 4.22 presents only the major LULC conversions from the LULC categories. The primary conversion of LULC changes are agricultural land, shrubland and paddy field, while the highest soil erosion rate happened to agricultural land ranging from 15.6 to 31.3 t/ha, and the soil erosion rate of shrubland is from 0.5 to 4.8 t/ha, while paddy field ranges from 1.9 to 3.0 t/ha. The mean soil erosion rate of the converted LULC varied from 0.3 to 22 t/ha (Figure 4.9). All LULC categories were changed to agricultural land which occupied the area of 125,546 ha which mainly converted from mixed forest (57,862.7 ha), deciduous forest (37,911.5 ha), evergreen forest (19,309.7 ha), shrubland (14,775.3 ha), grassland (6,348 ha) and paddy field (4,114 ha); resulted in total soil loss of 1,597,728.4 ha, 878,981.9 ha, 603,570.1 ha, 117,116.3 ha, 258,200.8 ha and 64,104.8 ha, respectively.

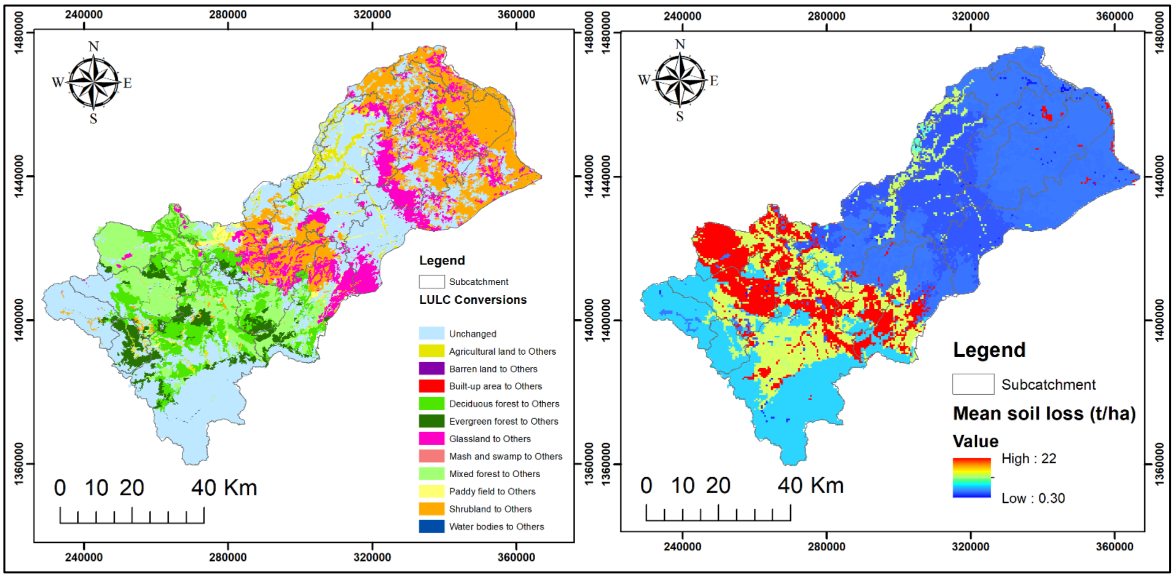

Figure 4.9. Spatial distribution of the conversions of the land use and cover (LULC) between 2002 and 2015

Table 4.22. Distribution of soil erosion loss under different LULC conversion categories in the in Stung Sangkae catchment

No	LULC Categories	Unchanged Area (ha)	Changed Area (ha)	Major LULC Conversions	Changed Area from LULC Categories (ha)	Soil Erosion (t/ha)	Soil Erosion (tons)
1	Agricultural land	11,299	14,328	Built-up area	11,789.3	7.2	85,319.6
				Paddy field	1,371.4	3.0	4,083.8
2	Deciduous forest	20,712	53,813	Agricultural land	37,911.5	23.2	878,981.9
				Shrubland	9,688.0	2.3	22,501.6
				Evergreen forest	3,583.2	0.2	611.5
3	Evergreen forest	83,150	27,324	Agricultural land	19,309.6	31.3	603,570.1
				Shrubland	6,878.9	4.8	32,931.1
4	Grassland	12,396	67,100	Paddy field	35,168.8	1.9	67,545.0
				Shrubland	18,624.0	0.5	9,767.2
				Agricultural land	6,348.1	18.4	117,116.3
5	Mixed forest	1,462	73,900	Agricultural land	57,862.7	27.6	1,597,728.4
				Shrubland	9,621.6	3.8	36,994.1
6	Paddy field	82,643	10,142	Built-up area	4,777.6	5.6	26,819.6
				Agricultural land	4,114.1	15.6	64,104.8
7	Shrubland	27,628	114,061	Mixed forest	56,712.5	2.1	116,896.8
				Paddy field	23,401.6	2.7	62,869.5
				Grassland	16,699.6	1.8	30,334.7
				Agricultural land	14,775.3	17.5	258,200.8

4.4. Discussions

This study applied the empirical RUSLE model to predict potential soil erosion in Stung Sangkae catchment, northwestern part of Cambodia, by integrating the RUSLE model into a GIS application based on the national LULC changes in the catchment between 2002 and 2015. As there is no available report or research on soil erosion with the RUSLE model applied in Cambodia, particularly to the catchment, the computation of the potential soil erosion is based on the literature on the assumption of land management and supporting practice; potential erosion is understood as the erosion processes that are only controlled by physical factors (Marondedze and Schütt, 2020). The R-factor is the main driver of soil erosion. There are many equations to estimate the rainfall erosivity factor based on the preferences of the individual researchers and the regions.

A review of the RUSLE model (Benavidez et al., 2018) showed that due to the detailed data requirements for the standard (R)USLE computation of rainfall erosivity, alternative equations have been used when studying in areas with less detailed data, depending on the temporal resolution and availability of the precipitation data. In the study, the equation recommended by El-Swaify et al. (1987), adopted by many researchers around the world, mostly in Africa (e.g., Ethiopia, Kenya, Zimbabwe) and the Asia (e.g., China, India, Malaysia, Nepal, Thailand, Philippine), particularly the South-East Asian countries and

MRB countries were chosen for soil erosion analysis. At the same time, the K-factor was calculated following the equation (Williams, 1995). According to Yang et al. (2013), soil loss is proportional to rainfall erosivity index when all the other factors are held constant; therefore, it is an important factor in the model. The study showed that the spatial distribution of rainfall-runoff erosivity in the catchment was consistent with the amount of precipitation received in various parts of the study catchment. The highest calculated erosivity indices were more in the southwestern regions of the study area, mainly in Phnom Samkos Wildlife Sanctuary, compared with central areas and floodplain areas. In Cambodia, the average annual rainfall is 1400 mm in the central lowland regions and can reach 4000 mm in some coastal areas or in the highlands (Thoeun, 2015). As a result, the high rainfall erosivity indices in the region are more likely to occur during the rainy season which runs from mid-May to early October.

The study also determined that the highest erodibility values were found in the upper regions of the catchment. This indicates that the soils in these areas have stability and low infiltration rates; therefore, they are susceptible to erosion in the event of large flows. The soil erosion rates between 0.2 and 62.9 t/ha/y (Table 4.7) estimated for the catchment were within similar studies carried out in the MRB. According to Chuenchum et al. (2020), in the Lancang MRB, soil erosion loss was mainly classified as moderate erosion in 45% of the study area. Furthermore, in the area around Tenle Sap's soil erosion, it was found that its erosion level was extreme, with more than 80 t/ha/y (Chuenchum et al., 2020). Chuenchum et al. (2020) reported that the soil erosion of the lower MRB was 198.2 t/km^2/y (1.9 t/ha/y), which represents approximately 64% of the total occurrence of soil erosion in the MRB. However, the results of Chuenchum et al. (2020) were close to the average values from the previous studies (Thuy and Lee, 2017), where soil erosion average was found to be between 1,400 to 8,500 t/km^2/y. The differences in these findings may be mainly because of R-factor and LS-factor values, as Chuenchum et al. (2020) found that the values of R-factor and LS-factor were 65.6–524.3 MJ.mm/(ha.hr.y) and LS-factor were in the range of 0–336. Meanwhile, Thuy et al. (2017) found that the R-factor was 1,886–9,725 MJ.mm/(ha.hr.y), and LS-factor was from 0.001 to 31.9. Kogo et al. (2020) emphasized that due to the variability of topographic features, erodibility, erosivity, and vegetation entrances, the estimated soil erosion rate varies between regions. Based on the Marondedze et al. (2020), in the tropical condition, the average soil loss rates of 5/t/ha/y were found in the previous studies (Bamutaze, 2015; Lufafa et al., 2003) while it also mentioned that a soil loss limit could be 11t/ha/y accepted as reasonably average annual loss due to soil erosion. However, Hudson (1995) believes that for sensitive and fragile lands, the rate of average soil loss tolerance of 2 t/ha/y can be recommended. Additionally, the potential and actual case studies of soil erosion have verified the sensitivity of the C and the P-factors to soil erosion. Natural vegetation covers, such as the forests (evergreen forest, deciduous forest, and mixed forest) in catchment decreased dramatically around 50,379.8 ha (8.32%), 20,136.4 ha (3.33%), and 10,650.6 ha (1.76%) from 2002 to 2015 (Tables 4.2 and 4.21 and Figure 4.3). Therefore, if forest area is converted into agricultural lands, the rate of soil erosion will increase significantly, especially in the upper reaches (Rangsiwanichpong et al., 2018). However, it is reported that the RUSLE model lacks the ability to calculate soil losses caused by gully or river channel erosion caused by raindrops (Wischmeier and Smith, 1978; Renard et al., 1997). Hence, it should be considered that the soil erosion rates found in this study mainly comes from sheet, rill (produced by runoff) and inter-rill (affected by raindrops on the ground) erosion. However, these are the most common processes leading to extensive soil loss in farmland (Borrelli et al., 2017).

In terms of the severity classes of soil loss, the results illustrated that 76.6% of the study areas experienced a very low rate of severe soil erosion. Cumulatively, the annual contribution of the low severe soil erosion class is highest due to the expansive extent of their occurrence. These areas cannot be ignored in the agricultural management of soil erosion, because soil loss in these areas will systematically reduce soil quality by removing silt, clay, and organic components that play a vital role in keeping the soil water holding capacity and structural integrity (Sanchez et al., 2003).

We also estimated gross soil erosion in the catchment. The results showed significant change in mean soil erosion due to LULC changes during the investigated periods between 2002 and 2015 LULC, in which agricultural land showed a significant increase. In contrast, forest lands (evergreen forest, deciduous forest and mixed forest), grassland and shrubland declined significantly. Soil erosion was considerably higher on cropland (agricultural land and paddy field), built-up area, shrubland and barren land, and low in forested areas (evergreen forest, deciduous forest and mixed forest) and grassland.

The relationship between LULC and estimated soil erosion was analyzed by overlaying LULC and the soil erosion maps in 2002 and 2015 (Table 4.21). This relationship is considered to be a valuable tool to monitor patterns of LULC change and the risk of soil erosion (Marondedze and Schütt, 2020; Khosrokhani and Pradhan, 2014). In comparison with the soil erosion based on the types of land use and land cover, the results revealed that human activities mainly influenced soil erosion concerning soil erosion risk, which was higher in rain-fed agricultural land and paddy field, highlighting their vulnerability to water-induced erosion, as compared to areas under forests (evergreen forest and deciduous forest), grassland, shrubland and built-up area. This can be explained by the intensive cultivation of crops in the Battambang province of Cambodia, the country's largest rice-producing province. As stated in the introduction (MRC, 2016) the area of rice production increased from 2.72 million ha in 2009 to 3.05 million ha in 2013. In the catchment, farmers practice conventional agricultural methods for crop production, leading to soil degradation. This tends to cause a higher rate of erosion and loss of soil organic matter content, which affects the stability of soil aggregate (Kogo et al., 2020; Barbera et al., 2012).

Forests, grassland and shrubland areas are also prone to soil erosion. However, due to better soil cover, the rate of erosion in these areas is lower than that of agricultural land and paddy fields. Table 4.21 shows that the forest lands under mixed forest experienced the highest soil erosion among the other types of land uses caused by the forest clearance by farmers to expand agricultural productivities. This observation aligns with a recent finding by Kong et al. (2019), which demonstrated that from 2002 to 2010, forest conversion was relatively more intensive and homogenous in Pailin Province where the Stung Sangkae catchment covers almost one-third part of it (Figure 4.1). If the trend of transforming forestlands to agricultural lands continues to increase, the possibility of soil erosion will be further expanded, which will affect the sustainability of agricultural lands in the catchment for crop production. Therefore, agricultural deforestation must be minimized, especially on steep slopes. Additionally, it is necessary to implement agricultural management practices, such as on-farm conservation agriculture practices (CAP), water conservation and management, agroforestry practices, vegetation cover restoration and the creation of slopes terraces (Kogo et al., 2020) to achieve sustainable control of soil erosion to improve the productivity of growing crops.

4.5. Conclusions of This Chapter

This study applied the empirical RUSLE model to predict potential soil erosion in Stung Sangkae catchment, northwestern part of Cambodia, by integrating the RUSLE model into a GIS application based on the national LULC changes in the catchment between 2002 and 2015. As there is no available report or research on soil erosion with the RUSLE model applied in Cambodia before, particularly to the catchment, the computation of the potential soil erosion is based on the literature on the assumption of land management and supporting practice; potential erosion is understood as the erosion processes that are only controlled by physical factors.

The map of LULC and findings clearly illustrate extensive soil erosion of very low to moderate severity rates ranging from 0.2 to 7.1 t/ha/y. With the application of the RUSLE equation show that 87% of the basin area is exposed to a low to moderate erosion risk (<10 t/ha/y) and 4.1% basin is in severe moderate risk based on the land use in 2015. The highest erosion rates of 14.3 to 62.9 t/ha/y were found in parts of the upland of the Stung Sangkae catchment, mainly due to steep slopes, high rate of erosion and degradation of the vegetation. Between 2002 and 2015, considerable changes in soil loss rate were observed in agricultural land. The forest lands decreased significantly during the investigated period, notably a massive shift in deciduous and mixed forest converted to agricultural land, paddy rice fields and other types of land use. Therefore, it is necessary to integrate protection measures at the farm level and target areas of high risk of erosion, mainly the degraded lands along the steep slopes, to limit the conversion of forest areas for agriculture and minimize the rate of erosion where the land is bare or with low vegetation cover. Some of the recommended measures to prevent soil erosion includes on-farm conservation agriculture practices (CAP), water conservation and management, agro-forestry practices, vegetation cover restoration and terracing. Future soil erosion assessment work in the study area should examine soil loss due to gully erosion, which is not currently possible using the RUSLE model. Additionally, calibration of the RUSLE results through field experiments helps to verify the accuracy of the estimated soil erosion in the study area.

Reference of this chapter

Abu Hammad, A., Lundekvam, H., and Børresen, T. 2005. Adaptation of RUSLE in the eastern part of the Mediterranean region, Environ. Manage., 34, 829–841, https://doi.org/ 10.1007 /s00267-003-0296-7, 2005.

Alewell, C., Borrelli, P., Meusburger, K., and Panagos, P. 2019. Using the USLE: chances, challenges and limitations of soil erosion modelling. International Soil and Water Conservation Research 7, 203–225. Retrieved from https://doi.org/10.1016/j.iswcr.2019.05.004

Adornado, H.A., Yoshida, M., Apolinares, H.A. 2009. Erosion vulnerability assessment in REINA, Quezon province, Philippines with raster-based tool built within GIS environment. Agricultural Information Research 18, 24–31. https://doi.org/10.3173/air.18.24

Aksoy, H. and Kavvas, M. L. 2005. A review of hillslope and watershed scale erosion and sediment transport models, Catena, 64, 247–271, https://doi.org/10.1016/j.catena.2005.08.008.

Arnoldus, H. M. J. 1980. An approximation of the rainfall factor in the Universal Soil Loss

Equation, in: De Boodt, M. and Gabriels, D., Assessment of Erosion, Wiley, 127–131, Chichester, UK.

Bagherzadeh, A. 2014. Estimation of soil losses by USLE model using GIS at Mashhad plain, Northeast of Iran, Arab. J. Geosci., 7, 211–220, https://doi.org/10.1007/s12517-012-0730-3.

Bamutaze, Y. 2015. Revisiting socio-ecological resilience and sustainability in the coupled mountain landscapes in Eastern Africa. Current Opinion in Environmental Sustainability 14, 257–265. https://doi.org/10.1016/j.cosust.2015.06.010

Barbera, V., Poma, I., Gristina, L., Novara, A., and Egli, M. 2012. Long-term cropping systems and tillage management effects on soil organic carbon stock and steady state level of C sequestration rates in a semiarid environment. Land Degrad. Dev. 23, 82–91. https://doi.org/10.1002/ldr.1055

Beck, M.B. 1987. Water quality modeling: A review of the analysis of uncertainty. Water Resour. Res. 23, 1393–1442. https://doi.org/10.1029/WR023i008p01393

Benavidez, R., Jackson, B., Maxwell, D., and Norton, K. 2018. A review of the (Revised) Universal Soil Loss Equation ((R)USLE): with a view to increasing its global applicability and improving soil loss estimates. Hydrol. Earth Syst. Sci. 22, 6059–6086. https://doi.org/10.5194/hess-22-6059-2018

Beskow, S., Mello, C.R., Norton, L.D., Curi, N., Viola, M.R., and Avanzi, J.C. 2009. Soil erosion prediction in the Grande River Basin, Brazil using distributed modeling. CATENA, 79(1), 49–59. https://doi.org/10.1016/j.catena.2009.05.010

Bezak, N., Ballabio, C., Mikoš, M., Petan, S., Borrelli, P., and Panagos, P. 2020. Reconstruction of past rainfall erosivity and trend detection based on the REDES database and reanalysis rainfall. Journal of Hydrology 590, 125372. https://doi.org/10.1016/j.jhydrol.2020.125372

Blanco-Canqui, H., Lal, R. 2008. Principles of soil conservation and management. Springer Netherlands, Dordrecht. https://doi.org/10.1007/978-1-4020-8709-7

Bonilla, C.A., Reyes, J.L., and Magri, A. 2010. Water erosion prediction using the Revised Universal Soil Loss Equation (RUSLE) in a GIS framework, Central Chile. Chilean J. Agric. Res. 70, 159–169. https://doi.org/10.4067/S0718-58392010000100017

Borrelli, P., Robinson, D.A., Panagos, P., Lugato, E., Yang, J.E., Alewell, C., Wuepper, D., Montanarella, L., and Ballabio, C. 2020. Land use and climate change impacts on global soil erosion by water (2015-2070). Proc Natl Acad Sci USA 117, 21994–22001. https://doi.org/10.1073/pnas.2001403117

Byizigiro, R.V., Rwanyiziri, G., Mugabowindekwe, M., Kagoyire, C., and Biryabarema, M. 2020. Estimation of soil erosion esing RUSLE model and GIS: The case of Satinskyi Catchment, Western Rwanda. RJESTE 3, 14–33. https://doi.org/10.4314/rjeste.v3i1.2S

Chen, T., Niu, R., Li, P., Zhang, L., and Du, B. 2011. Regional soil erosion risk mapping using RUSLE, GIS, and remote sensing: a case study in Miyun Watershed, North China. Environ Earth Sci 63, 533–541. https://doi.org/10.1007/s12665-010-0715-z

Chuenchum, P., Xu, M., and Tang, W. 2020. Predicted trends of soil erosion and sediment yield from future land use and climate change scenarios in the Lancang–Mekong River by using the modified RUSLE model. International Soil and Water Conservation Research 8, 213–227. https://doi.org/10.1016/j.iswcr.2020.06.006

Chuenchum, P., Xu, M., and Tang, W. 2019. Estimation of soil erosion and sediment yield in the Lancang–Mekong River using the modified revised universal soil loss equation and GIS techniques. Water 12, 135. https://doi.org/10.3390/w12010135

Da Silva, A. M. 2004. Rainfall erosivity map for Brazil, Catena, 57, 251–259. https://doi.org/10.1016/j.catena.2003.11.006

De Asis, A.M., and Omasa, K. 2007. Estimation of vegetation parameter for modeling soil erosion using linear spectral mixture analysis of Landsat ETM data. ISPRS Journal of Photogrammetry and Remote Sensing 62, 309–324. https://doi.org/10.1016/j.isprsjprs.2007.05.013

Desmet, P.J.J. and Govers, G. 1996. A GIS procedure for automatically calculating the USLE LS factor on topographically complex landscape units. Journal of Soil and Water Conservation, 51, 427-433.

Durigon, V.L., Carvalho, D.F., Antunes, M.A. H., Oliveira, P.T. S., and Fernandes, M.M. 2014. NDVI time series for monitoring RUSLE cover management factor in a tropical watershed, Int. J. Remote Sens., 35, 441–453. https://doi.org/10.1080/01431161.2013.871081

El-Swaify, S.A., Gramier, C.L., and Lo, A. 1987. Recent advances in soil conservation in steepland in humid tropics, in: International Conference on Steepland Agriculture in the Humid Tropics. Presented at the the International Conference on Steepland Agriculture in the Humid Tropics, Kuala Lumpur, MADI, pp. 87–100.

Evans, R. 2002. An alternative way to assess water erosion of cultivated land – field-based measurements and analysis of some results. Applied Geography 22, 187–207. https://doi.org/10.1016/S0143-6228(02)00004-8

Evans, R., and Brazier, R. 2005. Evaluation of modelled spatially distributed predictions of soil erosion by water versus field-based assessments. Environmental Science & Policy 8, 147 493–501. https://doi.org/10.1016/j.envsci.2005.04.009

Ferreira, V. and Panagopoulos, T. 2014. Seasonality of soil erosion under Mediterranean conditions at the Alqueva dam watershed, Environ. Manage., 54, 67–83. https://doi.org/10.1007/s00267-014-0281-3.

Food and Agriculture Organization of the United Nations (FAO). 2006. Guidelines for soil description, 4th ed.; Food and Agriculture Organization of the United Nations: Rome, Italy; ISBN 978-92-5-105521-2.

Gashaw, T., Tulu, T., Argaw, M., and Worqlul, A.W. 2019. Modeling the impacts of land use–land cover changes on soil erosion and sediment yield in the Andassa watershed, upper Blue Nile basin, Ethiopia. Environ Earth Sci 78, 679. https://doi.org/10.1007/s12665-019-8726-x

Hateffard, F., Mohammed, S., Alsafadi, K., Enaruvbe, G. O., Heidari, A., Abdo, H. G., and Rodrigo-Comino, J. 2021. CMIP5 climate projections and RUSLE-based soil erosion assessment in the central part of Iran. Sci Rep 11, 1–17. https://doi.org/10.1038/s41598-021-86618-z

Hernandez, E.C., Henderson, A., and Oliver, D.P. 2012. Effects of changing land use in the Pagsanjan–Lumban catchment on suspended sediment loads to Laguna de Bay, Philippines. Agricultural Water Management 106, 8–16. https://doi.org/10.1016/j.agwat.2011.08.012

Jain, M.K., Das, D. 2010. Estimation of sediment yield and areas of soil erosion and deposition for watershed prioritization using GIS and remote sensing. Water Resour Manage 24, 2091–2112. https://doi.org/10.1007/s11269-009-9540-0

Japan International Cooperation Agency (JICA). 2003. The study on the establishment of GIS base data of the Kingdom of Cambodia; Japan International Cooperation Agency (JICA): Phnom Penh, Cambodia; p. 120.

Jayasinghe, P.K.S. C., Adornado, H.A., Yoshida, M., and Leelamanie, D.A.L. 2010. A web-based GIS and remote sensing framework for Spatial Information System (SIS): a case study in Nuwaraeliya, Sri Lanka. Agricultural Information Research 19, 106–116. https://doi.org/10.3173/air.19.106

Kavian, A., Fathollah Nejad, Y., Habibnejad, M., and Soleimani, K. 2011. Modeling seasonal rainfall erosivity on a regional scale: A case study from Northeastern Iran, Int. J. Environ. Res., 5, 939–950.

Kebede, B., Tsunekawa, A., Haregeweyn, N., Adgo, E., Ebabu, K., Meshesha, D.T., Tsubo, M., Masunaga, T., and Fenta, A.A. 2021. Determining C- and P-factors of RUSLE for different land uses and management practices across agro-ecologies: Case studies from the upper Blue Nile Basin, Ethiopia. Phys. Geogr., 42, 160–182.

Khosrokhani, M., and Pradhan, B. 2014. Spatio-temporal assessment of soil erosion at Kuala Lumpur metropolitan city using remote sensing data and GIS. Geomatics, Natural Hazards and Risk 5, 252–270. https://doi.org/10.1080/19475705.2013.794164

Kim, J.B., Saunders, P., and Finn, J.T. 2005. Rapid assessment of soil erosion in the Rio Lempa Basin, Central America, using the universal soil loss equation and geographic information systems, Environ. Manage., 36, 872–885. https://doi.org/10.1007/s00267-002-0065-z

Kinnell, P.I.A. 2010. Event soil loss, runoff and the Universal Soil Loss Equation family of models: A review, J. Hydrol., 385, 384–397. https://doi.org/10.1016/j.jhydrol.2010.01.024

Kityuttachai, K., Heng, S., and Sou, V. 2016. Land cover information catalogue of the Lower Mekong Basin. MRC technical paper No. 58, information and knowledge management programme, Mekong River Commission, Phnom Penh, Cambodia 83 pp.

Klik, A., Haas, K., Dvorackova, A., and Fuller, I. C. 2015. Spatial and temporal distribution of rainfall erosivity in New Zealand, Soil Res., 53, 815–825.

Kogo, B.K., Kumar, L., and Koech, R. 2020. Impact of land use/cover changes on soil erosion in Western Kenya. Sustainability 12, 9740. https://doi.org/10.3390/su12229740

Kong, R., Diepart, J.-C., Castella, J.-C., Lestrelin, G., Tivet, F., Belmain, E., and Bégué, A. 2019. Understanding the drivers of deforestation and agricultural transformations in the Northwestern uplands of Cambodia. Applied Geography 102, 84–98. https://doi.org/10.1016/j.apgeog.2018.12.006

López-Vicente, M., Navas, A., and Machín, J. 2008. Identifying erosive periods by using RUSLE factors in mountain fields of the Central Spanish Pyrenees, Hydrol. Earth Syst. Sci., 12, 523–535, https://doi.org/10.5194/hess-12-523-2008

Loureiro, N.D.S. and Coutinho, M.D.A. 2001. A new procedure to estimate the RUSLE EI30 index, based on monthly rainfall data and applied to the Algarve region, Portugal, J. Hydrol., 250, 12– 18. https://doi.org/10.1016/S0022-1694(01)00387-0

Lufafa, A., Tenywa, M.M., Isabirye, M., Majaliwa, M.J.G., and Woomer, P.L. 2003. Prediction of soil erosion in a Lake Victoria basin catchment using a GIS-based universal soil loss model. Agricultural Systems 76, 883–894. https://doi.org/10.1016/S0308-521X(02)00012-4

Marondedze, A.K., and Schütt, B. 2020. Assessment of soil erosion using the RUSLE model for the Epworth district of the Harare Metropolitan province, Zimbabwe. Sustainability 12, 8531. https://doi.org/10.3390/su12208531

Mekong River Commission (MRC). 2005. Overviews of Hydrology of the Mekong Basin. Mekong River Commission, Vientiane.

Mekong River Commission (MRC). 2016. Land cover map of the Lower Mekong Basin (MRC Technical Paper No. 59), Information and knowledge management programme. Mekong River Commission, Phnom Penh, Cambodia.

Merritt, W.S., Letcher, R.A., and Jakeman, A.J. 2003. A review of erosion and sediment transport models. Environmental Modelling & Software 18, 761–799. https://doi.org/ 10.1016/S1364-8152(03)00078-1

Merritt, W.S., Croke, B.F.W., Jakeman, A. J., Letcher, R.A., and Perez, P. 2004. A biophysical toolbox for assessment and management of land and water resources in rural catchments in Northern Thailand. Ecological Modelling 171, 279–300. https://doi.org/ 10.1016/j.ecolmodel.2003.08.010

Mihara, M., Yamamoto, N., and Ueno, T. 2005. Application of USLE for the prediction of nutrient losses in soil erosion processes. Paddy Water Environ 3, 111–119. https://doi.org/10.1007/s10333-005-0006-6

Morgan, R.P.C. 2005. Soil erosion and conservation, 3rd ed. ed. Blackwell Pub, Malden, MA.

Nagle, G.N., Fahey, T. J., and Lassoie, J. P. 1999. Management of sedimentation in tropical watersheds, Environ. Manage., 23, 441–452, https://doi.org/10.1007/s002679900199

Naipal, V., Reick, C., Pongratz, J., and Van Oost, K. 2015. Improving the global applicability of the RUSLE model – adjustment of the topographical and rainfall erosivity factors, Geosci. Model Dev., 8, 2893–2913. https://doi.org/10.5194/gmd-8-2893-2015.

Nakil, M. and Khire, M. 2016. Effect of slope steepness parameter computations on soil loss estimation: review of methods using GIS. Geocarto International 31, 1078–1093. https://doi.org/10.1080/10106049.2015.1120349

Nigel, R. and Rughooputh, S.D.D.V. 2012. Application of a RUSLE based soil erosion modelling on Mauritius Island, Soil Res., 50, 645–651, 2012.

Ochoa-Cueva, P., Fries, A., Montesinos, P., Rodríguez-Díaz, J.A., and Boll, J. 2015. Spatial estimation of soil erosion risk by landcover change in the Andes of Southern Ecuador, Land Degrad. Dev., 26, 565–573, https://doi.org/10.1002/ldr.2219

Ozsahin, E., Duru, U., and Eroglu, I. 2018. Land use and land cover changes (LULCC), a key to understand soil erosion intensities in the Maritsa Basin. Water 10, 335. https://doi.org/10.3390/w10030335

Panagos, P., Meusburger, K., Ballabio, C., Borrelli, P., and Alewell, C. 2014. Soil erodibility in Europe: A high-resolution dataset based on LUCAS, Sci. Total Environ., 479–480, 189–200, https://doi.org/10.1016/j.scitotenv.2014.02.010

Panagos, P., Ballabio, C., Borrelli, P., Meusburger, K., Klik, A., Rousseva, S., and Alewell, C. 2015a. Rainfall erosivity in Europe, Sci. Total Environ., 511, 801–814. https://doi.org/10.1016/j.scitotenv.2015.01.008

Panagos, P., Borrelli, P., Poesen, J., Ballabio, C., Lugato, E., Meusburger, K., and Alewell, C. 2015b. The new assessment of soil loss by water erosion in Europe, Environ. Sci. Policy, 54, 438–447, https://doi.org/10.1016/j.envsci.2015.08.012

Panagos, P., Ballabio, C., Meusburger, K., Spinoni, J., Alewell, C., and Borrelli, P. 2017. Towards estimates of future rainfall erosivity in Europe based on REDES and WorldClim datasets. Journal of Hydrology 548, 251–262. https://doi.org/10.1016/j.jhydrol.2017.03.006

Panagopoulos, Y., Dimitriou, E., and Skoulikidis, N. 2019. Vulnerability of a Northeast Mediterranean Island to soil loss. Can crazing management mitigate erosion? Water 11, 1491. https://doi.org/10.3390/w11071491

Pham, T. G., Degener, J., and Kappas, M. 2018. Integrated universal soil loss equation (USLE) and Geographical Information System (GIS) for soil erosion estimation in A Sap basin: Central Vietnam. International Soil and Water Conservation Research 6, 99–110. https://doi.org/10.1016/j.iswcr.2018.01.001

Pimentel, D., and Burgess, M. 2013. Soil erosion threatens food production. Agriculture 3, 443–463. https://doi.org/10.3390/agriculture3030443

Prasannakumar, V., Vijith, H., Abinod, S., Geetha, N. 2012. Estimation of soil erosion risk within a small mountainous sub-watershed in Kerala, India, using Revised Universal Soil Loss Equation (RUSLE) and geo-information technology. Geoscience Frontiers 3, 209–215. https://doi.org/10.1016/j.gsf.2011.11.003

Rangsiwanichpong, P., Kazama, S., and Gunawardhana, L. 2018. Assessment of sediment yield in Thailand using revised universal soil loss equation and geographic information system techniques: Assessment of sediment yield in Thailand using geographic information system technique. River Res Applic 34, 1113–1122. https://doi.org/10.1002/rra.3351

Raza, A., Ahrends, H., Habib-Ur-Rahman, M., and Gaiser, T. 2021. Modeling approaches to assess soil erosion by water at the field scale with special emphasis on heterogeneity of soils and crops. Land 10, 422. https://doi.org/10.3390/land10040422

Renard, K. and Freimund, J.R. 1994. Using monthy precipitation data to estimate R-factor in the revised USLE, J. Hydrol., 157, 287–306

Renard, K.G., Foster, G.R., Weesies, G.A., McCool, D.K., and Yoder, D.C. 1997. Predicting soil erosion by water: a guide to conservation planning with the Revised Universal Soil Loss Equation (RUSLE), Handbook No. 703. United States Department of Agriculture.

Renschler, C. S., and Harbor, J. 2002. Soil erosion assessment tools from point to regional scales—the role of geomorphologists in land management research and implementation. Geomorphology 47, 189–209. https://doi.org/10.1016/S0169-555X(02)00082-X

Reyes, M.R., Raczkowski, C.W., Gayle, G.A., and Reddy, G.B. 2004. Comparing the soil loss predictions of GLEAMS, RUSLE, EPIC, and WEPP. Transactions of the ASAE 47, 489– 493. https://doi.org/10.13031/2013.16049

Sanchez, P.A., Palm, C.A., and Buol, S.W. 2003. Fertility capability soil classification: a tool to help assess soil quality in the tropics. Geoderma 114, 157–185. https://doi.org/10.1016/S0016-7061(03)00040-5

Schmitt, L. K. 2009. Developing and applying a soil erosion model in a data-poor context to an island in the rural Philippines, Environ. Dev. Sustain., 11, 19–42, https://doi.org/10.1007/s10668-007-9096-1

Shamshad, A., Azhari, M.N., Isa, M.H., Hussin, W.M.A.W., and Parida, B.P. 2008. Development of an appropriate procedure for estimation of RUSLE EI30 index and preparation of erosivity maps for Pulau Penang in Peninsular Malaysia, Catena, 72, 423–432, https://doi.org/10.1016/j.catena.2007.08.002

Sholagberu, A.T., Ul Mustafa, M.R., Wan Yusof, K., and Ahmad, M.H. 2016. Evaluation of rainfall-runoff erosivity factor for Cameron highlands, Pahang, Malaysia, J. Ecol. Eng., 17, 1–8, https://doi.org/10.12911/22998993/63338

Stefanidis, S., Alexandridis, V., Chatzichristaki, C., and Stefanidis, P. 2021. Assessing Soil Loss 157 by Water Erosion in a Typical Mediterranean Ecosystem of Northern Greece under Current and Future Rainfall Erosivity. Water 13, 2002. https://doi.org/10.3390/w13152002

Stefanidis, S., and Chatzichristaki, C. 2017. Response of soil erosion in a mountainous catchment to temperature and precipitation trends. Carpathian Journal of Earth and Environmental Sciences 12, 35–39.

Stewart, B., Woolhiser, D., Wischmeier, W., Caro, J., and Frere, M. H. 1975. Control of water pollution from cropland, United States Department of Agriculture, United States.

Tang, W., Shan, B., Zhang, H., Zhang, W., Zhao, Y., Ding, Y., Rong, N., and Zhu, X. 2014. Heavy metal contamination in the surface sediments of representative limnetic ecosystems in Eastern China. Sci Rep 4, 7152. https://doi.org/10.1038/srep07152

Talchabhadel, R., Nakagawa, H., Kawaike, K., and Prajapati, R. 2020. Evaluating the rainfall erosivity (R-Factor) from daily rainfall data: An application for assessing climate change impact on soil loss in Westrapti River Basin, Nepal. Model. Earth Syst. Environ., 6, 1741–1762.

Thoeun, H. C., 2015. Observed and projected changes in temperature and rainfall in Cambodia. Weather and Climate Extremes 7, 61–71. https://doi.org/10.1016/j.wace. 2015. 02.001

Thorne, C.R., Zevenbergen, L.W., Grissinger, E.H., and Murphey, J.B. 1985. Calculator programe and nomograph for on-site predictions of ephemeral gully erosion, United States Department of Agriculture Soil Conservation Service, United States.

Thuy, H.T., and Lee, G. 2017. Soil loss vulnerability assessment in the Mekong River Basin. Journal of the Korean Geo-Environmental Society 18, 37–47. https://doi.org/10.14481 /JKGES.2017.18.1.37

Van der Knijff, J. M., Jones, R. J. A., and Montanarella, L. 2000. Soil Erosion Risk Assessment in Europe, available at: https://www.preventionweb.net/files/1581_ ereurnew2.pdf (last access: 29 June 2020).

Van Oost, K., Quine, T.A., Govers, G., De Gryze, S., Six, J., Harden, J. W., Ritchie, J.C., McCarty, G.W., Heckrath, G., Kosmas, C., Giraldez, J.V., da Silva, J.R.M., and

Merckx, R. 2007. The Impact of agricultural soil erosion on the global carbon cycle. Science 318, 626–629. https://doi.org/10.1126/science.1145724

Wilkinson, B.H., McElroy, B.J. 2007. The impact of humans on continental erosion and sedimentation. Geological Society of America Bulletin 119, 140–156. https://doi.org/10.1130/B25899.1

Williams, J.R. 1975. Sediment-Yield Prediction with Universal Equation Using Runoff Energy Factor (Volume 40, p. 244). Washington DC: ARS-S, Southern Region, Agricultural Research Service, US Department of Agriculture.

Williams, J.R. 1995. The EPIC Model. In Computer Models of Watershed Hydrology; Singh, V.P., Ed.; Water Resources Publications: Highlands Ranch, CO, USA; ISBN 0-918334-91-8.

Williams, J.R., and Berndt, H.D. 1977. Sediment yield prediction based on watershed hydrology. Transactions of the ASAE 20, 1100–1104. https://doi.org/10.13031/2013.35710

Wilson, J.P. and Gallant, J.C. 2000. Digital terrain nalysis. In: Wilson, J.P. and Gallant, J.C., Eds., terrain analysis: Principles and applications, John Wiley & Sons, New York, 1-27.

Wischmeier, W.H.; Smith, D.D. 1958. Rainfall energy and its relationship to soil loss. Trans. AGU, 39, 285.

Wischmeier, W.H., and Smith, D.D. 1978. Predicting rainfall erosion losses: A guide to conservation planning. Department of Agriculture, Science and Education Administration, Washington, DC, USA.

Zhang, H., Yang, Q., Li, R., Liu, Q., Moore, D., He, P., Ritsema, C. J., and Geissen, V. 2013. Extension of a GIS procedure for calculating the RUSLE equation LS factor. Computers & Geosciences 52, 177–188. https://doi.org/10.1016/j.cageo.2012.09.027

Yang, D., Kanae, S., Oki, T., Koike, T., and Musiake, K. 2003. Global potential soil erosion with reference to land use and climate changes. Hydrol. Process. 17, 2913–2928. https://doi.org/10.1002/hyp.1441

CHAPTER 5

Effects of Reforestation or Agroforestry on Hydrological Responses in Stung Sangkae River Catchment

5.1. Introduction

Reforestation is essential to reduce or reverse biodiversity loss and mitigate climate change (Cunningham et al., 2015). Restoring forests can restore the biogeochemical cycling of carbon, oxygen, and nutrients between the atmosphere, biomass, pedosphere, and hydrosphere (Arneth et al., 2010). Reforestation of agricultural land can improve biodiversity, resulting in increased primary production, reduced susceptibility to invasion by exotic species, and increased ecological resistance to pressures such as climate change (Hooper et al., 2005). It offers several ecosystem facilities, such as improving soil water infiltration conditions, soil erosion control, and providing wood–related products like timber and fuelwood (Ong et al., 2006). Agroforestry is a prospective solution to reduce the rate of deforestation and overcome the food crisis problem (FAO, 2022; Mulia and Phuong, 2021). This is an integrated approach to a sustainable land-use system (traditional and modern) in which there are interactions between ecological and economic components (timber/forestry plants with seasonal/perennial tree crops, livestock, or fisheries inside or outside forest areas). Agroforestry provides ecosystem services, including climate change mitigation, benefits for smallholders, and prospects for sustainable food production (Bettles et al., 2021; Bishaw et al., 2022). The fertility potential of soils under forests and the need to increase crop production makes forests a target for conversion to agricultural land through deforestation (Laurance et al., 2014). Therefore, there would be high competition for land between forests and agricultural production in some regions of the world, particularly in the tropics (Laurance et al., 2014).

In such situations, agroforestry or reforestation is seen as a compromise between agricultural production and the provision of forest/tree–related benefits (Nair and Garrity, 2012). In agroforestry systems, trees in different arrangement forms are integrated into agricultural land (Nyaga et al., 2015). The World Commission on Water estimates that demand for water will increase by approximately 50% over the next 30 years, and about half of the world's population will live in severe water stress conditions by 2025 (Ong et al., 2006). The urgent need to increase water productivity is a growing global concern. Mwangi et al. (2016) reported that the increase in the agroforest would result in a decrease in the runoff. Therefore, increasing agroforestry is one of the solutions to reduce flood values in the catchment. After more than a century of forest hydrology, several controversial issues or 'beliefs' still hamper rational decision-making regarding land use. Several types of research summarized that forests increase rainfall, decrease runoff, regulate streamflow and increase dry-season streamflow (Wangpimool et al., 2013), reduce erosion, reduce floods, increase infiltration rates and soil moisture retention (Arancibia, 2013) improve water quality, minimizes the drought.

The Stung Sangkae river catchment is one of the major river basins of Tonle Sap basin that have high encroachment of forest areas which has impacted the watersheds of the river catchment and causes flooding almost every year, with frequent social and economic damages (Provincial Department of Water Resource and Meteorology, 2013). Land use change due to increased cultivated land has severely impacted the watershed area and decreased soil quality (Department of Agricultural Land Resources Management, 2019). Moreover, agricultural and ecological system reserves in the lower reaches of the Sangkae River catchment have water shortage problems in the dry season (December-April). The loss of forest area increases the flood potential and drought impacts in the catchment. On the other hand, increasing forest area after returning agricultural lands to the forest reduces the wet season stream flow. It raises it in dry seasons, thus reducing flood potential in the wet season and drought severity in the dry season (Guo et al., 2008). A significant number of studies have reported the impacts of land use on runoff (Costa et al., 2003; Mao and Cherkauer, 2009; Mueller et al., 2009; Cao et al., 2009; Mohammad and Adam, 2010, Schilling et al., 2010). Ouyang et al. (2008) have indicated that the highest peak runoff value is hillside cropland with a slope larger than 15°, which had been converted from the forest. The lowest is hillside cropland with a slope larger than 25° converted into the forest when compared with the cropland and forest area conditions before the implementation of converting cropland to forest policy.

In this regard, catchment management is necessary in order to protect the natural ecosystem as well as to achieve a sustainable use of agricultural land in degraded areas. Soil and water conservation practices also referred to as catchment management strategies (CMSs) are the primary steps of catchment management whose purpose is to enhance agricultural productivity and protect catchments. Specifically, they aim at decreasing runoff rates, improving soil fertility, retarding soil erosion, and thus increasing soil-moisture availability and groundwater recharge (WOCAT, 2007). Agroforestry has in particular, been the focus of many catchment management programs in the developing world (many countries in Africa, Asia, and Latin America whose economies are agriculture-driven) (World Agroforestry, 2021). Agroforestry has been considered a key pathway to restoring degraded ecosystems and achieving food security globally. Within these systems, reforestation efforts have been scaled up to combat the alarming deforestation and forest degradation rates. The contribution of trees to carbon sequestration, nitrogen fixation, and provision of a source of income has been ranked higher and is perceived as more sustainable than other CMSs (Speranza, 2010). However, to reap the numerous benefits offered by trees, it is imperative to determine at the catchment scale where and what proportion of land can reasonably be converted. Since trees consume more water than other vegetation (Mwangi et al., 2016; Kirschke et al., 2018) an improper allocation could magnify an already existing water scarcity situation.

Moreover, CMSs threaten the productive capacity of catchments as their implementation may lead to losses in agricultural production. Thus, there is a need for a comprehensive and systematic understanding of the possible adverse effects of agroforestry and its combination with other CMSs on the different ecosystem services. Tools such as hydrologic models have been used to conceptualize the impacts of climatic and anthropogenic changes on the various sub-processes within the hydrologic cycle (Legesse et al., 2003).

Therefore, the integration of forest cover for flood management and mitigation is a potential and cost-effective solution (Ellison et al., 2017; Jongman et al., 2015) for river management and development. Moreover, the Royal Government of Cambodia has a goal of maintaining at least 50% of its land under forest cover to contribute to the country's Sustainable Development Goals by 2030.

5.2. Materials and Methodology

The materials and methodology applied in section 3.2, which was already mentioned in chapter 3, were used in this chapter; however, some reforestation scenarios were made to understand the effects of reforestation on stream flow and soil erosion in the catchment, as described in the previous chapters. The location of the study area is shown in Figure 5.1.

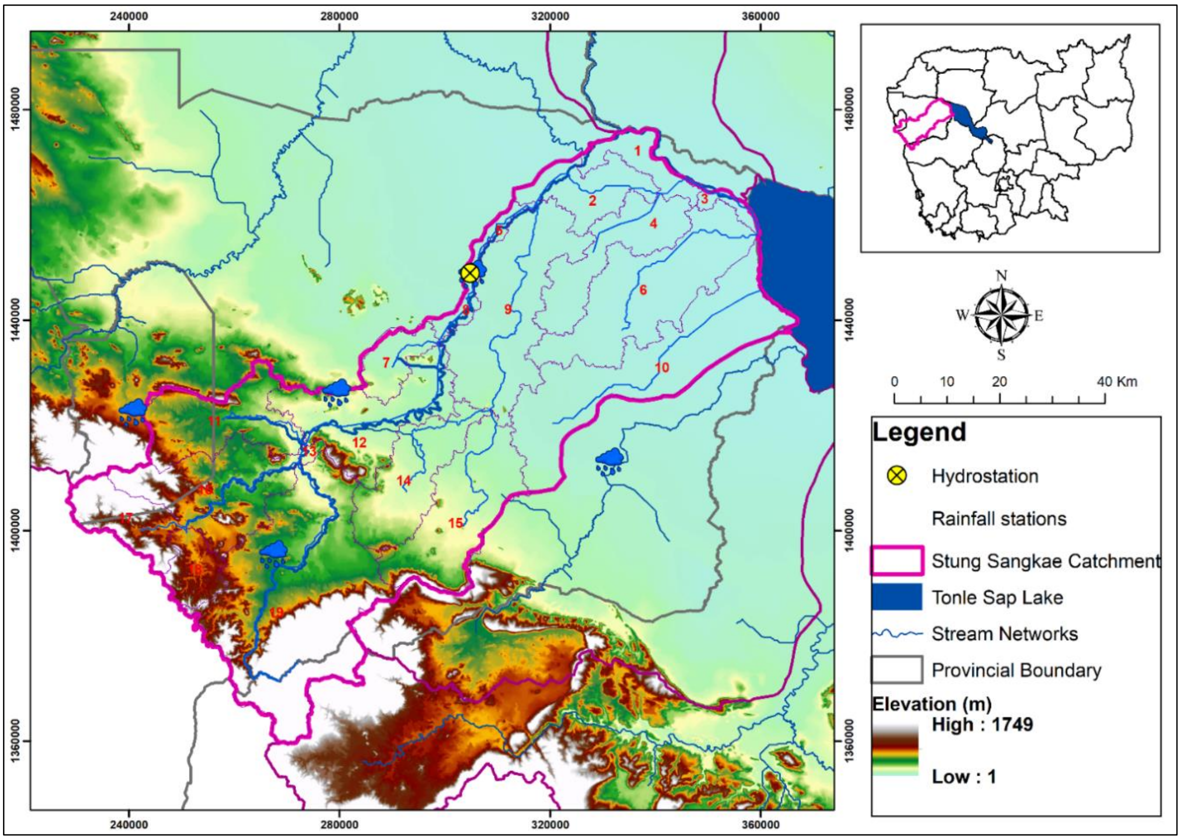

Figure 5.1. Location of the study area

5.2.1. Reforestation scenarios

The actual land use database, a digital map of land use in 2015, was defined as the baseline land use. Three scenarios were used to evaluate the effect of reforestation on stream flow and soil erosion in the Stung Sangkae River catchment, as shown in Table 5.1 and Figure. 5.1, 5.2, and 5.3. The scenario of an increased percentage of reforestation was based on the RGC's policy that by 2030, the goal is to maintain at least 50% of its land under forest cover to contribute to the country's Sustainable Development Goals (RGC, 2018). The three scenarios were:

Scenario-1: All areas of forest land (mixed and deciduous forest) were revived, and the other types of land use remained the same as the LULC MRC 2015 pattern. 15% of the forest land is reforested.

Scenario-2: The area of agricultural land was reforested, and the other types of land use remained the same as the LULC MRC 2015 pattern. 25% of the forest land is reforested.

Scenario-3: All the mixed forest, deciduous forest, and agricultural land were revived, and the other types of land use remained the same as the LULC MRC 2015 pattern. 40% of the forest land is reforested.

Table 5.1. Land use conditions in the three scenarios

No	LU categories	Baseline-MRC		Scenario-1		Scenario-2		Scenario-3	
		Area		Area		Area		Area	
		ha	%	ha	%	ha	%	ha	%
1	Agricultural Land	152,742.3	25.2	152,742.3	25.2	-	-	-	-
2	Barren land	274.3	0.0	274.3	0.0	274.3	0.0	274.3	0.0
3	Built-up area	20,870.1	3.4	20,870.1	3.4	20,870.1	3.4	20,870.1	3.4
4	Deciduous forest	24,144.9	4.0	-	-	24,144.9	4.0	-	-
5	Evergreen forest	90,338.0	14.9	179,193.8	29.6	243,080.3	40.2	331,936.0	54.9
6	Grassland	29,394.2	4.9	29,394.2	4.9	29,394.2	4.9	29,394.2	4.9
7	Marshes and swamp	35.8	0.0	35.8	0.0	35.8	0.0	35.8	0.0
8	Mixed forest	64,710.9	10.7	-	-	64,710.9	10.7	-	-
9	Paddy field	144,931.5	23.9	144,931.5	23.9	144,931.5	23.9	144,931.5	23.9
10	Shrubland	74,019.0	12.2	74,019.0	12.2	74,019.0	12.2	74,019.0	12.2
11	Water bodies	3,709.6	0.6	3,709.6	0.6	3,709.6	0.6	3,709.6	0.6
Total		**605,170.5**	**100.0**	**605,170.5**	**100.0**	**605,170.5**	**100.0**	**605,170.5**	**100.0**

a). Grassland

b). Broadleaved deciduous forest

c). Mixed forest

d). Broadleaved ever-green forest

Figure 5.2. Land use types in the study area

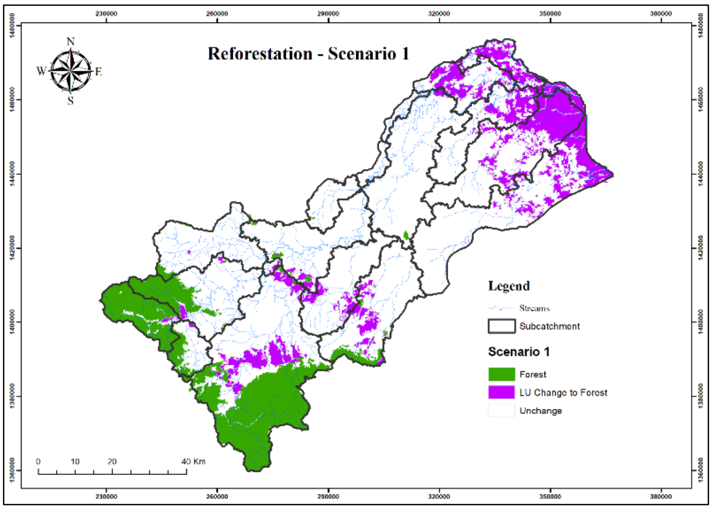

a). Reforestation scenario-1 in the catchment (15% forest increased)

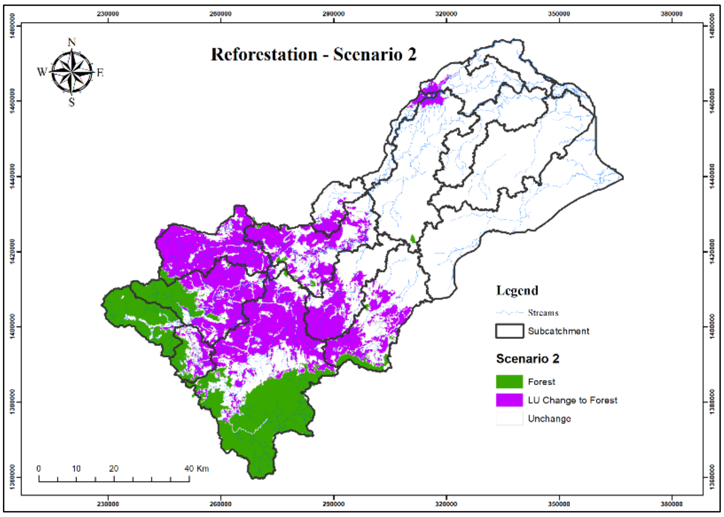

b). Reforestation scenario-2 in the catchment (25% forest increased)

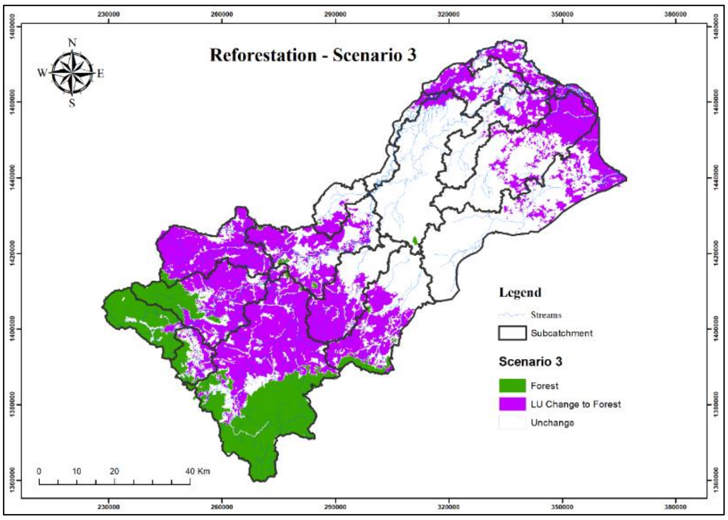

c). Reforestation scenario-3 in the catchment (40% forest increased)

Figure 5.3. Reforestation scenario conditions in the Stung Sangkae River catchment

5.3. Results and Discussion

5.3.1. Stream flow response to reforestation

The reforestation changes in the Stung Sangkae River catchment in each scenario and baseline were used in the SWAT simulation to investigate the effect on stream flow. The result of the simulation in the whole catchment of annual stream flow of baseline land use and three reforestation scenarios are shown in Figure 5.4 and Table 5.2. It showed that implementing reforestation activities in the catchment could dramatically reduce the annual stream flow in the Stung Sangkae River catchment compared to the reference or baseline land use. However, for the Scenarios, 2 (25% of the reforested land) and 3 (40% of the reforested land), the annual streamflow is almost the same. Thus, the reforestation above 25% is not recommended for implementation in the catchment.

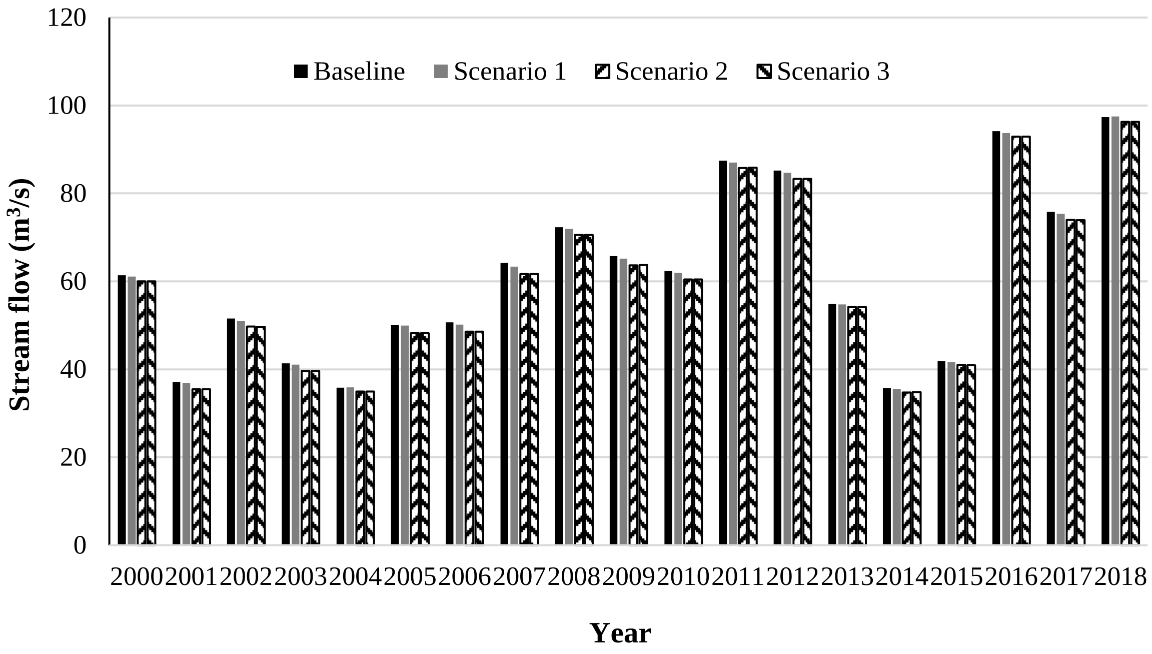

Figure 5.4. Annual stream flow (cms) for baseline and reforest scenarios

The effects of reforestation on stream flow, mainly seasonal stream flow, are more remarkable. The altered land use influences seasonal stream flow volumes. The volumes of seasonal stream flow of scenarios 1 - 3 and baseline are shown in Table 5.2. The results indicate that the volumes of seasonal stream flow in three scenarios decreased in the wet season and increased in the dry season compared with the baseline land use (Figure. 5.5). For the percentage of seasonal stream flow changes in scenarios 1 and 2, they decreased in the wet season at about 3%. They increased in the dry season also at about 3%. These stream flows are more important for water resource management in the dry season and also for flood reduction in the wet season. This finding is aligned with the (Wangpimool et al., 2013).

For the variation of streamflow in this study, the average in the reference period was significantly higher than that in the reforestation period, indicating that the flow velocity of streamflow was decreased by reforestation. This is likely because forest recovery through reforestation can effectively store water because of canopy interception, abundant underpants and forest floor, which leads to more soil infiltration and consequently more baseflow (Zhou et al., 2010).

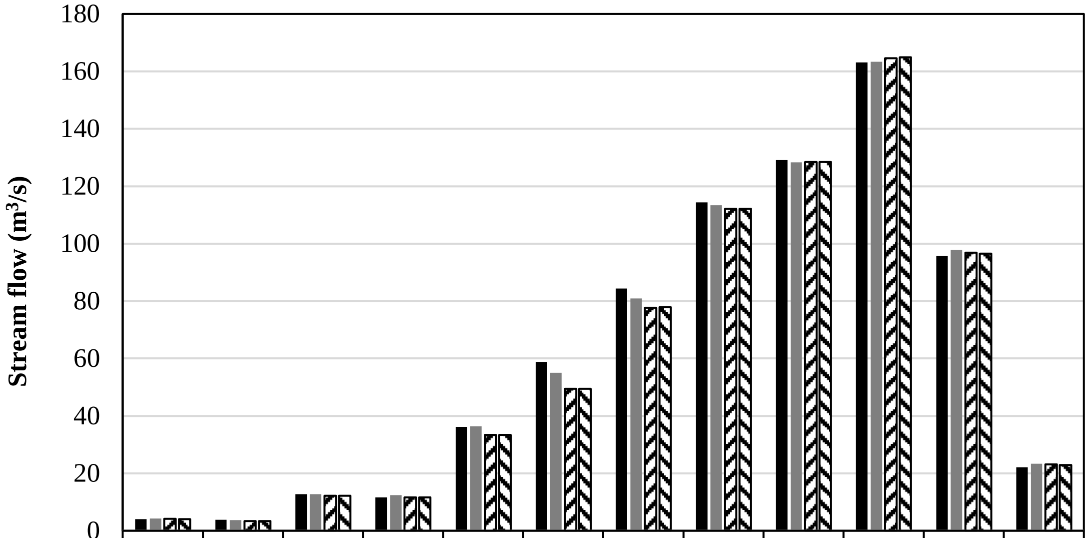

	Jan	Feb	Mar	Apr	May	Jun	Jul	Aug	Sep	Oct	Nov	Dec
Baseline	4.0	3.8	12.7	11.7	36.2	58.8	84.3	114.3	129.1	163.1	95.7	22.1
Scenario 1	4.2	3.7	12.8	12.4	36.4	55.0	80.9	113.4	128.4	163.3	97.8	23.4
Scenario 2	4.1	3.3	12.1	11.6	33.4	49.4	77.7	112.1	128.5	164.6	96.9	23.1
Scenario 3	4.1	3.4	12.1	11.6	33.4	49.5	77.9	112.1	128.5	164.9	96.5	22.9

Figure 5.5. Average monthly stream flow for baseline and reforestation scenarios

In this study, relative contributions of reforestation to total streamflow had similar effects in terms of magnitude as those from climate variability, indicating that hydrological effects of forest changes might be the same as those caused by climatic variability in the studied watershed (Table 5.2). The percentage of the change is less than one percent in wet and dry season, and if compared to the flow volume, it was reduced to around 50 million cubic meters (MCM) compared to the baseline. This conclusion is consistent with various studies. For example, the long-term and large-scale forest changes, including deforestation and reforestation, contributed to 50.31% and 49.3% of streamflow variations, respectively, in the upper reach of the Poyang Lake watershed of China (Liu et al., 2015). Similar results were also reported by Montenegro and Ragab (2012), Huang et al. (2016) and Li et al. (2017). However, some studies showed that the influences from climatic variability on regional discharge were more pronounced compared with those from forest change or land-use change. For example, Wei et al. (2018) quantitatively assessed the relative contributions of forest change and climatic variability on annual mean flow in forested watershed across the globe and found that average variation in annual streamflow ascribed to forest change is 31% while 69% from climate variability. This suggested that streamflow is more sensitive to climate variability on average at the global scale. Those inconsistent conclusions may be due to the difference in climate, the degree of forest changes, and spatial scale.

Table 5.2. Annual stream flow (MCM) for baseline and reforest scenarios

Scenarios	Annual stream flow	Wet season (May - Oct.)		Dry season (Nov. – Apr.)	
	MCM	MCM	%	MCM	%
Baseline	1907.4	1,518.6	79.6	388.9	20.4
Scenario-1	1,896.8	1,496.7	78.9	400.2	21.1
Scenario-2	1,858.2	1,466.3	78.9	391.8	21.1
Scenario-3	1,858.0	1,467.8	79.0	390.2	21.0

The effects of reforestation on stream flow, mainly seasonal stream flow, are more remarkable. The altered land use influences seasonal stream flow volumes. The results indicate that the discharge of seasonal stream flow of three scenarios decreased in the wet season (May-October) and increased in the dry season (November-April) compared with the baseline land use (Table 5.2 and Figure 5.6). The finding agreed with Wangpimool et al. (2013). In Figure 5.6, it was shown that 25% of reforestation increased flow volume in the dry season, which will be suitable for water resource management in the dry season.

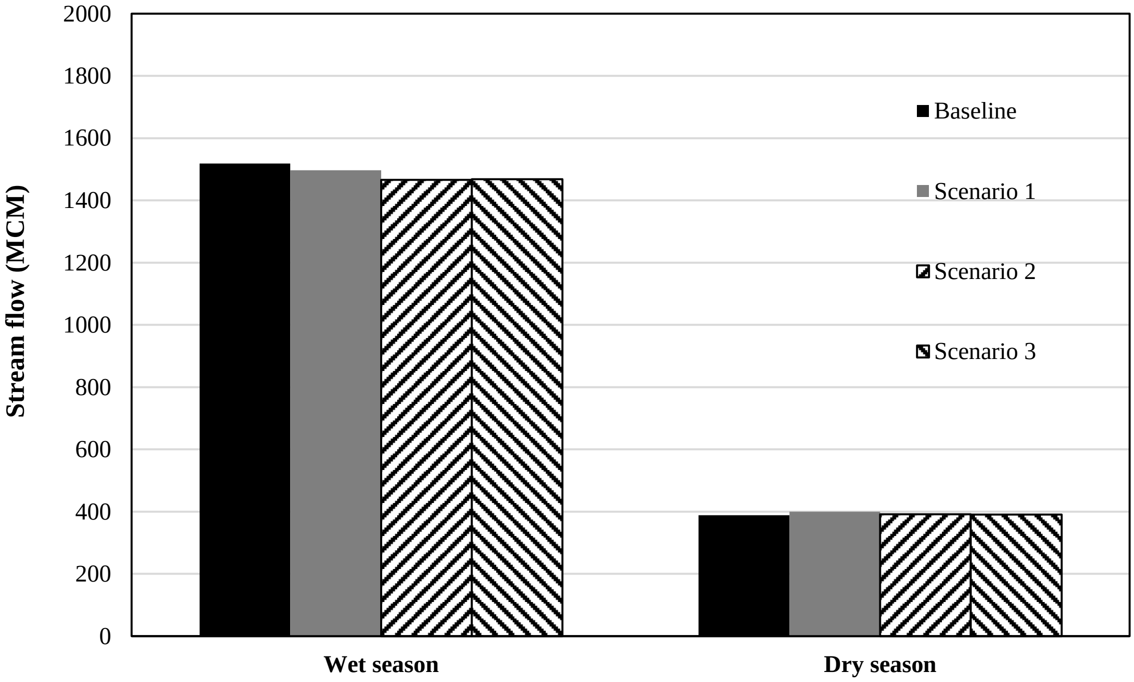

Figure 5.6. Seasonal stream flows for baseline and reforestation scenarios

5.3.2. Soil loss response to reforestation

The study of the effect of reforestation on soil loss in the Stung Sangkae catchment by the Soil and Water Assessment Tool (SWAT) model application designated the land use in 2015 as the baseline land use and assigned 3 reforestation land use scenarios. The effects of reforestation on soil loss, especially annual and monthly soil loss, are significantly different (Table 5.3 and Figure 5.7). The LULC changes significantly impacted soil loss in the Stung Sangkae River catchment, even though the stream flow is not significantly changed. Table 5.3 shows that under scenario 1 and 2, the soil loss is significantly reduced almost 30% (28.4%=15.5 ton/ha) with 15% increased reforestation and 50% (47.5%=11.4 ton/ha) with 25% increased reforestation in the catchment compared to the baseline soil loss (21.8 ton/ha) , respectively. For scenarios 2 and 3, the soil loss is almost unchanged. Thus, reforestation effectively prevents soil erosion in the catchment, particularly during the rainy season from August to October (Figure 5.7). However, 25% of reforestation (40% of forest cover in the catchment) is enough to prevent soil erosion in the catchment as it is not significant if it is increased more than this recommendation. The result could contribute to the RGC's policy toward the country's Sustainable Development Goals to maintain at least 50% of its land under forest cover in 2030 (RGC, 2018).

Table 5.3. Annual soil loss based on baseline and 3 reforestation scenarios (ton/ha)

No	Year	Baseline (ton/ha)	Scenario-1		Scenario-2		Scenario-3	
			ton/ha	%	ton/ha	%	ton/ha	%
1	2000	21.9	15.9	27.4	12.1	44.7	12.1	44.7
2	2001	5.4	4.0	25.9	2.9	46.3	2.9	46.3
3	2002	23.5	16.5	29.8	12.3	47.7	12.4	47.2
4	2003	21.9	15.9	27.4	11.8	46.1	11.8	46.1
5	2004	14.0	11.0	21.4	8.1	42.1	8.1	42.1
6	2005	20.9	15.3	26.8	10.9	47.8	10.9	47.8
7	2006	21.4	15.1	29.4	11.7	45.3	11.8	44.9
8	2007	37.5	25.8	31.2	18.7	50.1	18.7	50.1
9	2008	26.0	18.3	29.6	13.8	46.9	13.9	46.5
10	2009	16.5	11.4	30.9	8.1	50.9	8.2	50.3
11	2010	23.5	17.4	26.0	14.7	37.4	14.8	37.0
12	2011	22.6	16.3	27.9	12.4	45.1	12.5	44.7
13	2012	27.2	19.3	29.0	14.0	48.5	14.0	48.5
14	2013	33.4	24.1	27.8	18.3	45.2	18.3	45.2
15	2014	14.9	10.8	27.5	7.1	52.3	7.2	51.7
16	2015	22.1	15.9	28.1	10.8	51.1	10.8	51.1
17	2016	18.0	12.4	31.1	8.8	51.1	8.9	50.6
18	2017	22.5	15.4	31.6	10.9	51.6	11.0	51.1
19	2018	21.9	15.1	31.1	10.2	53.4	10.3	53.0

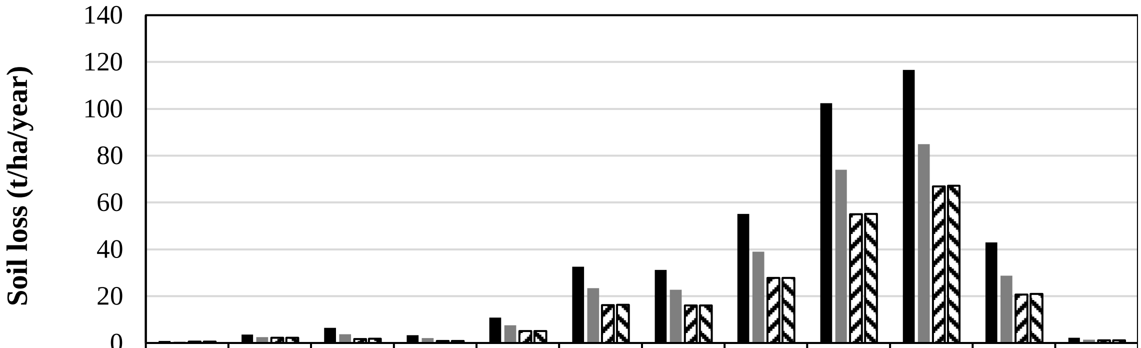

	Jan	Feb	Mar	Apr	May	Jun	Jul	Aug	Sep	Oct	Nov	Dec
Baseline	0.9	3.7	6.5	3.4	10.8	32.5	31.2	55.2	102.4	116.7	42.9	2.2
Scenario 1	0.7	2.6	3.7	2.1	7.6	23.4	22.7	39.1	74.1	84.9	28.8	1.5
Scenario 2	0.6	2.2	1.8	0.8	5.1	16.2	16.0	27.8	55.0	66.9	20.7	1.1
Scenario 3	0.6	2.3	1.8	0.8	5.1	16.3	16.0	27.8	55.1	67.2	20.9	1.2

Figure 5.7. Monthly soil loss based on baseline and 3 reforestation scenarios

The effects of reforestation on seasonal soil loss are very significant. The results indicate that the seasonal soil loss of three scenarios significantly decreased in the wet season (May-October) and the dry season (November-April) compared with the baseline land use

(Figure 5.8). The 25% reforestation could significantly decrease soil erosion in the wet season. Moreover, the soil loss in each sub-catchment is also dramatically reduced due to increased reforestation. The soil erosion at the upstream catchment decreased significantly, particularly in sub-catchment no. 11, 13, 15, 16, 18, and 19 (Table 5.4).

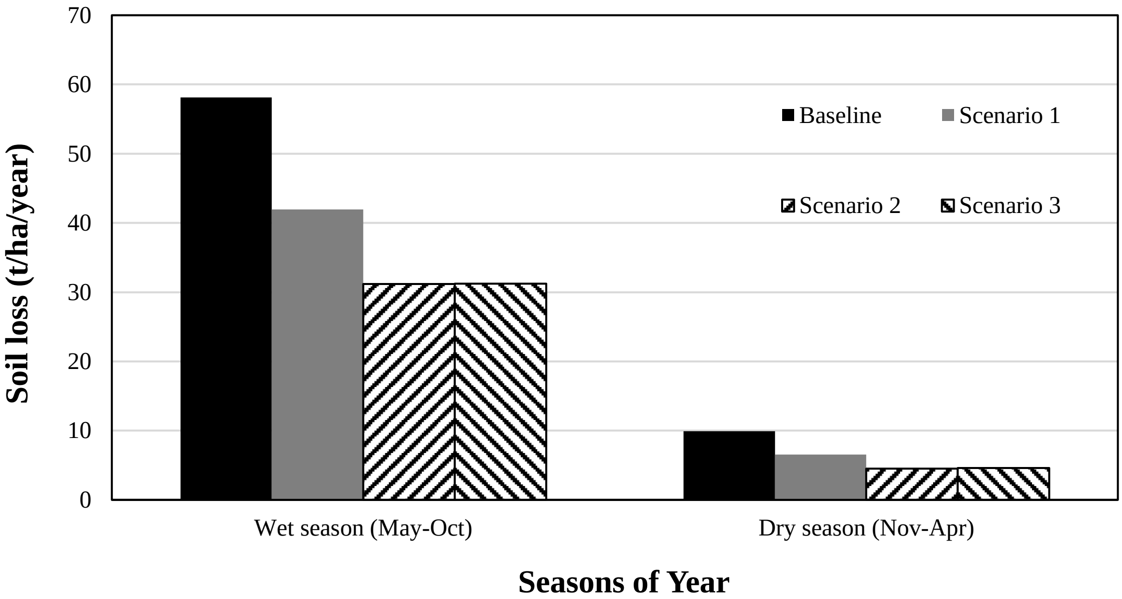

Figure 5.8. Soil loss based on season

Table 5.4. Soil loss from subbasin of baseline land use, and with 3 reforestation land use scenarios (ton/ha)

Subbasin	Area (ha)	Baseline	Scenario-1	Scenario-2	Scenario-3
1	12,384.1	17.2	16.2	16.2	16.2
2	20,512	9.1	7.5	7.5	7.5
3	3,693.6	0.5	0.4	0.4	0.4
4	28,800.2	18.6	15.7	15.7	15.7
5	3,843.0	13.5	10.6	10.6	10.6
6	55,486.7	8.2	7.1	7.1	7.1
7	12,185.1	12.5	8.3	6.8	6.8
8	4,455.8	6.5	6.1	6.1	6.1
9	56,913.7	4.0	3.5	3.5	3.5
10	69,949.8	4.6	4.3	4.3	4.3
11	33,473.9	38.6	21.0	13.1	13.1
12	40,221.9	6.4	5.1	4.5	4.6
13	1,548.3	29.3	19.7	17.2	17.3
14	32,385.2	7.7	4.4	3.0	3.2
15	45,275.3	40.2	25.5	13.4	13.7
16	41,340.6	40.5	25.3	15.1	15.1
17	19,966.2	8.3	7.1	6.3	6.3
18	12,324.5	45.5	29.4	16.4	16.4
19	110,409.4	22.3	13.8	6.8	7.1

5.4. Conclusion of This Chapter

The study of the effect of reforestation on stream flow and soil erosion in the Stung Sangkae catchment by the SWAT model application designated the land use in 2015 as the baseline land use and assigned 3 reforestation land use scenarios. The estimated stream flow and soil erosion with the SWAT model showed an annual average stream flow of about 1,907 MCM and an average annual soil loss of about 21.8 tons/ha. The average stream flow occurring during the wet season from May to October was about 1,517 MCM (80% of the average annual stream flow), and in the dry season, about nearly 389 MCM (20% of the average yearly average stream flow). The results of reforestation from scenarios 1 and 2 were predicted to increase annual stream flow in the dry season by about 3% and to reduce the flow in the wet season by about 3% in the mainstream and its tributaries. The soil loss was significantly reduced to 11.4 tons/ha, with a 25% increase in reforestation in the catchment compared to the baseline. For scenario 3, reforestation was predicted to neither increase nor decrease stream flow in wet or dry seasons. However, the effect of reforestation on water resources is both complex and uncertain; considering many alternatives and evaluations, the past will help in understanding the dynamic changes. However, the effect of reforestation on water resources is both complex and uncertain; considering many alternatives and evaluations, evaluation, and the past will help in understanding the dynamic changes. This study result will be a guideline for decision-making about land use and water resources management in the Stung Sangkae River catchment and other river basins in the Tonle Sap Basin of Cambodia.

Moreover, the increased 25% of reforestation (40% of forest cover in the entire catchment) is enough to prevent soil erosion. In contrast, the percentage of reforestation above this is not recommended. Furthermore, the result could contribute to the RGC's policy toward the country's Sustainable Development Goals to maintain at least 50% of its land under forest cover in 2030.

In this study, we conclude that forest recovery provided positive hydrological effects slightly on streamflow but significantly on soil loss. Forest changes (reforestation or fruit tree planting) can play a similar role in all streamflow components as climatic variability in magnitude. The different hydrological effects between reforestation and fruit tree planting suggest that fruit tree planting may not be effective in soil and water conservation as previously expected and should be managed cautiously. We also conclude that a combined research approach of the separation technique with the pair-wise method would provide a more robust research framework for assessing the hydrological effects of reforestation.

Reference of this chapter

Arneth, A., Harrison, S.P., Zaehle, S., Tsigaridis, K., Menon, S., Bartlein, P.J., Feichter, J., Korhola, A., Kulmala, M., O'Donnell, D., Schurgers, G., Sorvari, S., and Vesala, T. 2010. Terrestrial biogeochemical feedback in the climate system. Nature Geoscience, 3(8), 525–532. https://doi.org/10.1038/ngeo905

Arancibia, J.L.P. 2013. Impacts of land use change on dry season flows across the tropics (forests as 'Sponges' and 'Pumps'), 262p, PhD. Dissertation, University of London, UK.

Bettles, J., Battisti, D.S., Cook-Patton, S.C., Kroeger, T., Spector, J.T., Wolff, N.H., and Masuda, Y.J. 2021. Agroforestry and non-state actors: A review. Forest Policy and Economics, 130, 102538. https://doi.org/10.1016/j.forpol.2021.102538

Bishaw, B., Soolanayakanahally, R., Karki, U., and Hagan, E. 2022. Agroforestry for sustainable production and resilient landscapes. Agroforestry Systems, 96(3), 447–451. https://doi.org/10.1007/s10457-022-00737-8

Cao, W., Bowden, W.B., Davie, T., and Fenemor, A. 2009. Modeling impacts of land cover change on critical water resources in the Motueka river catchments,New Zealand. Water Resources Management, Vol. 23, pp. 137 151.

Costa, M.H., Botta, A., and Cardille, J.A. 2003. Effects of large-scale changes in land cover on the discharge of the Tocantins River, Southeastern Amazonia. J. Hydrol. (Amst), 283, pp. 206-217, 10.1016/S0022-1694(03)00267-1

Cunningham, S.C., Mac Nally, R., Baker, P.J., Cavagnaro, T.R., Beringer, J., Thomson, J.R., and Thompson, R.M. 2015. Balancing the environmental benefits of reforestation in agricultural regions. Perspectives in Plant Ecology, Evolution and Systematics, 17(4), 301–317. https://doi.org/10.1016/j.ppees.2015.06.001

Ellison, D., Morris, C.E., Locatelli, B., Sheil, D., Cohen, J., Murdiyarso, D., Gutierrez, V., Van Noordwijk, M., Creed, I.F., Pokorny, J. 2017. Trees, forests and water: cool insights for a hot world. Global Environ. Change 43, 51–61. https://doi.org/10.1016/j.gloenvcha.2017.01.002.

Food Agricultural Organization (FAO). 2022. Agroforestry. Retrieved from http://www.fao.org/forestry/agroforestry/en/

Guo, H., Hu, Q., & Jiang, T. (2008). Annual and seasonal streamflow responses to climate and land-cover changes in the Poyang Lake basin, China. Journal of Hydrology, 355(1–4), 106–122. https://doi.org/10.1016/j.jhydrol.2008.03.020

Hooper, D.U., Chapin, F.S., Ewel, J.J., Hector, A., Inchausti, P., Lavorel, S., Lawton, J.H., Lodge, D.M., Loreau, M., Naeem, S., Schmid, B., Setälä, H., Symstad, A.J., Vandermeer, J., and Wardle, D.A. 2005. Effects of biodiversity on ecosystem functioning: A consensus of current knowledge. Ecological Monographs, 75(1), 3–35. https://doi.org/10.1890/04-0922

Huang, X., Shi, Z., Zhu, H., Zhang, H., Ai, L., and Yin, W. 2016. Soil moisture dynamics within soil profiles and associated environmental controls. Catena 136:189–196.

Jongman, B., Winsemius, H.C., Aerts, J.C., de Perez, E.C., Van Aalst, M.K., Kron, W. and Ward, P.J. 2015. Declining vulnerability to river floods and the global benefits of adaptation. Proc. Natl. Acad. Sci.

Kirschke, S., Zhang, L., and Meyer, K. 2018. Decoding the wickedness of resource nexus problems—examples from water-soil nexus problems in China. Resources 7:67. https://doi.org/10.3390/resources7040067

Laurance, W.F., Sayer, J., and Cassman, K.G. 2014. Agricultural expansion and its impacts on tropical nature. Trends in Ecology & Evolution, 29(2), 107–116. https://doi.org/10.1016/j.tree.2013.12.001

Legesse, D., Vallet-Coulomb, C., and Gasse, F. 2003. Hydrological response of a catchment to climate and land use changes in Tropical Africa: case study South Central Ethiopia. J. Hydrol. 275, 67–85. https://doi.org/10.1016/S0022-1694(03)00019-2

Li, D., Wrzesien, M.L., Durand, M., Adam, J., and Lettenmaier, D.P. 2017. How much runoff originates as snow in the western United States, and how will that change in the future? Geophysical Research Letters, 44(12), 6163–6172. https://doi.org/10.1002/2017GL073551

Liu, W., Wei, X., Liu, S., Liu, Y., Fan, H., Zhang, M., et al. 2015. How do climate and forest changes affect long-term streamflow dynamics? A case study in the upper reach of Poyang River basin. Ecohydrology, 8(1), 46–57. https://doi.org/10.1002/eco.1486

Mao, D., and Cherkauer, K.A. 2009. Impacts of land-use change on hydrologic responses in the Great Lakes region, Journal of Hydrology, 374, 1–2, 71-82.

Mohammad, A.G., and Adam, M.A. 2010. The impact of vegetative cover type on runoff and soil erosion under different land uses, CATENA, 81, 2, 97-103.

Montenegro, S., and Ragab, R. 2012. Impact of possible climate and land use changes in the semi arid regions: a case study from North Eastern Brazil. J Hydrol 434-435:55–68.

Mulia, R.; Phuong, N.M. 2021. Diversity of agroforestry practices in Viet Nam; World Agroforestry (ICRAF): Hanoi, Vietnam. Retrieved from https://apps.worldagro forestry.org /region/sea/publications/detail?pubID=4709

Mueller, E.N, Francke, T., Batalla, R.J., and Bronstert, A. 2009. Modelling the effects of land-use change on runoff and sediment yield for a meso-scale catchment in the Southern Pyrenees, CATENA, 79, 3, 288-296. https://doi.org/10.1016/j.catena.2009. 06.007.

Mwangi, H.M., Julich, S., Patil, S.D., McDonald, M.A., and Feger, K.H. 2016. Modelling the impact of agroforestry on hydrology of Mara River Basin in East Africa: Impact of agroforestry on hydrology of Mara River Basin. Hydrological Processes, 30(18), 3139–3155. https://doi.org/10.1002/hyp.10852

Nair, P.K.R., and Garrity, D.P. (Eds.). 2012. Agroforestry - The future of global land use, Springer, ISBN 978-94-007-4676-3

Nyaga, J., Barrios, E., Muthuri, C.W., Öborn, I., Matiru, V., and Sinclair, F.L. 2015. Evaluating factors influencing heterogeneity in agroforestry adoption and practices within smallholder farms in Rift Valley, Kenya. Agriculture, Ecosystems & Environment, 212, 106–118. https://doi.org/10.1016/j.agee.2015.06.013

Ong, C.K., Black, C.R., and Muthuri, C.W. 2006. Modifying forestry and agroforestry to increase water productivity in the semi-arid tropics. CABI Reviews, 2006. https://doi.org/10.1079/PAVSNNR20061065

Ouyang, W., Hao, F.-H., Wang, X., and Cheng, H.-G. 2008. Nonpoint source pollution responses simulation for conversion cropland to forest in mountains by SWAT in China. Environmental Management, 41(1), 79–89. https://doi.org/10.1007/s00267-007-9028-8

Royal Government of Cambodia (RGC). 2018. Cambodian Sustainable Development Goals (CSDGs) Framework (2016-2030).

Schilling, K.E., Chan, K.-S., Liu, H., and Zhang, Y.-K. 2010. Quantifying the effect of land use land cover change on increasing discharge in the Upper Mississippi River, Journal of Hydrology, 387, 3–4, 343-345.

Speranza, C.I. 2010. Resilient Adaptation to Climate Change in African Agriculture. Bonn: Deutsches Institut für Entwicklungspolitik.

Wangpimool, W., Pongput, K., Sukvibool, C., Sombatpanit, S., and Gassman, P. W. 2013. The effect of reforestation on stream flow in Upper Nan River basin using Soil and Water Assessment Tool (SWAT) model. International Soil and Water Conservation Research, 1(2), 53–63. https://doi.org/10.1016/S2095-6339(15)30039-3

Wei, X.; Li, Q., Zhang, M., Giles-Hansen, K., Liu, W., Fan, H., Wang, Y., Zhou, G., Piao, S., and Liu, S. 2018. Vegetation cover—Another dominant factor in determining global water resources in forested regions. Glob. Change Biol., 24, 786–795.

WOCAT. 2007. Where the land is greener: Case studies and analysis of soil and water conservation initiatives worldwide (2007). Switzerland: WOCAT.

World Agroforestry. 2021. What is agroforestry? World agroforestry | Transforming lives and landscapes with trees. Available online at: https://www.worldagroforestry.org/about/agroforestry (accessed on September 22, 2021).

Zhou, G., Wei, X., Luo, Y., Zhang, M., Li, Y., Qiao, Y., et al. 2010. Forest recovery and river discharge at the regional scale of Guangdong Province, China. Water Resources Research, 46, W09503. https://doi.org/10.1029/2009WR008829

CHAPTER 6

Deeping Public Perception on the Importance of Conservation Strategies against Flood/Drought and Soil Loss

6.1. Introduction

The problems of global, regional, national, and ground soil fertilizers, decline in wildlife habitats, fauna and flora, changing of water flow pattern, farming system, poor nutrition, and unhealthy people have been caused by land use and land cover (LULC) change (Desalegn et al., 2014; Intergovernmental Panel on Climate Change (IPCC), 2014; Manandhar et al., 2009; Montalván-Burbano et al., 2021; Shi et al., 2018; Xu et al., 2018). Most of developing countries, the majority of citizens' jobs rely on natural resources and agriculture (Desalegn et al., 2014; Mwavu and Witkowski, 2008). For instance, in Cambodia, approximately 13.6 million people live in rural areas,, and about 11 million people's livelihoods are based on farming, fisheries, and natural resources (USAID, 2021).

In a worldwide context, the supply of land resources for producing food, fiber, and biofuels is limited (Lambin and Meyfroidt, 2011). Otherwise, land should be taken attention to be prepared, developed, and used sustainably (Desalegn et al., 2014; Mwavu and Witkowski, 2008; Nut, et al., 2021; Sourn et al., 2021). According to Bonilla-Moheno and Aide, (2020); le Polain de Waroux et al., (2016); Kong et al., 2019; Nut et al., 2021), the conversion of forest land to farming land happened in Mexico, South America, and Cambodia due to the rise of pastures, soybeans, cassava, corn and other fruit trees and paddy rice fields. These changes impacted negatively on soil erosion, in particular in Battambang province of Cambodia (Nut, et al., 2021, Sourn et al., 2022). For instance, the casava field was eroded around 60 to 119 t/ha/262 days in an upland area of Battambang (CARDI, 2016). Otherwise, conservation agriculture was recommended practiced as a mitigation measure against soil degradation (Pheap et al., 2019). The high crop potential in Cambodia, the land area for casava, corn and fruit tree, is increased by the expense of natural resources (Sourn et al., 2021). Crop plantation, particularly casava, was also defined as a main crop for socioeconomic development and was a key. Consequently, land use change is increasingly occurring throughout Cambodia, especially the conversion from forest to cultivated land.

In addition, for comprehensive and scientific research of natural and social change, some tools, such as key informants, in-depth interviews, and focus-group discussions in the study area, should be applied to get information on past, present and expected future land use and land cover changes (Gashaw et al., 2017; Sandewall et al., 2001). To deeply understand local perceptions of land use change, the approach of qualitative research in social science and survey research was used, to answer the question “why change happens” and “so what” (Maro, 2011). This methods was also used by Desalegn et al., (2014) and Toh et al., (2018) to know the relationship between LULC change and socioeconomic condition in Cameroon and Ethiopia. Using individual semi-structured interviews with local farmers to understand the relation between national and local perceptions of environmental change in central Northern Namibia found that a combination of local and scientific knowledge enables a more beneficial evaluation of land use and land cover change and their impact on local land users and managers (Klintenberg et al., 2007).

6.2. Research Methodology

Structured questionnaire design was used for a household survey (HS), focusing on the impacts of LULC changes on soil fertility changes and flooding/drought happening in the catchment, particularly relating to agricultural expansion, fertilizer consumption etc., and soil erosion. The survey was carried out in August 2021 and adopted a purposive sampling method of study site selection such as upstream catchment (Samlout and Rattanak Mondul district) and downstream (Sangkae and Ak Phnom district located along Stung Sangkae River) to understand the people perception on soil fertility changes and flood/drought impacts during the last 18 years from 2002 to 2020. 200 respondents (100 HS at the upstream and 100 HS at the downstream of Stung Sangkae River catchment) were chosen randomly. The main reason of site selection is due to Battambang, considered as agricultural hub and the largest area in the country. The agricultural expansion in Battambang province for cassava, corn and other fruit trees in the uplands (Kong et al., 2019), was to booster agricultural product in line with the goal of the Cambodian agricultural sector development strategy plan (2019–2023) is to increase all type of agricultural production approximately 10% in annual (MAFF, 2019). The challenge of cultivated area expansion in upland was decline of soil fertilizer (Kong et al., 2019). Two stages were organized for this research study. The first stage, we have observed the field to receive contextual information on agricultural systems in accordance with first draft of structured questionnaire for pretesting before survey starting. The second phase, information collected, was used to finalize the structured questionnaire in order to gather qualitative and quantitative data. Deep interview, semi-structured face-to-face individual interviews, four focused group discussion (two focused group discussion for upstream and downstream) and key informants were carried out to get the information relating land use change, information of flooding/drought, agricultural practice and other challenges. To overcome the problem of data scarcity and evaluate soil erosion in a relatively short period, a unique approach for assessing land degradation from the standpoint of farmers was used. It was based on farmer assessments and observations of changes in their fields. These changes were expressed as soil and productivity loss through visible and comprehensible indicators by the farmers.

Photo 1-2. Interviwing commune leader (Left) and key farmer (Right)

Photo 3-4. Interviewing villagers in Rotanak Mondol (Left) and Sangkae District (Right)

Additional assessment of soil fertility changes and flood/drought was assessed through farmers' perceptions through the household survey (HS) of 200 respondents (100 HS at the upstream and 100 HS downstream of the Stung Sangkae catchment) in 2021. To overcome the problem of data scarcity and evaluate soil erosion in a relatively short period, a unique approach for assessing land degradation from the standpoint of farmers was used. It was based on farmer assessments and observations of changes in their fields. These changes were expressed as soil and productivity loss through visible and comprehensible indicators by the farmers. For the field survey, four districts were selected from each ecological zone (2 districts at the upstream and 2 districts at the downstream catchment). The villages were selected based on their agricultural practices and accessibility. Of the total participants in focus group discussion (FGDs), 35% of respondents were female. The FGDs consisted of a mixture of closed- and open-ended questions.

6.3. Results and Discussion

6.3.1. Assessment of Farmers' Perceptions of Soil Erosion

Additional assessment of soil loss was assessed through farmers' perceptions through household survey (HS). To overcome the problem of data scarcity and evaluate soil erosion in a relatively short period, a unique approach for assessing land degradation from the standpoint of farmers was used. It was based on farmer assessments and observations of changes in their fields. These changes were expressed as soil and productivity loss through visible and comprehensible indicators by the farmers. For the field survey, four districts were selected from each ecological zone (2 districts at the upstream catchment and 2 districts at the downstream catchment). A total of 200 questionnaires and 3 focus group discussions (FGDs) were performed in nine villages from each ecological zone, i.e., high, mid, and low, for the assessment of soil erosion indicators during the year 2002–2020. The villages were selected based on their agriculture practices and accessibility. Of the total participants in FGDs, 35% of respondents were female. The FGDs consisted of a mixture of closed-and open-ended questions.

According to the results of the household survey (HS) of 200 respondents (100 HS at upstream and 100 HS downstream of the Stung Sangkae River catchment) in 2021 showed that all respondents claimed that during 18 years from 2002 to 2020, soil fertility declined significantly. In the catchment, mainly the soil fertility occurred at a fair decline to a strong decline which was 44% and 35%, respectively (Figure 6.1), while the rate of soil fertility tended to slightly increase from a fair decline to a strong decline of 33% to 36% and 40% to 43 % at the upstream and downstream catchment, respectively which was 44% and 35%, respectively (Figure 6.2). In constract, the rate of very strong decline of soil fertility was mainly happened at the upstream catchment rather than at the downstream catchment, which was 18% and 11%, respectively. The response from the farmer was agreed with the simulation of the SWAT and RUSLE that mostly the soil erosion happened at the upstream catchment. However, based on the focus group discussion, the farmers responded that their agricultural yield only slightly declined during the stuy period. This was because the amount of chemical fertilizer consumption were used more than before to sustain the yield of the products. Similarly, previous researchers proved that the soil loss could reduce agricultural productivity. Soil erosion could reduce corn productivity by 12 % to 21 % in Kentucky, 0–24% in Illinois, 25%–65% in Georgia, and 21% in Michigan, USA (Frye, et al., 1982; Olson and Nizeyimana, 1988; Mokma and Sietz, 1992). Furthermore, Jie (2010) reported that if the current rate of soil loss in China continues over the next 50 years, food production would decrease by 40%.

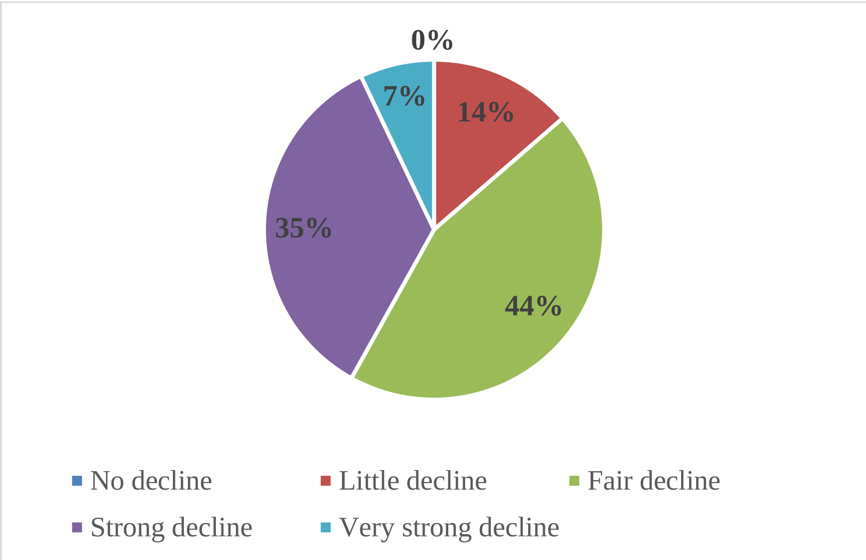

Figure 6.1. Soil fertility

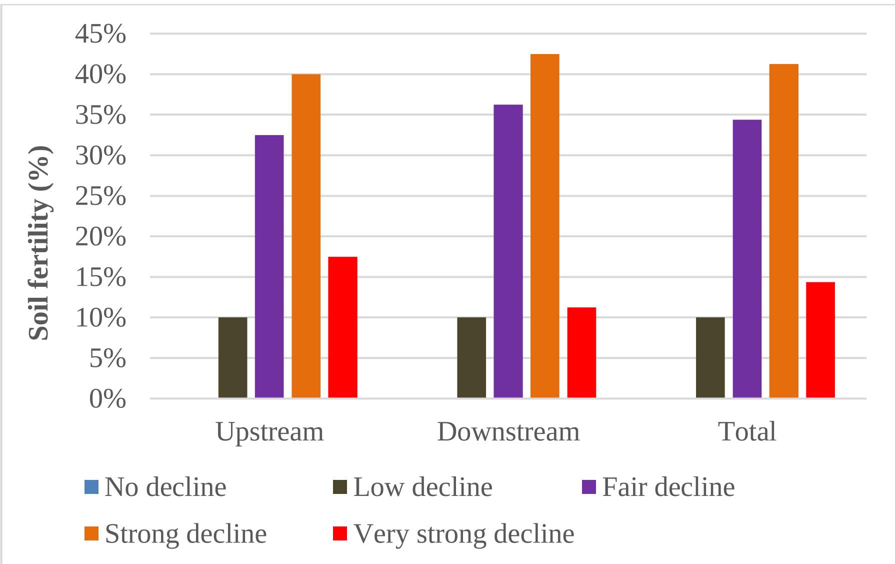

Figure 6.2. Perception of soil fertility decline in the catchment from 2002 to 2015

6.3.2. Assessment of Farmers' Perceptions of Dought and Flooding

The results of the household survey (HS) in 2021 showed that all respondents claimed that during 18 years from 2002 to 2020, the catchment mainly experienced low drought at the upstream and downstream catchment in 2002 and 2015; however, in 2020, the catchment experienced extreme drought rather than low drought in the catchment, particularly in lowland catchment (Figure 6.3).

Figure 6.4 shows that the flooding occurred at a moderate level at the upstream and downstream catchment. In 2002, the flooding occurrence at the upstream catchment (42%) was higher than at the downstream catchment (33%); however, in 2015-2020, the flooding experienced at the downstream catchment, while the rate of flooding also increased from moderate to an extreme level, particularly in 2020. Farmers confirmed that they experienced drought and flooding while water was released from the dam at the upstream catchment.

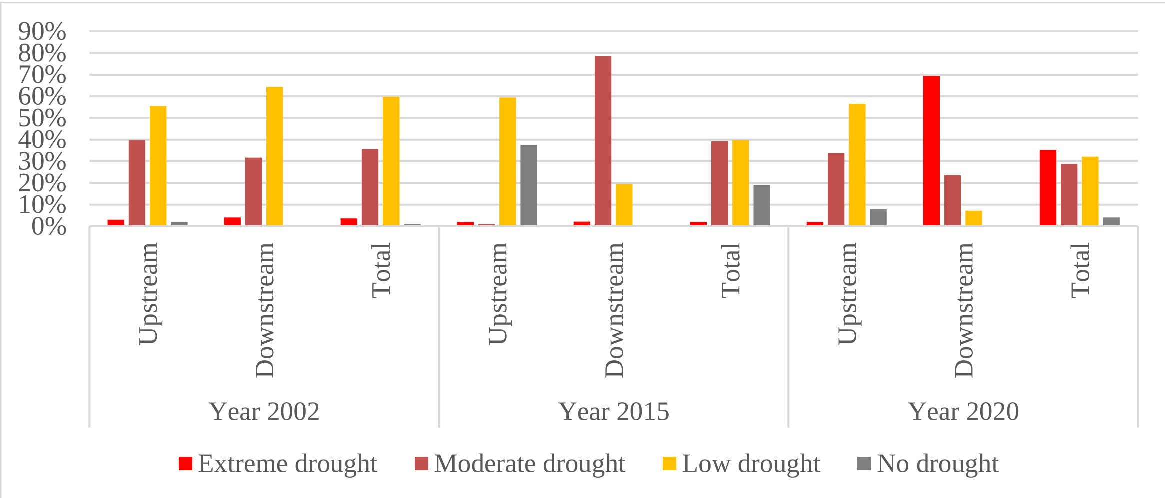

Figure 6.3. Perception of drought in the catchment from 2002 to 2020

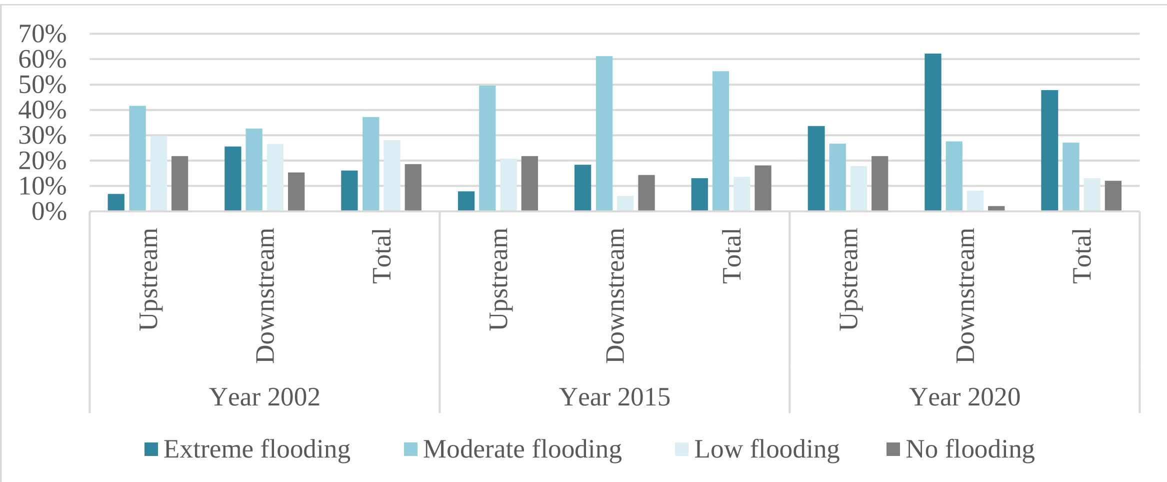

Figure 6.4. Perception of flooding in the catchment from 2002 to 2020

6.4. Discussion

This study is concerned with the impacts of LULC change on hydrological responses in Stung Sangkae catchment. We are concerned that changes in land use will result mainly in changes to stream flow, evapotranspiration, water yield, and soil erosion. This study used the LULC baseline scenario in 2002 compared with the LULC scenario in 2015 for the stream flow, evapotranspiration, water yield, and soil erosion simulation period from 2000 to 2018, while the field survey was done to confirm with simulation results, particularly drought, flooding, and soil fertility decline due to the soil erosion in the catchment based on the perception of the farmers.

In our study, the SWAT model proved satisfactory for modeling river flows in the Stung Sangkae catchment. Results obtained from the SWAT model were improved when calibration was completed by adjusting the parameters that affect the flow rate. According to Moriasi et al. (2007), calibrated and validated results were adequately acceptable for the Stung Sangkae catchment following the performance evaluation criteria. Similarly, the study of Oeurng et al. (2019) reported that calibration and validation performance for monthly time-step simulations at Stung Sangkae River in the Tonle Sap Lake basin obtained R^2 = 0.55, NSE = 0.32, and PBIAS = −30% for calibration and R^2 = 0.70, NSE = 0.19, and PBIAS = −62% for validation. In contrast, according to the performance evaluation criteria, our calibrated and validated results for NSE > 0.40 and PBIAS < ±15% were performed well for Stung Sangkae river in Tonle Sap Lake basin. In addition, all R^2 values for the monthly calibration and validation were above 0.50, suggesting good model performance (Moriasi et al., 2007). The model's overall performance was satisfactory as presented in Figures 3.3 and 3.5.

The result of soil loss simulated from the SWAT model significantly caused my LULC changes even though the streamflow was not significantly influenced. The soil loss led to a decline in soil fertility, which strongly affected farmers' agricultural practices at the upstream and downstream catchment. Based on the HS, the farmer’s responses agreed with the SWAT model as the soil fertility declined at the upstream and downstream catchment. In contrast, the RUSLE model could provide a reasonable result of soil erosion which occurred mainly at the upstream catchment, like the SWAT model, but failed to predict the erosion at the downstream catchment. However, the farmers responded that their crop yield was not much reduced as they applied more chemical fertilizer on their fields due to the soil degradation.

Moreover, the farmers experienced drought and flooding in the catchment, while some years they experienced at the same time drought and flooding. Besides these, the policy of RGC is to increase the forest cover through reforestation activities in the country up to 50% of the SDG on the UN agenda. Also, it tries to intensify agricultural production by promoting some farming techniques such as conservation agriculture and agroforestry to prevent soil erosion and reduce runoff from the farming fields etc. Different studies in different countries have also been conducted to evaluate the impacts of LULC changes on stream flow; a modeling study of Anger watershed, in Ethiopia (Brook et al., 2011) introduced that the surface runoff increased, and the base flow decreased due to the expansion of agricultural land and declined of forest land. In the study of Chemoga watershed, in Blue Nile basin, (Abebe, 2005) also reported that a large volume of surface runoff occurs during storm events since the area under forest cover decreased.

Nevertheless, without including climate change factors, our study provided new sights on the impacts of land use change on stream flow evapotranspiration, water yield, and soil erosion. Similar to several studies, Lin et al. 2007 and Wijesekara et al. 2012 have integrated the hydrologic models with only land use change models to study the impact of foreseeable changes. In addition, the changes observed in the Stung Sangkae catchment hydrology (stream flow) due to land use change in this study align with hydrological studies in different countries from Anand et al., 2018; Remondi et al., 2016; Wagner et al., 2017. Moreover, this study can assess the potential impacts of land use change on hydrological responses (stream flow, evapotranspiration, water yield, and soil erosion, etc.) in the Stung Sangkae catchment; however, water quality is also accounted for the other priority. Based on this study scenario, exploring the associations of hydrologic changes in Stung Sangkae catchment will be helpful for decision-makers and policymakers for the conservation of natural water resources and ecosystems.

Reference of this chapter

Abebe, S. 2005. Land-Use and Land-Cover Change in Headstream of Abbay Watershed, Blue Nile Basin, Addiss Ababa University, Ethiopia.

Anand, J., Gosain A.K. and Khosa, R. 2018. Prediction of land use changes based on land change modeler and attribution of changes in the water balance of Ganga basin to land use change using the SWAT model. Science of the Total Environment, 644, 503-519, Retrieved from Doi: 10.1016/j.scitotenv.2018.07.017

Bonilla-Moheno, M., and Aide, T.M. 2020. Beyond deforestation: Land cover transitions in Mexico. Agricultural Systems, 178, 102734. https://doi.org/10.1016/j.agsy.2019.102734

Brook, H., Argaw, M., Sulaiman, H. and Abiye, T.A. 2011. The Impact of land use/cover change on hydrology components due to resettlement activity: SWAT model approach. International Journal of Ecology and Environmental Sciences 37 (1): 49-60.

Cambodian Agricultural Research and Development Institute (CARDI). 2016. *Annual Research Report for 2015*; CARDI: Phnom Penh, Cambodia.

Desalegn, T., Cruz, F., Kindu, M., Turrión, M.B., and Gonzalo, J. 2014. Land-use/land-cover (LULC) change and socioeconomic conditions of local community in the central highlands of Ethiopia. International Journal of Sustainable Development & World Ecology, 21(5), 406–413. https://doi.org/10.1080/13504509.2014.961181

Frye, W.W.; Ebelhar, S.A.; Murdock, L.W.; Bevins, R.L. 1982. Soil erosion effects on properties and productivity of two Kentucky soils. Soil Sci. Soc. Am. J., 46, 1051–1055.

Gashaw, T., Tulu, T., Argaw, M., and Worqlul, A.W. 2017. Evaluation and prediction of land use/land cover changes in the Andassa watershed, Blue Nile Basin, Ethiopia. Environmental Systems Research, 6(1), 17. https://doi.org/10.1186/s40068-017-0094-5

Intergovernmental Panel on Climate Change (IPCC). 2019. Climate Change and Land. Retrieved from www.ipcc.ch.

Jie, D. 2010. Chinese soil experts warn of massive threat to food security. SciDevNet. Available online: https://www.scidev.net/global/news/chinese-soil-experts-warn-of-massive-threat-to-food-security/ (accessed on 05 February 2021).

Klintenberg, P., Seely, M., and Christiansson, C. 2007. Local and national perceptions of environmental change in central Northern Namibia: Do they correspond? Journal of Arid Environments, 69(3), 506–525. https://doi.org/10.1016/j.jaridenv.2006.10.015

Kong, R., Diepart, J.-C., Castella, J.-C., Lestrelin, G., Tivet, F., Belmain, E., and Bégué, A. 2019. Understanding the drivers of deforestation and agricultural transformations in the Northwestern uplands of Cambodia. Applied Geography 102, 84–98. https://doi.org/10.1016/j.apgeog.2018.12.006

le Polain de Waroux, Y., Garrett, R.D., Heilmayr, R., and Lambin, E.F. 2016. Land-use policies and corporate investments in agriculture in the Gran Chaco and Chiquitano. Proceedings of the National Academy of Sciences, 113(15), 4021–4026. https://doi.org/10.1073/pnas.1602646113

Lambin, E.F., and Meyfroidt, P. 2011. Global land use change, economic globalization, and the looming land scarcity Proc. Natl. Acad. Sci., 108, pp. 3465-3472

Lin, Y.-P., Hong, N.-M., Wu, P.-J., Wu, C.-F., and Verburg, P. H. 2007. Impacts of land use change scenarios on hydrology and land use patterns in the Wu-Tu watershed in Northern Taiwan. Landscape and Urban Planning, 80(1–2), 111–126. https://doi.org/10.1016/j.landurbplan.2006.06.007

Manandhar, R., Odeh, I., and Ancev, T. 2009. Improving the accuracy of land use and land cover classification of landsat data using post-classification enhancement. Remote Sensing, 1(3), 330–344. https://doi.org/10.3390/rs1030330

Maro, P. 2011. Environmental change in Lesotho: An analysis of the causes and consequences of land-use change in the Lowland Region. Springer International Publishing. https://doi.org/10.1007/978-94-007-1881-4

Mokma, D.L.; Sietz, M.A. 1992. Effects of soil erosion on corn yields on Marlette soils in South-Central Michigan. J. Soil Water Conserv., 47, 325–327.

Montalván-Burbano, N., Velastegui-Montoya, A., Gurumendi-Noriega, M., Morante-Carballo, F., and Adami, M. 2021. Worldwide research on land use and land cover in the Amazon Region. Sustainability, 13(11), 6039. https://doi.org/10.3390/su13116039

Moriasi, D.N., Arnold, J.G., Van Liew, M.W., Binger, R.L., Harmel, R.D., and Veith, T. 2007. Model evaluation guidelines for systematic quantification of accuracy in watershed simulations. Trans. ASABE 50(3): 885-900.

Mwavu, E.N., and Witkowski, E.T.F. 2008. Land-use and cover changes (1988-2002) around budongo forest reserve, NW Uganda: Implications for forest and woodland sustainability. Land Degradation & Development, 19(6), 606–622. https://doi.org/10.1002/ldr.869

Nut, N., Mihara, M., Jeong, J., Ngo, B., Sigua, G., Prasad, P.V.V., and Reyes, M.R. 2021. Land use and land cover changes and its impact on soil erosion in Stung Sangkae Catchment of Cambodia. *Sustainability*, *13*(16), 9276. https://doi.org/10.3390/su13169276

Oeurng, C., Cochrane, T., Chung, S., Kondolf, M., Piman, T., and Arias, M. 2019. Assessing Climate Change Impacts on River Flows in the Tonle Sap Lake Basin, Cambodia. Water, 11(3), 618. https://doi.org/10.3390/w11030618

Olson, K.R.; Nizeyimana, E. 1998. Effects of soil erosion on corn yields of seven Illinois soils. J. Prod. Agric., 1, 13–19

Pheap, S., Lefèvre, C., Thoumazeau, A., Leng, V., Boulakia, S., Koy, R., Hok, L., Lienhard, P., Brauman, A., and Tivet, F. 2019. Multi-functional assessment of soil health under conservation agriculture in Cambodia. Soil and Tillage Research, 194, 104349. https://doi.org/10.1016/j.still.2019.104349

Remondi, F., Burlando, P. and Vollmer, D. 2016. Exploring the hydrological impact of increasing urbanisation on a tropical river catchment of the metropolitan Jakarta, Indonesia. Sustain. Cities Soc., 20, 210-221, Retrieved from https://doi.org/10.1016/j.scs.2015.10.001

Sandewall, M., Ohlsson, B., and Sawathvong, S. 2001. Assessment of historical land-use changes for purposes of strategic planning—A case study in Laos. AMBIO: A Journal of the Human Environment, 30(1), 55–61. https://doi.org/10.1579/0044-7447-30.1.55

Shi, Z., Crowell, S., Luo, Y., and Moore, B. 2018. Model structures amplify uncertainty in predicted soil carbon responses to climate change. Nature Communications, 9(1), 2171. https://doi.org/10.1038/s41467-018-04526-9

Sourn, T., Pok, S., Chou, P., Nut, N., Theng, D., Rath, P., Reyes, M.R., Prasad, P.V.V., 2021. Evaluation of Land Use and Land Cover Change and Its Drivers in Battambang Province, Cambodia from 1998 to 2018. Sustainability 13, 11170. https://doi.org/10.3390/su132011170

Sourn, T., Pok, S., Chou, P., Nut, N., Theng, D., and Prasad, P.V.V. 2022. Assessment of land use and land cover changes on soil erosion using remote sensing, GIS and RUSLE Model: A case study of Battambang Province, Cambodia. *Sustainability*, *14*(7), 4066. https://doi.org/10.3390/su14074066

Toh, F.A., Angwafo, T.E., Ndam, L.M., and Antoine, M.Z. 2018. The socio-economic impact of land use and land cover change on the inhabitants of Mount Bambouto Caldera of the Western Highlands of Cameroon. Advances in Remote Sensing, 07(01), 25–45. https://doi.org/10.4236/ars.2018.71003

USAID. 2021. Agriculture and food security. Retrieved from https://www.usaid.gov/cambodia/agriculture-and-food-security.

Wagner, P.D., Bhallamudi, S.M., Narasimhan, B., Kumar, S., Fohrer, N. and Fiener, P. 2017. Comparing the effects of dynamic versus static representations of land use change in hydrologic impact assessments. Environ. Model. Softw., Retrieved from https://doi.org/10.1016/j.envsoft.2017.06.023

Wijesekara, I., Senevirathne, M., Li, Y.-X., and Kim, S.-K. 2012. Functional ingredients from marine algae as potential antioxidants in the food industry. In S.-K. Kim (Ed.), Handbook of marine macroalgae (pp. 398-402). Hoboken: John Wiley & Sons, Inc.

Xu, X., Xie, Y., Qi, K., Luo, Z., and Wang, X. 2018. Detecting the response of bird communities and biodiversity to habitat loss and fragmentation due to urbanization. Science of The Total Environment, 624, 1561–1576. https://doi.org/10.1016/j.scitotenv.2017.12.143

CHAPTER 7
Conclusion and Recommendations

7.1 General Conclusion

This research used different land use and land cover change (LULC) to evaluate their impacts on the hydrological responses, such as streamflow, water balance, and soil erosion in Stung Sangkae River catchment. During the investigated periods from 2002 to 2015, the upland fields increased by 20.8% from 4.4% to 25.2%. The forest land decreased significantly from 43% to 29.6% due to a massive shift in deciduous and mixed forest converted to agricultural land, paddy rice fields, and other land use types.

For both reference land uses in 2002 LULC and 2015 LULC, the sensitive stream flow parameters were the same, although the sensitivity rank of the exact parameters varies. Hence, these calibrated parameters can be used for further future hydrological and environmental studies in the Stung Sangkae River catchment without doing a sensitivity analysis. In general, the calibrated model reasonably explained the variability in hydrological responses of streamflow affected by different LULC maps in the sub-catchment and catchment scales under the evaluation of LULC 2002 and 2015. The statistical agreement was R^2=0.58, NSE=0.55, PBIAS=5 (including the dam construction period) and R^2=0.64, NSE=0.62, and PBIAS=15 (excluding the dam construction period).

As LULCs changed from 2002 to 2015, individual LULCs' contribution to catchment WY changed too, but the change process was complex because the WY is an integrated result of LULCs, soil, topography, and climate. For the contribution of each LULC to the total WY of the catchment, the forested area, shrubland, and grassland were the main contributors, with up to about 40%, 12%, and 13%, respectively. The land use that generated the largest water yield was presented to be agricultural activities and urban area, which was higher than any other land use type, followed by forested area, shrubland, and grassland. Furthermore, accompanying the LULC changes in the Stung Sangkae catchment, an increase in PET, ET, and WY indicated that soil and water conservation practices increased stream flow. In contrast, expanding the agricultural land, rice, and urban area increased the ET and WY.

Even though the LULC in 2002 and 2015 had significantly changed from forest land to agricultural land and other types, the SWAT streamflow simulation was not very different, but it significantly impacted soil erosion in the Stung Sangkae catchment.

In terms of soil erosion analysis with SWAT and RUSLE models, the mean annual soil loss of the Stung Sangkae catchment was approximately 12 t/ha/yr and 21.8 t/ha/yr for the LULC 2002 and LULC 2015 based on SWAT model simulation which agreed with the experimental corn field of CARDEC in 2019. For the soil erosion analysis with the RUSLE model, the average soil loss from the catchment was 3.1 in 2002 and 7.6 t/ha/y in 2015, while the highest erosion rates of 14.3 to 62.9 t/ha/y were found in parts of the upland of the Stung Sangkae catchment, mainly due to steep slopes, high rate of erosion and degradation of the vegetation. Considerable changes in soil loss rate were observed in agricultural land. The application of the RUSLE equation shows that 87% of the catchment area is exposed to a low to moderate erosion risk (<10 t/ha/y), and 4.1% basin is in severe, moderate risk, while the application of the SWAT model shows that 74.5 % of the surface area of the Stung Sangkae catchment is exposed to a low to moderate risk of erosion (<10 t/h/y) and 17.4% basin is at severe risk. The most affected areas are in the west of the catchment, where the upland agriculture was expanded. Generally, both models have shown that the risk of erosion in the Stung Sangkae catchment is considered as low to moderate erosion risk. However, if compared with the results of the questionnaire survey, the SWAT model is better than RUSLE for predicting soil erosion as it could capture the soil erosion at the downstream catchment, while the RUSLE could not do that. This is because the RUSLE model is based on kinetic energy in the delivery of potential erosion quantities in a terrestrial phase, while the SWAT model works in two phases, the terrestrial first which consists of quantifying the amounts of the sediment to be delivered at the level of each sub-basin discretized in several hydrological units, and the second fluvial phase, which makes it possible to evaluate the quantities of the transported sediments. In our case, the amount of soil erosion from the SWAT model is increased because of the porous nature of the Stung Sangkae catchment soil, which consequently can raise or minimize the amount of erosion delivered by each sub-basin. Moreover, this can happen due to the inappropriate estimation of the C and P factors in the catchment while using the RUSLE model, as they effectively prevented soil loss.

Countermeasures of reforestation or agroforestry of 25% (40% forest of the total area) had less impact on streamflow. Still, it significantly prevented soil erosion in the catchment, while the increased reforestation of more than 25% is not recommended.

It could also be concluded that the approach used in this research simply evaluates the contributions of individual LULC classes to the hydrological responses, providing quantitative information for decision-makers to make better options for land and water resource planning and management. This approach also provides a solid example of the potential of hydrologic modeling using national LULC maps in understanding the impacts of hydrological change on runoff, water yield, soil erosion etc. in the Stung Sangkae River catchment of Cambodia. It can be widely applied to a variety of catchments, where time-sequenced digital land cover data is available, and to predict hydrological consequences to LULC changes. Moreover, the applicability of the SWAT model in simulating the soil erosion and flow dynamics of the Stung Sangkae River catchment was validated based on the satisfactory values of the statistical measures of the model efficiency. Therefore, the model simulation results provide confidence for further application of the model to assess hydrological response analysis, as the spatial and temporal variability of the catchment features within the Stung Sangkae River basin will show minimal bias. However, the changes in LULC have impacted the environmental sustainability, especially the streamflow that caused flooding at the downstream watershed due to declined forest cover at the watershed, sediment yield, soil erosion, and other environmental issues.

7.2 Recommendations

Based on the study's outcome, it recommends that some further things and studies should be considered.

- As the LULC could more or less impact hydrological components (stream flow, groundwater, water yield, evapotranspiration etc.) in the Stung Sangkae River catchment due to the population growth and required agricultural land for crop production, which are the main factors leading to the decrease of forest land, a proper integrated forest resource management to balance forest conversion to agriculture and built-up areas, should be considerably taken into consideration by the policy-marker as well as urban planning designer.
- The other thing which is highly recommended is that the weather stations should be improved both in quality and quantity in order to improve the performance of the model. Hence, it is highly recommended to establish good meteorological stations.

- Hydrological modeling integrating future climate change and LULC changes scenarios can effectively plan future water resource management strategies. Thus, the next research should focus on integrating these scenarios to understand how much changing impervious land use contributes more clearly to water quantity.
- The study developed R-factor from six meteorological stations, which may introduce uncertainties in the estimated soil loss. Therefore, more stations of meteorology should be further used to estimate soil erosion based on the RUSLE model, while the R-factor equation for the Cambodia context should be formulated for better results.
- The estimation of the K-factor should be made based on national or local soil type to compare with the soil type extracted from the Soil Grids database of ISRIC-World Soil Information.
- The estimation of the C and P factors in the catchment should be carefully selected for use with the RUSLE model as they are susceptible to estimating soil loss.
- Integrated protection measures at the farm level and target areas of high risk of erosion, mainly the degraded lands along the steep slopes, to limit the conversion of forest areas for agriculture and minimize the rate of erosion where the land is bare or with low vegetation cover should be taken into consideration. Some recommended measures to prevent soil erosion include on-farm conservation agriculture practices (CAP), water conservation and management, agro-forestry practices, vegetation cover restoration, and terracing.
- This study result will be a guideline for decision-making about land use and water resources management in the Stung Sangkae Catchment and other river catchments of the Tonle Sap tributaries of Cambodia.

APPEXDIX I

List of Publications

This dissertation is based on the work contained in the following papers, referred to by Roman numerals in the text:

I. **Nareth Nut**, Machito Mihara, Jaehak Jeong, Bunthan Ngo, Gilbert Sigua, P.V. Vara Prasad and Manuel R. Reyes (2021). Land Use and Land Cover Changes and Its Impact on Soil Erosion in Stung Sangkae Catchment of Cambodia. *Sustainability* 2021, 13(16), 9276. https://doi.org/10.3390/su13169276

II. **Nareth Nut**, Machito Mihara, Jaehak Jeong, Bunthan Ngo, Sakdanuphol Chan, Gilbert Sigua and Manuel R. Reyes. (2021). Impacts of Land Use-Land Cover Changes on Streamflow and Water Balance of Stung Sangkae Catchment Using SWAT. *International Journal of Environmental and Rural Development (IJERD).* 12(2): 201-208. https://doi.org/10.32115/ijerd.12.2_201

III. **Nareth Nut**, Manuel R. Reyes, Gilbert Sigua, Machito Mihara, Sakdanuphol Chan and Taingaun Sourn (2021). Application of APEX Model in Evaluating Streamflow and Sediment Yield in Stung Chinit Catchment. International Journal of Environmental and Rural Development (IJERD). 12(2): 161-170. https://doi.org/10.32115/ijerd.12.2_160

Other publications associated with the PhD dissertation is contained in the following papers:

I. Sourn, T., Pok, S., Chou, P., **Nut, N.**, Theng, D., Rath, P., Reyes, M.R., Prasad, P.V.V., 2021. Evaluation of Land Use and Land Cover Change and Its Drivers in Battambang Province, Cambodia from 1998 to 2018. Sustainability 13, 11170. https://doi.org/10.3390/su132011170

II. Sourn, T.; Pok, S.; Chou, P.; **Nut, N.**; Theng, D.; Prasad, P.V. Assessment of Land Use and Land Cover Changes on Soil Erosion Using Remote Sensing, GISand RUSLE Model: A Case Study of Battambang Province, Cambodia. Sustainability 2022, 14(7), 4066. https://doi.org/10.3390/su1407406

APPEXDIX II

Table A.1. Rating curve developed to estimate stream flows for the monitored water levels at the outlets of the 11 Tonle Sap sub-catchments (Kummu, et al., 2014)

Sub-catchments	**Rating curve**	**Observed flow**
ST. Chinit	$Q = 15.49 - 36.8088 \times \mathrm{H_{KgThom}} + 36.3032 \times \mathrm{H^2_{KgThom}} - 8.5957 \times \mathrm{H^3_{KgTmar}} + 0.7869 \times \mathrm{H^4_{KgTmar}}$	2000-2019
ST. Sen	$Q = 0.000013 \times \left(\mathrm{H_{KgThom}} - 1.21\right)^{6.8178} \times \mathrm{F}^{0.2}$; where, $\mathrm{F} = \mathrm{H_{KgThom}} - \mathrm{H_{KgLuong}}$	2000-2019
ST. Staung	$Q = 0.8554 \times \mathrm{H^{2.7794}_{KgChen}} \times \mathrm{F}^{0.5}$; where, $\mathrm{F} = \mathrm{H_{KgChen}} - \mathrm{H_{KgLuong}} + 7$	2000-2019
ST. Chikreng	$Q = 0.1017 \times \mathrm{H^{3.3034}_{KgKdey}} \times \mathrm{F}^{0.5}$; where, $\mathrm{F} = \mathrm{H_{KgChen}} - \mathrm{H_{KgKdey}} + 7$	2000-2018
ST. Siem Reap	$Q = 4.1059 \times \left(\mathrm{H_{UntacBridge}} - 0.0936\right)^2$	2000-2016
ST. Sreng	$Q = 0.01299 \times \mathrm{H^{4.3665}_{Kralanh}} \times \mathrm{F}^{0.5}$; where, $\mathrm{F} = \mathrm{H_{Kralanh}} - \mathrm{H_{BacPrea}} + 4$	2000-2017
ST. Mongkol Borey	$Q = \mathrm{y} \times (\mathrm{F} + 6.09)^{0.69}$; $\mathrm{y} = -0.5665 + 2.212 \times \mathrm{H_{MongkolBorey}} - 0.8243 \times \mathrm{H^2_{MongkolBorey}} - 0.1796 \times \mathrm{H^3_{MongkolBorey}}$ $\mathrm{F} = \mathrm{H_{MongkolBorey}} - \mathrm{H_{BacPrea}} + 6$	2000-2017
ST. Sangke	$Q = \mathrm{y} \times (\mathrm{F} + 0.3)^{0.18}$; $\mathrm{y} = -28.2541 + 33.8995 \times \mathrm{H_{Battambang}} - 9.5551 \times \mathrm{H^2_{Battambang}} - 0.8092 \times \mathrm{H^3_{Battambang}}$ $\mathrm{F} = \mathrm{H_{MongkolBorey}} - \mathrm{H_{BacPrea}}$	2000-2018
ST. Dauntri	$Q = 12.4 \times \left(\mathrm{H_{MaungRussey}} - 1.2439\right)^2$	2000-2008
ST. Pursat	$Q = 25.5 \times (\mathrm{H_{BacTrakuon}} - 0.0856)^2$	2000-2016
ST. Baribo	$Q = 37.1593 \times \mathrm{H^{1.6195}_{Baribo}}$	2000-2014

APPEXDIX III

Household Questionnaire Survey

1. Interniewee's Information

Interviewee's name		**Sex**		**Age**	
Village name		Commune		District	
GPS ID		Coordinate x		Coordinate y	
Household ID					
Date of interview		Starting time		Ending time	
Do she/he Consent to provide information for this survey? Yes ☐ No ☐					

Section 1: Social Economic Profile

(For interviewer: please ask the questions below to head of the family for both husband and wife.)

N°	1. Ages	2. Gender (1=male, 2=female)	3. Marital Status	4. Level of Education	5. Ethnic	6. Religious
1						

Marital Status	Level of Education	Ethnic	Religious
1. Single 2. Married 3. Divorced 4. Widow/widower	1. Illiterate 2. Primary school 3. Secondary Scholl 4. High school 5. Vocational trainings 6. College/University 7. Informal education 8. Others	1. Khmer 2. Kuoy 3. Bunong 4. Krol 5. Lao 6. Kinh 7. Others (Please specify)	1. Buddhist 2. Catholic 3. Protestant 4. Islam 5. Ancestors worship 6. No religious

7. How many people in your family based on age classification below? ☐

7.1 Children under 1 year old ☐

7.2 Children from 1 to 5 years old ☐

☐

7.3 Children age from 5 to 17years old

7.4 Adults age from 18 to 59 years old ☐

7.5 Elder age above 59 years old ☐

8. Can you read any announcement or information? ☐ 1= No ☐ 2 = Yes

9. What is the source of lighting in the house?
☐ 1 = Electricity ☐ 2 = Biogas ☐ 3 = Kerosene
☐ 4 = Battery ☐ 5 = Other _______________

10. What is the main fuel used for cooking in the house?
☐ 1 = Electricity ☐ 2 = Gas ☐ 3 = Firewood
☐ 4 = Kerosene ☐ 5 = Charcoal ☐ 6 = Other

11. How many of the following devices does your household have?

Households' asset	Number	Households' asset	Number
11.1 Sewing machine		11.8 Mobile Phone	
11.2 Ox cart		11.9 Motorcycle	
11.3 Tractor		11.10 Bicycle/electric bicycle	
11.4 Television		11.11 Car	
11.5 DVD/VCD/VHS player		11.12 Boat with engine	
11.6 Rice miller		11.13 Boat without engine	
11.7 Sawing machine		11.14 others	

12. How many in your household, including yourself, can earn income? ☐

13. What is the main occupation for sustaining your family livelihood? *(Please tick only one.)*

1.Farming/gardening	5. Fishing	9. Aquaculture
2. Handicraft	6. Collecting TFP/NTFP	10. Middleman
3. Rented labors	7. Own business	11. Service providers
4. Government officer	8. NGO/Company staff	12. Others, specify…………….

14. What are the secondary occupations for sustaining your family livelihood? *(Can be ticked more than one.)*

1.Farming/gardening	5. Fishing	9. Aquaculture
2. Handicraft	6. Collecting TFP/NTFP	10. Middleman
3. Rented labors	7. Own business	11. Service providers
4. Government officer	8. NGO/Company staff	12. Others, specify…………….

15. Please indicate your average monthly household income (Riels).

1	Less than R200,000	7	From R1,200,000 to R1,400,000

2	From R200,000 to R400,000	8	From R1,400,000 to R1,600,000
3	From R400,000 to R600,000	9	From R1,400,000 to R1,600,000
4	From R600,000 to R800,000	10	From R1,600,000 to R2,000,000
5	From R800,000 to R1,000,000	11	From R2,000,000 to R2,400,000
6	From R1,000,000 to R1,200,000	12	More than R 2,400,000

Section 2: Agricultural Practices

16. Please indicate the amount of land (in hectares) that your household currently own and have rented in/out.

Land category	Land ownership (ha)	Total land rented out (ha)	Total land rented in (ha)	Total areas (ha)
16. Agricultural land				
16.1 Paddy land				
16.2 Chamkar (crop land)				
16.3 Pasture (natural or planted)				
16. Total land owned				

Section 3: Soil Erosion Impacts on Agricultural Potential and Performance

17. Distance from your house to farmland (…………km)

18. What type of road in your village?

Year	1. Earth road	2. Laterite road	3. Concrete road	4. BST road
2002				
2015				
2020				

19. How big is your farm size?

Year	1. < 1 ha	2. 1 ha < & < 3 ha	3. 3 ha< & < 5 ha	4. 5 ha < & < 10 ha	5. > 10 ha
2002					
2015					
2020					

20. Fertilizer Consumption:

20.1. Do you apply chemical fertilizer on your fields?

☐ 1. No, ☐ 2. Yes (*How many sack of chemical fertilizer is applied per hectares?)*

Year	1. < 1 sack	2. 1 < & < 3 sack	3. 3 < & < 5 sack	4. > 5 sack	Cost of fertilizer per sack
2002					
2015					
2020					

Note: One sack = 50 kg

20.2. Do you apply compost fertilizer or cow/chicken manures on your fields?

☐ 1. No, ☐ 2. Yes (*How many sack of chemical fertilizer is applied per hectares?)*

Year	1. < 1 ton	2. 1 < & < 3 tons	3. 3 < & < 5 tons	4. > 5 tons	Cost of compost per ton
2002					
2015					
2020					

Section 4: Constraints to Agricultural Production

21. Does the soil fertilizer decline in the last 20 years?
☐ a. No decline, ☐ b. Little, ☐ c. Fair, ☐ d. Strong, ☐ e. Very strong
22. Do you lack of credit for agricultural production?
☐ a. No, ☐ b. Little, ☐ c. Fair, ☐ d. Much, ☐ e. Very much
23. Do you lack of labor for agricultural production?
☐ a. No, ☐ b. Little, ☐ c. Fair, ☐ d. Much, ☐ e. Very much
24. Do you have any problem with flooding?
☐ a. No, ☐ b. Little, ☐ c. Fair, ☐ d. Strong, ☐ e. Very strong
25. Do you have any problem with drought?
☐ a. No, ☐ b. Little, ☐ c. Fair, ☐ d. Strong, ☐ e. Very strong
26. How much is chemical peticide applied in the field?

Year	1. No	2. little	3. Fair	4. Very	5. Very Strong
2002					
2015					
2020					

27. How much is chemical fertilizer applied in the field?

Year	1. No	2. little	3. Fair	4. Very	5. Very Strong
2002					
2015					
2020					

Section 5: Impacts of Land Use Change on Hydrological characteristics in 2002-2020

28. Rainfall pattern: Have you noticed about the rainfall pattern changed in your areas during these years: 2002, 2015 and 2020? ☐ 1. No, ☐ 2. Yes (*Please answer below.)*

Year	1. Low rainfall	2. Moderate rainfall	3. Extreme rainfall
2002			
2015			
2020			

29. Flooding occurrences: Is there any flooding occurrence during these year: 2002, 2015 and 2020? ☐ 1. No, ☐ 2. Yes (*Please answer below.)*

Year	1. Low flooding	2. Moderate flooding	3. Extreme flooding
2002			
2015			
2020			

30. Erosion occurrences: Is there any erosion occurrence during these year: 2002, 2015 and 2020? ☐ 1. No, ☐ 2. Yes (Please answer below.)

Year	1. Low erosion	2. Moderate erosion	3. Extreme erosion
2002			
2015			
2020			

31. Drought occurrences: Is there any drought occurrence during these year: 2002, 2015 and 2020? ☐ 1. No, ☐ 2. Yes (Please answer below.)

Year	1. Low drought	2. Moderate drought	3. Extreme drought
2002			
2015			
2020			

32. Do you use water from the Stung Sangkae during these year: 2002, 2015 and 2020? ☐ 1. No, ☐ 2. Yes (Please answer below.)

Year	1. Low use	2. Normal use	3. Much use
2002			
2015			
2020			

33. Do you irrigate your crop fields during these year: 2002, 2015 and 2020? ☐ 1. No, ☐ 2. Yes (Please answer below.)

Year	1. Less irrigate	2. Normal irrigate	3. Much irrigate
2002			
2015			
2020			

34. Do you change the crop type (different crop; plant new crop) between 2002 and 2020?

☐ 1. No

(Reason: ....)

☐ 2. Yes

(Reason: ....)

35. Do you change the crop variety (same crop; but different varieties) between 2002 and 2020?

☐ 1. No

(Reason: ....)

☐ 2. Yes

(Reason: ....)

36. Do you change to drought resistant crop between 2002 and 2020?

☐ 1. No

(Reason: ....)

☐ 2. Yes

(Reason: ....)

37. Do you change in sowing/planting dates between 2002 and 2020?

☐ 1. No

(Reason: ....)

☐ 2. Yes

(Reason: ....)